1463

ProQuest Number: 10702812

ProQuest 10702812

Studies of Biomarkers in Temporal Lobe epilepsy

Mariam Abdelghani Sheilabi

A thesis submitted in partial fulfilment of the requirements of
Sheffield Hallam University for the degree of Doctor of
Philosophy

July 2016

Abstract

Purpose: Refractory temporal lobe epilepsy associated with hippocampal sclerosis (TLE-HS) affects about 30% of TLE patients, where antiepileptic drugs are not effective in controlling seizures. These patients become candidates for surgical treatment which is effective in only 60-70% of cases. In addition, surgical treatment causes memory and cognitive impairments as well as psychopathological disturbance. Therefore, the aim of this study is to investigate potential biomarkers in surgically resected sclerotic TLE-HS (n = 49) and non-spiking superior temporal gyrus samples (TLE-STG; n = 25) from TLE patients and *post-mortem* hippocampi (PMC; n = 10), in order to increase our understanding of refractory TLE pathophysiology and help in identifying new potential drug targets for treatment of TLE patients. **Methods:** $GABA_B$ receptor subunits were investigated in TLE-HS, TLE-STG and PMC tissue by quantitative real time polymerase chain reaction (qRT-PCR) and quantitative western blot (WB) techniques. Alterations in expressions of SGK1, SCN4B, IP3R1 and SYNPR were investigated in TLE-HS, TLE-STG and PMC specimens by qRT-PCR and WB. The transcriptome profiling of TLE-HS, TLE-STG and PMC samples was done by microarray analysis (MA). MA was followed by functional annotation clustering analysis (FAC) of the MA differentially expressed genes (DEGs). Genes from FAC analysis were further investigated by qRT-PCR. MA Aquaporin (AQP1, 3, 4, 5, 8, 9, 11) expressions were further validated by qRT-PCR. **Results:** Expression of the inhibitory $GABA_{B2}$ receptor subunit was significantly up regulated in TLE-HS compared to PMC but its expression was reduced in TLE-HS compared to TLE-STG.The expression of SCN4B, IP3R1 and SYNPR, which are involved in regulating neuronal excitability, were significantly reduced in TLE-HS compared to TLE-STG and were significantly increased compared to PMC. The expression of SGK1 mRNA was significantly increased in TLE-HS compared to both TLE-STG and PMC. MA analysis revealed 1821 genes were significantly up regulated and 1511 genes were significantly down regulated in TLE-HS compared to TLE-STG and PMC. The first cluster from FAC analysis of DEGs showed that the up regulated inflammatory genes such as cytokines had the highest enrichment score. The qRT-PCR data showed that expression of IL-1β, IL-18, Fas, ICAM-1, CCL2, CCL4, CXCL1, CXCL2, CXCL12, CXCR4 and CX3CR1 were significantly higher in TLE-HS compared to TLE-STG and PMC therefore validating MA data. AQP1 and -4, which are involved in water homeostasis, were significantly up regulated in TLE-HS compared to TLE-STG. AQP11 expression was significantly reduced in TLE-HS while AQP3, -5, -8 and -9 were not significantly altered in TLE-HS compared to TLE-STG and PMC. **Discussion:** The significant dysregulation of biomarker expression investigated in this study indicate that different biological processes such as neuronal excitability, neuronal and astrocytic energy metabolism, neurogenesis, apoptosis, neuroinflammation, intracellular calcium and water homeostasis are affected in the epileptogenic TLE-HS tissue. These biomarkers seem to be associated with TLE-HS pathophysiology. Furthermore, they highlight the role of neuronal, astrocytic, microglia and endothelial cell dysfunction in TLE-HS pathology. **In conclusion**, the biomarkers investigated increased our understanding of biological processes affected in TLE-HS pathophysiology and they represent potential drug targets for refractory TLE-HS. However, further research is still needed to understand the temporal and spatial changes of those genes and their proteins during TLE.

Table of Contents

List of Figures

List of Tables

Abbreviations

a.u.	Arbitrary unit
A_{230}	Absorbance at 230 nm
A_{260}	Absorbance at 260 nm
A_{280}	Absorbance at 280 nm
ACTB	β-actin
AEDs	Antiepileptic drugs
AMPA	α-amino-3-hydroxy-5-methyl-4-isoxazolepropionic acid receptor
AQP	Aquaporin
BBB	Blood brain barrier
BCA	Bicinchoninic acid
BDNF	Brain-derived neurotrophic factor
BSA	Bovine serum albumin
BZs	Benzodiazepines
CA	*Cornu ammonis*
CA1-CA4	Cornu ammonis area 1-4
cAMP	3'-5'-cyclic adenosine monophosphate
CBZ	Carbamazepine
CCL	Chemokine (C-C motif) ligand
CDKN1B	Cyclin-dependent kinase inhibitor 1B
cDNA	Complementary DNA
CGR	Centre for Genomic research
CLB	Clobazam
CNP	Clonazepam
C_t	Threshold cycle
CV	Coefficient of variation
CX3CR1	Chemokine (C-X3-C motif) receptor 1
CXCL	Chemokine (C-X-C motif) ligand
CXCR	Chemokine (C-X-C motif) receptor
Cy3	Cyanine 3 dye

Cy5	Cyanine 5 dye
DAG	Diacylglycerol
DAVID	Database for Annotation, Visualisation and Integrated Discovery
DEGs	Differentially expressed genes
DG	Dentate gyrus
DH	Dentate hilus
DTT	Dithiothreitol
EAAT	Excitatory amino acids transporter
EDTA	Ethylenediaminetetraacetic acid
ER	Endoplasmic reticulum
FADD	Fas-Associated protein with Death Domain
FDR	False discovery rate
GABA	γ- amino butyric acid
GABA$_A$	γ- amino butyric acid receptor type A
GABA$_B$	γ- amino butyric acid receptor type B
GABA$_{B1a}$	γ- amino butyric acid receptor type B, subunit 1, isoform a
GABA$_{B1b}$	γ- amino butyric acid receptor type B, subunit 1, isoform b
GABA$_{B2}$	γ- amino butyric acid receptor type B, subunit 2
GABAT	γ- aminobutyric acid transaminase enzyme
GAD	Glutamate decarboxylase
GALGO	R package for multivariate variable selection using genetic algorithms
GAT1	γ- aminobutyric acid transporter 1
GBP	Gabapentin
GCL	Granule cell layer
GFAP	Glial fibrillary acidic protein
GIRKs	G protein-activated inwardly rectifying potassium channels
Glut	Glutamate
GOTERM_BP	Gene ontology term: Biological Processes
GOTERM_CC	Gene ontology term: Cellular Components
GOTERM_MF	Gene ontology term: Molecular Functions
G-protein	Guanine nucleotide binding protein
Gαi/o	Guanine nucleotide binding protein, alpha subunit

HKG	Housekeeping gene
HMGB1	High-mobility group box 1
HS	Hippocampal sclerosis
HVA	High-voltage activated
ICAM-1	Intercellular adhesion molecule 1
IFN-γ	Interferon-gamma
IL-1R	Interleukin-1 type 1 receptor
IL-1β	Interleukin-1 beta
ILAE	International League Against Epilepsy
IP3R1	Inositol 1,4,5-trisphosphate receptor, type 1
IPSP	Inhibitory postsynaptic potential
IR	Near-infrared
KCNQ2	Potassium voltage-gated channel, KQT-like subfamily, member 2
KCNQ3	Potassium voltage-gated channel, subfamily Q, member 3
KCTD	Potassium channel tetramerization T1 domain- containing protein
KDa	kilo Dalton
KEGG	Kyoto Encyclopaedia of Genes and Genome pathways
Kir4.1	Inward rectifier K^+ channels
K_V	Voltage-gated potassium channels
Kv7.2	Potassium voltage-gated channel, subfamily Q, member 2
Kv7.3	Potassium voltage-gated channel, subfamily Q, member 3
LCS	Lacosamide
LEV	Levetiracetam
LMT	Lamotrigine
LOWESS	Locally weighted scatter plot smoothing
LTLE	Lateral temporal lobe epilepsy
MA	Microarray analysis
MA1	TLE-HS vs TLE-STG analysis
MA2	TLE-HS vs PMC analysis
MAPK	Mitogen-activated protein kinase
MeV	TM4 Multi-Experiment Viewer
MGB	Minor groove binder

mGluRs	Metabotropic glutamate receptors
ML	Molecular layer
MMPs	Matrix metalloproteinase
MRI	Magnetic resonance imaging
ms	Milliseconds
MTLE	Medial temporal lobe epilepsy
NA	Not available
Na$_V$	Voltage-gated sodium channels
NC	Nitrocellulose membrane
NeuN	Neuronal nuclei or RNA binding protein, fox-1 homolog
NFDM	Non-fat dry milk
NF-L	Neurofilament-Light
NFQ	Non-fluorescent quencher
NMDA	*N*-methyl-D-aspartate
OXC	Oxcarbazepine
PB	Phenobarbital
PBS	Phosphate buffered saline
PBST	Phosphate buffered saline with Tween 20
PCL	Pyramidal cell layer
PER	Perampanel
PGB	Pregabalin
PHT	Phenytoin
PIP$_2$	Phosphatidylinositol 4, 5-bisphosphate
PKA	Protein kinase A
PKC	Protein kinase C
PLC	Phospholipase C
PMC	*Post-mortem* control sample
PMI	*Post-mortem* Interval
PPIA	Peptidylprolyl isomerase A (cyclophilin A)
QC	Quality control
qRT-PCR	Quantitative real- time polymerase chain reaction
R^2	Linear regression

RP	Rank Product
SCN4B	Sodium channel, voltage-gated, type IV, beta subunit gene
SDS	Sodium dodecylsulphate
SDS-PAGE	Sodium dodecyl sulfate polyacrylamide gel electrophoresis
SE	Status epilepticus
SGK1	Serum/glucocorticoid regulated kinase 1
SGZ	Subgranular zone
SNARE	Soluble *N*-ethylmaleimide-sensitive factor attachment protein receptor
SSA	Succinic semi-aldehyde
SUDEP	Sudden unexpected death in epilepsy
SV2A	Synaptic vesicle glycoprotein 2A
SYNPR	Synaptoporin
TAE	Tris acetate EDTA buffer
TGB	Tiagabine
TLE	Temporal lobe epilepsy
TLE-HS	Temporal lobe epilepsy associated with hippocampus sclerosis
TLE-STG	Superior temporal gyrus from temporal lobe epilepsy
TLR	Toll-like receptor
TM	Transmembrane domain
TNFR1	Tumour necrosis factor receptor 1
TNF-α	Tumour necrosis factor alpha
TPM	Topiramate
VFTD	Venus flytrap domain
VGB	Vigabatrin
VGCCs	Voltage-gated calcium channels
VGKCs	Voltage-gated potassium channels
VGSCs	Voltage-gated sodium channels
VPA	Valproate
WB	Quantitative western blot
ZNS	Zonisamide
ΔRn	Sample fluorescence minus background fluorescence

Publications:

Manuscripts submitted:

M Sheilabi, D. Battacharyya, L. Caetano, J.S. Duncan, M.Thom, N.G. Bowery and A.P. Princivalle (**2016**). Quantitative expression and Localization of $GABA_{B1a}$, $GABA_{B1b}$ and $GABA_{B2}$ receptor subunits in hippocampi from temporal lobe epilepsy patients with hippocampal sclerosis. Submitted to *Epilepsia.*

Manuscripts in preparation:

1. **M.A. Sheilabi**, E. Sims, M. Hellewell, D. Bhattacharyya and A.P. Princivalle (**2016**). Hippocampal SCN4B expression in patients with temporal lobe epilepsy. To be submitted to *Epilepsia brief communication*.

2. **M.A. Sheilabi**, M. Salman, F. Falciani, D. Bhattacharyya, M. Conner and A.P. Princivalle (**2016**). Characterisation of AQPs and MAPK pathway in temporal lobe epilepsy patients with hippocampal sclerosis. To be submitted to *Glia*.

3. **M.A. Sheilabi**, D. Bhattacharyya, F. Falciani and A.P. Princivalle (**2016**). The up regulation of chemokines and cytokines in sclerotic hippocampi from temporal lobe epilepsy patients. To be submitted to *Journal of Neuroinflammation.*

Presented work:

Oral presentations:

1. The expression of $GABA_B$ receptor subunits in human TLE hippocampi (**2014**). *ILAE British Chapter annual Scientific meeting*, Nottingham.

2. Transcriptome analysis of sclerotic hippocampi from patients with refractory Temporal Lobe Epilepsy (**2015**). *ILAE British Chapter annual Scientific meeting*, London.

Posters:

1. **M.A. Sheilabi**, D. Bhattacharyya and A.P. Princivalle **(2013)**. Quantitative fluorescence western blot expression analysis Of GABA$_B$ receptors in human TLE hippocampi. *ILAE British Chapter annual scientific meeting*, Glasgow.

2. **M.A. Sheilabi**, D. Bhattacharyya and A.P. Princivalle **(2014)**. Quantitative fluorescence western blot expression analysis Of GABA$_B$ receptors in human TLE hippocampi. *Libya higher education forum,* London.

3. **M.A. Sheilabi**, D. Bhattacharyya and A.P. Princivalle **(2014)**. Characterisation of temporal lobe epilepsy biomarkers in human sclerotic hippocampi. *9th FENS Forum of Neuroscience FENS,* Milan.

4. **M.A. Sheilabi**, D. Bhattacharyya and A.P. Princivalle **(2014)**. The expression of GABA$_B$ receptor subunits in human TLE hippocampi. *ILAE British Chapter annual Scientific meeting*, Nottingham.

5. **M.A. Sheilabi**, D. Bhattacharyya and A.P. Princivalle **(2015)**. The expression of GABA$_B$ receptor subunits in human TLE hippocampi. *HWB faculty research day, Sheffield Hallam University.* **Awarded 1st Prize.**

6. **M.A. Sheilabi**, D. Bhattacharyya and A.P. Princivalle **(2015)**. Characterisation of temporal lobe epilepsy biomarkers in human sclerotic hippocampi. *HWB faculty research day, Sheffield Hallam University.*

7. **M.A. Sheilabi**, D. Bhattacharyya, F. Falciani and A.P. Princivalle **(2016)**. Transcriptome analysis of sclerotic hippocampi from patients with refractory temporal lobe epilepsy. *HWB faculty research day, Sheffield Hallam University.*

8. M. Salman, **M.A. Sheilabi**, F. Falciani, D. Bhattacharyya, M. Conner and A.P. Princivalle **(2016)**. The expression and trafficking profile of the aquaporin (AQP) water channels and potassium channel in the hippocampi of TLE patients. *HWB faculty research day, Sheffield Hallam University.*

Meetings and courses attended:

1. Training course on research ethics in studies with human participants, Sheffield Hallam University **(2012)**.

2. Sheffield epilepsy workshop, University of Sheffield **(2013)**.

3. "Researchers who teach" course, Sheffield Hallam University **(2013)**.

4. Yorkshire Immunology group symposium, University of Sheffield **(2013)**.

5. Oxford masterclass in epileptology: epilepsy genomics, Corpus Christi College, Oxford **(2015)**.

6. Sheffield Glial symposium, Sheffield institute for translational neuroscience **(2015)**.

7. MicroRNAs and Other Non-Coding RNAs Symposium, Sheffield institute for translational neuroscience **(2015)**.

Acknowledgments

1 General Introduction

1.1 Epilepsy

Epilepsy is a common neurological condition that is defined by a tendency to have recurrent unprovoked seizures. The International League Against Epilepsy (ILAE) defines epilepsy as *"Epilepsy is a disease of the brain defined by any of the following conditions: (1) At least two unprovoked (or reflex) seizures occurring >24 h apart. (2) One unprovoked (or reflex) seizure and a probability of further seizures similar to the general recurrence risk (at least 60%) after two unprovoked seizures, occurring over the next 10 years. (3) Diagnosis of an epilepsy syndrome"* (Fisher *et al.*, 2014).

Epilepsy affects about 0.8 % of the human population and its prevalence in the UK is estimated to be about 0.5 − 1 % of the population (Pitkänen and Sutula, 2002; Smithson and Walker, 2012; Rang *et al.*, 2014; Johnson *et al.*, 2015). According to Epilepsy Action; in the UK, 600,000 or one in every 103 people have epilepsy (www.epilepsy.org.uk).

An important concept that must be clarified is the difference between epilepsy and acute symptomatic seizures. In epilepsy the seizures are frequent and unprovoked while acute symptomatic seizures are triggered and provoked by a specific cause such as hypoglycaemia, fever or head injury. Epileptic seizures are brief with a sudden onset and normally are divided into phases; the pre-ictal, ictal, post-ictal and inter-ictal phases (Rang *et al.*, 2014). The epileptic seizure is caused by synchronised excessive discharge of action potentials or impulses from a group of neurons in the brain. This is due to abnormal neuronal firing from excitatory neurons, reduced inhibition or both.

2

The underlying mechanism of epileptic seizure is still poorly understood (Smithson and Walker, 2012; Rang *et al.*, 2014).

The prognosis of epilepsy depends upon many factors such as gender, age, genetic background and the cause of epilepsy. A study done on the population of Rochester, Minnesota, USA, found that the risk of developing epilepsy increased with age in both males and females. It also found that males had higher risk of developing epilepsy compared to females in the same age group (Hesdorffer *et al.*, 2011).

In addition to the fact that epilepsy has a significant negative effect on individuals' social lives, it has a high mortality rate due to accidents, suicides and sudden unexpected death in epilepsy (SUDEP) (Smithson and Walker, 2012).

1.2   Classification of epilepsy

The classification of epilepsy is difficult and complicated. However, it has been clinically classified into two broad categories partial and generalized seizures based on the origin of seizure in the brain, and the speed and distance over which it spreads. Some seizures start as partial then become generalized seizures as in tonic-clonic seizures (Berg and Scheffer, 2011; Smithson and Walker, 2012).

1.2.1   Partial or focal seizures

Partial seizures originate from a localized cortical area in the brain and they normally affect one hemisphere. They account for 60 % of all adult epilepsy cases. Partial seizures are further divided into:

- Simple partial seizures: they are brief, intense, stereotypical, and there is no loss of consciousness.

- Complex partial seizures: there is loss of consciousness in addition to confusion after the seizure.

- Secondary generalized seizures begin as partial and then spread to both hemispheres (Berg and Scheffer, 2011; Smithson and Walker, 2012; Téllez-Zenteno and Hernández-Ronquillo, 2012).

1.2.2 Generalized seizures

Generalized seizures originate from a local brain area, then they spread to both hemispheres and they normally affect the whole brain. The two most common types of generalized seizures are tonic- clonic seizure and absence seizures (Berg and Scheffer, 2011).

1.3 Temporal lobe epilepsy

Temporal lobe epilepsy (TLE) is one of the most common partial seizures as 60% of all partial seizures originate from the temporal lobe. TLE often starts as a simple partial seizure that extends to become a complex partial seizure (Smithson and Walker, 2012; Téllez-Zenteno and Hernández-Ronquillo, 2012). According to the ILAE (2010), TLE is classified into 3 main types:

1. Mesial temporal lobe epilepsy (MTLE): seizures start from amygdalohippocampal area (hippocampus, parahippocampal gyrus and amygdala).

4

2. Lateral temporal lobe epilepsy (LTLE): seizures start from the neocortex lateral to the temporal area.

3. Mesial temporal lobe epilepsy with hippocampal sclerosis (MTLE-HS): it is one of the most common types of epilepsy referred to surgery and it is often refractory to antiepileptic drugs (Blümcke *et al.*, 2012; Téllez-Zenteno and Hernández-Ronquillo, 2012).

The common symptoms in TLE include motor arrest followed typically by chewing, lip smacking and swallowing, fiddling with the hands, illusions, auditory hallucinations and complex visual hallucinations (Smithson and Walker, 2012).

1.4 Temporal lobe epilepsy pathogenesis

In most patients with symptomatic TLE, the epileptic process includes three phases: the epileptogenic lesion, the latent period and the development of seizures and epilepsy as in figure 1.1. In the **epileptogenic lesion** phase there is an identifiable brain-damaging insult that is thought to underlie the cause of seizures. This brain injury could be a brain infection, a stroke, a head trauma or *status epilepticus* (SE). SE is a life threatening condition characterized by a continuous seizure activity without recovery of consciousness (Pitkänen and Sutula, 2002; Kuruba *et al.*, 2009).

Following the epileptogenic lesion comes the **latent period** where there are no seizures. The epileptogenesis process starts when the epileptogenic lesion triggers a cascade of neurobiological events leading to the development of spontaneous seizures and the diagnosis of epilepsy. After the diagnosis of epilepsy patients are treated with antiepileptic drugs (Pitkänen and Sutula, 2002; Kuruba *et al.*, 2009).
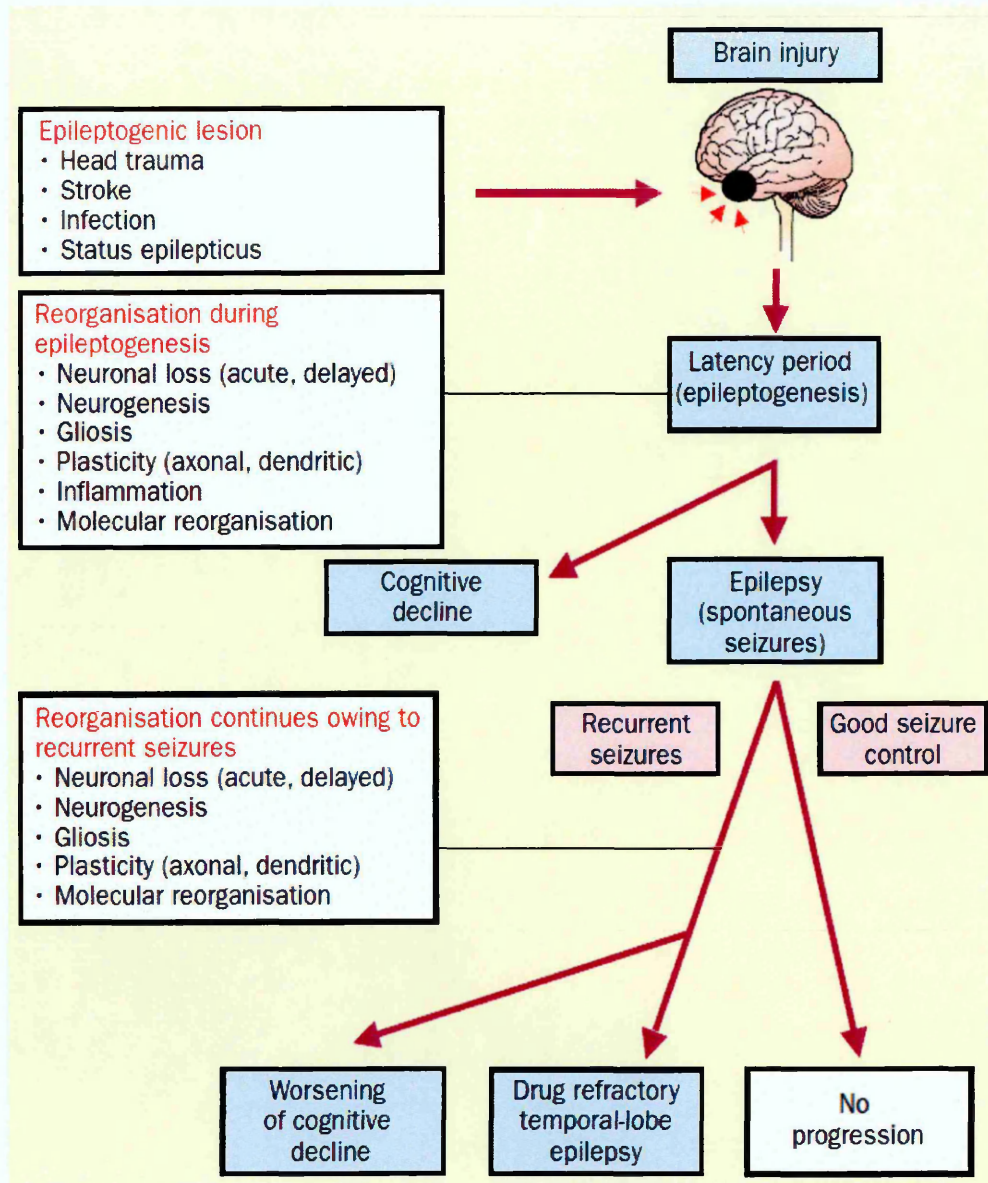
Figure 1.1 TLE pathogenesis

TLE pathogenesis includes an epileptogenic lesion, latent period and development of spontaneous seizures. Adapted from Pitkänen and Sutula (2002).

1.5   Temporal lobe epilepsy drug treatment

1.5.1   Neuronal action potential:

Epileptic seizures are caused by excessive discharge of action potentials. Therefore to treat epileptic seizures, it is vital to understand what a neuronal action potential is and

how it is generated. An action potential is a pulse of electrical activity which is very important in neuronal communication. It starts at the axon initial segment then propagates along the axon to the nerve terminal. At the nerve terminal it activates voltage-gated calcium channels, which play a major role in the release of synaptic vesicles containing neurotransmitters into the synapse (Lai and Jan, 2006).

Normally at **resting potential** - 70 mV there are: high extracellular sodium ion (Na^+) concentration and high intracellular potassium ion (K^+) concentration, which is maintained by Na^+/K^+ ATPase activity. At this stage both voltage-gated Na^+ and K^+ channels are closed as in figure 1.2. When a stimulus is strong enough to reach the threshold (- 50 mV), it opens the voltage-gated sodium channels (Na_V) allowing the influx of Na^+ inside the cell. This results in membrane **depolarization**. The sodium ions will continue flowing into the cell until the membrane potential reaches +40 mV. Then the Na_V channels become inactive and the voltage-gated potassium channels (K_V) open allowing the flux of K^+ ions outside the cell. This results in the membrane repolarisation and leading to **hyperpolarisation**. The hyperpolarisation stage is also known as refractory period (Na channels are inactive) where the cell can not fire another action potential. Then the Na^+/K^+ ATPase will help in returning the membrane to its resting potential and Na_V channels will return to their closed position (Namadurai *et al.*, 2015)
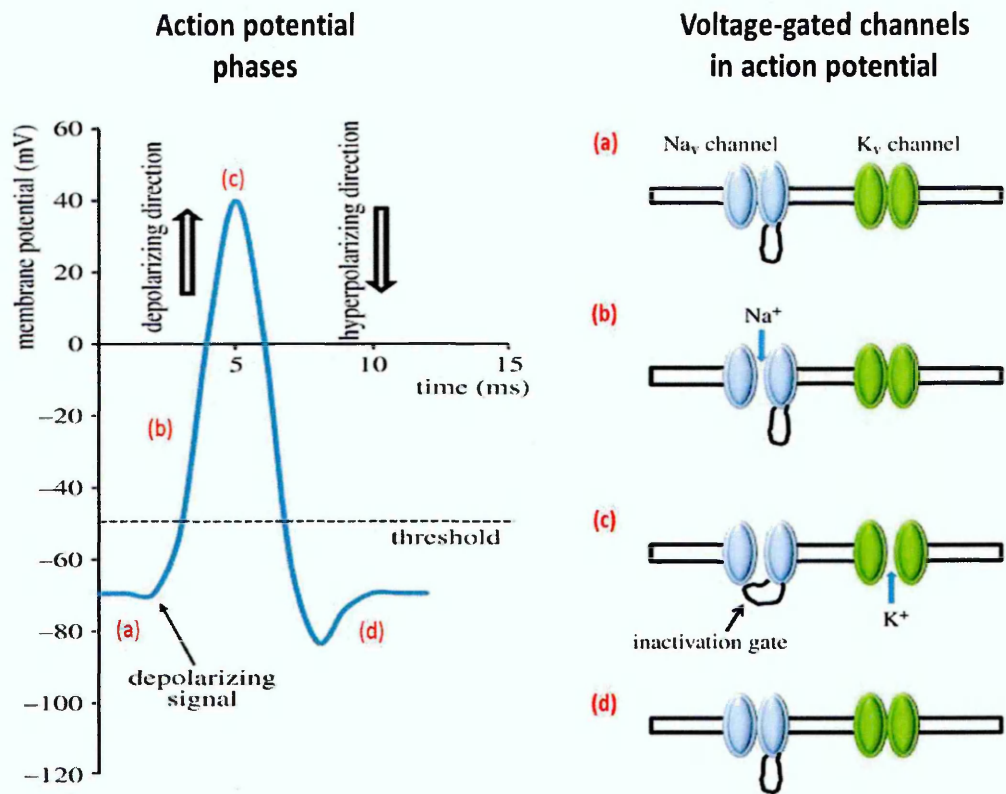
Figure 1.2 Schematic presentation of the main events in a neuronal action potential

The neuronal action potential phases include: **(a)** Resting potential, where both Na_V and K_V channels are closed. **(b)** Depolarization following a stimuli, where Na_V channels open causing the influx of Na^+ in the cell. **(c)** Repolarisation, where Na_V channels become inactive and K_V channels open allowing the flux of K^+ ions. **(d)** Return to resting potential after hyperpolarisation, Na_V channels change into their closed conformation. Adapted from Namadurai *et al.* (2015).

1.5.2 Antiepileptic drugs (AEDs)

The purpose of giving antiepileptic drugs (AEDs) is to reduce the synchronised excessive discharge of impulses firing from the neurons during seizures without affecting the normal non-epileptic impulses. This is achieved by acting on one or many molecular targets such as ion channels, neurotransmitter transporters and metabolic enzymes at the same time (Rogawski and Löscher, 2004).   The AEDs available on the market today work with a diverse mechanism of actions that can be summarised as:

- Modulation of voltage-gated ion channels such as voltage-gated sodium, potassium and calcium channels.

- Enhancement of synaptic inhibition: drugs act on γ-amino butyric acid (GABA) receptors (the main inhibitory neurotransmitter in the brain).

- Inhibition of synaptic excitation: drugs that block glutamate receptors (excitatory neurotransmitter).

1.5.2.1 Voltage-gated sodium channel modulators

The voltage-gated sodium channels (VGSCs) are responsible for the depolarisation phase in the neuronal action potential. They are composed of a main α-subunit and two auxiliary β subunits as in figure 1.3 (Namadurai *et al.*, 2015). There are four β subunits β1 - β4, that play an important role in modifying voltage dependence and gating kinetics of VGSC (Cannon and Bean, 2010; Catterall *et al.*, 2010). The presence of β subunits with sodium channel α subunits accelerates the activation and inactivation rate of the channel. While, β1 and β3 favour the Na^+ channel inactivation, the β4 subunit favours Na^+ channel activation and makes neurons more susceptible to excitation (Yu *et al.*, 2003).

9
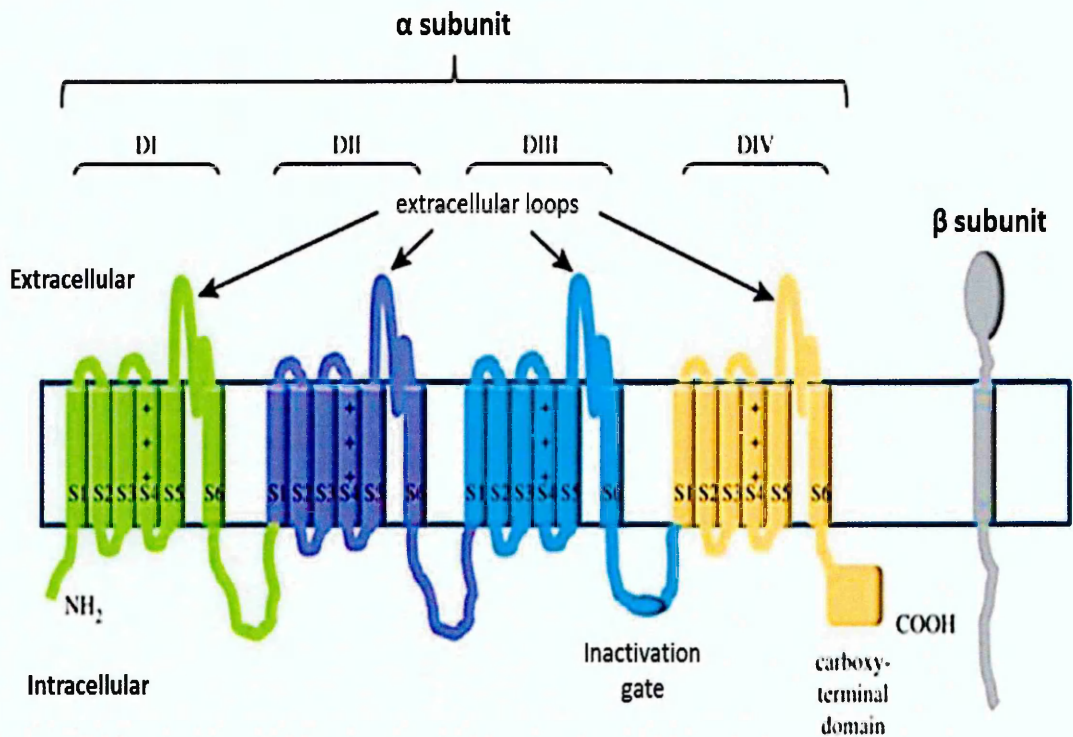
Figure 1.3 Schematic diagram of voltage-gated sodium channel subunits

VGSCs are composed of a main α subunit associated with two auxiliary β subunits (β1-β4). The α subunit consists of 4 homologous domains (I, II, III and IV) and each domain has 6 transmembrane segments (S1-S6). The pore of the channel is formed by **S5** and **S6** from each domain and the channel's voltage sensor segment is **S4**. The fast inactivation gate that closes the channel in a hinge-like mechanism located between DIII and DIV. Sodium channel modulating drugs such as lamotrigine stabilizes the inactive form by binding to S6 in domain III and IV. Adapted from Yarov-Yarovoy *et al.* (2001) and Namadurai *et al.* (2015).

The VGSCs undergo three conformational changes (closed, open and inactive forms) within milliseconds (ms) range during the action potential. In the depolarisation phase the sodium channels change from closed state to the open conducting state. The channels then change to the inactive form and when repolarisation is reached the channel changes back to the resting closed state (Kuo and Bean, 1994; Cannon and Bean, 2010).

The sodium channel inactivation process is very important as it determines the frequency of action potential firing. There are two main types of inactivation, fast and slow. The fast inactivation occurs via the inactivation particle which is a short loop of amino acid residues between α subunit domain III and IV. It occludes the channel like a hinged lid. The slower inactivation is associated with the pathological prolonged depolarization such as seen in epileptic activity. The channel pore undergoes molecular rearrangement to stop the sodium flux (Goldin, 2003).

As mentioned previously the voltage-gated sodium channels are responsible for the depolarization phase in the action potential. Thus, voltage-gated sodium channel blockers protect against seizures by inactivating sodium channels and subsequently blocking the depolarization in the high-frequency repetitive action potential (which happens during the spread of the seizure). On the other hand, they do not interfere in the physiological generation of action potentials; as they bind slowly to sodium channels and will only affect the long pathological depolarization events that are associated with the epileptic activity. Examples of AEDs that stabilize fast inactivation state of VGSCs are: phenytoin, carbamazepine, lamotrigine, oxcarbazepine and rufinamide (Rogawski and Löscher, 2004; Brodie *et al.*, 2011). A recently developed

AEDs, lacosamide and eslicarbazepine acetate, act via selective enhancement of the slow inactivation state of VGSCs (Perucca *et al.*, 2008; Park *et al.*, 2013).

1.5.2.2 Voltage-gated potassium channel modulators

The voltage-gated potassium (K^+) channels (VGKCs) are responsible for the repolarization phase in the neuronal action potential and thus they stabilize the membrane potential by controlling the neuronal excitability. The M-type potassium channels are low-threshold voltage-gated channels that are widely distributed in the central and peripheral neurons including hippocampal and cortical pyramidal cells. They are heterotetramers composed of 4 α subunits; two Kv7.2 subunits and two Kv7.3 subunits that are products of *KCNQ2* and *KCNQ3* genes respectively as in figure 1.4. (Telezhkin *et al.*, 2012).

Many studies found that mutations in *KCNQ2* and *KCNQ3* genes caused a familial neonatal convulsion which is a form of congenital epilepsy (Tatulian *et al.*, 2001) and thus came the idea behind developing an anti-epileptic drug that enhances the M channel activity. Accordingly retigabine, an anticonvulsant drug, was developed; it activates Kv7.2 and Kv7.3 and enhances the opening of the M type potassium channel causing hyperpolarization of the membrane and longer refractory period that reduces the number of firing action potentials (Wickenden *et al.*, 2000; Tatulian *et al.*, 2001).
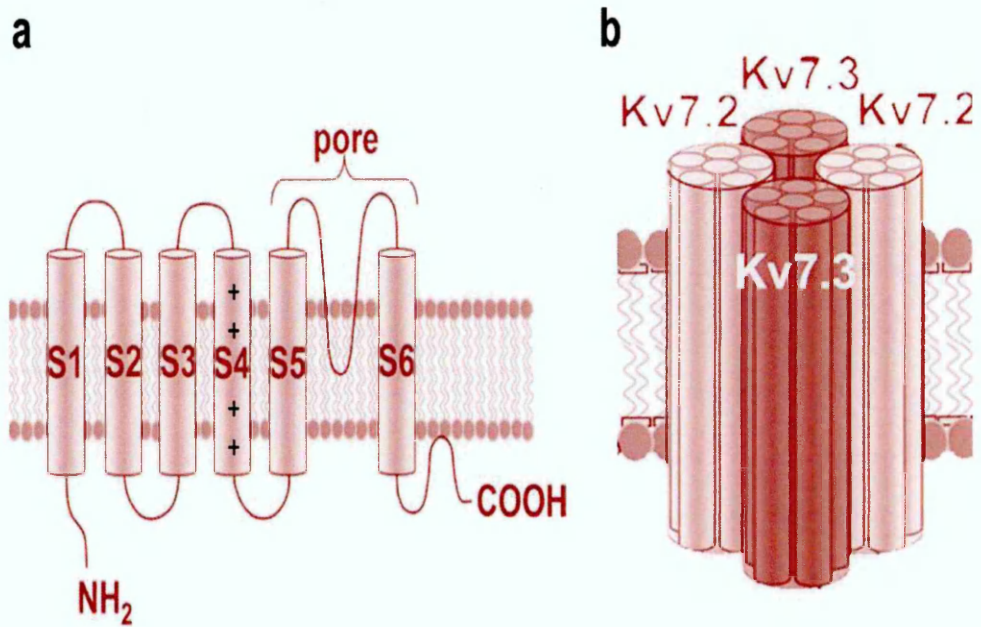
Figure 1.4 Schematic diagram of voltage-gated M-type potassium channel

M-type potassium channel is composed of 4 α subunits, **(a)** each α subunit consists of 6 transmembrane domains (S1-S6). S4 is the voltage-sensing domain. S5 and S6 are the pore-forming domains. **(b)** M-type potassium channel is composed of two Kv7.2 and two Kv7.3 subunits that are arranged in an alternative manner. Adapted from Telezhkin *et al.* (2012).

1.5.2.3 Calcium channel modulators

There are two broad groups of voltage-gated calcium channels: the high-voltage activated (HVA) calcium channels (P/Q type) and the low-voltage activated calcium channels (T type). The HVA calcium channels are a potential AED target as they regulate the neurotransmitter release from presynaptic nerve terminals. AEDs such as gabapentin and pregabalin act in part by blocking HVA calcium channels (Rogawski and Löscher, 2004; Bialer and White, 2010).

The low-voltage activated calcium channels regulate neuronal firing. AED ethosuximide blocks the T-type calcium channels in the thalamic neurons and it is effective in the treatment of absence seizures (Rogawski and Löscher, 2004).

1.5.2.4 GABA mediated AEDs

Most of the broad spectrum antiepileptic drugs act by mechanisms that influence GABA, which is the main inhibitory neurotransmitter in the brain. GABA acts on two types of receptors: $GABA_A$ receptors are ligand-gated chloride channels (ionotropic receptors) and $GABA_B$ receptors are G-protein- coupled metabotropic receptors (Jacob *et al.*, 2008).

$GABA_A$ receptor

GABA causes a fast post synaptic inhibition upon its binding to $GABA_A$ receptor. It opens the chloride channel allowing the Cl^- anion influx. This will result in a hyperpolarized membrane potential that stops the firing of the next action potential. The $GABA_A$ receptor is composed of 5 subunits (2α, 2β and γ) that are assembled to from a chloride channel. Each subunit is composed of 4 transmembrane domains

(TM1-TM4); TM2 domain forms the chloride channel pore. The ligand binding site is at the large N-terminal extracellular domain as in figure 1.5 (Jacob *et al.*, 2008).

GABA$_B$ receptors

GABA$_B$ receptors are G-protein coupled receptors that are responsible for the slow synaptic inhibition and prolonging inhibitory postsynaptic potentials (IPSP) (Benarroch, 2012). It was found that mice which are lacking functional GABA$_B$ receptors developed epileptic activity and spontaneous seizures supporting the inhibitory role of GABA$_B$ (Schuler *et al.*, 2001).

GABA$_B$ receptors are present on both the pre- and postsynaptic membranes in the neuronal synapses. The activation of presynaptic GABA$_B$ receptor inhibits the release of GABA by the inhibition of voltage-gated Ca^{2+} channels. The activation of postsynaptic GABA$_B$ receptor activates the K^+ channels causing hyperpolarisation and prolonged IPSP (Benarroch, 2012).

Drugs acting on GABAergic system

The AEDs that enhance GABA inhibition either act as GABA agonists or inhibitors of GABA transaminase enzyme and GABA transporters to increase GABA levels in the synaptic cleft. **Barbiturates** and **benzodiazepines** are GABA agonists that bind to allosteric sites in GABA$_A$ receptor potentiating the effect of GABA. While, the barbiturates prolong the channel opening time; the benzodiazepines increase the number of channels opening resulting in more hyperpolarized membrane potential. The barbiturates also act on sodium and calcium ion channels (Rogawski and Löscher, 2004; Johnston, 2005).
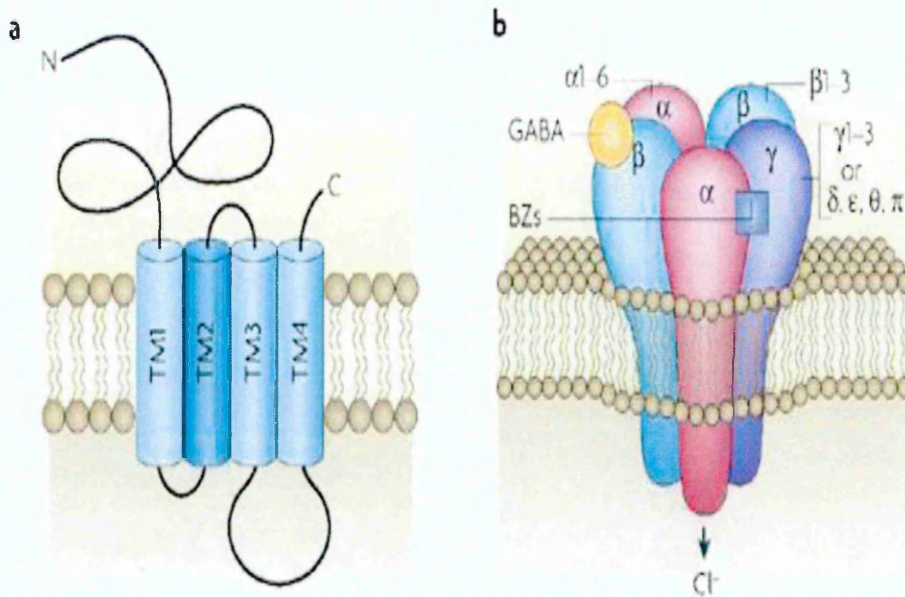
Figure 1.5 Ligand-gated GABA$_A$ receptor structure

(a) The four transmembrane domains (TM1-4) of a single GABA$_A$ subunit. TM2 domains line the chloride channel pore. The large N-terminal extracellular domain is the site for binding neurotransmitters and AEDs such as benzodiazepines (BZs). **(b)** GABA$_A$ receptor is composed of five subunits to from a heteropentameric chloride channel. The most common type of GABA$_A$ receptor found in the brain consists of 2α, 2β, and 1γ subunits. Adapted from Jacob *et al.* (2008).

The AED **vigabatrin** increases GABA levels via inhibition of GABA degradation. It irreversibly inhibits GABA transaminase enzyme (GABAT) that is responsible for converting GABA to succinic semi-aldehyde (SSA) as in figure 1.6. **Tiagabine** increases GABA concentration by inhibiting its reuptake by neurons and astrocytes. It is a potent selective inhibitor of GABA transporter 1 (GAT1), which is the most abundant GABA transporter that reuptakes GABA and terminates its action. Tiagabine binds to GAT1 with high affinity slowing the reuptake of GABA. Therefore, it prolongs the inhibitory postsynaptic potential (Sills *et al.*, 1999; Brodie *et al.*, 2011; Besag and Patsalos, 2012).

It was found that **gabapentin** and **pregabalin** also have a GABA-mediated action. It is thought that gabapentin and pregabalin increase cellular GABA levels by enhancing GABA transporter GAT1 (Whitworth and Quick, 2001; Errante *et al.*, 2002; Sills, 2006). In addition, valproate also increases GABA synthesis and turnover (Rogawski and Löscher, 2004).
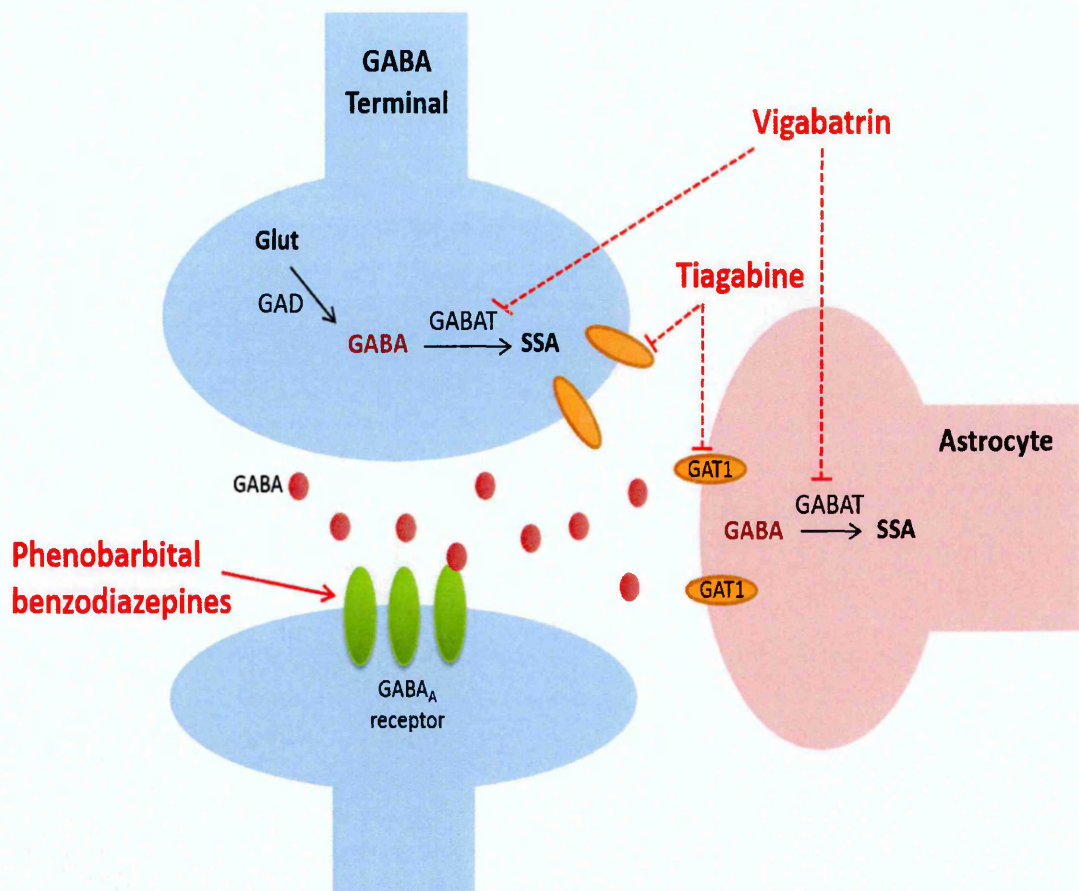
Figure 1.6 GABA-mediated antiepileptic drugs

In the presynaptic terminal GABA is synthesized from Glutamate (**Glu**) by glutamate decarboxylase (**GAD**). GABA is released in the synapse where it acts on the postsynaptic $GABA_A$ receptor. The action of GABA is terminated by its reuptake by GABA transporter 1 (**GAT1**) into presynaptic neurons and astrocytes; where it is degraded into succinic semi-aldehyde (**SSA**) by the GABA transaminase (**GABAT**). GABA-mediated AEDs: **phenobarbital and benzodiazepines** are allosteric $GABA_A$ receptor agonists. **Tiagabine** inhibits GABA reuptake by selective inhibition of GAT1 and **Vigabatrin** inhibits GABA degradation by irreversible inhibition of GABAT. Adapted from Rogawski and Löscher (2004).

1.5.2.5 Inhibitors of synaptic excitation

Glutamate is the main excitatory neurotransmitter that mediates most of the fast excitatory neurotransmission in the brain. There are 3 families of ionotropic glutamate receptors: N-methyl-D-aspartate (NMDA), α-amino-3-hydroxy-5-methyl-4-isoxazolepropionic acid receptor (AMPA) and kainate receptors. In epilepsy there is an over excitation state, theoretically glutamate receptor blockers make ideal drugs in treatment of TLE (Rogawski and Löscher, 2004). However, the results of preclinical and clinical trials of selective NMDA antagonists were disappointing and so far there are no marketed AEDs that act predominantly on the NMDA receptors (Rogawski, 2011; Besag and Patsalos, 2012). Nevertheless, some of the available AEDs do act partly on glutamate receptors such as: **felbamate** that acts partly by blocking NMDA receptors (Kuo *et al.*, 2004) and **topiramate** that acts partly by blocking kainate and AMPA receptors (Gryder and Rogawski, 2003).

Recently a new AED perampanel was introduced to the market for treatment of partial seizures that significantly reduced seizure frequencies in patients. Perampanel acts as a highly selective non-competitive AMPA antagonist that was well tolerated in epilepsy patients (Besag and Patsalos, 2012; Trinka *et al.*, 2016).

1.5.2.6 Synaptic vesicle modulators

Synaptic vesicles play a major role in regulating neurotransmitter release. They are responsible for neurotransmitter exocytosis and endocytosis and therefore are very important in regulating the efficiency of synaptic transmission (Casillas-Espinosa *et al.*, 2012).

The synaptic vesicle glycoprotein 2A (SV2A), found in presynaptic terminals in neurons, has a regulatory role in synaptic vesicle exocytosis and calcium-dependent neurotransmitter release. SV2A down regulation was reported in both animal models and refractory TLE patients. Its dysfunction was associated with increased neurotransmitter via the presynaptic calcium accumulation (Bialer and White, 2010; Sills, 2010).

It was found that there is strong correlation between the binding affinity to SV2A and anticonvulsant potency of AEDs in animal models. The AED levetiracetam binds to SV2A with high affinity, inhibiting the recycling of SV2A neurotransmitter vesicles and thus decreasing the vesicular release. In addition, levetiracetam also blocks the HVA calcium channels (Rogawski and Löscher, 2004; Bialer and White, 2010).

Brivaracetam is a selective SV2A ligand that binds to SV2A with high affinity. It is about 6 to 12 times more potent and has more rapid brain penetration compared to levetiracetam. The preclinical trials suggest that it may provide an effective treatment for refractory epilepsy (Bialer and White, 2010; Klitgaard et al., 2016). Brivaracetam is one of the newest AEDs to be approved for treatment of epilepsy (Zaccara, 2016).

The presynaptic vesicle protein synaptoporin (SYNPR) is highly expressed in adult hippocampus and it plays a vital role in regulating synaptic transmission in both physiological and pathological conditions (Singec et al., 2002; Sun et al., 2006).

Neurotransmitter release via presynaptic vesicle proteins such as S2VA and SYNPR is a calcium dependent process that is affected by intracellular Ca^{2+} level (Chen et al., 1996; Matsumoto and Nagata, 1999). Inositol 1, 4, 5-trisphosphate receptor 1 (IP3R1)

is one of the main IP3 receptors in neurons that is found on the endoplasmic reticulum. IP3R1 regulates intracellular Ca^{2+} levels, neuronal excitability and neurotransmitter release (Nicolay et al., 2007).

1.5.2.7   AEDs that act on multiple targets

The mechanism of action of some AEDs is not fully understood and some others are complex and acting on many targets such as valproate, felbamate, topiramate, zonisamide and acetazolamide. **Valproate** is thought to block HVA calcium channels, fast and slow voltage-gated sodium channels in addition to its role in increasing GABA turnover (Rogawski and Löscher, 2004). **Felbamate** multiple mechanisms of action include possible actions on both GABA and NMDA receptors in addition to its actions on fast VGSCs and HVA calcium channels. **Topiramate** acts as sodium channel and kainate/AMPA receptor blocker, it enhances GABAergic transmission and inhibits carbonic anhydrase. **Zonisamide** anticonvulsant activity is thought to act mainly by blocking of VGSCs and HVA calcium channels (Rogawski and Löscher, 2004; Baulac and Leppik, 2007; Besag and Patsalos, 2012).

1.5.2.8 Summary of antiepileptic drugs

The main issue with the present AEDs, summarized in table 1.1, is that they only treat the symptoms and do not reverse or stop the progression of epilepsy (Brodie *et al.*, 2011). Therefore, the ultimate goal of epilepsy treatment should be to prevent and reverse the progression of epilepsy. In order to achieve that, understanding the epileptogenic process that underlines the mechanism of enhanced seizure susceptibility, is vital to develop anti-epileptogenic drugs. Those drugs will inhibit and stop the process of epileptogenesis. In addition, AEDs are only effective in controlling seizures in about 70 % of TLE patients and the remaining 30 % of patients are refractory to AEDs. For these patients, the uncontrolled recurrent seizures contribute to the severity of TLE as well as the deterioration of the patient's cognitive functions (Pitkänen and Sutula, 2002).

Table 1.1 Summary of antiepileptic drugs and their targets

AEDs target and mechanism of action	AEDs
1. Sodium channel actions	
• Blockade by stabilizing fast-inactivated state	Phenytoin, carbamazepine, lamotrigine, oxcarbazepine, rufinamide.
• Blockade by stabilizing slow-inactivated state	Lacosamide, eslicarbazepine
2. Potassium channel actions	
• Opens Kv7 potassium channels	Retigabine
3. Calcium channel actions	
• Blockade of high voltage-activated channel (P/Q type)	Gabapentin, pregabalin
• Blockade of low voltage-activated channel (T type)	Ethosuximide
4. GABA-mediated actions	
• GABA$_A$ receptor agonists	Phenobarbital Benzodiazepines
• Blockade of GABA transporter GAT1	Tiagabine
• Inhibition of GABA transaminase	Vigabatrin
5. AMPA receptor action	
• selective AMPA receptor antagonist	Perampanel
6. Synaptic vesicle protein 2A actions	
• Modulation of SV2A	Levetiracetam, brivaracetam
7. Multiple actions	
• Various actions on multiple targets	Valproate, felbamate, topiramate, zonisamide,

Adapted from (Brodie *et al.*, 2011)

1.6 Pathogenesis of refractory temporal lobe epilepsy associated with hippocampal sclerosis (TLE-HS)

According to ILAE drug resistant or refractory epilepsy is defined as "failure *of adequate trials of two tolerated, appropriately chosen and used antiepileptic drug schedules (whether as monotherapies or in combination) to achieve sustained seizure freedom"* (Kwan *et al.*, 2010).

Since the 19th century epilepsy has been associated with brain damage and hippocampal sclerosis especially the drug refractory TLE. About 30% of epilepsy patients are drug resistant and the majority of those patients have hippocampal sclerosis (Blümcke *et al.*, 2012). Hippocampal sclerosis is a lesion characterised by neuronal loss in the main *cornu ammonis* (CA) CA1 - CA4 and the dentate gyrus regions of the hippocampus as in figure 1.7 (Pitkänen and Sutula, 2002; Coras and Blümcke, 2015).

In refractory TLE associated with hippocampal sclerosis (TLE-HS), there is continuous seizure-induced plasticity in neural circuits as part of the epileptogenic process. There is also a continuous seizure-induced neuronal loss, neurogenesis, axonal and dendritic plasticity, gliosis and molecular reorganization (Pitkänen and Sutula, 2002; Coras and Blümcke, 2015).
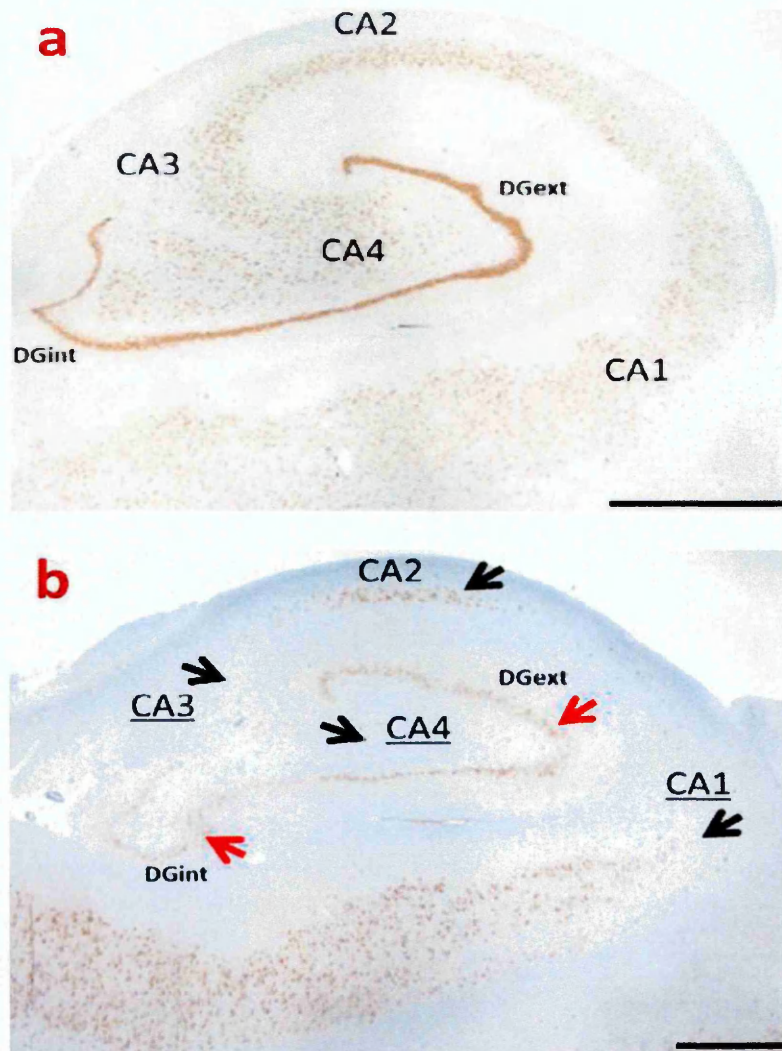
Figure 1.7 Hippocampal sclerosis in TLE-HS

(a) The anatomically normal hippocampus showing the staining of pyramidal neurons in *cornu ammonis* (CA) CA1 - CA4 subregions. It also shows the staining of granular neurons in external and internal limbs of dentate gyrus (DGext, DGint). (b) Sclerotic hippocampus from TLE patient showing the significant neuronal loss in the pyramidal neurons of CA1 - CA4 areas (indicated by black arrows). In addition, it shows the significant neuronal density reduction and dispersion in both external and internal DG hippocampal areas (indicated by red arrows). NeuN immunohistochemistry with hematoxylin counterstaining using 4 µm thin paraffin embedded sections. CA: *cornu ammonis*. DGext: External limb of dentate gyrus. DGint: Internal limb of dentate gyrus. Scale bar = 2000 µm. Adapted from Coras and Blümcke (2015).

1.6.1   Neuronal loss and damage in TLE-HS

Many histological studies have been undertaken on brain tissue resected from TLE patients undergoing surgical treatment. These studies indicated the association of recurrent seizures and long duration of epilepsy with the severity of neuronal loss in different hippocampal subregions (Mathern *et al.*, 1995; Yilmazer-Hanke *et al.*, 2000; Pitkänen and Sutula, 2002). According to Mathern *et al.* (1995) the type of neuronal damage in TLE depends on age of the patient at the initial epileptogenic lesion and the age of developing epilepsy. The hippocampal damage was greater in patients where the initial epileptogenic lesion occurred in childhood.

Many animal model experiments were performed to assess the effect of seizure on hippocampal neuronal loss. Those studies showed that hippocampal neuronal loss was induced by brief seizures and as the number of seizures increased, the neuronal loss also increased in a pattern similar to hippocampal sclerosis seen in TLE patients (Cavazos and Sutula, 1990; Cavazos *et al.*, 1994). It was suggested that the primary cause of seizure-induced neuronal death is glutamate excitotoxicity. The over-activation of the glutamate gated ion channels leads to the neurons being flooded with sodium and calcium ions. This leads to the neurone swelling and membrane rupture. Some animal studies showed that the administration of glutamate receptor-blocker (such as NMDA antagonists) had a neuroprotective effect. They reduced the hippocampus damage after *status epilepticus* but the rats still developed epilepsy later due to the disruption of normal brain function (Engel and Henshall, 2009).

The neuronal loss in TLE-HS is caused by cellular mechanisms such as apoptosis (Xu *et al.*, 2007). Many studies indicated that the seizure-induced neuronal death may involve

26

the activation of apoptosis, probably the intrinsic pathway. The intrinsic pathway is activated by internal changes within a cell such as DNA damage and calcium overload. Studies on the human hippocampi obtained from patients with refractory TLE, found an alteration in expression of Bcl-2 (pro-apoptotic) and caspase family genes. There was evidence of up-regulation of anti-apoptotic genes (Bcl-2, Bcl-xL and Bcl-w) as well as pro-caspases genes (2, 6, 7, 8 and 9) in TLE patients. This indicated that apoptosis seem to be contributing to the neuronal loss seen in TLE-HS (Henshall *et al.*, 2000; Engel and Henshall, 2009; Thompson *et al.*, 2011).

Neuroinflammation mediated by the pleiotropic cytokine tumour necrosis factor alpha (TNF-α), also has a role in seizure-induced neuronal loss and damage. Data from both animal and human studies showed that seizures induce TNF-α that activates TNF receptor 1 (TNFR1). The prolonged activation of TNFR1 (that contains a death domain) will activate apoptosis via caspase 8 (Thompson *et al.*, 2011). In addition, Fas-mediated neuronal loss was also reported in resected sclerotic hippocampi obtained from TLE patients. This further implicates the role of extrinsic apoptotic pathway in TLE-HS neuronal loss (Xu *et al.*, 2007).

1.6.2   Gliosis in TLE-HS

In the sclerotic hippocampus there is a prominent proliferation of glial cells such as astrocytes, microglia, and oligodendrocytes. Alterations in glial cell functions such as growth-factor production, pH regulation and transmitter uptake may play a major role in hippocampal circuit excitability and seizure susceptibility (Pitkänen and Sutula, 2002; Lee *et al.*, 2004; Verkhratsky *et al.* 2013; Steinhäuser *et al.*, 2016).

1.6.2.1 Role of astrocytes in TLE-HS

TLE-HS is characterized by reactive astrogliosis (Lee *et al.*, 2004; Verkhratsky *et al.* 2013; Steinhäuser *et al.*, 2016). Astrocytes are important in maintaining brain physiological function. They maintain extracellular K^+ homeostasis by K^+ uptake and spatial buffering. The control of K^+ homeostasis is very important for maintaining normal brain function as high extracellular K^+ concentrations can cause a significant increase in neuronal excitability (Steinhäuser *et al.*, 2016).

Unlike normal neuronal activity, where there is a transient increase in K^+ concentration, in epilepsy there is an excessive accumulation of extracellular K^+ concentration that is cleared by the astrocytic inward rectifier K^+ channels (Kir4.1). However in epileptic tissue from TLE-HS patients; there is a down-regulation in astrocytic Kir4.1 channels. This causes an impaired K^+ buffering and contributes to increased seizure susceptibility in TLE-HS (Lee *et al.*, 2004; Binder *et al.*, 2012; Heuser *et al.*, 2012). In addition, the down regulation of perivascular aquaporin 4 (AQP4) in TLE-HS is accompanied by impaired extracellular K^+ homeostasis that caused prolonged and aggravated epileptic seizures (Eid *et al.*, 2005).

Astrocytes also play a critical role in maintaining extracellular glutamate levels. High level of extracellular glutamate causes glutamate neurotoxicity and increased seizure susceptibility. At excitatory terminals, astrocytes are responsible for glutamate reuptake via the excitatory amino acid transporters (EAAT) EAAT1-EAAT2. Therefore, they reduce extracellular glutamate levels and limit activation of extrasynaptic glutamate receptors. Serum- and glucocorticoid-inducible kinase-1 (SGK1) up-regulates glutamate EAAT transporters in astrocytes and induces the clearance of accumulated

glutamate in the synaptic space (Rothstein *et al.*, 1996; Boehmer *et al.*, 2006). The glutamate in astrocytes is converted into glutamine by glutamine synthetase enzyme. The glutamine is taken up by neurons and used as a precursor for the synthesis of both glutamate and GABA (Steinhäuser *et al.*, 2016).

In sclerotic hippocampi obtained from TLE patients, there were high levels of extracellular glutamate (Cavus *et al.*, 2005). This was accompanied with the down regulation of EAAT-1 and EAAT-2 glutamate transporters (Proper *et al.*, 2002; Sarac *et al.*, 2009) and astrocytic glutamine synthetase (Eid *et al.*, 2004; van der Hel *et al.*, 2005). In addition, there is an up-regulation of ionotropic and metabotropic glutamate receptors in astrocytes from epileptic tissues that contribute to increased seizure susceptibility (Verkhratsky *et al.* 2013; Steinhäuser *et al.*, 2016). Therefore, reactive astrogliosis seen in TLE-HS appears to play a vital role in epileptogenesis and pathophysiology of TLE-HS (Steinhäuser *et al.*, 2016).

1.6.2.2 Role of activated microglia in TLE-HS

One of the characteristics of TLE-HS epilepsy is microglia activation (Kang *et al.*, 2006; Shapiro *et al.*, 2008; Yeo *et al.*, 2011; Xu *et al.*, 2015; Abiega *et al.*, 2016). Microglia are the main immune cells in the CNS that play a central role in mediating immune responses and maintaining homeostasis (Xu *et al.*, 2015). Activated microglia have a phagocytic function, they engulf and degrade apoptotic cells and damaged cell debris. It They also have the ability to release inflammatory mediators such as interleukin-1 beta (IL-1β) and TNF-α as well as matrix metalloproteinases (Felderhoff-Mueser *et al.*, 2005; Xu *et al* 2015; Abiega *et al.*, 2016).

In patients with intractable epilepsy, there is a significant elevation in the number of activated microglia in the epileptogenic tissue indicating neuroinflammation (Choi *et al.*, 2009). Following SE in animal models, rapid microglial activation in the hippocampus preceded the SE-induced neuronal damage, suggesting a possible role in the epileptogenesis process (Kang *et al.*, 2006; Shapiro *et al.*, 2008).

In physiological conditions there is coupling between apoptosis and phagocytosis in the hippocampus. In TLE there is an increase in the number of apoptotic cells that need to be phagocytosed by microglia. A recent study that investigated the role of microglia phagocytic ability in human and experimental TLE found that the activated microglia had an impaired phagocytic function that caused uncoupling between apoptosis and phagocytosis. It also found that the loss of coupling was correlated to high expression of pro-inflammatory cytokines such as IL-1β in the epileptogenic tissue (Abiega *et al.*, 2016). Therefore, microglial activation seems to plays a vital role in TLE epileptogenesis (Kang *et al.*, 2006; Abiega *et al.*, 2016).

In summary, gliosis in TLE-HS is involved in the TLE epileptogenic process and developing drugs that target activated microglia or reactive astrocytes in early stages of epilepsy could have an anti-epileptogenic effect.

1.6.3   Mossy fibre sprouting in TLE-HS

The mossy fibres are the axons of the granule cells in the dentate gyrus (DG). They project through the dentate hilus (DH) to CA3, where they make synaptic contacts with hilar and CA3 pyramidal cells. Normally the majority of mossy fibres project towards the inhibitory GABAergic interneurons rather than the excitatory cells (Frotscher *et al.*, 2006).

The mossy fibres sprouting is a phenomenon seen in both human and animal models of TLE. It is a form of synaptic reorganization in the DG where the mossy fibres develop collaterals that project into abnormal locations to form new functional synapses on neurons that they do not normally innervate (Koyama and Ikegaya, 2004; Ben-Ari and Dudek, 2010). These mossy fibres form new excitatory synapses on the dendrites of granule cells in the inner third of the DG molecular layer, CA1 and CA3 pyramidal neurons as in figure 1.8 (Ben-Ari and Dudek, 2010).

Some studies suggested that the mossy fibres sprouting has a role in developing the epileptiform activity during and after the latent period of epileptogenesis as the majority of these new synapses are excitatory. Therefore there is an increase in number of excitatory synapses in granular cells and CA3 pyramidal neurons that are innervated by sprouting mossy fibres as in figure 1.9 (Bragin *et al.*, 2000; Scharfman *et al.*, 2003; Koyama and Ikegaya, 2004; Ben-Ari and Dudek, 2010).

On the other hand, some studies suggested that sprouting mossy fibres form synapses with inhibitory interneurons in DG, inhibit the excitability of granule cells and lead to hyper-inhibition state that resist the generation of epileptiform discharges (Frotscher *et al.*, 2006; Sloviter *et al.*, 2006). Hence, the role of mossy fibre sprouting in epileptogenesis needs to be further investigated.
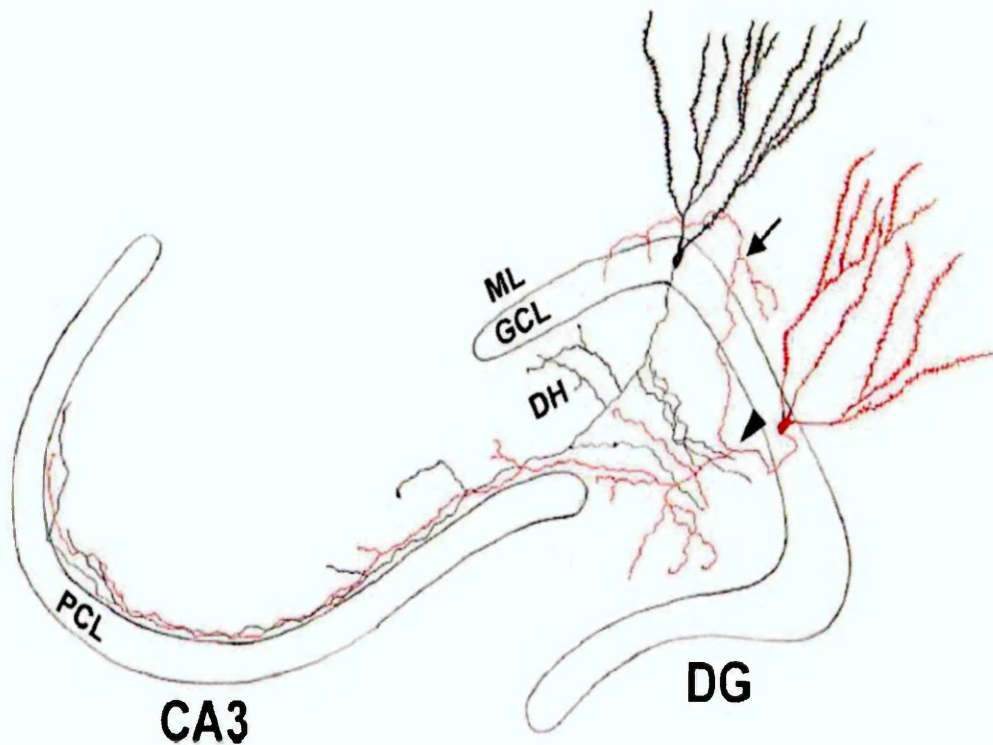
Figure 1.8 Mossy fibre sprouting in TLE-HS

The normal mossy fibres (**black**) are the axons of the granule cells in the dentate gyrus (**DG**) and they project through the dentate hilus (**DH**) to CA3. They make new synaptic contacts with hilar cells, CA3 pyramidal cell layer (**PCL**) and interneurons. In TLE the new sprouting mossy fibres (**Red**) will arise from dentate hilus (**arrowhead**) and run across the granule cell layer (**GCL**). They will also project to the inner third molecular layer (**ML**) (**arrow**). They will contact other granule cell's dendrites and form excitatory synapses. Adapted from Koyama and Ikegaya (2004).

Before epileptogenesis
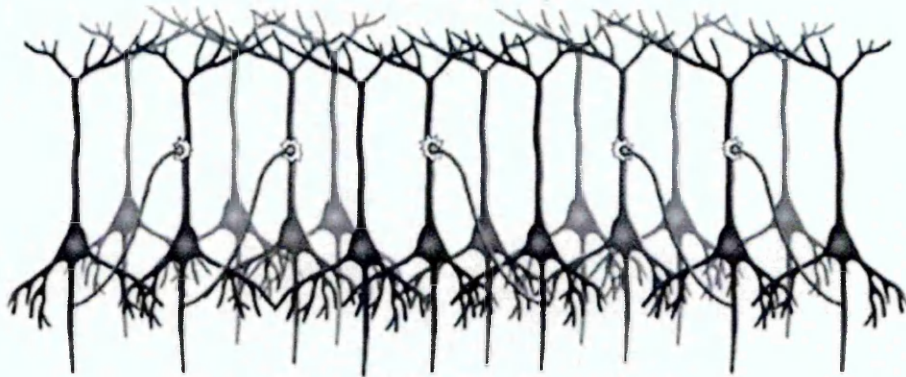
Normal recurrent excitation

After epileptogenesis
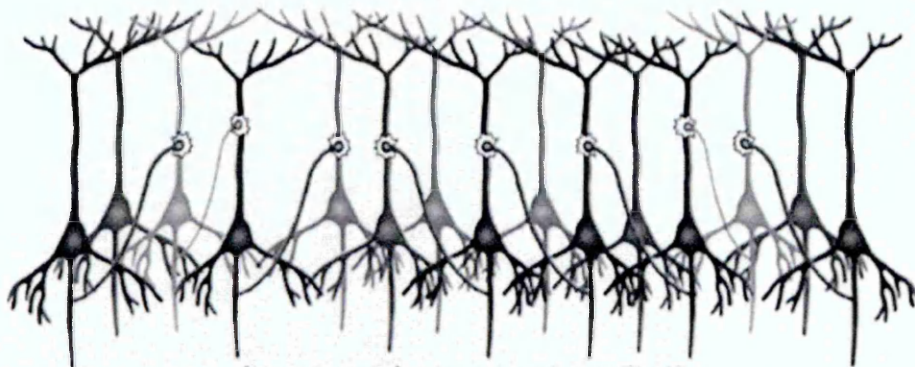
Increased recurrent excitation

Figure 1.9 Schematic representation of mossy fibre sprouting in the CA3 area of the hippocampus before and after epileptogenesis

The numbers of excitatory synapses in CA3 pyramidal cells formed by mossy fibre sprouting are increased after epileptogenesis leading to an increased excitation. Adapted from Ben-Ari and Dudek, (2010).

1.6.4 Neurogenesis in TLE-HS

Neurogenesis in the hippocampus is seen in all mammals throughout life. It has an important role in cognitive functions such as learning and memory. It also has a reparative function, as neurogenesis is increased after an acute cerebral injury to help in neuronal recovery. The rate of neurogenesis declines with age (Kuruba *et al.*, 2009). Neurogenesis occurs within the subgranular zone (SGZ) of the hippocampal dentate gyrus. The progenitor cells mature into granule neurons then migrate into the granule cell layer and send their axons to the hilus and CA3 subfield (Engel *et al.*, 2011).

Many animal studies reported that acute seizures were associated with an increase in hippocampal neurogenesis. In contrast, chronic seizures were associated with severe reduction in hippocampal neurogenesis. Human studies also showed a decrease in the sclerotic hippocampal neurogenesis that supports the finding from chronic seizures animal studies (Engel, *et al.*, 2011). However, the functional significance of neurogenesis is still poorly understood, as some studies suggest that the new neurons that migrate to the granular cell layer may have a pro-epileptogenic effect (Kuruba *et al.*, 2009).

1.6.5 Neuroinflammation in TLE-HS

Many experimental and clinical studies highlighted the role of inflammatory pathways in epilepsy pathogenesis. Many cells such as infiltrated leukocytes, endothelial cells of the blood brain barrier (BBB), activated microglia, astrocytes and neurons, contribute to neuroinflammation in TLE-HS by the synthesis and secretion of high levels of pro-inflammatory cytokines (Maroso *et al.*, 2011).

In an experimental model of acute TLE, there was an induction of pro-inflammatory cytokines such as interleukin-1 beta (IL-1β) and TNF-α in glia and neurons after acute seizures (Ravizza and Vezzani, 2006). In addition, in a chronic model of TLE the IL-1β expression showed persistent up regulation in astrocytes and activated microglia. While the chronic up regulation of astrocytic IL-1β did not depend on the frequency of seizures, microglial IL-1β up regulation was dependent on frequency of seizures and was only found in areas with high seizure frequency (Ravizza et al., 2008). Furthermore, there was up regulation of IL-1β and TNF-α as well as their downstream inflammatory mediators such as prostaglandins and complement in the epileptogenic tissue from TLE patients (Ravizza et al., 2008; Maroso et al., 2011).

Many studies found that Interleukin-1 type 1 receptor ∕ Toll-like receptor (IL-1R1∕ TLR) signalling pathways contribute to seizure activity in epilepsy. The IL-1β that is released from astrocytes and activated microglia in response to seizures, acts on neuronal IL1-R1 and increase the NMDA-mediated Ca^{2+} influx. Hence leads to increase in neuronal excitability. The High-mobility group box 1 (HMGB1) is a danger molecule that is released from injured neurons following a seizure. It acts on TLRs and increases neuronal excitability also via increasing the NMDA-mediated Ca^{2+} influx (Maroso et al., 2011). Therefore, drugs targeting (IL-1R1∕ TLR) signalling will help reduce inflammatory processes in the epileptic brain as well as counteracting the neuronal hyperexcitability (Maroso et al., 2011).

Recent evidence also highlighted the role of up regulated pro-inflammatory chemokines such as CCL2, CCL3 and CCL4 in TLE neuropathology (Van Gassen et al., 2008; Kan et al., 2012; Arisi et al., 2015). Activated microglia and astrocytes are

primary sources of chemokines following CNS injury. Chemokines are a class of cytokines that play an important role in neuroinflammation. They are leukocyte chemoattractants; they facilitate leukocyte infiltration across BBB. Once leukocytes are within the brain, together with microglia and astrocytes, they accelerate the inflammatory process by inducing the release of pro-inflammatory cytokines, cytotoxic substances and proteolytic enzymes (Mantovani *et al.*, 2006; Louboutin *et al.*, 2011).

In summary, TLE-HS prolonged chronic inflammation appears to participate in its pathophysiology and targeting inflammation provides a new therapeutic approach in TLE treatment that may have an anti-epileptogenic effect (Vezzani *et al.*, 2013).

1.6.6   Water homeostasis in TLE-HS

Water and ion homeostasis are important factors that modulate seizure susceptibility (Andrew, 1990; Schwartzkroin *et al.*, 1998; Lee *et al.*, 2012). It was found that hippocampus excitability is affected by alteration in water movement and osmotic changes as hypotonic solutions promoted epileptiform activity in hippocampal brain slices (Andrew, 1990). Magnetic resonance imaging in TLE-HS patients shows water accumulation in sclerotic hippocampi, compared to non-sclerotic ones and indicates impaired water homeostasis in TLE-HS (Bronen *et al.*, 1991; Dawe *et al.*, 2014).

Aquaporins (AQPs) are membrane transporter proteins that mainly regulate the bidirectional water movement across cell membranes in response to osmotic gradients (Amiry-Moghaddam and Ottersen, 2003). A few studies on human TLE-HS specimens reported dysregulation in AQP4 and AQP1 expression in HS. They also suggested that AQPs are implicated in water accumulation seen in TLE-HS (Lee *et al.*, 2004; Eid *et al.*,

2005; Bebek *et al.*, 2013). However little is known about the expression of other AQPs such as AQP3, AQP5 AQP8, AQP9 and AQP11 in TLE-HS.

1.7 Surgical treatment of refractory TLE-HS

The TLE-HS patients that are refractory to the available AEDs become candidates for surgical treatment where the epileptogenic focus is resected. They either undergo selective amygdalohippocampectomy or temporal lobectomy. The surgical treatment is effective in controlling seizures in 60 - 70% of patients. It also stops the cognitive decline associated with recurrent and uncontrolled seizures (Blümcke et al., 2012; Coras and Blümcke, 2015). However, TLE surgery does have many complications; it causes memory and cognitive impairments such as verbal memory decline. It also increases patient's risk of accelerated mental ageing compared to medically treated patients (Helmstaedter *et al.*, 2008). Another significant complication following surgery is the worsening of previously existing psychiatric disorders, in addition, it causes the development of *de novo* psychopathological disorder in patients such as depression, anxiety and to less extent psychosis (Cleary *et al.*, 2012).

Nevertheless, 40% of TLE patients suffer from surgery failure (Blümcke et al., 2012). So in addition to their uncontrolled seizures, patients still suffer from the surgery complications which could be very distressing to them and their families (Cleary *et al.*, 2012).

1.8 Aims and objectives

Refractory TLE is a common adult epilepsy where antiepileptic drugs are not effective in controlling seizures. Those patients become candidates for surgical treatment which is effective in only 60 - 70% of TLE patients. Although surgical treatment can control recurrent seizures and halt cognitive decline, it causes memory and cognitive impairments as well as psychopathological disturbance. Therefore, further research is needed to further understand the pathophysiology of refractory TLE in order to develop effective drug treatments for refractory TLE-HS. Consequently, the objective of this study is to investigate potential biomarkers, which will increase our understanding of refractory TLE pathophysiology and help in the identification of new potential drug targets. Thus, the aims of this study are to do:

1. Quantitative investigation of inhibitory $GABA_B$ receptor expression in sclerotic hippocampi obtained from TLE patients undergoing surgical resection.

2. Quantitative investigation of IP3R1, SGK1, SCN4B and SYNPR biomarkers, which are involved in regulating neuronal excitability, in sclerotic hippocampi obtained from TLE patients undergoing surgical resection.

3. Transcriptome analysis of sclerotic hippocampi obtained from TLE patients undergoing surgical resection and further validating microarray expression data of inflammatory cytokines by qRT-PCR.

4. Quantitative investigation of AQP1, AQP3, AQP4, AQP5, AQP8, AQP9 and AQP11 biomarkers, which are involved in water homeostasis, in sclerotic hippocampi obtained from TLE patients undergoing surgical resection.

Chapter 2

Materials and Methods

2 Materials and Methods

2.1 Human sample collection and patients' clinical data

2.1.1 Surgical samples

All surgical samples were obtained from the Royal Hallamshire Hospital (Sheffield, UK). The research was approved by South Yorkshire Research Ethics Committee (08/H1310/49) and it followed the Code of Ethics of the World Medical Association (2001). The samples were obtained with the understanding and the written consent of each patient.

We recruited patients with pharmacoresistant TLE associated with unilateral HS. The diagnosis of TLE-HS was made by the treating clinician based on brain MRI scan and inter-ictal and ictal EEG characteristics being consistent with a seizure focus in the hippocampus within the temporal lobe. The patients' relevant clinical data are shown in Table 2.1. These patients underwent a therapeutic selective amygdalohippocampectomy. After surgery two samples were obtained; sclerotic hippocampi (TLE-HS, n = 49), which are the epileptogenic and seizure focus specimens and superior temporal gyrus specimens (TLE-STG, n = 25), which are the part of the temporal lobe that showed no ictal or inter-ictal activity.

Table 2.1 Patient clinical data

Patient No	Sex	Family history	Age at surgery (yrs)	Epilepsy duration (yrs)	samples (side)	Current AED	previous AEDs
Pt. 01	M	No	59	15	TLE-HS (Rt) TLE-STG (Rt)	PGB	LMT, LEV, CBZ
Pt. 02	M	No	40	32	TLE-HS (Rt) TLE-STG (Rt)	PHT	PHT, LEV,CBZ
Pt. 03	M	No	37	12	TLE-HS (Lt) TLE-STG (Lt)	CBZ, LEV	VPA
Pt. 04	M	No	50	48.5	TLE-HS (Lt) TLE-STG (Lt)	LEV, ZNS,PGB	CBZ, TPM, PB, VPA, GBP, PHT
Pt. 05	F	NA	34	NA	TLE-HS (Rt)	NA	NA
Pt. 06	F	NA	44	28	TLE-HS (Rt) TLE-STG (Rt)	TPM	LMT, CBZ, LEV, CLB
Pt. 07	F	No	39	26	TLE-HS (Lt) TLE-STG (Lt)	None	CBZ, PHT, LEV, LMT
Pt. 08	F	No	26	18	TLE-HS (Lt)	LEV, PHT, CLB	CBZ,LMT
Pt. 09	F	No	34	33.5	TLE-HS (Rt) TLE-STG (Rt)	LMT,LEV	PB, PHT, CBZ, VPA
Pt. 10	F	No	36	32	TLE-HS (Lt)	PHT,VPA	PGB, LEV, LMT, CBZ, TPM, ZNS
Pt. 11	M	No	42	40	TLE-HS (Lt)	CBZ,ZNS, PHT	PB,VPA, GBP,LEV
Pt. 12	M	NA	54	NA	TLE-HS (Rt)	CBZ, ZNS	PB, PHT, PGB, CNP,LEV
Pt. 13	F	No	24	23	TLE-HS (Lt)	LCS, LEV	CBZ, LMT
Pt. 14	M	NA	42	NA	TLE-HS (Lt) TLE-STG (Lt)	CBZ,CNP, ZNS	NA
Pt. 15	F	Yes	32	13	TLE-HS (Rt) TLE-STG (Rt)	LMT, CBZ, GBP	LEV
Pt. 16	M	No	25	23	TLE-HS (Lt)	ZNS, TPM	CBZ, VPA, GBP
Pt. 17	M	NA	61	NA	TLE-HS (Lt) TLE-STG (Lt)	NA	NA
Pt. 18	M	Yes	48	47	TLE-HS (Rt) TLE-STG (Rt)	PER,CBZ	PHT,LEV,LMT,GBP, TPM,PGB,ZNS
Pt. 19	F	No	51	11	TLE-HS (Lt) TLE-STG (Lt)	LCS, LEV	CBZ, LMT, VPA

Hippocampal sclerotic specimens (**TLE-HS**) and superior temporal gyrus specimens (**TLE-STG**) obtained from temporal lobe epilepsy patients. Antiepileptic drugs (**AEDs**): **CBZ,** Carbamazepine; **CLB**, Clobazam; **CNP**, Clonazepam; **GBP**, Gabapentin; **LCS**, Lacosamide; **LEV**, Levetiracetam; **LMT**, Lamotrigine; **OXC**, Oxcarbazepine; **PB**, Phenobarbital; **PER**, Perampanel; **PGB**, Pregabalin, **PHT**, Phenytoin; **TGB**, Tiagabine; **TPM**, Topiramate; **VGB**, Vigabatrin; **VPA**, Valproate; **ZNS**, Zonisamide. **NA**: not available.

Table 2.1 Patient clinical data (continued):

Patient No	Sex	Family history	Age at surgery (yrs)	Epilepsy duration (yrs)	samples (side)	Current AED	previous AEDs
Pt. 20	M	No	30	2	TLE-HS (Lt)	LEV, TPM, LCS	LMT
Pt. 21	M	Yes	32	3	TLE-HS (Rt) TLE-STG (Rt)	LMT, OXC	CBZ, LEV
Pt. 22	M	No	51	6	TLE-HS (Lt) TLE-STG (Lt)	NA	NA
Pt. 23	M	No	35	18	TLE-HS (Lt) TLE-STG (Lt)	CBZ, LEV	TPM, LMT, VPA
Pt. 24	F	No	54	53	TLE-HS (Lt) TLE-STG (Lt)	LMT,PGB	GBP,VPA,PHT,CBZ,PB, LEV, CNP,LCS
Pt. 25	M	No	41	29	TLE-HS (Lt) TLE-STG (Lt)	NA	NA
Pt. 26	F	No	22	13	TLE-HS (Rt) TLE-STG (Rt)	LCS, LMT, TPM, PB	VPA
Pt. 27	F	No	25	6	TLE-HS (Lt) TLE-STG (Lt)	NA	NA
Pt. 28	F	No	44	22	TLE-HS (Rt) TLE-STG (Rt)	LMT,VPA, PHT	CBZ,LEV,TPM
Pt. 29	F	No	24	20	TLE-HS (Rt) TLE-STG (Rt)	LMT	VPA, TPM, CBZ
Pt. 30	M	NA	35	NA	TLE-HS (Rt) TLE-STG (Rt)	NA	NA
Pt. 31	F	NA	44	10	TLE-HS (Lt)	LCS, LEV, PHT	OXC, LMT
Pt. 32	M	NA	32	NA	TLE-HS	NA	NA
Pt. 33	M	NA	35	14	TLE-HS (Lt)	LMT, CLB	VPA, ZNS, CBZ
Pt. 34	F	NA	31	NA	TLE-HS TLE-STG	NA	NA
Pt. 35	M	NA	NA	NA	TLE-HS TLE-STG	NA	NA
Pt. 36	M	NA	42	NA	TLE-HS TLE-STG	NA	NA
Pt. 37	F	No	45	16	TLE-HS (Lt)	None	CBZ,LEV,PGB,CLB
Pt. 38	M	NA	33	24	TLE-HS (Lt)	None	CBZ,VPA, LEV

Hippocampal sclerotic specimens (**TLE-HS**) and superior temporal gyrus specimens (**TLE-STG**) obtained from temporal lobe epilepsy patients. Antiepileptic drugs (**AEDs**): **CBZ,** Carbamazepine; **CLB**, Clobazam; **CNP**, Clonazepam; **GBP**, Gabapentin; **LCS**, Lacosamide; **LEV**, Levetiracetam; **LMT**, Lamotrigine; **OXC**, Oxcarbazepine; **PB**, Phenobarbital; **PER**, Perampanel; **PGB**, Pregabalin, **PHT**, Phenytoin; **TGB**, Tiagabine; **TPM**, Topiramate; **VGB**, Vigabatrin; **VPA**, Valproate; **ZNS**, Zonisamide. **NA**: not available.

Table 2.1 Patient clinical data (continued):

Patient No	Sex	Family history	Age at surgery (yrs)	Epilepsy duration (yrs)	samples (side)	Current AED	previous AEDs
Pt. 39	M	No	33	31	TLE-HS (Lt)	LEV, LMT	CBZ,VPA, CLB
Pt. 40	F	NA	22	NA	TLE-HS (Lt)	CBZ,LMT	CNP,LEV,ZNS
Pt. 41	F	No	39	37	TLE-HS (Rt)	None	GBP,LEV, LMT
Pt. 42	F	No	29	28	TLE-HS (Lt)	CBZ,LMT	CLB, LCS, LEV,PGB,VPA, ZNS
Pt. 43	M	No	23	16	TLE-HS (Lt)	LMT	CLB,LEV, TPM
Pt. 44	F	No	27	9	TLE-HS (Rt)	CBZ, LEV	CLB,LMT, TPM
Pt. 45	M	No	31	20	TLE-HS (Rt)	CBZ,LEV, LCS	PGB, VGB
Pt. 46	M	No	48	41	TLE-HS (Rt)	None	CBZ,LMT, VPA, PHT, VGB, CLB, TPM,TGB
Pt. 47	M	NA	48	NA	TLE-HS (Lt)	LEV, VPA	OXC
Pt. 48	F	NA	44	NA	TLE-HS (Lt)	PGB,VPA	LEV, LMT
Pt. 49	M	No	63	46	TLE-HS (Lt)	LEV,CLB	VPA,VGB, PB,ZNS
Total	M=27 F =22				TLE-HS (49) TLE-STG (25)		

Hippocampal sclerotic specimens (**TLE-HS**) and superior temporal gyrus specimens (**TLE-STG**) obtained from temporal lobe epilepsy patients. Antiepileptic drugs (**AEDs**): **CBZ,** Carbamazepine; **CLB**, Clobazam; **CNP**, Clonazepam; **GBP**, Gabapentin; **LCS**, Lacosamide; **LEV**, Levetiracetam; **LMT**, Lamotrigine; **OXC**, Oxcarbazepine; **PB**, Phenobarbital; **PER**, Perampanel; **PGB**, Pregabalin, **PHT**, Phenytoin; **TGB**, Tiagabine; **TPM**, Topiramate; **VGB**, Vigabatrin; **VPA**, Valproate; **ZNS**, Zonisamide. **NA**: not available.

2.1.2 Post-mortem hippocampi samples

The post-mortem hippocampi samples were obtained from UCL Brain Bank (08/H0718/54). They were from individuals with no previous medical history of neurological or psychiatric disease (Table 2.2). At autopsy the hippocampi were dissected, pH was checked to be between 6 and 7 (optimal for RNA stability), and then they were snap frozen and stored at - 80°C (Kingsbury *et al.*, 1996).

Table 2.2 Post-mortem hippocampi samples

Sample	Gender	Age (yrs)	PMI (hrs)	Cause of death	Method
PMC 1	F	64	79	Bowel cancer	RT-PCR
PMC 2	M	38	80.35	Gastric cancer	RT-PCR
PMC 3	M	63	42	Congestive Heart Failure	RT-PCR
PMC 4	M	43	15	Heart attack	RT-PCR
PMC 5	F	53	29.5	Intra-cerebral haemorrhage	RT-PCR
PMC 6	M	71	38.5	Mesothelioma	RT-PCR / MA
PMC 7	F	78	23.3	Endometrium cancer	RT-PCR / WB /MA
PMC 8	F	80	49.1	Pancreas cancer	RT-PCR / WB /MA
PMC 9	M	85	51.3	Multiple organ failure	RT-PCR / WB /MA
PMC 10	F	78	51.3	Colon cancer	RT-PCR / WB /MA

PMC: Post-mortem control sample. **PMI**: Post-mortem Interval in hours. **qRT-PCR**: Quantitative real- time polymerase chain reaction. **WB**: Quantitative Western blot. **MA**: Microarray analysis.

2.2 Experimental design

The human samples obtained were used to investigate both mRNA and protein levels of potential biomarkers involved in TLE-HS pathophysiology. The mRNA levels were investigated by quantitative real-time polymerase chain reaction (qRT-PCR) and microarray analysis technique, while protein expression was investigated by two-colour quantitative western blot (WB) as in figure 2.1.

Human samples :
- Sclerotic hippocampi obtained from TLE-HS surgery (n = 49)
- Superior temporal gyrus obtained from TLE-HS surgery (n = 25)
- *Post-mortem* control (n = 10)

Investigating mRNA expression

Investigating protein expression

RNA extraction
cDNA synthesis

Protein extraction
Protein quantification

qRT-PCR
Microarray analysis

Quantitative western blot
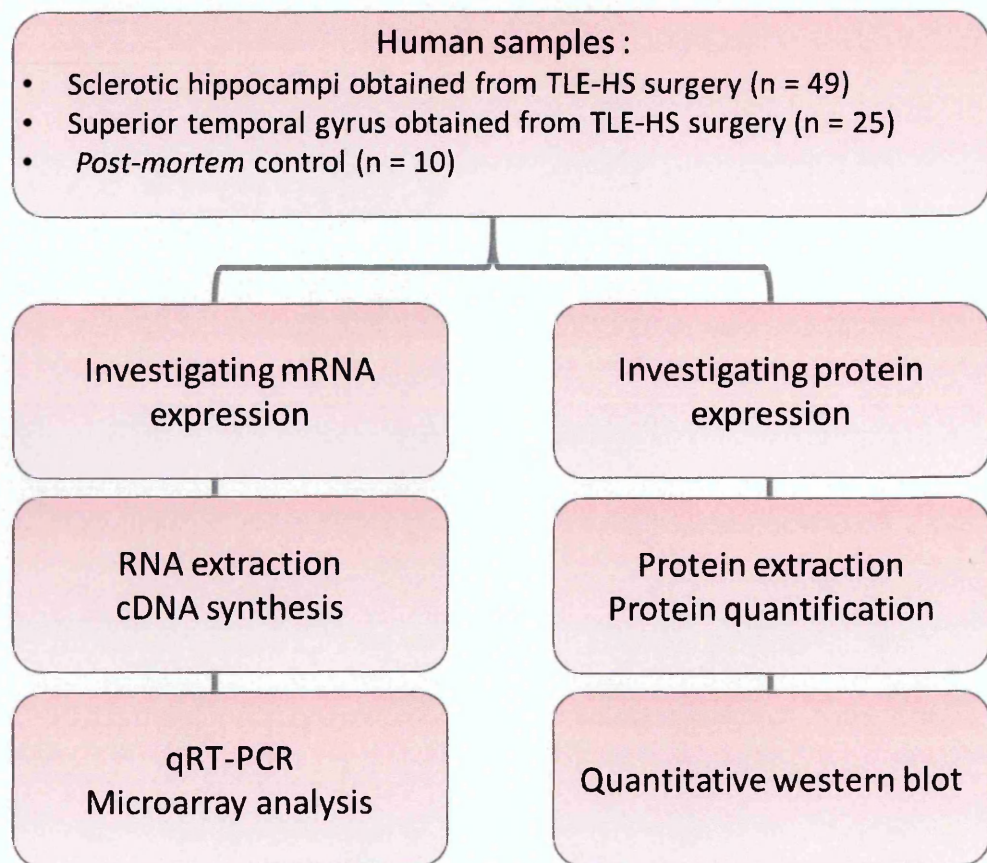
Figure 2.1 Experimental design of the study

Potential biomarkers involved in TLE-HS pathophysiology were investigated by techniques such as quantitative real-time polymerase chain reaction (qRT-PCR), microarray analysis and quantitative western blot.

2.3 RNA extraction

2.3.1 RNA extraction protocol

RNA extraction: The SV Total RNA Isolation System (Promega, Z3100) was used to extract the total RNA from samples according to the manufacturer's instructions. The hippocampus tissue lysate was prepared by adding 1ml of RNA lysis buffer to 342 mg of tissue, and then homogenized using a manual homogenizer. 175µl of tissue lysate was diluted with 350µl SV RNA dilution buffer before it was incubated at 70°C for 3 minutes. The lysate was then centrifuged at 13,000 xg for 10 minutes at 25°C and the clear lysate solution was transferred to a fresh microcentrifuge tube without disturbing the pelleted debris. All centrifugation steps were done at 13,000 xg unless they are stated.

RNA purification by centrifugation: the clear lysate was mixed with 200µl 95% ethanol and then transferred to the Spin Column Assembly (Promega, Z3100) before it was centrifuged for 1 minute. The liquid in the collection tube was discarded and 600µl of SV RNA wash solution was added to the spin basket and centrifuged for 1 minute followed by emptying the collection tube.

DNase treatment: 50µl of freshly prepared **DNase incubation mix** (40µl Yellow Core Buffer, 5µl 0.09M $MnCl_2$ and 5µl of DNase I enzyme) was added directly to the membrane of spin basket where it was then incubated for 15 minutes at room temperature (RT). Following DNase incubation, 200µl of SV DNase stop solution was added to the spin basket and then centrifuged for 1 minute.

RNA washing and elution: The RNA adsorbed on the spin basket membrane was washed by adding 600µl of SV RNA wash solution followed by centrifugation for 1 minute. The collection tube was emptied and 250µl of SV RNA wash solution was added to the spin basket before it was centrifuged again for 2 minutes. The spin basket was then transferred to a sterile elution tube and RNA was eluted in 100µl of nuclease-free water by centrifugation for 1 minute. The basket was discarded and the purified RNA solution collected in the elution tube was stored at - 80°C.

RNA quantification and purity: the NanoDrop-1000 spectrophotometer was used to determine RNA concentration (ng/µl), yield and purity. A pure RNA sample has A260/A280 ratio of (1.8 - 2.0) and A260/A230 ratio of (1.8 - 2.2) to dismiss any protein and guanidine contamination respectively.

2.3.2 Ethanol precipitation of RNA

If an RNA sample was very dilute or inadequately pure (A260/A280 and A260/A230 ratios lower than 1.8), it underwent a further ethanol precipitation step to concentrate and purify it. For 100µl RNA sample, 10µl of sodium acetate (3M, pH 5-5.2) and 250µl of 100 % ethanol were mixed gently with the RNA sample and then incubated overnight at -20°C. The sample was then centrifuged at 12,000 xg for 30 minutes at 4°C and the supernatant was removed carefully without disturbing the RNA pellet (gel-like pellet). The RNA pellet was resuspended in 250µl of 70% ethanol and then centrifuged at 12,000 xg for 15 minutes at 4°C. The supernatant was removed carefully and the RNA pellet was air-dried for 10 minutes at RT. The RNA was resuspended in 20µl nuclease-free water and RNA concentration and purity were checked by NanoDrop-1000 spectrophotometer as in figure 2.2.

47

2.3.3 Agarose gel electrophoresis of total RNA

The overall RNA quality and integrity was checked by running the sample on 1% agarose gel electrophoresis. The pre-stained agarose gel was prepared by adding 1 g of agarose (A9537, Sigma-Aldrich) to 100ml 1X Tris acetate EDTA (TAE) buffer (40mM Tris-acetate, 1mM EDTA, pH 8.2 - 8.4). The agarose was dissolved by heating the mixture in a microwave for about 2 minutes. The solution was then allowed to cool for a few minutes before adding 7.5μl of ethidium bromide (5mg/ml). The solution was poured into a sealed gel tray with an 8-well comb and it was allowed to set for about 40 minutes. The gel was transferred to an electrophoresis tank after removing the comb. The tank was filled with 1X TAE buffer until the gel was completely submerged. The RNA samples were mixed with a loading dye (5μl RNA sample and 1μl loading dye) then they were loaded into the wells (wells at negative electrode side). The electrophoresis was run at 90 volts for 45 minutes then the gel was visualized using a UV transilluminator. The images were captured on Labworks software version 4. A good RNA sample with no degradation or contamination should have 2 bands for 28S and 18S ribosomal RNAs in a 2:1 ratio approximately shown in figure 2.3.

Figure 2.2 RNA sample purity assessment by NanoDrop-1000 spectrophotometer

RNA sample purity assessed by NanoDrop-1000 spectrophotometer before and after ethanol precipitation. (**A**) RNA extraction of C28 RNA sample concentration was 101.4 ng/µl, 260/280 ratio was 2.10 and 260/230 ratio was 1.78. (**B**) C28 RNA sample concentration after ethanol precipitation was increased to 425.9 ng/µl. 260/230 ratio was increased to 1.92 and 260/280 ratio decreased to 1.96 indicating a more pure RNA sample.

Figure 2.3 RNA sample integrity assessed by 1 % agarose gel electrophoresis

The RNA samples showed 2 clear bands for 28S and 18S ribosomal RNA in a 2:1 ratio indicating no degradation of the RNA.

2.4 Complementary DNA (cDNA) synthesis

The mRNA was reverse transcribed to cDNA using SuperScript^{TM} III first strand synthesis system (Life Technologies, 18080-051). Starting from 1 µg of total RNA, 1µl of 50 µM oligo (dT)$_{20}$ primer and 1µl of 10 mM deoxyribonucleotide triphosphate (dNTPs) mix were added to 8µl of total RNA before they were incubated at 65°C for 5 minutes and then placed on ice. A cDNA synthesis mix (10µl) was then prepared in the following order : 2µl of 10X RT buffer, 4µl of 25 mM MgCl$_2$, 2µl of 0.1 M dithiothreitol (DTT), 1µl of RNaseOUT^{TM} (40 U/µl) and 1µl of SuperScript^{TM} III RT$^{©}$. The 10µl cDNA synthesis mix was added to RNA, oligo (dT)$_{20}$ primer and dNTP mix, before it was mixed gently and incubated at 50°C for 50 minutes. The reaction was terminated by incubation at 85°C for 5 minutes then it was placed on ice.

The cDNA was then purified using a QIAquick PCR purification kit (Qiagen, 28104) according to the manufacturer's instructions. The cDNA sample (20µl) was mixed gently with 100µl of buffer PB before it was transferred to a QIAquick spin column and then centrifuged at 13,000 xg for 1 minute. The collection tube was emptied and 750µl of Buffer PE was added to column and centrifuged at 13,000 xg for 1 minute. The collection tube was emptied and the column was centrifuged again at 13,000 xg for 1 minute. The spin column was then transferred to a sterile elution tube and cDNA was eluted by adding 30µl of nuclease-free water and centrifuged at 13,000 xg for 1 minute. The cDNA was quantified using NanoDrop-1000 spectrophotometer and stored at - 80°C.

2.5 Quantitative real-time polymerase chain reaction (qRT-PCR)

2.5.1 Principle of qRT-PCR using TaqMan© gene expression assays

qRT-PCR is one of the most powerful and sensitive techniques used for investigating gene expression. Some of the advantages of qRT-PCR include: it collects the data in real time as amplification and detection are done simultaneously and it does not need post amplification processing; it is very accurate and can detect small changes in gene expression between samples; it needs small amounts of starting cDNA and is more accurate and sensitive than end point PCR (Wong and Medrano, 2005).

qRT-PCR phases: The PCR process is divided into 4 phases: linear ground, early exponential, log-linear, and plateau phases as shown in figure 2.4. The **Linear ground phase** is the first few cycles of PCR where the fluorescence baseline is being calculated. The **early exponential phase** is the starting point in which the gene of interest is first detected and threshold cycle (C_t) is determined. The C_t is the cycle in which the fluorescence becomes higher than the background level. The C_t value is inversely proportional to cDNA quantity in the samples. In **log-linear phase** the PCR products are doubling with every cycle and when PCR components are depleted the PCR reaches the **plateau phase**.

Amplification Plot
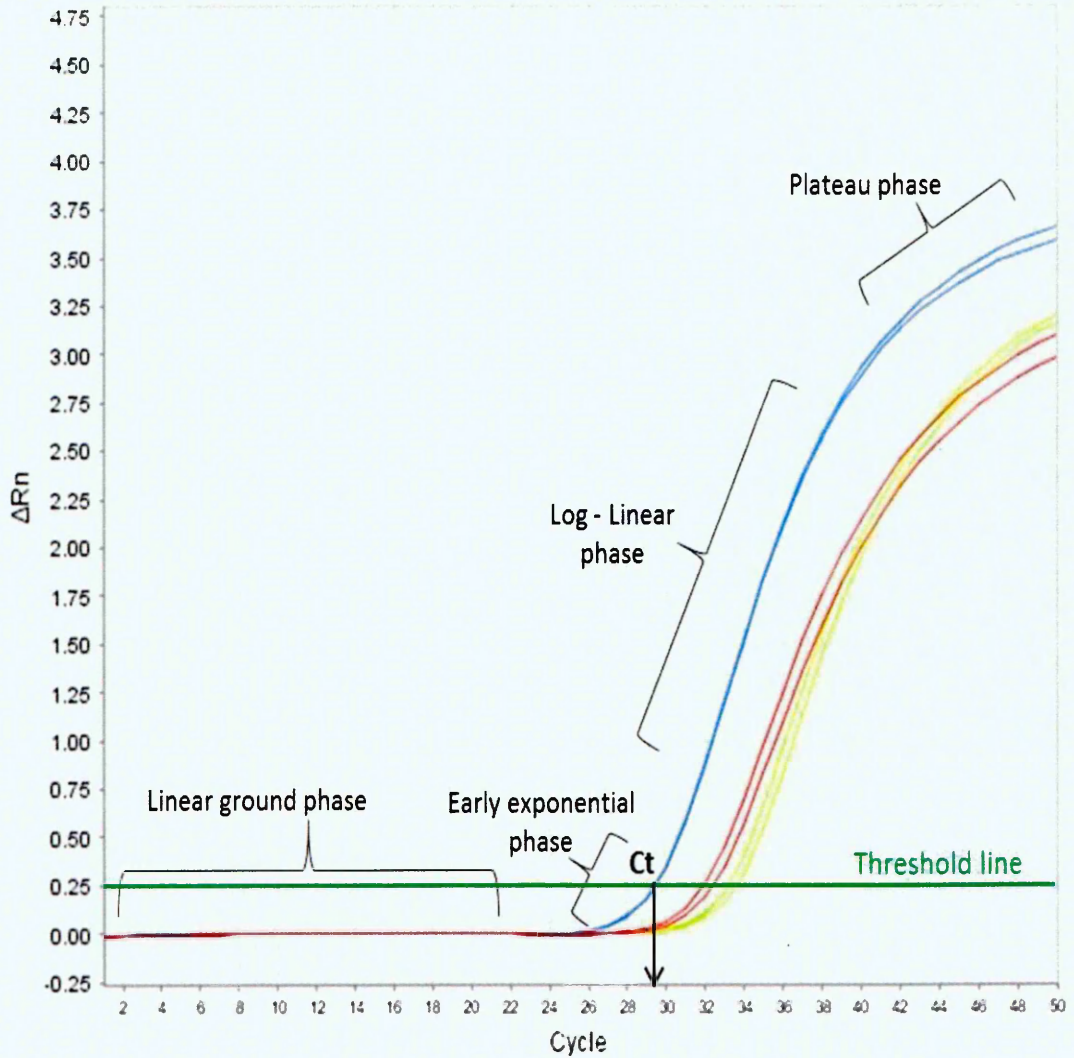
Figure 2.4 qRT-PCR amplification plot phases

There are 4 phases: In linear ground phase the baseline fluorescence is measured. In the early exponential phase, the threshold cycle (C_t) is the intersection between an amplification curve and a threshold line. The target C_t is the cycle that target fluorescence exceeds the background signal and it reflects the relative target concentration in the sample. The log-linear phase shows the optimal amplification as PCR product is doubled with every cycle. In the plateau phase the PCR component starts to be depleted. The ΔRn signal is fluorescence of sample minus background fluorescence. This graph was generated on StepOnePlus™ Real-Time PCR System (Applied Biosystems).

52

TaqMan® Gene Expression Assays consists of 2 unlabelled PCR primers specific to target sequence and a TaqMan® minor groove binder (MGB) probe that is designed to anneal specifically to a sequence between forward and reverse primer. This gives further specificity to TaqMan assays compared to non-probe SYBR Green I dye chemistry. The TaqMan probe is a double-dye oligonucleotide hydrolysis probe that contains fluorescent reporter fluorochrome (FAM™ dye) at the 5′ end, MGB and non-fluorescent quencher (NFQ) fluorochrome at the 3′ end of the probe as in figure 2.5. In the intact probe, NFQ supresses the reporter dye fluorescence due to proximity distance between the 2 fluorochrome. However during the PCR amplification, the reporter dye is hydrolysed by 5′ exonuclease activity of Taq DNA polymerase enzyme and the reporter dye fluorescence is emitted and detected. The FAM reporter fluorescence is increased with every PCR cycle providing real time measurement of target gene (Van der valden *et al.,* 2003).

There is no non-specific amplification detected when using TaqMan MGB probes for many reasons: (1) the probe is specifically designed to anneal to complementary sequence in the target gene. (2) The MGB in the probe increases the melting temperature and allows the design of shorter more specific primers. (3) The probe is conjugated with non-fluorescent quencher making it more accurate to measure the reporter fluorescence. (4) The reporter dye fluorescence is only detected when it is separated from the quencher. (5) Taq DNA polymerase cleaves only probes that are annealed to target gene. (6) The 3′ end of the probe is locked so the probe doesn't extend and cause any non-specific amplification (Van der valden *et al.,* 2003).
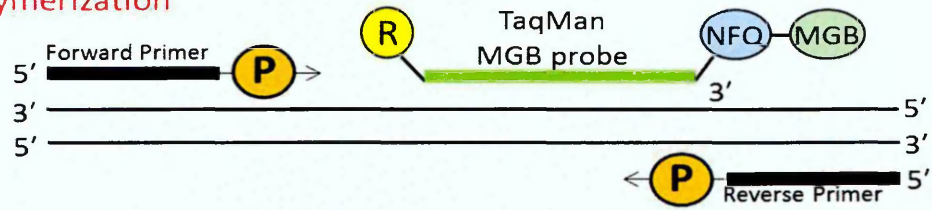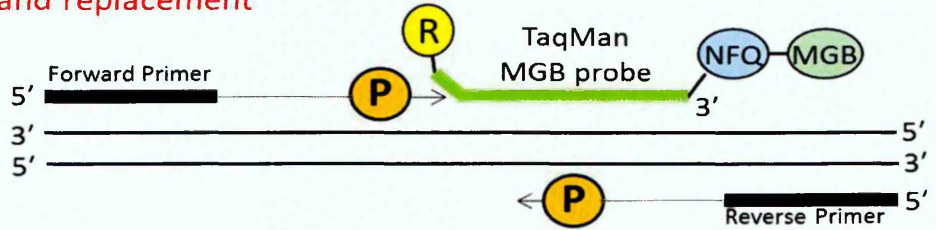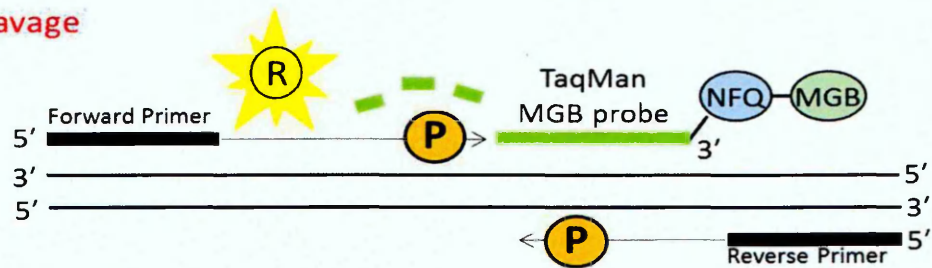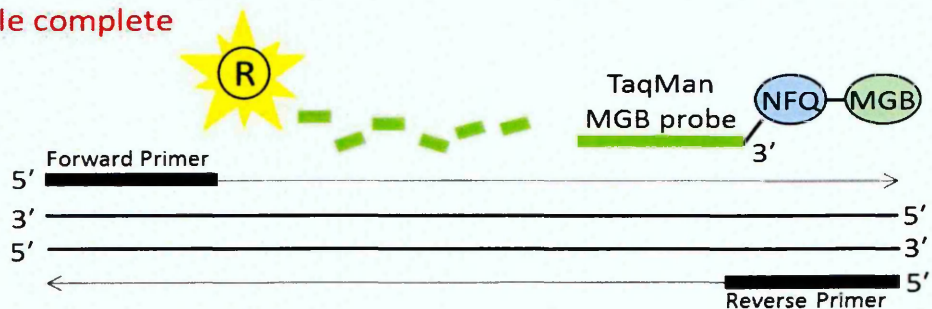
Figure 2.5 Principle of qRT-PCR using TaqMan® MGB probes

a) In polymerization forward and reverse primers anneal to specific sequences in target gene. TaqMan® Minor grove binder (**MGB**) probe binds specifically down steam of the primer. At this stage the probe is intact and there is no emitted fluorescence from the reporter dye (**R**) due to close distance to non-fluorescent quencher (**NFQ**). **b)** During the extension of the primers, the Taq DNA polymerase (**P**) initially displaces the probe. **c)** The 5′ exonuclease activity of DNA polymerase cleaves the reporter dye separating it from NFQ allowing R fluorescence to be detected. **d)** The polymerization of the strand continues until the first cycle is complete and then this process is repeated in the following PCR cycles (Adapted from TaqMan® gene expression assays protocol, Applied Biosystems™, PN 4333458N).

2.5.2   RT-PCR Relative quantification using the comparative CT method

There are two ways of analysing RT-PCR data, absolute and relative quantification methods. In the absolute quantification method, the transcript of interest absolute copy number is determined by a standard curve. In the comparative C_t ($2^{-\Delta\Delta Ct}$) method, relative change in gene expression in tested sample is determined as a fold change compared to the control sample. For each sample, the gene of interest expression is first normalised to a stable housekeeping gene that acts as an internal control (Linvak and Schmittgen, 2001; Wong and Medrano, 2005).

The raw data obtained at the end of the qRT-PCR experiment is C_t values for genes in diseased and control sample. The RT-PCR assay for target and housekeeping gene are done in triplicates and therefore, the first step in data analysis is to average C_t values for each gene to account for any inter-assay variability. Then the target gene expression in different samples is normalized to housekeeping gene and ΔC_t calculated as following:

The ΔC_t in diseased sample:

$$\Delta C_{t\,(Dis)} = \text{Housekeeping gene } C_{t\,(Dis)} - \text{Target gene } C_{t\,(Dis)}$$

The ΔC_t in control sample:

$$\Delta C_{t\,(cont)} = \text{Housekeeping gene } C_{t\,(cont)} - \text{Target gene } C_{t\,(cont)}$$

The $2^{-\Delta\Delta Ct}$ method is calculated as following:

$$\Delta\Delta C_t = \Delta C_{t\,(Dis)} - \Delta C_{t\,(cont)}$$

$$\text{Fold-change ratio} = 2^{-\Delta\Delta Ct}$$

The qRT-PCR data could then be presented as fold-change compared to control sample ($2^{-\Delta\Delta Ct}$), where control equals 1. However, data can also be presented as gene expression normalized to housekeeping gene ($2^{-\Delta Ct}$), showing the actual expression of gene in both control and diseased samples (Linvak and Schmittgen, 2001).

2.5.3 Selection of stable housekeeping genes

The qRT-PCR is an outstanding accurate and sensitive method for mRNA quantification but it critically depends on the selection of a good stable internal control or a housekeeping gene (HKG). The first step in data analysis by ΔCt method (section 1.6.2) is to normalise target gene expression to a stable HKG, to eliminate any variation between samples that may be caused by different amount or quality of starting RNA or cDNA. Therefore in relative qRT-PCR quantification, it is vital to evaluate and select the most stable HKGs that are not affected by experimental and pathological conditions (Radonić et al., 2004; Wierschke et al., 2010). It is also recommended to use 2 or more HKGs as normalization factor, rather than just one, as this provides the most accurate method for gene expression determination (Vandesompele et al., 2002).

The selection of stable housekeeping genes was done using Fast 96 -well TaqMan® Express Human Endogenous Control plates (Life technologies,4426700). Those plates contained dried-down TaqMan® assays specific for 32 housekeeping genes in triplicates, the HKG TaqMan®assay IDs are in table 2.3 and plate layout in figure 2.6. Those candidate HKGs were selected from literature search and whole genome microarray analysis as they were constitutively expressed at moderate abundance.

Table 2.3 TaqMan®assay IDs in TaqMan® express human endogenous control plates

#	Gene symbol	Gene name	Assay IDs
1	18S	Eukaryotic 18S rRNA	Hs99999901_s1
2	GAPDH	Glyceraldehyde-3-phosphate dehydrogenase	Hs99999905_m1
3	HPRT1	Hypoxanthine phosphoribosyltransferase 1 (Lesch-Nyhan syndrome)	Hs99999909_m1
4	GUSB	Glucuronidase, beta	Hs99999908_m1
5	ACTB	Actin, beta	Hs99999903_m1
6	B2M	Beta-2-microglobulin	Hs99999907_m1
7	HMBS	Hydroxymethylbilane synthase	Hs00609297_m1
8	IPO8	Importin 8	Hs00183533_m1
9	PGK1	Phosphoglycerate kinase 1	Hs99999906_m1
10	RPLP0	Ribosomal protein, large, P0	Hs99999902_m1
11	TBP	TATA box binding protein	Hs99999910_m1
12	TFRC	Transferrin receptor (p90, CD71)	Hs99999911_m1
13	UBC	Ubiquitin C	Hs00824723_m1
14	YWHAZ	Tyrosine 3-monooxygenase/tryptophan 5-monooxygenase activation protein, zeta polypeptide	Hs00237047_m1
15	PPIA	Peptidylprolyl isomerase A (cyclophilin A)	Hs99999904_m1
16	POLR2A	Polymerase (RNA) II (DNA directed) polypeptide A, 220kDa	Hs00172187_m1
17	CASC3	Cancer susceptibility candidate 3	Hs00201226_m1
18	CDKN1A	Cyclin-dependent kinase inhibitor 1A (p21, Cip1)	Hs00355782_m1
19	CDKN1B	Cyclin-dependent kinase inhibitor 1B (p27, Kip1)	Hs00153277_m1
20	GADD45A	Growth arrest and DNA-damage-inducible, alpha	Hs00169255_m1
21	PUM1	Pumilio homolog 1 (Drosophila)	Hs00206469_m1
22	PSMC4	Proteasome (prosome, macropain) 26S subunit, ATPase, 4	Hs00197826_m1
23	EIF2B1	Eukaryotic translation initiation factor 2B, subunit 1 alpha, 26kDa	Hs00426752_m1
24	PES1	Pescadillo homolog 1, containing BRCT domain (zebra fish)	Hs00362795_g1
25	ABL1	V-abl Abelson murine leukemia viral oncogene homolog 1	Hs00245445_m1
26	ELF1	E74-like factor 1 (ets domain transcription factor)	Hs00152844_m1
27	MT-ATP6	Mitchondrially encoded ATP synthase 6	Hs02596862_g1
28	MRPL19	Mitochondrial ribosomal protein L19	Hs00608519_m1
29	POP4	Processing of precursor 4, ribonuclease P/MRP subunit (S. cerevisiae)	Hs00198357_m1
30	RPL37A	Ribosomal protein L37a	Hs01102345_m1
31	RPL30	Ribosomal protein L30	Hs00265497_m1
32	RPS17	Ribosomal protein S17	Hs00734303_g1
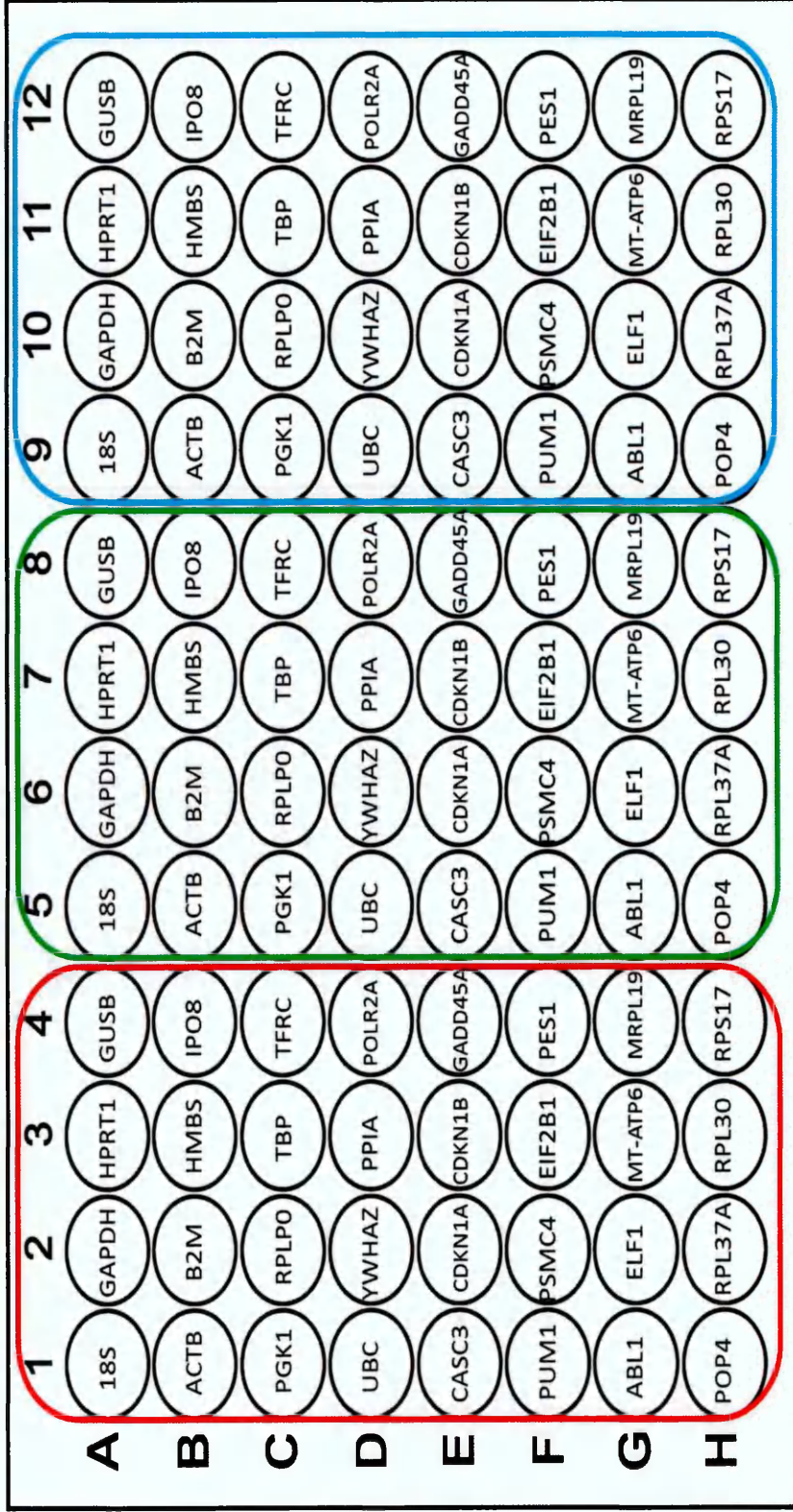
Figure 2.6 Fast 96 -well TaqMan® express human endogenous control plates layout

The Fast 96 -well TaqMan® Express Human Endogenous Control plates contains 32 housekeeping genes in triplicates.

58

Protocol: for every sample the PCR reaction mix (10µl final volume), per well, was prepared by adding 5µl of cDNA template (10ng cDNA in RNase-free water) and 5µl of 2X TaqMan® fast universal PCR master mix (Life Technologies,4352042). The TaqMan® express human endogenous control plate was centrifuged briefly at 1000 xg for 1 min and then 10µl PCR reaction mix was added to each well. The plate was covered by MicroAmp® optical adhesive film and centrifuged at 1000 xg for 1 min. The plate was loaded in StepOnePlus™ Real-Time PCR instrument (Applied Biosystems) and fast thermal cycling conditions were set on the instrument (polymerase activation 95°C for 20 sec, 40 cycles of denaturing at 95°C for 3 sec, and annealing and extension at 60°C for 30 sec).

The data analysis: was done according to Applied Biosystems Application Note (127AP08) and Radonić *et al.* (2004). For every gene, the average C_t values and standard deviation (Stdev) were calculated using Microsoft® Excel 2010 software and data plotted using GraphPad Prism 6 software for Windows, version 6.05 (www.graphpad.com). The genes with lowest variability were selected as internal controls for data analysis.

2.5.4   Determination of primer efficiencies

The comparative C_t method (section 1.6.2) used for qRT-PCR analysis, is based on the assumption that the amplification efficiencies of both target and housekeeping genes are 100% and within 5% of each other. The ideal 100% amplification efficiency means that PCR products are doubling with each PCR cycle during the exponential phase. Therefore it is essential to validate this assumption by determining primer efficiencies of all genes prior to data analysis (Wong and Medrano, 2005).

The primer efficiencies are assessed by using 5 different dilutions of cDNA samples starting from 100 ng concentration. The average C_t value was plotted against Log 10 cDNA concentration. The linear regression (R^2) and linear equation were determined and plotted on graph. The slope of the standard curve is obtained from the linear equation and primer efficiency was calculated using the following equation:

$$\text{Primer efficiency E} = [10^{-1/slope}] - 1$$

Primers efficiency ranging from 90 -110% within 5% of each other is considered acceptable and could be used for comparative C_t data analysis (Wong and Medrano, 2005).

2.5.5 qRT-PCR protocol

For all investigated genes, 10ng of sample cDNA and final PCR reaction volume of 10µl were used (2µl of cDNA and 8µl of PCR reaction mix). For every sample tested, the 2 HKGs and investigated genes were run on the same PCR plate in duplicate.

The PCR mix, per well, was prepared by adding 0.5µl of 20X TaqMan® gene expression assay (Assay IDs for investigated genes are in table 2.4), 2.5µl RNase-free water and 5µl 2X TaqMan® fast universal PCR master mix (Life technologies, 4352042). To each well of 96-well PCR plate, 2µl of sample cDNA template was loaded followed by addition of 8µl of PCR mix. The plate was then sealed by MicroAmp® optical adhesive film (Life technologies, 4360954) and centrifuged at 1000 xg for 1 min. The qRT-PCR was run on StepOnePlus™ Real-Time PCR instrument (Applied Biosystems) using fast thermal cycling conditions (polymerase activation 95°C for 20 sec, 40 cycles of denaturing at 95°C for 1 sec, and annealing and extension at 60°C for 20 sec).

2.5.6 qRT-PCR data statistical analysis

The data obtained from RT-PCR is average C_t values; these were exported to Microsoft® Excel (2010) software. The data was analysed by calculating $2^{-\Delta Ct}$ (fully described in section 2.5.2). Relative mRNA expression was normalised to cyclophilin A (PPIA) and cyclin-dependent kinase inhibitor 1B (CDKN1B) housekeeping genes as they were among most stably expressed genes in our samples (fully described in section 2.5.3) and Wierschke *et al.*, (2010).

The StatsDirect statistical software (www.statsdirect.co.uk) and GraphPad Prism 6 software for Windows, version 6.05 (www.graphpad.com) were used for the statistical analysis and data presentation. The Shapiro-Wilk test was performed to test the normality of the data and Kruskall–Wallis with Conover–Inman *post hoc* analysis test was then used to identify significant differences between samples ($P < 0.05$).

Table 2.4 TaqMan® gene expression assay IDs for all genes investigated

	Gene symbol	Gene Name	mRNA accession number	Function	TaqMan ID assay	Amplicon length
1	PPIA	Peptidylprolyl isomerase A (cyclophilin A)	NM_021130.3	Protein metabolism and folding	Hs04194521_s1	97
2	CDKN1B	Cyclin-dependent kinase inhibitor 1B (p27, Kip1)	NM_004064.3	Cell growth and division	Hs01597588_m1	151
3	GABA$_{B1}$	Gamma-aminobutyric acid (GABA) B receptor, 1	NM_001470.2	Synaptic transmission, GABA signalling pathway	Hs00559488_m1	68
4	GABA$_{B2}$	GABA B receptor, 2	NM_005458.7	Synaptic transmission, GABA signalling pathway	Hs01554998_m1	158
5	NeuN	Neuronal nuclei or RNA binding protein, fox-1 homolog (C. elegans) 3	NM_001082575.2	mRNA processing and neuronal marker	Hs01370653_m1	58
6	GFAP	Glial fibrillary acidic protein	NM_001131019.2	Astrocyte cytoskeletal protein	Hs00909233_m1	57
7	SGK1	Serum/glucocorticoid regulated kinase 1	NM_001143676.1	Regulate neuronal function and Ion channel activity	Hs00178612_m1	81
8	IP3R1 (ITPR1)	Inositol 1,4,5-trisphosphate receptor, type 1	NM_001099952.2	Intracellular ligand-gated calcium channel activity	Hs00181881_m1	64
9	SCN4B	Sodium channel, voltage-gated, type IV, beta subunit	NM_174934.3	Positive regulation of voltage-gated sodium channel	Hs00545394_m1	71
10	SYNPR	Synaptoporin	NM_001130003.1	Synaptic vesicles protein	Hs00376149_m1	70
11	AQP1	Aquaporin 1	NM_001185060.1	Water transport and cell homeostasis	Hs01028916_m1	96
12	AQP3	Aquaporin 3	NM_004925.4	Water transport and cell homeostasis	Hs00185020_m1	63
13	AQP4	Aquaporin 4	NM_001650.4	Brain water homeostasis	Hs00242342_m1	92
14	AQP5	Aquaporin 5	NM_001651.3	Water channel protein	Hs00387048_m1	68
15	AQP8	Aquaporin 8	NM_001169.2	Water channel protein	Hs00154124_m1	73

Table 2.4 TaqMan® gene expression assay IDs for all genes investigated (continued):

#	Gene symbol	Gene Name	mRNA accession number	Function	TaqMan ID assay	Amplicon length
16	AQP9	Aquaporin 9	NM_020980.3	Water-selective membrane channels	Hs01035888_m1	98
17	AQP11	Aquaporin 11	NM_173039.2	Water transport	Hs00542682_m1	111
18	CCL2	Chemokine (C-C motif) ligand 2	NM_002982.3	Cytokine signalling pathway and neuroinflammation	Hs00234140_m1	101
19	CCL4	Chemokine (C-C motif) ligand 4	NM_002984.2	Cytokine signalling pathway and neuroinflammation	Hs00237011_m1	137
20	CXCL1	Chemokine (C-X-C motif) ligand 1	NM_001511.3	Inflammatory and immune response	Hs00236937_m1	70
21	CXCL2	Chemokine (C-X-C motif) ligand 2	NM_002089.3	Inflammatory and immune response	Hs00601975_m1	100
22	CXCL12	Chemokine (C-X-C motif) ligand 12	NM_000609.6	Inflammatory and immune response, tissue homeostasis neurogenesis	Hs03676656_mH	88
23	CXCR4	Chemokine (C-X-C motif) receptor 4	NM_0010008540.1	Inflammatory and immune response, CXCL12 receptor	Hs00607978_s1	153
24	CX3CR1	Chemokine (C-X3-C motif) receptor 1	NM_001171171.1	Inflammatory and immune response	Hs01922583_s1	162
25	IL1B	Interleukin 1, beta	NM_000576.2	Inflammatory and immune response	Hs01555410_m1	91
26	IL-18	Interleukin 18	NM_001243211.1	Cytokine signalling pathway and interferon-gamma-inducing factor	Hs01038788_m1	115
27	ICAM1	Intercellular adhesion molecule 1	NM_000201.2	Cytokine-mediated signalling pathway	Hs00164932_m1	87
28	Fas	Fas cell surface death receptor	NM_000043.4	Cytokine signalling pathway and apoptosis	Hs00236330_m1	125

63

2.6 Protein extraction

Protein extraction from human hippocampal specimens was done using CelLytic^{TM}MT mammalian tissue Lysis/Extraction reagent (Sigma-Aldrich, C3228) and protease inhibitor cocktail (Sigma-Aldrich, P8340). The cocktail contains inhibitors with a broad specificity for serine, cysteine, and acid proteases, and aminopeptidases. For every 1 gram of tissue, 10ml of CelLytic^{TM} lysis buffer and 10µl of protease inhibitor cocktail were added to the sample in a pre-chilled manual homogenizer. The sample was then homogenized at 4°C and the lysate was centrifuged twice at 500 xg for 15 minutes at 4°C. The pellet was discarded and the collected supernatant was centrifuged at 20,000 xg for 40 minutes at 4°C. The pellet was washed twice with 50mM TrisHCl, pH 7.5 (TBS) and was then re-suspended in TBS according to the original 1 : 10 ratio. The 50µl resuspended pellet aliquots were then stored at - 20°C until further use.

2.7 Total protein determination by BCA assay

The concentration of total proteins extracted from hippocampal specimens were determined by bicinchoninic acid (BCA) assay. The principle of the assay relies on the formation of a stable purple-blue complex between BCA and Copper I (Cu^{1+}) in an alkaline environment. The protein's peptide bond reduces Cu^{2+} to Cu^{1+} and the Cu^{1+} produced from this reaction then forms the stable coloured complex with BCA. Therefore the colour produced is directly proportional to protein concentration (Brown *et al.*, 1989; Walker, 2009).

The BCA reagent was freshly prepared by mixing 50 parts of bicinchoninic acid solution (Sigma-Aldrich, B9643) with 1 part of 4% copper (II) sulphate pentahydrate solution (Sigma-Aldrich, C2284). Bovine serum albumin (BSA) standards were then prepared by making serial dilutions of the stock BSA solution (10µg/µl). The BSA standards concentration were (1, 2, 3, 4, 5, 6, 7, 8, 9, 10) µg/µl. In a 96 well plate, the protein sample (10µl) at a 1:20 dilution was added to the BCA reagent (200µl); every sample was tested in triplicate. The plate was incubated for 1 hour at room temperature on a shaker. The absorbance was measured at 562 nm on a Tecan-Control spectrophotometer. The standard curve was then generated by plotting absorbance against concentration of BSA standards. The protein concentration of unknown sample was calculated from the linear equation of the standard curve with regression (R^2) $\geq$ 0.95.

2.8   Quantitative two colour western blot analysis (WB)

Western blotting also known as protein blotting or immunoblotting is a powerful technique used to identify, quantify and determine the size of specific proteins. The proteins are separated, based on their size, by polyacrylamide gel electrophoresis then they are transferred to a membrane. The target proteins are then identified by using primary antibody, specific to the target, and secondary labelled-antibodies that allow visualization and quantification of target proteins (Kurien and Scofield, 2006; Jensen, 2012). The advantage of WB is that the membrane is easily handled and the proteins transferred on to a membrane, unlike in a gel, are more accessible to many probes (Kurien and Scofield, 2006).

There are many methods of protein detection by WB depending on the secondary antibody used. In the colorimetric method, the secondary antibody is conjugated to an enzyme that produces colour when it reacts with its substrate. In the fluorescence detection method the secondary antibody is labelled with fluorophores. Recently a new method of detection was developed, it involved the use of near-infrared (IR) fluorophores directly conjugated to the secondary antibodies. Those fluorophores need to be excited by a laser beam before they can emit fluorescence such as IRDye™ 800 labelled antibodies (excitation at 778 nm and emission at 800 nm) and IRDye™ 680 labelled (excitation at 680 nm and emission at 700 nm) antibodies (Schutz-Geschwender *et al.*, 2004).

The use of (IR) fluorophores in WB provide many advantages to the technique; it provides a highly sensitive and accurate method for quantifying proteins, low abundant proteins from as small as 1 pg can be accurately quantified, very low background auto fluorescence is detected in the near-IR spectrum, and it allows two - colour WB detection method (Schutz-Geschwender *et al.*, 2004; Ambroz 2006).

The quantitative two-colour WB, provides the detection and quantification of two target proteins simultaneously on the same blot by hybridizing them with two different IR labelled antibodies (700 nm and 800 nm) at the same time. This is a fast and more precise quantification of protein expression as it eliminates the variability due to stripping or comparing separate blots. It also enables more accurate normalization of target protein to a housekeeping control (Picariello *et al.*, 2006).

2.8.1   Protein sample preparation for loading into gels

The proteins were extracted from the samples and quantified by BCA assay (described in sections 1.7 and 1.8). For all proteins investigated by WB, the same amount of total protein (20µg) was loaded in each gel well. The protein samples were prepared by adding 10µl of 2X sample buffer [20% Glycerol, 4.6% SDS, 0.02% Bromophenol blue, 2% DTT and 130 mM Tris-Cl, pH 6.8] to 10µl of protein sample (20µg). The proteins in the mixture were denatured and reduced by incubation at 72°C for 4 minutes, then samples were placed on ice until loaded onto the gel.

2.8.2   Sodium Dodecyl Sulphate Polyacrylamide Gel Electrophoresis (SDS-PAGE)

The SDS-polyacrylamide gel (8%) was placed in the BIO-RAD Mini-protean®Tetra electrophoresis tank filled with 1 X Tris-glycine SDS running buffer (10X running buffer: 0.25 M Tris,1.92 M glycine and 1% SDS in 1 L deionized water). Then 2µl of ColorPlus prestained protein marker (New England BioLab, P7711S) and 20µl protein samples were loaded into the wells. The proteins were then separated by electrophoresis at 120 volts for about 1 hour or until the dye front reached the bottom of the gel.

2.8.3   Protein electro-blotting

Following electrophoresis the SDS-PAGE gel, sponges, blotting paper and Hybond-C Extra nitrocellulose (NC) membrane (Fisher Scientific, 10564755) were submerged in cold Tris-glycine transfer buffer (100 ml 10X transfer buffer, 200 ml methanol and 700 ml water; 10X transfer buffer: 0.25 M Tris and 1.92 M glycine in 1 L deionized water). The WB sandwich was prepared and placed in the BIO-RAD Mini-protean® II cell transfer tank filled with pre-chilled transfer buffer. The proteins were electro-

transferred onto the NC membrane at 100 volts for one hour at 4°C. The membrane was washed briefly in phosphate buffer saline (PBS) for a few minutes then it was blocked with 5% w/v non-fat dry milk (5% NFDM) in PBS and 0.1% Tween 20 (PBST) for one hour at room temperature.

2.8.4   Incubation with antibodies

The primary antibodies were diluted with 0.1% PBST according to table 2.5. The NC membrane was incubated over night at 4°C with gentle shaking and sufficient volume of antibody to completely cover the membrane. Then it was washed 4 times with 0.1% PBST for 5 minutes. The IRDye® secondary antibodies were diluted with 0.1% PBST according to table 2.5 and were incubated with the NC membrane for 1 hour at room temperature. The NC membrane was incubated with both IRDye® 680LT goat anti-mouse IgG (for β-actin detection) and IRDye® 800CW goat anti-rabbit IgG (for target detection) at the same time. Following the incubation time, NC membrane was washed four times with PBS for 5 minutes.

The NC membrane was scanned on an Odyssey infrared imaging system (LI-COR, Biosciences, NE, U.S.A). Typically for each membrane, the instrument "Preset" is set to membrane, 169mm resolution, medium quality and 0 focus offset. Then scanning intensity for both 700 and 800 nm channels are adjusted to get the optimal image of the blot. The band quantification was done on the Odyssey software version 1.2, and Image studio™ lite 4 software (LI-COR, Biosciences). The band signal of target protein was normalized to β-actin band in the same lane, to eliminate any loading variation, as following:

Normalized intensity = Target protein signal / β-actin signal

Table 2.5 Primary and secondary antibodies and their dilutions used in western blot

Target	Primary antibodies	Dilution	Secondary antibodies	Dilution
ACTB	Mouse monoclonal β-actin antibody (S3700, Cell Signaling Technology®)	1 : 1000	IRDye® 680LT goat anti-mouse IgG (926-68020, LI-COR® Bioscience)	1 : 10,000
GABA$_{B1}$	Rabbit polyclonal GABA$_{B1}$ antibody (S3835, Cell Signaling Technology®)	1 : 500	IRDye® 800CW goat anti-rabbit IgG (926-32211, LI-COR® Bioscience)	1 : 5000
GABA$_{B2}$	Rabbit monoclonal GABA$_{B2}$ antibody (ab75838, Abcam®)	1 : 500	IRDye® 800CW goat anti-rabbit IgG (926-32211, LI-COR® Bioscience)	1 : 10,000
NF-L	Rabbit monoclonal Neurofilament-L antibody (S2837, Cell Signaling Technology®)	1 : 500	IRDye® 800CW goat anti-rabbit IgG (926-32211,LI-COR® Bioscience)	1 : 10,000
NeuN	Rabbit polyclonal Anti-NeuN antibody (ABN78, Merck Millipore®)	1 : 2000	IRDye® 800CW goat anti-rabbit IgG (926-32211,LI-COR® Bioscience)	1 : 5000
SGK1	Rabbit monoclonal Anti-SGK1[Y238] antibody (Abcam, ab32374)	1 : 500	IRDye® 800CW goat anti-rabbit IgG (926-32211,LI-COR® Bioscience)	1 : 10,000
SYNPR	Rabbit polyclonal Synaptoporin (H-60) (sc-99075, SANTA CRUZ BIOTECHNOLOGY)	1 : 200	IRDye® 800CW goat anti-rabbit IgG (926-32211,LI-COR® Bioscience)	1 : 5000
SCN4B	Rabbit polyclonal Anti-SCN4B antibody (Abcam,ab80539)	1 : 500	IRDye® 800CW goat anti-rabbit IgG (926-32211,LI-COR® Bioscience)	1 : 5000

Antibodies were diluted with 0.1% PBST

2.8.5 Western blot statistical analysis

The Shapiro-Wilk test was performed to test the normality of the data and Kruskall–Wallis with Conover–Inman *post hoc* analysis test was then used to identify significant differences between samples ($P < 0.05$). StatsDirect statistical software (www.statsdirect.co.uk) and GraphPad Prism 6 software for Windows, version 6.05 (www.graphpad.com) were used for the statistical analysis and data presentation.

2.9 Microarray analysis

DNA microarrays consist of complementary DNA strands called probes which are chemically bound to a solid surface such as a glass slide. The glass slides, unlike nylon membranes, are insensitive to light and provide excellent support to the DNA probes while allowing the use of smallest amount of sample (Stekel, 2003; Trevino *et al.*, 2007).

The probes can be single stranded PCR products or oligonucleotides depending on the type of microarray. The probes can either be ink-jet printed or microspotted on the microarray glass surface. The oligonucleotide microarrays are high quality arrays that have thousands of single-stranded nucleotide probes complementary to target genes in a test sample. Arrays are designed species-specific and they could cover the whole genome or a group of selected genes (Stekel, 2003)

Microarray analysis (MA) is a hybridization-based technique that allows the testing of thousands of genes simultaneously. It has many applications in biomedical and clinical research such as transcriptome profiling in physiological and disease conditions. This helps in understanding the underlying cause of a disease and the identification of new

drug targets. The oligo-based microarrays are the most common arrays used in biomedical research (Trevino *et al.*, 2007; Lemuth and Steffen, 2015).

The Agilent SurePrint microarrays are high quality arrays that are prepared by applying a thin film of an activated monolayer substrate to the glass slide which tightly binds to nucleic acids that are printed on its surface. The oligonucleotide probes are printed by an inkjet method. The probes are synthesized directly on the glass microarray surface via base-by-base repetitive printing rather than printing the full probe. Once the probe is printed it is called a feature. The inkjet printing undergoes multiple real-time monitoring to make sure that features present, size, shape and location are all consistent. Following the probe printing, the glass surface around the feature is deactivated to minimize the background signal (Agilent technologies, 5988-8171EN).

2.9.1   Microarray analysis experimental design

There are many microarray platforms in order to investigate gene expression. Here the two SurePrint G3 Human Gene Expression 8x60K Microarrays (Agilent technologies, Cat. number: G4851A, design ID: 028004) were used; the eight 60K microarrays were printed on 1-inch × 3-inch glass slides. The first microarray slide was used for the transcriptome analysis of TLE-STG and TLE-HS surgical samples. The second slide was used for transcriptome analysis of sclerotic TLE-HS and *post-mortem* hippocampi samples as shown in figure 2.7.
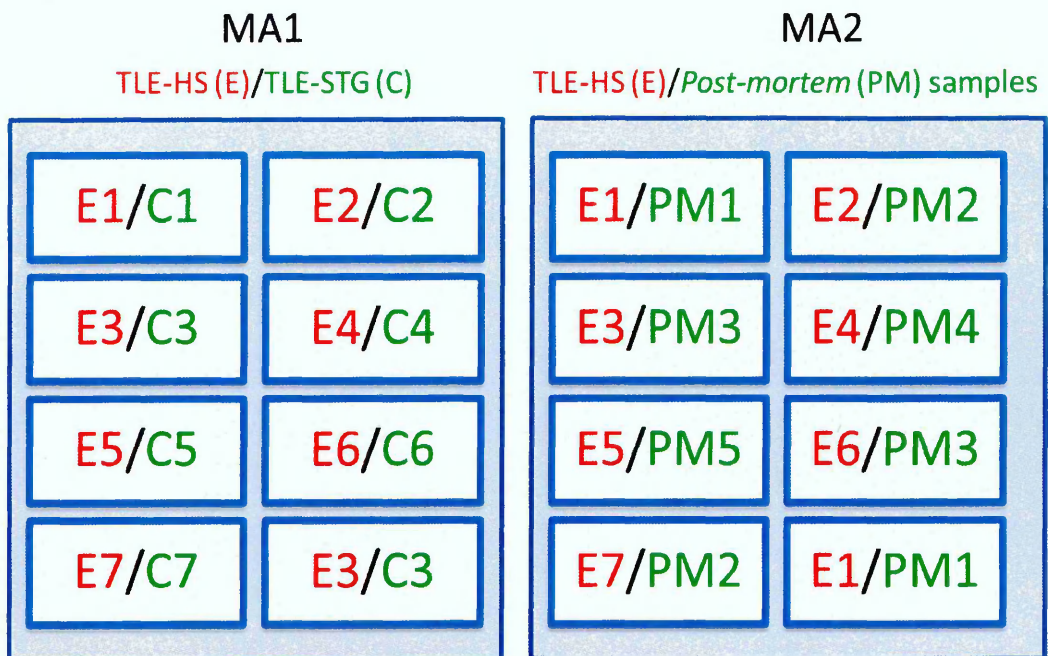
Figure 2.7 Experiment design of microarray analysis

The SurePrint G3 Human gene expression Microarrays (8x60K) slides were used to investigate hippocampal gene expression in sclerotic TLE-HS, TLE-STG and post-*mortem* samples. **E:** sclerotic hippocampi from TLE patients (n = 7). **C:** Non-spiking superior temporal gyrus TLE-STG from TLE patients (n = 7). **PM:** *post-mortem* hippocampi (n = 5). **MA:** Microarray analysis slide.

2.9.2 Microarray analysis workflow

The standard workflow of a two-colour based microarray gene expression analysis shown in figure 2.8; is based on RNA extraction, cDNA and cRNA synthesis, and labelling the target and control samples with fluorescent dyes, cyanine 3 (Cy3) and cyanine 5 (Cy5). Then an equal amount of both labelled samples are hybridized to the microarray at 65°C for 17 hours. This is followed by washing steps, scanning and feature extraction. After RNA extraction, the following steps of RNA amplification, labelling, hybridization and microarray scanning were done in the Centre for Genomic research (CGR) , University of Liverpool, UK.

2.9.3 Sample preparation for microarray analysis

2.9.3.1 RNA extraction

The RNA was extracted from samples by SV Total RNA Isolation System (Promega, Z3100) as described in section 2.3. The RNA concentration (ng/µl) and purity were checked by NanoDrop-1000 spectrophotometer and its integrity was checked by 1% agarose gel electrophoresis. Only high quality total RNA samples with A260/A280 ratio of 1.8 to 2.0 and an A260/A230 ratio of > 2.0 were used for microarray study. The RNA concentrations and integrity were also checked on Agilent 2100 Bioanalyzer in CGR.
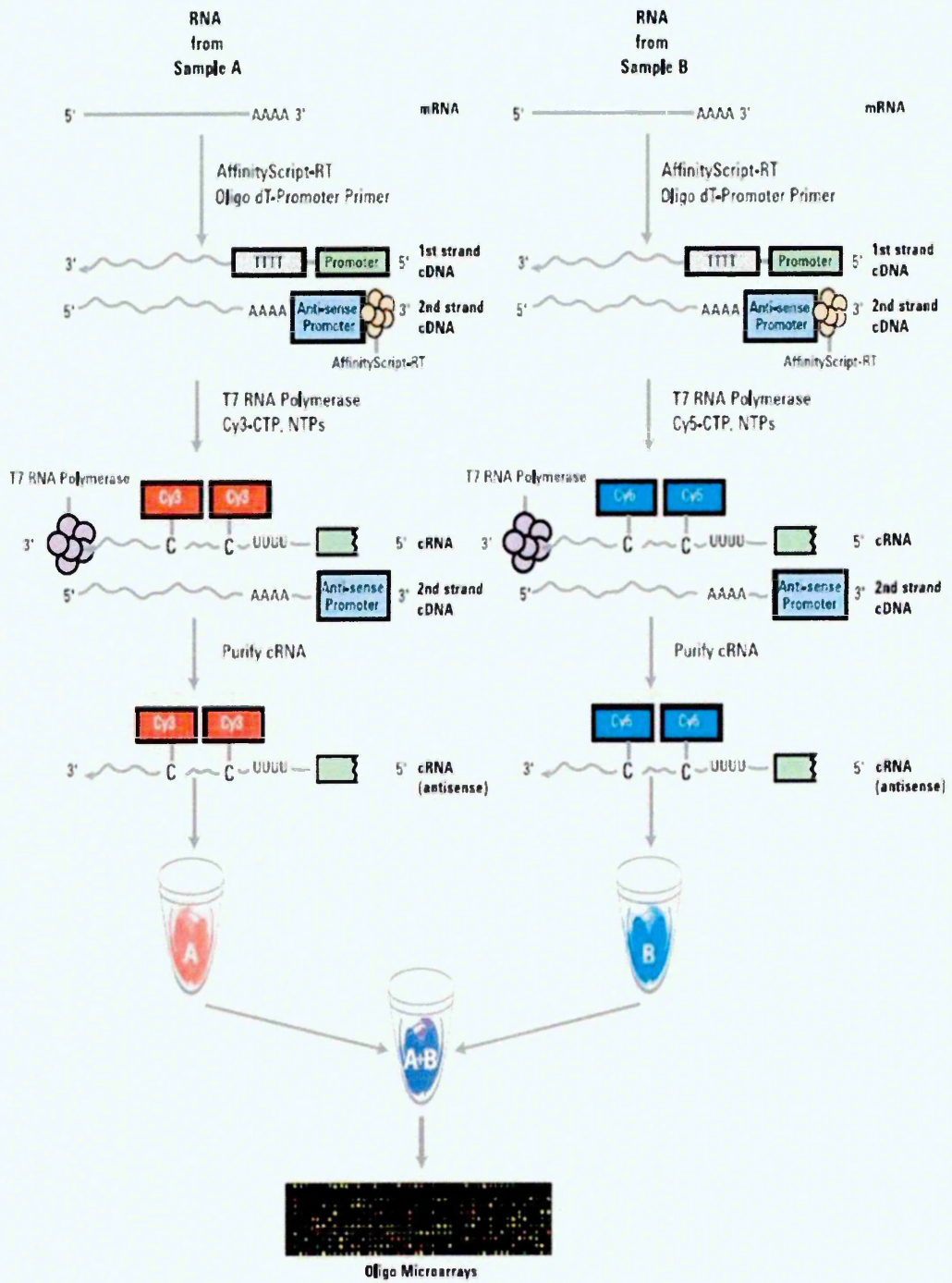
Figure 2.8 Workflow in two-colour microarray gene expression analysis

Adapted from Agilent technologies protocol, G4140-90050.

2.9.3.2 Preparation of spike-in Mix A and B

The RNA Two colour spike-in kit (Agilent technologies, 5188-5279) contains spike-in mix A and B. The spike-in mixes are positive controls that are added to the target RNA, in order to monitor microarray workflow such as amplification, labelling and hybridization. The spike-in is a mixture of 10 *in vitro* synthesized, polyadenylated transcripts (E1A transcripts) which are premixed at various ratios. The spike-in mix A is always labelled with Cy3 while spike-in mix B is labelled with Cy5. For each of the E1A transcripts, the calculated Log ratio of Cy5/Cy3 is plotted against the expected Log ratio and a correlation coefficient ≥ 0.9 demonstrates a high quality microarray data.

The spike-in mix A and B were pre-heated at 37°C for 5 minutes and then mixed well. For each spike-in mix, starting from 2μl of stock solution, four serial dilutions were done according to manufacturer's instructions and in the following order 1:20, 1:40, 1:16 and 1:4. From the fourth dilution 2μl were added to 50 ng of target RNA sample.

2.9.3.3 The cRNA amplification and labelling

RNA samples were processed by using the Two-colour Low Input Quick Amp Labelling Kit (Agilent technologies, 5190-2306). The starting RNA input that could be used is between 10 - 200 ng. The kit uses T7 RNA polymerase to simultaneously amplify and label the target mRNA (with Cy3 or Cy5) with about a 100-fold amplification. In our experiment there are three types of samples that are investigated: the TLE-HS hippocampi samples were labelled with Cy5, while TLE-STG and PMC samples were labelled with Cy3.

cDNA synthesis: 2µl of diluted spike-in mix were added to 50 ng of RNA sample (1.5µl) . Spike-in mix A was added to TLE-STG and PMC samples, while spike-in mix B was added to TLE-HS samples. Then 1.8µl of T7 oligo dT primer and 3.5µl target RNA sample (contain spike-in mix) were mixed and incubated at 65°C for 10 minutes and then they were placed on ice for 5 minutes. The 5X first strand buffer was incubated at 80°C for 4 minutes and was then allowed to cool to room temperature before it was added to the cDNA master mix. The cDNA master mix (4.7µl) was prepared by adding; 2µl of pre-heated 5X first stand buffer, 1µl of 0.1M DTT, 0.5µl of 10mM dNTPs mix, 1.2µl of Affinity Script RNase Block Mix. To each sample, a 4.7µl of cDNA master mix was added and reaction was incubated at 40°C for 2 hours then at 70°C for 15 minutes to stop the reaction. The cDNA samples synthesized (10µl) were then placed on ice for 5 minutes.

cRNA synthesis and labelling: two transcription master mixes were prepared as in table 2.6 , one with Cy3-CTP and the other with Cy5-CTP depending on the sample. Then to 10µl of cDNA samples previously synthesised, 6µl of transcription master mix were added and the reaction was incubated at 40°C for 2 hours, followed by placing the sample on ice.

Table 2.6 Transcription master mix components

Component	TLE-HS samples volume per reaction (µl)	TLE-STG, PMC samples volume per reaction (µl)
Nuclease-free water	0.75	0.75
5× transcription buffer	3.2	3.2
0.1 M DTT	0.6	0.6
NTPs Mix	1	1
T7 RNA polymerase blend	0.21	0.21
Cyanine 3-CTP	-	0.24
Cyanine 5-CTP	0.24	-
Total volume	**6**	**6**

The labelled cRNA purification was purified by RNeasy Mini Kit (Qiagen, 74104). 84µl nuclease-free water was added to the 16µl of labelled cRNA. First 350µl of buffer RLT and then 250µl of 96% ethanol were mixed with the diluted cRNA. The mixture was transferred to an RNeasy Mini Spin Column and was then centrifuged at 4°C for 30 sec at 13,000 xg. The RNeasy column was then transferred to a new collection tube and 500µl of buffer RPE were added to the column and then centrifuged at 4°C for 30 sec at 13,000 xg. The collection tube was emptied and another 500µl of buffer RPE was added to the column and then it was centrifuged at 4°C for 60 sec at 13,000 xg. The collection tube was emptied and the column was centrifuged again at 4°C for 30 sec at 13,000 xg to remove any traces of Buffer RPE. The column was transferred to a sterile collection tube and the pure cRNA was eluted by adding 30µl RNase-Free water directly onto the RNeasy filter membrane. After waiting for 1 minute the column was centrifuged at 4°C for 30 sec at 13,000 xg. The cRNA sample was stored at - 80°C.

2.9.3.4 The labelled cRNA quantification

The cRNA concentration (ng/µl), the Cy3 and Cy5 concentrations (pmol/µl) were all determined using the NanoDrop ND-1000 UV Spectrophotometer. The cRNA yield and Cy3 and Cy5 specific activity were calculated according to the following formulas:

$$\mu g \text{ of cRNA} = \frac{\text{cRNA Conc. (ng/µl)} \ X \ 30 \ \mu l \text{ (elution volume)}}{1000}$$

$$\text{pmol of Cy3 or Cy5 /µg cRNA} = \frac{\text{Cy3 or Cy5 Conc. (pmol/µl)}}{\text{cRNA Conc. (ng/µl)}} \ X \ 1000$$

For optimal microarray hybridization the cRNA yield should be at least 0.825 µg and Cy3 or Cy5 specific activity should be at least 6 pmol /µg cRNA.

2.9.3.5 Microarray hybridization

The hybridization was done using the Gene Expression Hybridization Kit (Agilent technologies, 5188-5242). For each microarray, equal amounts of the two samples were mixed gently with 10× gene expression blocking agent and 25× fragmentation buffer as in table 2.7. The mix was incubated at 60°C for 30 minutes to fragment the RNA and was then placed on ice for 1 minute. 25µl of 2× Hi-RPM hybridization buffer was mixed gently with the cRNA sample without introducing bubbles then it was centrifuged at room temperature for 1 min at 13,000 xg.

Table 2.7 Sample preparation for hybridization

Components	Volume/Mass
Cy3 labelled cRNA (TLE-STG or PMC)	300 ng
Cy5 labelled cRNA (TLE-HS)	300 ng
10× gene gxpression blocking agent	5µl
Nuclease-free water	bring volume to 24µl
25× fragmentation buffer	1µl
Total volume	25µl

The hybridization sample was then loaded onto the microarray by slowly dispensing 40µl of the sample onto the gasket well, without introducing any air bubbles. Then samples were hybridized at 65°C for 17 hour by placing the assembled slide chamber into a rotating hybridization oven. Following hybridization, the microarray hybridization chamber was disassembled at room temperature in gene expression wash buffer 1 (Agilent Technologies, 5188-5327). The microarray slide was placed into the slide rack and was washed with gene expression wash buffer 1 for 1 minute at room temperature. Then it was washed for another minute with the pre-warmed gene expression wash buffer 2 (warmed overnight to 37°C). The microarray slide was placed in a slide holder ready for scanning.

2.9.3.6 Microarray scanning and feature extraction

Following the washing steps, the microarrays were scanned immediately on Agilent Technologies SureScan Microarray Scanner and data was extracted using Agilent feature extraction software version 10.7.1. The features background signal was subtracted by local subtractions method. The raw data obtained was Log_2 ratio of Cy5/Cy3. The analysis of microarray data is fully described in chapter 5 (section 5.2.4).

Chapter 3

Expression of GABA$_B$ receptor in sclerotic hippocampi from refractory TLE-HS patients

3   Expression of GABA$_B$ receptor in sclerotic hippocampi from refractory TLE-HS patients

3.1   Introduction

In the brain γ-amino butyric acid (GABA) is the main inhibitory neurotransmitter. It acts on 2 types of receptors: ionotropic and metabotropic. The ionotropic GABA$_A$ and GABA$_C$ receptors are responsible for fast synaptic inhibition. The metabotropic GABA$_B$ receptors are G-protein-coupled receptors that are present on pre- and postsynaptic membranes in neuronal synapses (Jacob *et al.*, 2008; Benarroch, 2012). They are responsible for the slow and prolonged inhibitory postsynaptic potential (IPSP). GABA$_B$ receptors are also expressed in astrocytes and microglia (Charles *et al.*, 2003; Oka *et al.*, 2006). Many studies suggested that GABA$_B$ receptor could be implicated in TLE-HS pathophysiology (Billinton *et al.*, 2001a; 2001b; Muñoz *et al.*, 2002; Princivalle *et al.*, 2002 ; 2003; Benke *et al.*, 2012).

3.1.1   GABA$_B$ receptors subunits

3.1.1.1   Principal or core subunits

The functional GABA$_B$ receptor is an obligatory heterodimer composed of two principal subunits, GABA$_{B1}$ and GABA$_{B2}$. The core subunits are seven-transmembrane domain (7TM) subunits that have large extracellular N-terminal domains known as 'venus flytrap domain' (VFTD) and a large intracellular C-terminal domain that forms the coiled-coil dimerization domain. The GABA$_{B1}$ extracellular N-terminal domain contains the GABA binding site and its C-terminal domain contains the endoplasmic reticulum

(ER) retention/retrieval signal. The GABA$_{B2}$ N-terminal domain does not have a ligand binding site but the transmembrane-domain has an allosteric binding site, which influences the GABA binding affinity to GABA$_{B1}$ (Billinton *et al.*, 2000; Benarroch, 2012; Benke *et al.*, 2012; Gassmann and Bettler, 2012). The GABA$_{B1}$ subunit has two isoforms, GABA$_{B1a}$ and GABA$_{B1b}$ which are splice variants from the *GABA$_{B1}$* gene. The GABA$_{B1a}$ differs from GABA$_{B1b}$ by having an additional two protein-protein domains at the extracellular N-terminal known as sushi domains as in figure 3.1 (Bettler *et al.*, 2004).

3.1.1.2 Auxiliary subunits

Recent research found that the GABA$_B$ receptor is also composed of auxiliary subunits. The C-terminus of GABA$_{B2}$ is tightly associated with those auxiliary subunits which are potassium channel tetramerization T1 domain-containing (KCTD) protein members as in figure 3.1. Those protein members are KCTD8, KCTD12, KCTD12b and KCTD16 and they bind to the receptor in tetramers to form a stable receptor complex at the cell membrane (Gassmann and Bettler, 2012; Turecek *et al.*, 2014; Xu *et al.*, 2014; Rajalu *et al.*, 2015).

The KCTD auxiliary proteins could influence the GABA binding-affinity of the receptor, KCTD8 and 16 were found to slightly increase the GABA binding-affinity (Rajalu *et al.*, 2015). KCTD could also bind to the G-protein at the receptor and differentially regulate the G-protein signalling. KCTD12 reduced the receptor internalization and therefore increasing the magnitude of receptor signalling (Turecek *et al.*, 2014; Xu *et al.*, 2014; Rajalu *et al.*, 2015).
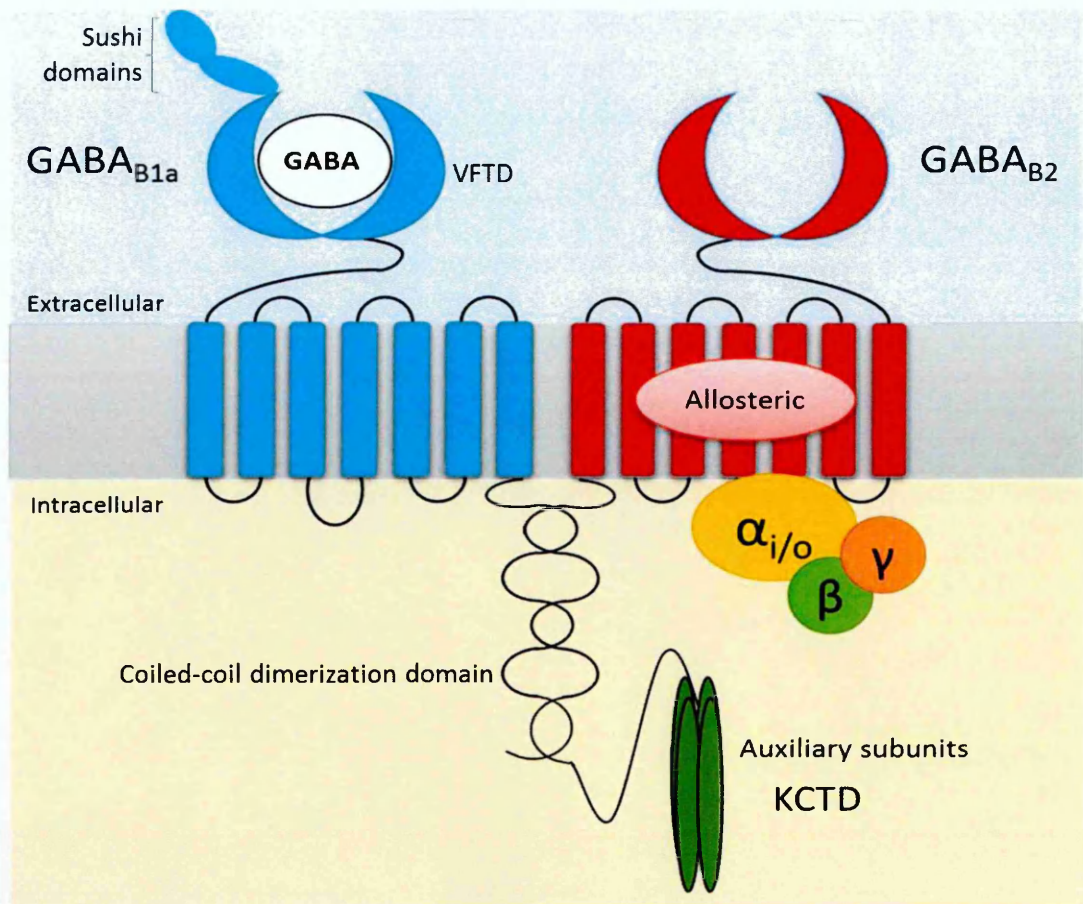
Figure 3.1 GABA$_B$ receptor principal and auxiliary subunits

GABA$_B$ is composed of 2 seven-transmembrane-domain (7TM) principal subunits: GABA$_{B1}$ and GABA$_{B2}$. The N-terminal venus flytrap domain (VFTD) of GABA$_{B1}$ subunit contain GABA binding site. GABA$_{B1a}$ isoform has two additional protein domains at the extracellular N-terminal known as sushi domains. The GABA$_{B2}$ 7TM domain has an allosteric binding site and its C-terminal binds to potassium channel tetramerization domain-containing protein (KCTD) auxiliary subunits. Adapted from Benke *et al*. (2012).

3.1.2 GABA$_B$ receptor assembly and trafficking

The GABA$_{B1}$ with GABA$_{B2}$ subunits are synthesized in the endoplasmic reticulum from *GABBR1* and *GABBR2* genes respectively, where they are assembled into a complex by the coiled-coil interaction between the 2 subunits. This assembly will mask the endoplasmic reticulum-retention signal (ER retention signal), in the GABA$_{B1}$ C- terminal domain, ensuring that only the heteromeric GABA$_{B1}$ and GABA$_{B2}$ receptor could be exported from the ER as in figure 3.2. Therefore, heteromeric assembly of GABA$_{B1}$ with GABA$_{B2}$ subunits is vital for the receptor trafficking to the cell surface (Benke *et al.*, 2012; Valenzuela *et al.*, 2014).

3.1.3 GABA$_B$ receptors mechanism of action

GABA$_B$ receptors are responsible for slow synaptic inhibition as they prolong the late inhibitory postsynaptic potential (IPSP) (Billinton *et al.*, 2001a; Benarroch, 2012). The activation of presynaptic GABA$_B$ receptors inhibits the release of neurotransmitters such as GABA and glutamate, while the activation of postsynaptic GABA$_B$ causes prolonged IPSP (Benke *et al.*, 2012).

The GABA$_B$ receptor is activated by binding of GABA to GABA$_{B1}$ subunit and this will lead to the recruitment and activation of the G-protein (G$\alpha_{i/o}$) by GABA$_{B2}$ subunit. The activated G-protein will act on three targets; adenylyl cyclase, voltage-gated calcium channels (VGCCs) and G protein-activated inwardly rectifying potassium channels (GIRKs) as in figure 3.3.
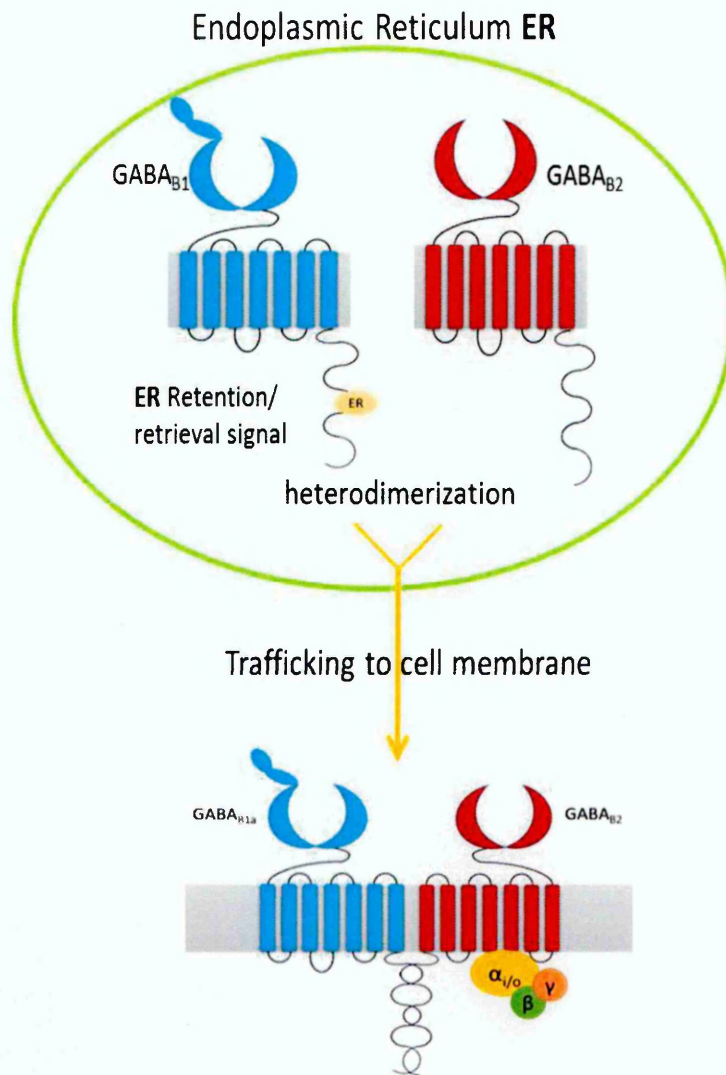
Figure 3.2 GABA$_B$ receptor assembly and trafficking to cell membrane

The heteromeric assembly of GABA$_{B1}$ and GABA$_{B2}$ subunits hides the endoplasmic reticulum-retention signal in GABA$_{B1}$ subunit and allows the receptor to be exported from the endoplasmic reticulum and trafficked to the cell membrane. Adapted from Valenzuela *et al*. (2014).
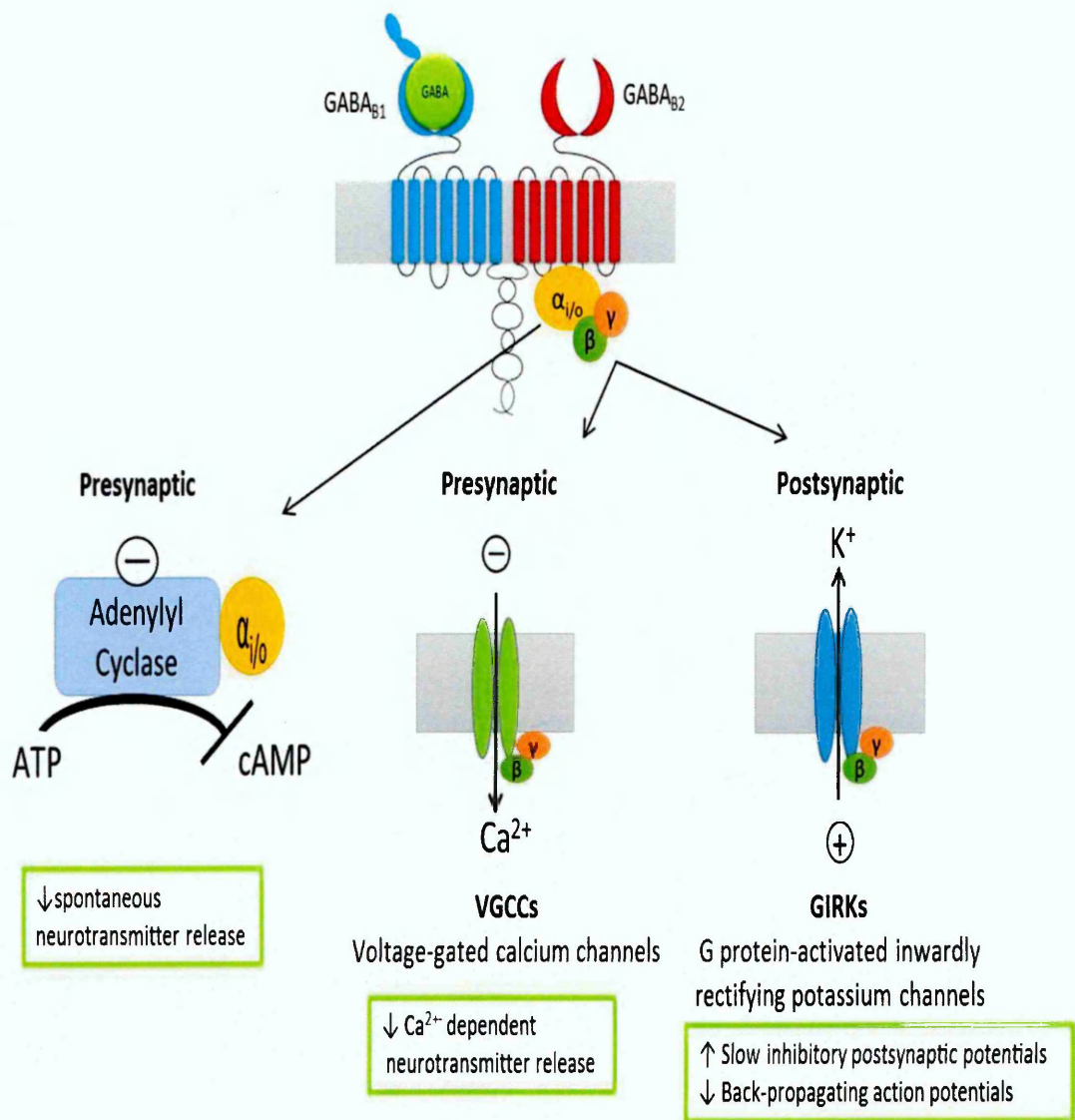
Figure 3.3 GABA$_B$ receptor activation and mechanism of action

The binding of GABA to GABA$_{B1}$ subunit leads to the activation of the G-protein which subsequently acts on three targets; adenylyl cyclase, voltage-gated calcium channels (VGCC) and G protein-activated inwardly rectifying potassium channels (GIRKs). Adapted from Gassmann and Bettler (2012).

The α-subunit of the activated G protein will inhibit adenylyl cyclase and lowers the level of cyclic adenosine monophosphate (cAMP). In pre-synapse, the reduced cAMP levels will hinder synaptic vesicle fusion and reduce the spontaneous neurotransmitter release. In postsynapse, the low cAMP levels will reduce cAMP dependent protein kinase A (PKA) activity and inhibit the calcium permeability of NMDA glutamate receptor (Skeberdis *et al.*, 2006; Gassmann and Bettler, 2012).

The βγ dimer subunits of the activated G protein reduce calcium dependent neurotransmitter release by inhibiting presynaptic VGCCs and by interacting directly with SNARE (soluble *N*-ethylmaleimide-sensitive factor attachment protein receptor) a synaptic vesicle fusion complex (Yoon *et al.*, 2007). The βγ dimer also activates the postsynaptic GIRKs causing an outward K^+ current and hyperpolarized membrane that leads to prolonged IPSP and the subsequent inhibition of back propagating action potentials (Benarroch, 2012; Benke *et al.*, 2012).

In addition to $GABA_B$ inhibition function, it was reported that $GABA_B$ receptors in hippocampal neuronal cultures promoted $GABA_A$ receptor surface expression via increasing the secretion of endogenous brain-derived neurotrophic factor (BDNF). The βγ subunits released from Gi/o proteins leads to the activation of phospholipase C, generation of diacylglycerol, and activation of protein kinase C (PKC). PKC mediates the phosphorylation of L-type VGCCs and subsequent secretion of BDNF (Kuczewski *et al.*, 2011).

3.1.4 GABA$_B$ receptors in TLE-HS

GABA$_B$ receptors were hypothesised to have an important role in the pathophysiology of TLE associated with HS. Many studies suggested that there was a reduction in the GABA-mediated inhibition in the neurons of the sclerotic hippocampus of temporal lobe epilepsy (Mangan and Lothman, 1996; Billinton *et al.*, 2001a; Princivalle *et al.*, 2003). Electrophysiological studies also showed a reduction in the inhibitory postsynaptic potential in sclerotic hippocampal neurons (Mangan and Lothman, 1996; Teichgräber *et al.*, 2009).

The distribution and expression levels of GABA$_{B1a}$, GABA$_{B1b}$ and GABA$_{B2}$ mRNA were studied in human TLE-HS samples by *in situ hybridisation*; neuronal loss was evident compared to the control hippocampi and there were alterations in the expression levels of GABA$_B$ subunits in the different subregions of the hippocampus. However, when the expression level was calculated per neuron to normalize for the neuronal loss, it showed that expression levels of GABA$_{B1a}$, GABA$_{B1b}$ and GABA$_{B2}$ were significantly higher in the surviving neurons (Billinton *et al.*, 2001a; Princivalle *et al.*, 2003).

The investigation of protein expression level is required to extend our understanding of the role of the GABA$_B$ in TLE-HS. The GABA$_B$ receptor distribution was studied in the animal models of TLE (Benke *et al.*, 1999; Straessle *et al.*, 2003) and in human TLE-HS specimens (Muñoz *et al.*, 2002). However, so far no quantitative studies of GABA$_{B1a}$, GABA$_{B1b}$ and GABA$_{B2}$ subunits were performed in human TLE-HS specimens.

3.1.5 Aims of the study

The aim of this study was to do: **1)** Quantitative analysis of $GABA_B$ subunits transcript levels in TLE-HS and PMC samples to further corroborate the *in situ hybridisation* data (Billinton *et al.*, 2001a; Princivalle *et al.*, 2003). **2)** mRNA quantitative analysis of $GABA_B$ subunits in the TLE-STG samples. **3)** Quantitative analysis of $GABA_B$ subunits protein level in TLE-HS, TLE-STG and PMC. This will lead to further understanding of the role of $GABA_B$ receptor in refractory TLE-HS pathophysiology.

3.2 Materials and methods

3.2.1 Patient clinical information

Clinical information for TLE-HS, TLE-STG and PMC samples investigated in this chapter is described in Appendix I.

3.2.2 Study design

The selection of a stable housekeeping gene was followed by the investigation of mRNA levels of PPIA, CDKN1B, $GABA_{B1}$, $GABA_{B2}$ and NeuN by qRT-PCR in TLE-HS (n = 26), TLE-STG (n = 11) and PMC (n = 10) samples. The protein expression of $GABA_{B1a}$, $GABA_{B1b}$, $GABA_{B2}$, NeuN, NF-L and β-actin (ACTB) were investigated by two-colour quantitative western blot in TLE-HS (n = 9), TLE-STG (n = 6) and PMC (n = 4) samples. Significant difference between the samples was identified by Kruskal-Wallis with Conover-Inman *post hoc* analysis test.

3.2.3 Methods

qRT-PCR: In brief, the total RNA was extracted by SV Total RNA Isolation System (section 2.3.1) and then was reverse transcribed using SuperScript^{TM} III first strand synthesis system (section 2.4). Stable housekeeping genes were selected for the normalization of target gene expression (section 2.5.3). The TaqMan$^{©}$ primers amplification efficiency of housekeeping and target genes was assessed first (section 2.5.4) prior to performing the qRT-PCR using TaqMan$^{©}$ gene expression assays (section 2.5.5).

WB: Briefly the total proteins were extracted from hippocampi samples using CelLytic^{TM}MT mammalian tissue extraction reagent (section 2.6).Then total protein determination was assessed by the BCA assay (section 2.7). Quantitative two colour western blotting was done for all samples by electrophoresis of 10μg protein followed by electro-transfer onto a nitrocellulose membrane. The membrane was then blocked, incubated with primary and secondary antibodies before it was scanned on the Odyssey infrared imaging system (section 2.8).

3.3 Results

3.3.1 RNA purity and integrity

High quality and pure RNA is essential for an effective and good reverse transcription reaction and qRT-PCR analysis. The extracted total RNA purity was assessed by the NanoDrop-1000 spectrophotometer, A260/A280 ratio indicated the presence of protein contamination and A260/A230 ratio indicated the presence of guanidine thiocyanate and alcohol contamination.

Only RNA samples with A260/A280 ratio of 1.8 - 2.0 and A260/A230 ratio of 2.0 - 2.2 as in figure 3.4 were considered free of contaminants and were used for qRT-PCR analysis. The integrity of total RNA extracted was also assessed by running 1% agarose gel electrophoresis. An intact RNA sample with no degradation should have 2 distinct bands for 28S and 18S ribosomal RNAs in an approximately 2:1 ratio as in figure 2.5.
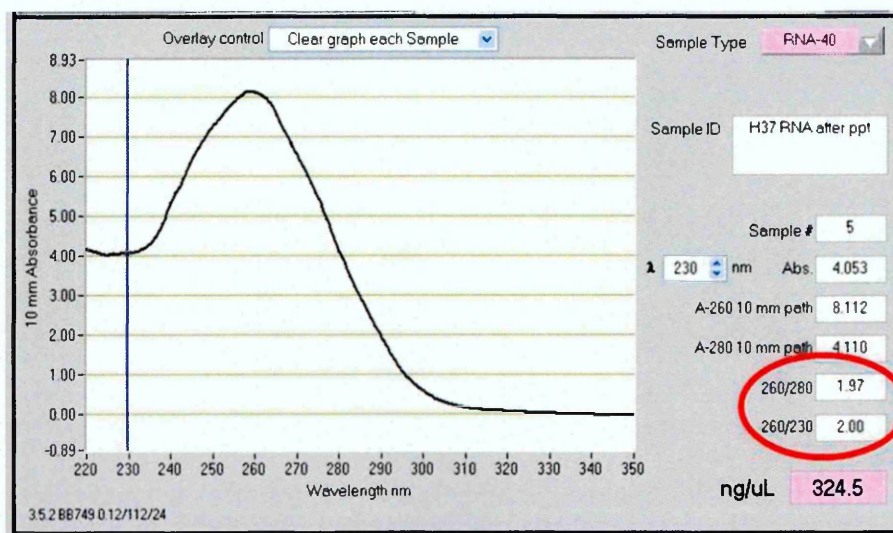
Figure 3.4 RNA sample purity assessed by the NanoDrop-1000 spectrophotometer
The RNA samples 260/280 ratio was 1.97 and 260/230 ratio was 2.00 indicating a pure RNA sample suitable for further investigations such reverse transcription, RT-PCR and MA analysis.

3.3.2 Selection of stable housekeeping genes for qRT-PCR analysis

In the relative qRT-PCR analysis, the expression of target gene is normalized to HKGs and thus it is vital to select the most stable HKGs that are not affected by experimental and pathological conditions (Radonić *et al.*, 2004; Wierschke *et al.*, 2010). Therefore in our study, 32 HKGs were tested in 6 samples, in triplicates, to check their stability. The analysis was done according to Applied Biosystems Application Note (127AP08) and Radonić *et al.* (2004). For every gene, the average C_t values and standard deviation (Stdev) were calculated and then plotted as in figure 3.5. The gene variability for each HKG was determined and plotted as in figure 3.6, and PPIA and CDKN1B were selected as normalization genes for subsequent qRT-PCR analysis as they were most stable. The Ct values of PPIA and CDKN1B in all the samples used were determined and plotted as in figure 3.7 to ensure their stability in all samples.

3.3.3 Primer efficiency

Once the HKGs were selected the primer efficiency for each gene was determined. For every gene the standard curve was done by plotting the average C_t value against Log_{10} cDNA concentration as in figure 3.8. The standard curve slope was used to calculate primers efficiency. The resulting primer efficiencies ranged from 96 % to 99.6 % and were within 5% of each other (table 3.1), making them very suitable for comparative qRT-PCR analysis.
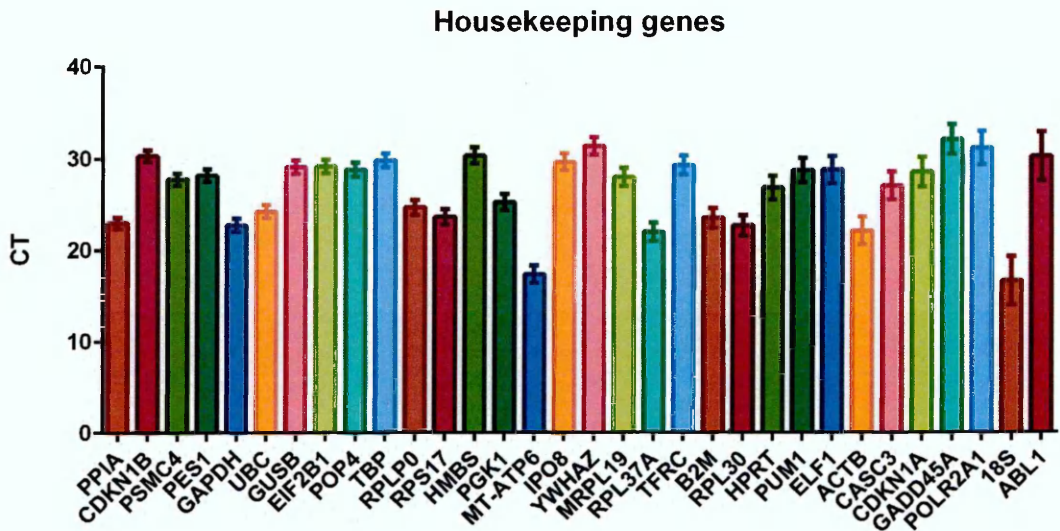
Figure 3.5 Threshold cycle (C$_t$) of 32 housekeeping genes in 6 samples

The C$_t$ is the cycle number at which the target fluorescence exceeds the threshold fluorescence. Refer to table 2.3 in section 2.5 for HKGs names. Data presented as the C$_t$ mean ± StDev (n = 6). **CT**: Threshold cycle (C$_t$).
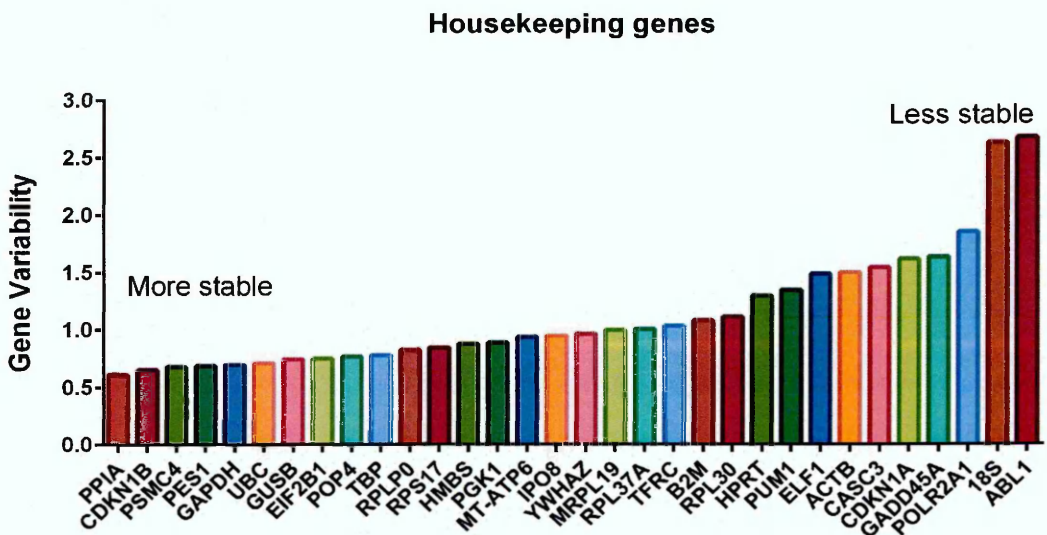
Figure 3.6 Variability of 32 housekeeping genes in 6 samples

The variability of each gene in the 6 samples is C$_t$ standard deviation. The PPIA and CDKN1B were selected as normalizing genes as they were 2 of the most stable genes. Refer to table 2.3 in section 2.5 for HKGs names.
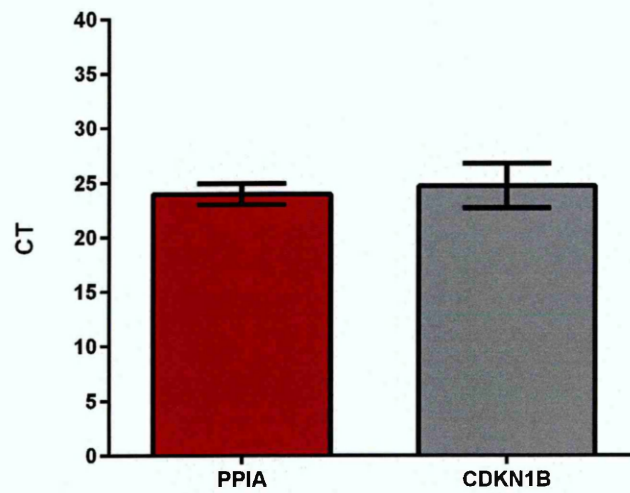
Figure 3.7 PPIA and CDKN1B gene variability

The C_t values of PPIA and CDKN1B obtained from RT-PCR were determined in all TLE-HS, TLE-STG and PM control samples. Data presented as C_t mean ± standard deviation. Number of samples: TLE-HS (n =26), TLE-STG (n = 11) and PM control (n = 10). **CT**: Threshold cycle (C_t).
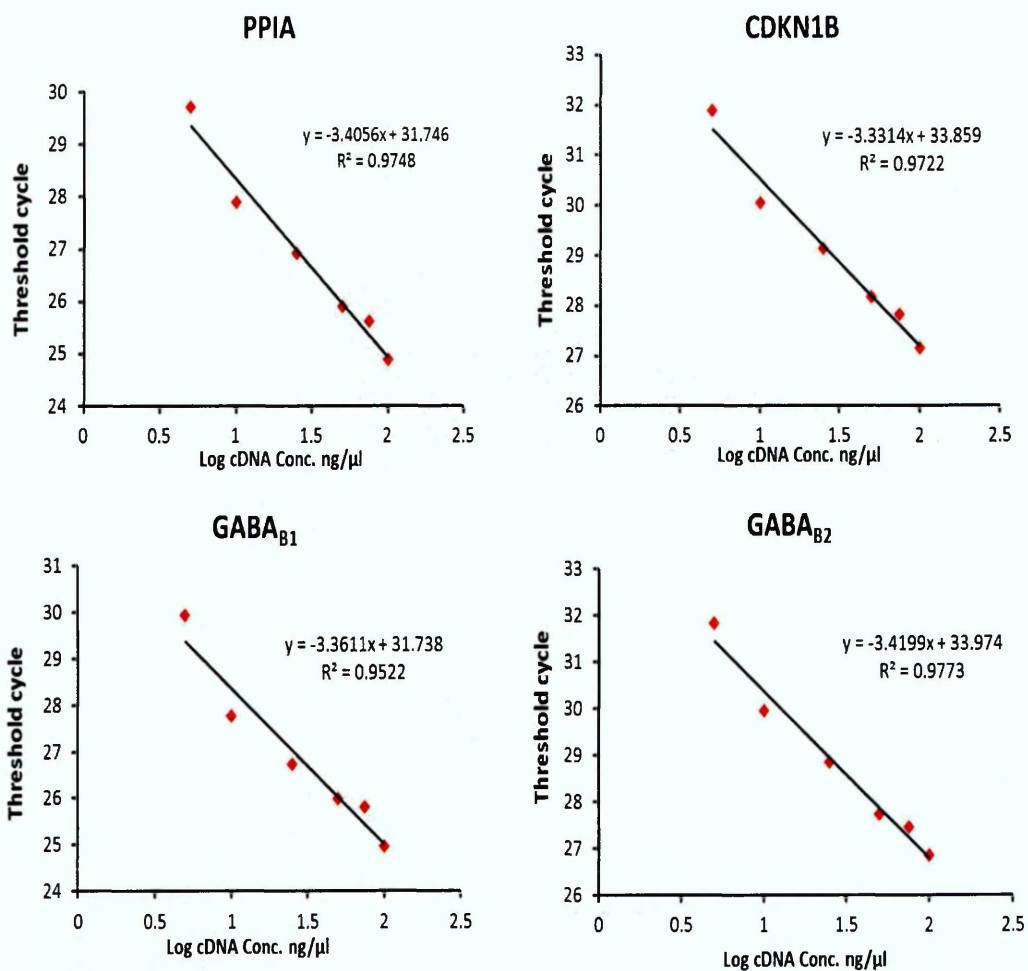
Figure 3.8 Standard curves for primer efficiency determination

PPIA, CDKN1B, GABA$_{B1}$ and GABA$_{B2}$ primers had good linear regression R^2 = 0.95-0.98

Table 3.1 TaqMan© assay primer amplification efficiency for all housekeeping and target genes used for qRT-PCR

Gene	Slope	R²	Primer efficiency (%)
PPIA	-3.4	0.97	96.84
CDKN1B	-3.33	0.97	99.66
GABA$_{B1}$	-3.36	0.95	98.03
GABA$_{B2}$	-3.41	0.98	96.45
NeuN	-3.42	0.98	96.06

3.3.4   Relative $GABA_{B1}$ and $GABA_{B2}$ mRNA expression

The data from qRT-PCR show a very similar trend for both $GABA_{B1}$ and $GABA_{B2}$ subunits. Comparing TLE-HS to PMC sample it can be seen that $GABA_{B1}$ mRNA is not varying whereas $GABA_{B2}$ mRNA level demonstrated an increased expression in TLE-HS. On the contrary, comparing TLE-HS to TLE-STG, both subunits mRNA level showed a reduced level of expression in TLE-HS. However, only $GABA_{B2}$ mRNA expression was significantly decreased in TLE-HS compared to TLE-STG as shown in figure 3.9.

3.3.5   Relative Neuronal nuclei (NeuN) mRNA expression

The neuronal marker NeuN mRNA expression obtained from qRT-PCR analysis showed a significant decrease in TLE-HS tissue compared to PMC. It also showed a decreased expression in TLE-HS tissue compared to TLE-STG, thought it was not significant as in figure 3.10.
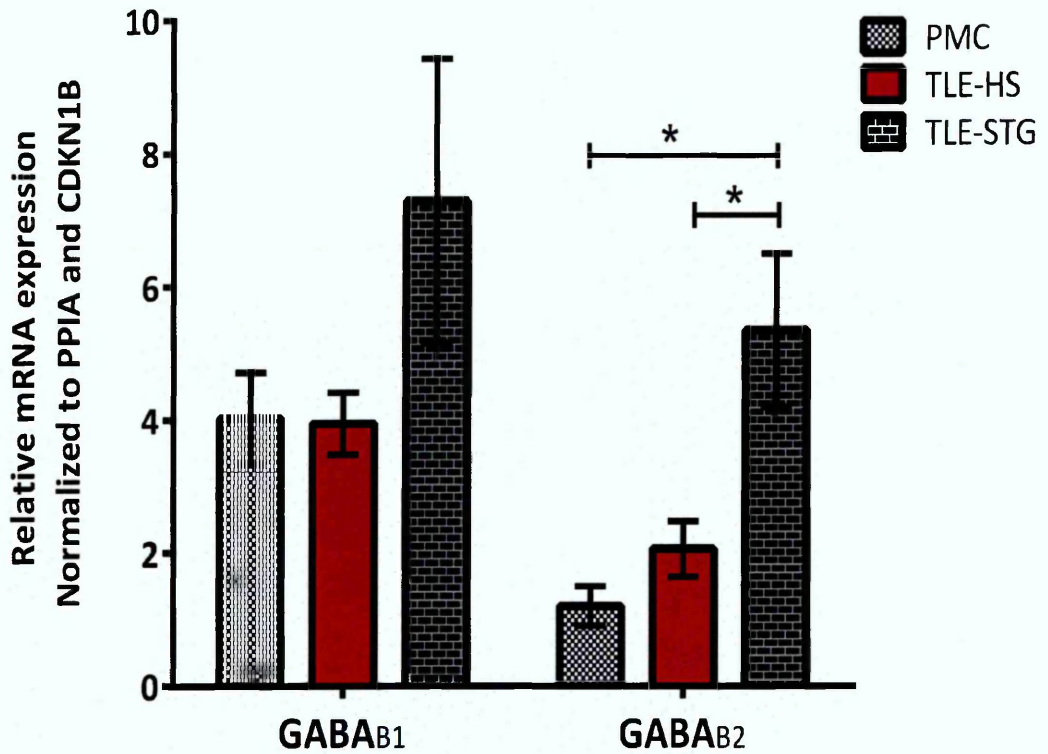
Figure 3.9 qRT-PCR data showing the relative mRNA expression of GABA$_{B1}$ and GABA$_{B2}$ in TLE-HS, TLE-STG and PMC

The GABA$_{B1}$ mRNA level in TLE-HS was not significantly altered compared to PMC and was decreased compared to TLE-STG. The GABA$_{B2}$ mRNA level in TLE-HS was increased compared to PMC but was significantly reduced compared to TLE-STG. qRT-PCR data analysis was done by $2^{-\Delta CT}$ method. Statistical analysis: Kruskal-Wallis with Conover-Inman *post hoc* analysis test was used to identify significant differences between samples (* $P < 0.05$). Number of samples: TLE-HS (n =26), TLE-STG (n = 11) and PMC (n = 10). Data presented as mean ± S.E.M.
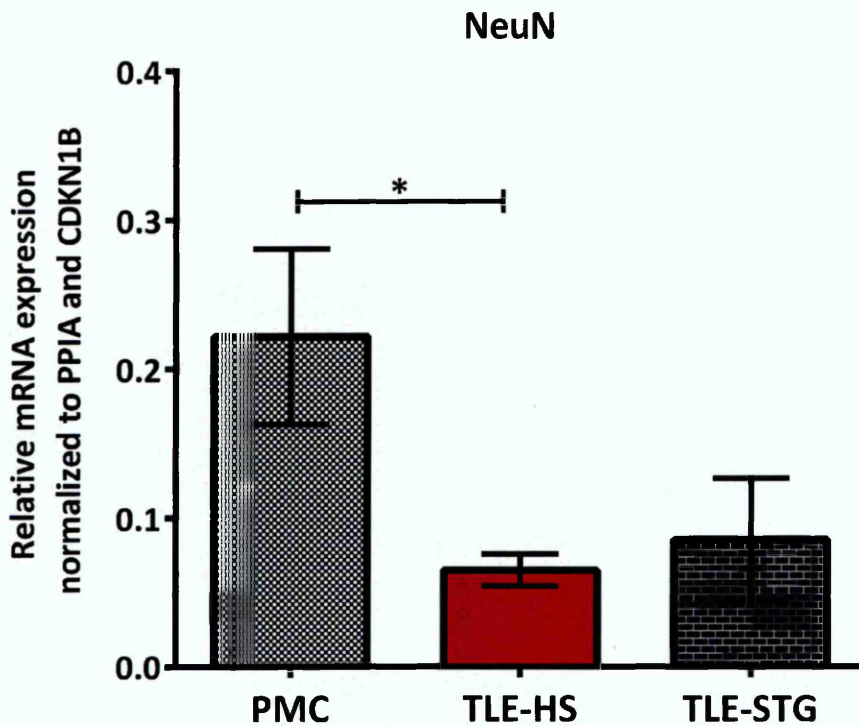
Figure 3.10 qRT-PCR data showing the relative mRNA expression of NeuN in TLE-HS, TLE-STG and PMC

The NeuN mRNA was significantly reduced in TLE-HS compared to PMC. The TLE-HS NeuN mRNA level was slightly decreased compared to TLE-STG. The qRT-PCR data analysis was done by $2^{-\Delta CT}$ method. Statistical analysis: Kruskal-Wallis with Conover-Inman *post hoc* analysis test was used to identify significant differences between samples (* $P < 0.05$). Number of samples: TLE-HS (n =26), TLE-STG (n = 11) and PMC (n = 10). Data presented as mean ± S.E.M.

3.3.6 Total protein quantification in hippocampi samples

The extracted total proteins were quantified by the bicinchoninic acid (BCA) assay to ensure the same amount of proteins was loaded for WB analysis. A standard curve was generated by plotting bovine serum albumin (BSA) concentrations against their absorbance at 562 nm as in figure 3.11. The protein concentration of unknown samples were calculated using linear equation of the standard curve $y = 0.2766 x + 0.3757$, where y = absorbance and x = protein concentration.

Protein Standard Curve

$y = 0.2766 x + 0.3757$
$R^2 = 0.9817$
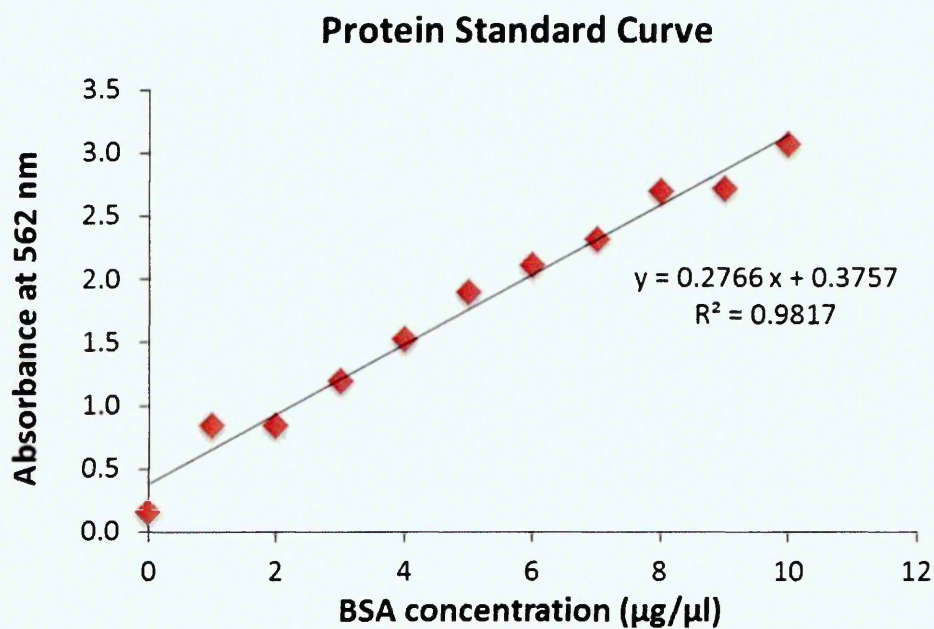
Figure 3.11 BSA standard curve for protein determination

The protein concentration of unknown sample was determined from the curve linear equation $X = (y - 0.375)/0.2766$, where x = protein concentration and y = unknown sample absorbance at 562 nm.

3.3.7 Western blot quantification of GABA$_{B1}$ and GABA$_{B2}$ receptor subunits

The double-labelled western blots in TLE-HS, TLE-STG and PMC samples demonstrated an alteration in expression of GABA$_B$ isoforms and subunits compared to the consistent expression of β-actin. In all samples GABA$_{B1}$ subunit showed a distinct 2 bands at 130 and 95 KDa for GABA$_{B1a}$ and GABA$_{B1b}$ isoforms respectively. The GABA$_{B2}$ subunit showed one distinct band at 106 KDa as in figure 3.12a. The densitometric analysis of the WB bands showed that, the expression of GABA$_B$ isoforms and subunit follows the same trend as in figure 3.12b. The results demonstrated that GABA$_{B1a}$, GABA$_{B1b}$ and GABA$_{B2}$ protein levels in TLE-HS samples showed a significant up regulation compared to PMC samples. On the other hand, they showed a decreased protein levels compared to TLE-STG samples although only GABA$_{B2}$ subunit was significantly down regulated.

3.3.8 Western blot quantification of NeuN and NF-L200

The double-labelled western blots of neurofilament-light (NF-L) in TLE-HS and TLE-STG samples, showed as expected 2 bands specific to NF-L at about 60 and 70 kDa and band specific to ACTB at about 45 kDa as in figure 3.13a. The WB also showed nonspecific band at about 50 kDa in the TLE-STG samples. The double-labelled western blots of NeuN protein in TLE-HS and TLE-STG samples, showed multiple bands, a band specific to NeuN at about 48 kDa, a band specific to ACTB at about 45 kDa and nonspecific band at about 50 kDa as in figure 3.13b. The WB quantification analysis of the bands intensities showed a significant reduction of both NF-L and NeuN protein levels in TLE-HS compared to TLE-STG samples, indicating neuronal loss in TLE-HS specimens as in figure 3.13c.

100
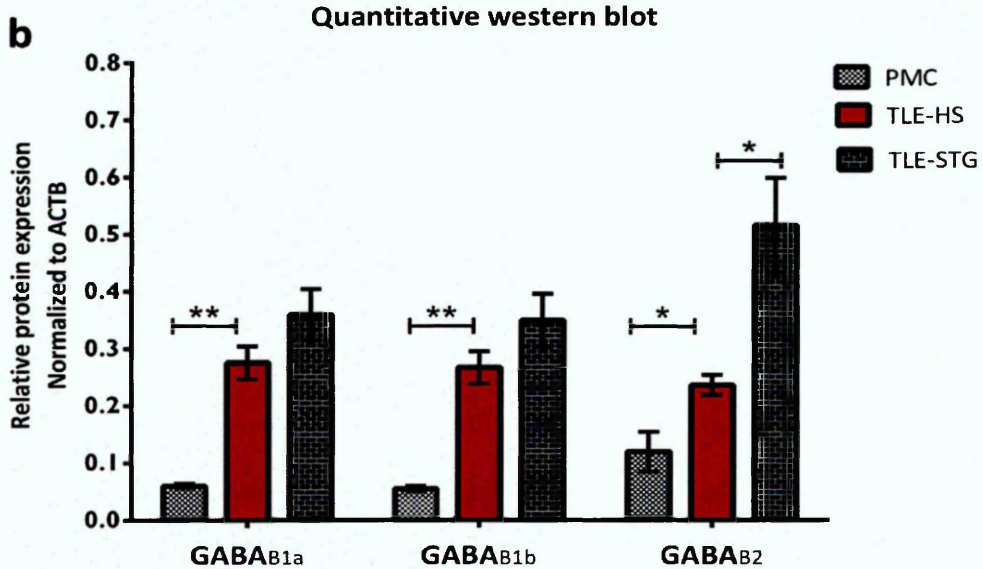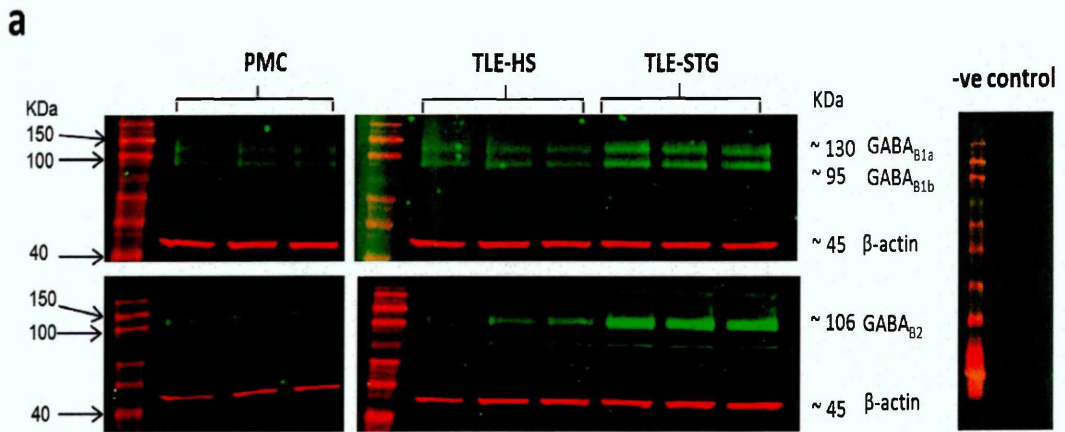
Figure 3.12 Quantitative western blotting of GABA$_{B1a}$, GABA$_{B1b}$ and GABA$_{B2}$ subunits in TLE-HS, TLE-STG and PMC

(a) Two-colour WBs showing expression of GABA$_{B1a}$, GABA$_{B1b}$, GABA$_{B2}$ and ACTB and the negative control for IRDye 680 and 800 secondary antibodies. (b) Quantitative expression of GABA$_{B1a}$, GABA$_{B1b}$ and GABA$_{B2}$ relative to ACTB expression. All GABA$_B$ subunits were significantly up regulated in TLE-HS compared to PMC and only GABA$_{B2}$ subunits was significantly down regulated in TLE-HS compared to TLE-STG. The band quantification was done by Odyssey (1.2) and Image Studio Lite (4.0) software. Statistical analysis: Kruskal-Wallis with Conover-Inman *post hoc* analysis test was used to identify significant differences between samples (* $P < 0.05$, ** $P < 0.01$). Number of samples: TLE-HS (n =9), TLE-STG (n = 6) and PMC (n = 4). Data presented as mean ± S.E.M.
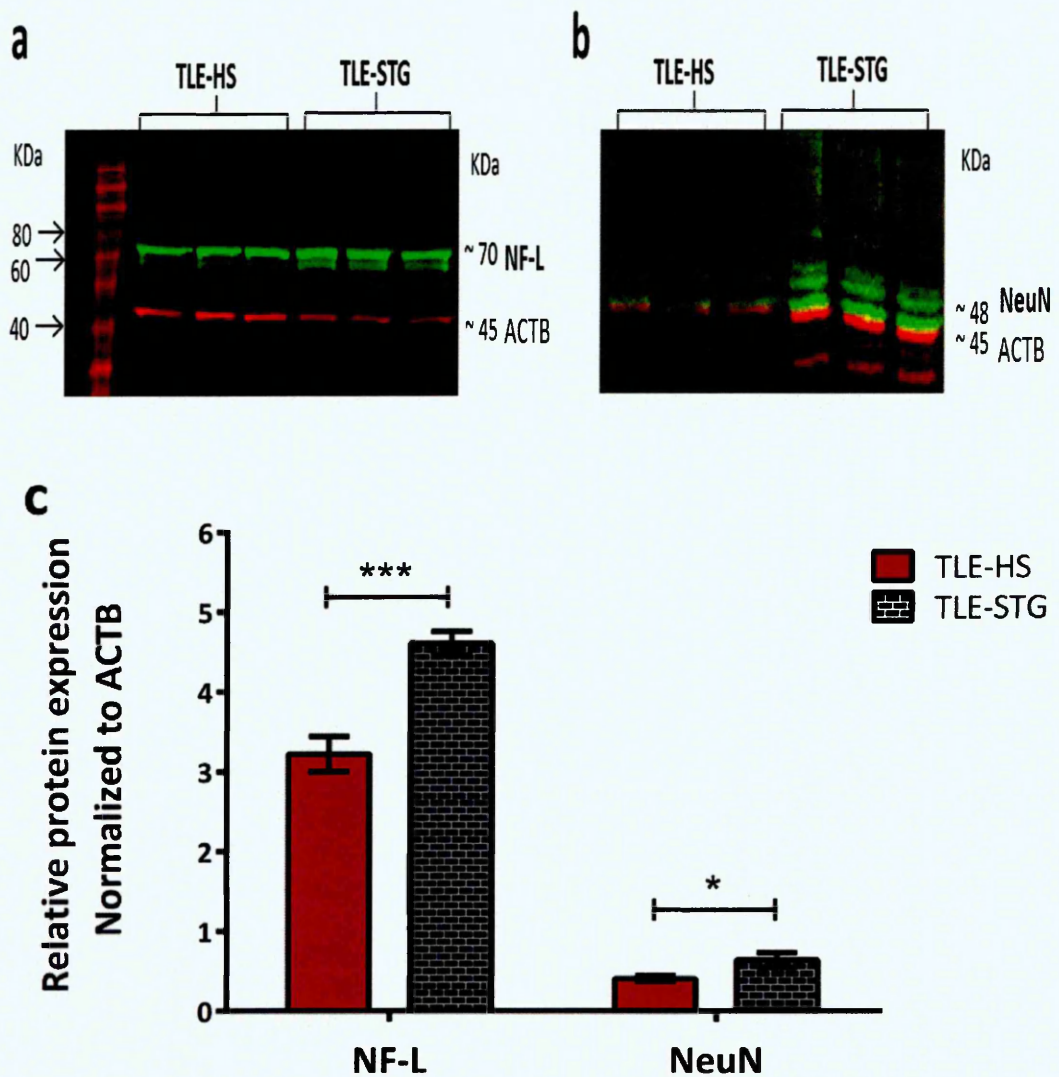
Figure 3.13 Quantitative western blotting of NF-L and NeuN in TLE-HS and TLE-STG

Two-colour WB using IRDye 680 and 800 secondary antibodies showing bands for **(a)** NF-L (~ 70 KDa) and β-Actin (~ 45 KDa) **(b)** NeuN (~ 48 KDa) and and β-Actin. **(c)** Quantitative expression of NF-L and NeuN was normalized to ACTB. The NF-L and NeuN expression were significantly reduced in TLE-HS indicating a degree of neuronal loss compared to TLE-STG. Statistical analysis: Kruskal-Wallis with Conover-Inman *post hoc* analysis test was used to identify significant differences between samples (* *P* < 0.05, *** *P* < 0.001). Number of samples: TLE-HS (n =9), and TLE-STG (n = 6). Data presented as mean ± S.E.M.

3.3.9   Neuronal GABA$_{B1}$ and GABA$_{B2}$ protein expression

The relative protein level of neuronal GABA$_B$ subunits was determined in TLE-HS and TLE-STG samples by normalizing GABA$_B$ subunit expression against two neuronal markers which are NF-L and NeuN to give us an indication of GABA$_B$ neuronal expression. The GABA$_B$ subunit, NF-L and NeuN expression values obtained from the two-colour western blot analysis were used to calculate the neuronal expression as a ratio of GABA$_B$ to NF-L or NeuN.

The neuronal protein expression of GABA$_B$ subunits followed the same trend when normalized against both NF-L and NeuN. The neuronal GABA$_{B1a}$ and GABA$_{B1b}$ protein level was slightly increased in TLE-HS compared to TLE-STG samples. While the neuronal GABA$_{B2}$ expression showed a reduction in GABA$_{B2}$ protein level in TLE-HS specimens compared to TLE-STG as in figure 3.14.
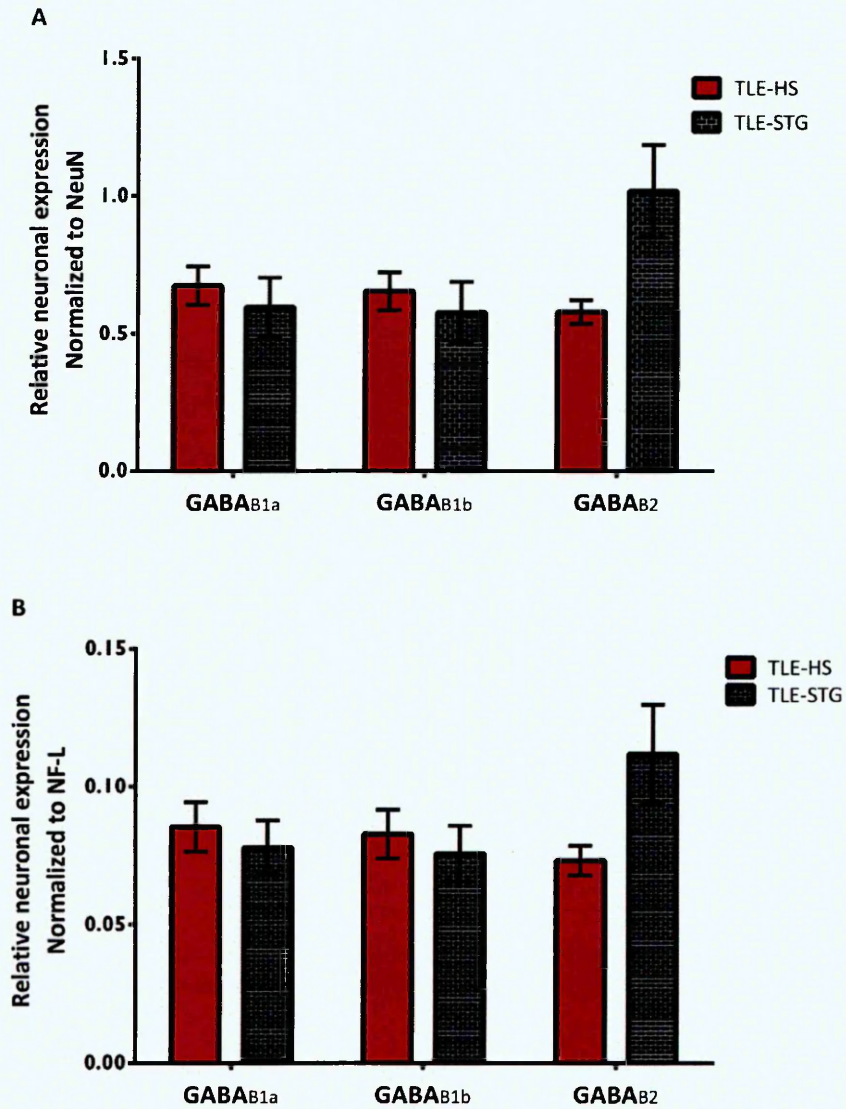
Figure 3.14 Neuronal GABA$_{B1}$ and GABA$_{B2}$ protein expression in TLE-HS and TLE-STG determined by western blotting.

The WB densitometic analysis values of GABA$_B$ subunits were expressed as a ratio to NeuN protein level **(a)** and as a ratio to NF-L protein level **(b)**. The neuronal GABA$_{B1}$ expression was increased while GABA$_{B2}$ was decreased in TLE-HS but they were not significant. Statistical analysis: Kruskal-Wallis with Conover-Inman *post hoc* analysis test was used to identify significant differences between samples. Number of samples: TLE-HS (n = 9), and TLE-STG (n = 6). Data presented as mean ± S.E.M.

3.4 Discussion

Previous studies indicated that changes in $GABA_B$ receptor subunits could be implicated in the pathophysiology of pharmacoresistant TLE associated with HS (Billinton et al., 2001a; 2001b; Muñoz et al., 2002; Princivalle et al., 2003). In summary the novel contributions of this study were: 1) the determination of both mRNA and protein levels of $GABA_{B1}$ and $GABA_{B2}$ subunits in TLE-HS and PMC hippocampal homogenates, which contain neurons, microglia and astrocytes from all hippocampal subregions: 2) the quantification of mRNA and protein levels of both $GABA_{B1}$ and $GABA_{B2}$ subunits in TLE-STG samples, which are non-spiking, non-sclerotic surgical specimens: 3) the determination of relative neuronal protein level of $GABA_{B1}$ and $GABA_{B2}$ subunits in TLE-STG and TLE-HS.

3.4.1 Expression of $GABA_B$ receptor in TLE-HS compared to *post-mortem* control

Quantifying mRNA and proteins in *post-mortem* brain tissue has the frequent problem of confounding factors such as gender, age at death, post-mortem interval and agonal state. Those factors influence the quantification and they need to be considered in studies using *post-mortem* tissues (Preece and Carins, 2003; Tomita et al., 2004). In the present study there was no regression between the age at death, *post-mortem* interval and mRNA expression (Appendix II).

The qRT-PCR results obtained in this study showed that the overall $GABA_{B1}$ mRNA expression in TLE-HS hippocampi, compared to PMC, was not significantly altered. This was the same trend demonstrated by Billinton et al., (2001a) *in situ* hybridization data. The $GABA_{B2}$ mRNA expression in this study was increased in TLE-HS compared to PMC,

though it was not significant. The *in situ* hybridization data (Princivalle *et al.*, 2003) of GABA$_{B2}$ mRNA expression also demonstrated an overall increase in GABA$_{B2}$ mRNA in 4 out of 6 hippocampal subregions supporting our data. An important point that needs to be considered, is that hippocampi specimens used in our study were homogenates of all hippocampal subregions rather than neuronal expression of an individual hippocampal area. Therefore it was challenging comparing GABA$_B$ subunits mRNA level of our qRT-PCR to *in situ* hybridization data of Billinton *et al.* (2001a) and Princivalle *et al.* (2003). However, both techniques did show the same overall trend which is a higher expression of GABA$_{B2}$ mRNAs in TLE-HS compared to PMC.

There are not many studies that investigated the protein level of GABA$_B$ subunit in human TLE-HS. The expression of GABA$_{B1a-b}$ subunit was investigated by semi-quantitative immunohistochemistry and its expression was significantly reduced in TLE-HS dentate gyrus granular cells compared to post-mortem controls (Muñoz *et al.*, 2002). The WB protein quantification obtained in our study demonstrated that, the overall protein expression of GABA$_{B1}$ isoforms (1a and 1b) and GABA$_{B2}$ were significantly up regulated in TLE-HS compared PM control. The GABA$_{B2}$ protein level reflects the increased mRNA levels obtained from qRT-PCR. The increased GABA$_B$ protein expression could be a compensatory mechanism to the hyperexcitability in TLE-HS tissue. However there seem to be an imbalance in expression of GABA$_{B1}$ to GABA$_{B2}$ ratio in TLE-HS samples.

The GABA$_B$ receptor autoradiography binding assays using both agonist and antagonist showed a significant reduction in receptor density in the overall TLE-HS tissue compared to PM control (Billinton *et al.*, 2001b; Princivalle *et al.*, 2002). It may be

106

argued that these finding contradict our results however, it is vital to point out that we investigated the protein levels of $GABA_B$ receptor subunits separately not knowing if these subunits are part of a functional receptor. While autoradiography binding assays done by Billinton *et al.*, (2001b) and Princivalle *et al.* (2002) investigated the functional heterodimeric receptor. Therefore even though both $GABA_B$ receptor subunits were significantly increased in TLE-HS compared to PM control It is hard to know what proportion of those subunits actually heterodimerize to form the full receptor.

Recent evidence show that $GABA_B$ receptor subunits are also expressed in hippocampal astrocytes and activated microglia (Charles *et al.*, 2003; Oka *et al.*, 2006; Huyghe *et al.*, 2014). In this study mRNA and proteins levels of $GABA_B$ receptor subunits represent the overall total $GABA_B$ expression including astrocytic expression however the astrocytic expression of $GABA_B$ receptors needs to be further explored.

3.4.2   Expression of $GABA_B$ receptor in TLE-HS compared to TLE-STG

In recent years many studies investigating the TLE pathophysiology have started comparing their results to surgically resected control samples to overcome agonal and *post-mortem* factors (Lee *et al.*, 2006; Ravizza *et al.*, 2008; Teichgräber *et al.*, 2009; Rocha *et al.*, 2015). In the present study for the first time, $GABA_B$ expression was investigated in TLE-STG surgically resected samples as well as in TLE-HS. The mRNA and protein levels of $GABA_{B1}$ subunit and its isoforms were decreased in TLE-HS compared to TLE-STG though the reduction was not significant. On the other hand, mRNA and protein levels of $GABA_{B2}$ subunit were significantly reduced in TLE-HS compared to TLE-STG specimens. The relative neuronal protein level of $GABA_{B2}$ subunit was also reduced in TLE-HS compared to TLE-STG.

It is now well recognised that heterodimeric GABA$_B$ receptor composed of GABA$_{B1}$ and GABA$_{B2}$ subunits is vital for trafficking of receptor complex to cell surface and G-protein activation. Therefore a fully functional receptor needs to be composed of GABA$_{B1}$ and GABA$_{B2}$ subunits (Kaupmann *et al.*, 1998; Gassmann and Bettler, 2013). The reduction in GABA$_{B2}$ subunit compared to GABA$_{B1}$ will lead to a decrease in formation of a functional heterodimeric receptor and the reduction in the density of functional GABA$_B$ receptor in TLE-HS patients. This supports the hypothesis of a compromised GABA$_B$ function in drug resistant TLE-HS pathophysiology.

Electrophysiological studies done on neurons from drug resistant TLE-HS patients, showed an impaired function of both pre- and post- synaptic GABA$_B$ receptor compared to neurons from TLE-STG tissue (Teichgräber *et al.*, 2009). Those findings support our results and indicate an altered GABA receptor function in TLE-HS patients.

3.5 Conclusion

In summary, there was an apparent increase in the total GABA$_{B1}$ and GABA$_{B2}$ subunits expression in TLE-HS compared to PM controls but there was an imbalance in the expression ratio of GABA$_{B1}$ to GABA$_{B2}$ subunit in TLE-HS cases. On the other hand, there was a persistent significant reduction in TLE-HS GABA$_{B2}$ subunits compared to TLE-STG which seems to contribute to reduction in functional GABA$_B$ receptor density and therefore, contribute to the increased excitatory hyperactivity in TLE-HS patients. This supports the role of a compromised GABA$_B$ function in drug resistant TLE-HS pathophysiology and suggests that GABA$_B$ receptor should be further investigated as a potential drug target for those patients with drug resistant TLE-HS.

Chapter 4

Expression of serum- and glucocorticoid-inducible kinase-1 (SGK1), Sodium channel β4 subunit (SCN4B), Inositol 1,4,5-trisphosphate receptor 1 (IP3R1) and Synaptoporin (SYNPR) in sclerotic TLE-HS hippocampi from refractory TLE-HS patients

4 Expression of SKG1, SCN4B, IP3R1 and SYNPR in sclerotic hippocampi from refractory TLE-HS patients

4.1 Introduction

A vast amount of research has been done on experimental animal models of *status epilepticus* (SE) to try and understand TLE-HS pathophysiology and to discover new drug targets. The microarray analysis data obtained from an animal model of *status epilepticus* (Borges *et al.*, 2007) was analysed by the GALGO multivariate method (Trevino and Falciani, 2006), it suggested that SCN4B, SGK1, IP3R1 and SYNPR genes could be indicators of seizures in epileptic hippocampi. Many other studies also suggested that those genes could be implicated in TLE-HS pathophysiology (Singec *et al.*, 2002; Cai *et al.*, 2004; Lang *et al.*, 2006; Lee *et al.*, 2013; Miyazaki *et al.*, 2014).

4.1.1 Serum- and glucocorticoid-inducible-kinase-1 (SGK1)

The serum- and glucocorticoid-inducible kinase-1 (SGK1) is a member of the serine/threonine protein kinase family. It was identified as SGK1 because its transcription was highly induced by serum and glucocorticoids in a mammary tumour cell line (Webster *et al.*, 1993). SGK1 plays a vital role in neuronal functions; it is a potent regulator of ion channels activity as it activates certain potassium, sodium, and chloride channels and therefore it regulates neuronal excitability and cell survival (Lang *et al.*, 2006; 2010). The SGK1 up-regulates glutamate transporters (EAAT1- EAAT4) that help clear the accumulated glutamate in the synaptic space and therefore protects neurons from excitotoxicity and neuronal death (Rothstein *et al.*, 1996; Boehmer *et al.*,

2006). On the other hand, SGK1 increases the abundance of kainate receptor GluR6 protein in the plasma membrane and therefore contributes to the excitatory postsynaptic potentials (Strutz-Seebohm *et al.*, 2005; Wang *et al.*, 2010).

The SGK1 activates the voltage-gated potassium channels (VGKCs). The VGKCs participate in maintaining the neuronal membrane potential as they are responsible for the repolarization phase in the neuronal action potential. Therefore their activation will lead to prolonged IPSP and the subsequent reduction of back propagating action potentials. It was also found that SGK1 up regulation causes the increased expression of VGKCs (Gamper *et al.*, 2002a; 2002b; Lang *et al.*, 2006). Therefore, due to the role of SGK1 in regulating neuronal excitability any alterations in its expression could be involved in pathophysiology of TLE.

4.1.2 Sodium channel beta 4 subunit (SCN4B)

The voltage-gated sodium channels (VGSCs) are very important in neuronal action potential generation and propagation. They are responsible for the depolarisation phase and therefore play a critical role in controlling neuronal excitability. They are composed of α-subunits that are associated with auxiliary β subunits. The α subunit forms the ion-conducting pore and it contains the voltage sensors segments. The auxiliary β subunits modify the gating kinetics and voltage dependence of the VGSCs. They are also adhesion molecules that interact with the extracellular matrix and the cellular cytoskeleton (Cannon and Bean, 2010; Catterall *et al.*, 2010).

There are four known β subunit genes *(SCN1B-4B)* that encode β1-β4 proteins. The β subunits are intrinsic membrane proteins that belong to immunoglobulin (Ig) domain

family of cell adhesion molecules. They have a large extracellular N - terminal domain which contains a single immunoglobulin (Ig) domain, a single transmembrane domain and an intracellular C - terminal domain (Liu *et al.*, 2014; Namadurai *et al.*, 2015). In neurons the presence of β subunits with sodium channel α subunits shifts the VGSCs gating properties from slow to fast mode and thus accelerating the rate of channel activation and inactivation (Yu *et al.*, 2003).

The novel β4 subunit is widely distributed in neurons of the brain. In the hippocampus, β4 was found to be expressed in the pyramidal cells and in the hilar neurons in the dentate gyrus. The β4 subunit has molecular mass of 38 kDa and it is covalently bound to α-subunits of VGSCs and therefore it is likely that it has an effect on the physiological function of multiple sodium channels (Yu *et al.*, 2003).

The β4 subunit favours the Na^+ channel activation and it causes a significant negative shift in the voltage dependence activation of Na^+ channel. Subsequently this will allow sodium channel to be activated at more negative voltages, resulting in the generation of an action potential in response to milder depolarizing stimuli. This will make the neurons more sensitive to excitatory inputs and hence making them more susceptible to excitation (Yu *et al.*, 2003). On the other hand, β1 and β3 subunits have opposite effect to β4, they favour the Na^+ channel inactivation and they cause positive shifts in the voltage dependence of activation making neurons less susceptible to excitation. However, the presence of β4 subunit overrides the effect of β1 and β3 subunits leading to a facilitated action potential firing in the neurons that express the β4 subunit (Amen *et al.*, 2009).

In addition, β4 subunit is responsible for resurgent kinetics of Na^+ channels that occurs during repolarization phase of the membrane after action potentials. A major site of resurgent Na^+ current is the hippocampus where about ~60% of DG granule cells and ~35% of CA1 pyramidal cells show those resurgent currents. The resurgent Na^+ currents significantly enhance firing frequency of action potential in response to depolarizing stimuli that is slightly above-threshold (Grieco et al., 2005; Castelli et al., 2007; Zhou et al., 2012). The β4 subunit is necessary for generating those resurgent currents which in turn influence the action potential firing of the neurons (Grieco et al., 2005; Zhou et al., 2012). Therefore, alteration in β4 subunit expression could play a role in seizure susceptibility and TLE-HS pathophysiology.

4.1.3   Inositol 1, 4, 5-trisphosphate receptor 1 (IP3R1)

IP3R1 is the main inositol trisphosphate (IP3) receptor in neurons. It is a ligand-gated calcium channel that is found on the endoplasmic reticulum. Its main function is to regulate the intracellular calcium (Ca^{2+}) concentrations. It is widely expressed in CA and DG subregions in the hippocampus (Nicolay et al., 2007).

The IP3 acts as a second messenger that is released in response to the binding of neurotransmitters such as glutamate to their metabotropic receptors (mGluRs). The activated coupled G-proteins subsequently lead to the activation of phospholipase C (PLC). PLC will cause the hydrolysis of the membrane phosphatidylinositol 4, 5-bisphosphate (PIP_2) to diacylglycerol (DAG) and IP3. Then the generated IP3 could act on its receptors (Taylor and Tovey, 2010; Kuczewski et al., 2011). The activation of IP3R1 by IP3 and cytosolic Ca^{2+} will lead to the mobilization of Ca^{2+} from the endoplasmic reticulum into the cytoplasm and this will lead to increase in the

intracellular Ca^{2+} concentrations (Matsumoto and Nagata, 1999). The intracellular Ca^{2+} acts as a second messenger playing an important role in neuronal functions such as gene transcription, neuronal excitability and neurotransmitter release (Nicolay *et al.*, 2007). The Ca^{2+} can regulate neuronal excitability by binding to ion channels and modulating their activity such as activation of calcium-dependent potassium channels or by inactivation of voltage-dependent calcium channels (Steinlein, 2014).

Many studies indicate that the calcium signalling pathway has a major role in the generation of seizures and epilepsy (Matsumoto and Nagata, 1999; Pal *et al.*, 2001; Cai *et al.*, 2004; Steinlein, 2014). An increased level of intracellular Ca^{2+} is cytotoxic to neurons and is believed to be the cause of many types of seizures. This increased intracellular Ca^{2+} is caused by defects in the mechanisms that regulate the intracellular Ca^{2+} homeostasis (Matsumoto and Nagata, 1999; Cai *et al.*, 2004; Steinlein, 2014). In neurons there are 2 major sources of calcium, external and internal, Ca^{2+} entering cells through VGCCs and NMDA receptors and the intracellular Ca^{2+} released from ER. The later was suggested to be responsible for most of the neurotoxic Ca^{2+} in neurons (Pal *et al.*, 2001). IP3R1 is very important in regulating the intracellular released calcium and therefore alteration in IP3R1 expression seems to be implicated in TLE-HS pathophysiology.

4.1.4 Synaptoporin (SYNPR)

Synaptoporin is a highly conserved synaptic vesicle membrane protein that belongs to synaptophysin family. The major members of the synaptic vesicle synaptophysin family are synaptophysin, synaptoporin, synaptogyrin, pantophysin and mitsugumin29 (Dai *et al.*, 2003). Synaptoporin is a glycoprotein that is specifically expressed in the brain and

114

it is composed of 4 transmembrane domains and C- and N-terminals (Cowan *et al.*, 1990). Synaptoporin is highly expressed in granule cells, CA3 pyramidal cells and it is also found in various interneurons in adult hippocampus (Grabs *et al.*, 1994; Singec *et al.*, 2002). Synaptoporin expression co-localized with GAD65 (GABA synthesizing enzyme), indicating that it is expressed in the inhibitory GABAergic nerve terminals in the different hippocampal layers (Singec *et al.*, 2002).

In the brain, synaptic vesicles play a major role in regulating neurotransmitter release as they are responsible for the neurotransmitter storing, exocytosis and endocytosis. Therefore they are very important in regulating the efficiency of synaptic transmission (Casillas-Espinosa *et al.*, 2012). Synaptophysin is a membrane protein associated with presynaptic vesicles that is vital for the calcium dependent neurotransmitter release (Chen *et al.*, 1996). It is found in synaptic terminals in all regions of the hippocampus and was found to be down regulated in sclerotic hippocampi obtained from drug resistant TLE patients (Grabs *et al.*, 1994; Davies *et al.*, 1998). There was also a reduced expression of synaptophysin in the hippocampi of spontaneous recurrent seizures in a rat model, indicating that the loss in synaptic vesicles seems to be involved in the pathogenesis of TLE (Zhang *et al.*, 2014).

The novel presynaptic synaptoporin expression, was found to be increased in response to nerve injury in the peripheral nervous system indicating its role in regulating synaptic transmission in both physiological and pathological conditions (Sun *et al.*, 2006). In the hippocampus, Grabs *et al.* (1994) suggested that synaptoporin seems to have a distinct function in the mossy fibre terminals that needs to be further explored. Recently Lee *et al.* (2013) found that the presynaptic synaptoporin at the mossy fibre-

CA3 synapse is crucial for maintaining homeostatic synaptic plasticity in hippocampus, which is important for regulating neuronal activity. Therefore changes in synaptoporin expression in the hippocampus could play an important role in refractory TLE-HS pathophysiology.

4.1.5 Aims of the study

SGK1, SCN4B, IP3R1 and SYNPR are potential biomarkers in TLE, they all play a role in regulating neuronal excitability and so far their expression has not been investigated in hippocampi from TLE-HS patients. Therefore the aim of this study was to do quantitative analysis of these potential biomarkers; in sclerotic TLE-HS and non-sclerotic TLE-STG tissue obtained from TLE patients and in post-mortem hippocampi, as this will also provide an insight into their roles in the pathophysiology of refractory TLE-HS.

4.2 Materials and methods

4.2.1 Patient clinical information

Clinical information for TLE-HS, TLE-STG and PMC samples investigated in this chapter is described in Appendix I.

4.2.2 Study design

The mRNA level of SGK1, SCN4B, IP3R1 and SYNPR was investigated by qRT-PCR in TLE-HS (n = 10), TLE-STG (n = 5) and PMC (n = 8) samples. The protein expression of SGK1, SCN4B, SYNPR and ACTB was investigated by two-colour quantitative western blot in

TLE-STG (n = 4) and TLE-HS (n = 7) samples. Significant difference between the samples was identified by Kruskal-Wallis with Conover-Inman *post hoc* analysis test.

4.2.3   Methods

qRT-PCR: In brief, the total RNA was extracted by SV Total RNA Isolation System (scetion 2.3.1) and then was reverse transcribed using SuperScript™ III first strand synthesis system (section 2.4). Stable housekeeping genes were selected for the normalization of target gene expression (section 2.5.3) which was then followed the qRT-PCR using TaqMan© gene expression assays (section 2.5.5).

WB: Briefly the total proteins were extracted from hippocampi samples using CelLytic™ MT mammalian tissue extraction buffer (section 2.6). Then total protein determination was assessed by the BCA assay (section 2.7). Quantitative two colour western blotting was done for all samples by electrophoresis of 20µg protein followed by electro-transfer onto a nitrocellulose membrane. The membrane was then blocked, incubated with primary and secondary antibodies before it was scanned on the Odyssey infrared imaging system (section 2.8).

4.3 Results

4.3.1 Relative mRNA and protein expression of SGK1

The SGK1 mRNA level in TLE-HS, TLE-STG and PMC samples was determined by qRT-PCR. Data showed a significant up regulation of SGK1 mRNA in the TLE-HS samples compared to both TLE-STG and PMC specimens as in figure 4.1. The densitometric analysis of WBs bands of SGK1 and ACTB in TLE-HS and TLE-STG samples revealed that the relative SGK1 protein level was higher in TLE-HS than in TLE-STG samples, though it was not statistically significant as in figure 4.2.

qRT-PCR SGK1
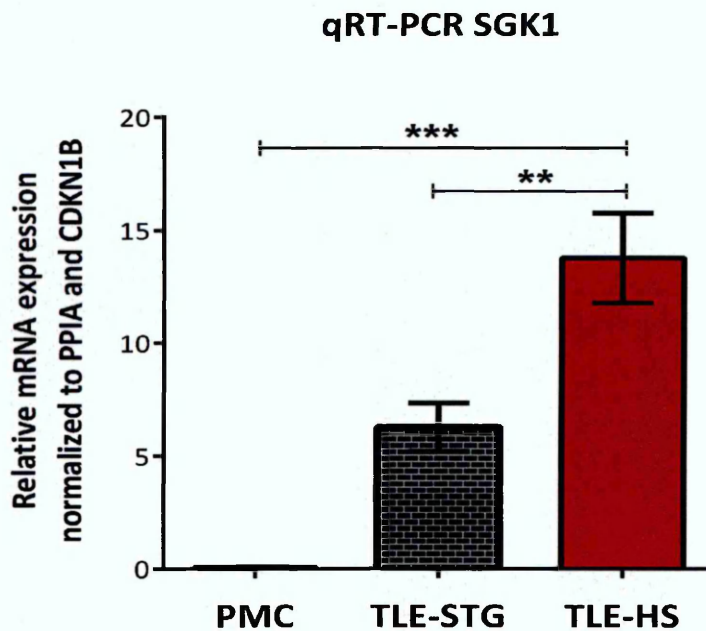
Figure 4.1 qRT-PCR data showing the relative mRNA expression of SGK1 in TLE-HS, TLE-STG and PMC

qRT-PCR data shows that SGK1 mRNA level in TLE-HS was significantly up regulated compared to both PMC and TLE-STG samples. Statistical analysis: Kruskal-Wallis with Conover-Inman *post hoc* analysis test was used to identify significant differences between samples (* $P < 0.05$, ** $P < 0.01$, *** $P < 0.001$). Number of samples: TLE-HS (n =10), TLE-STG (n = 5) and PMC (n = 8). Data presented as mean ± S.E.M.

118
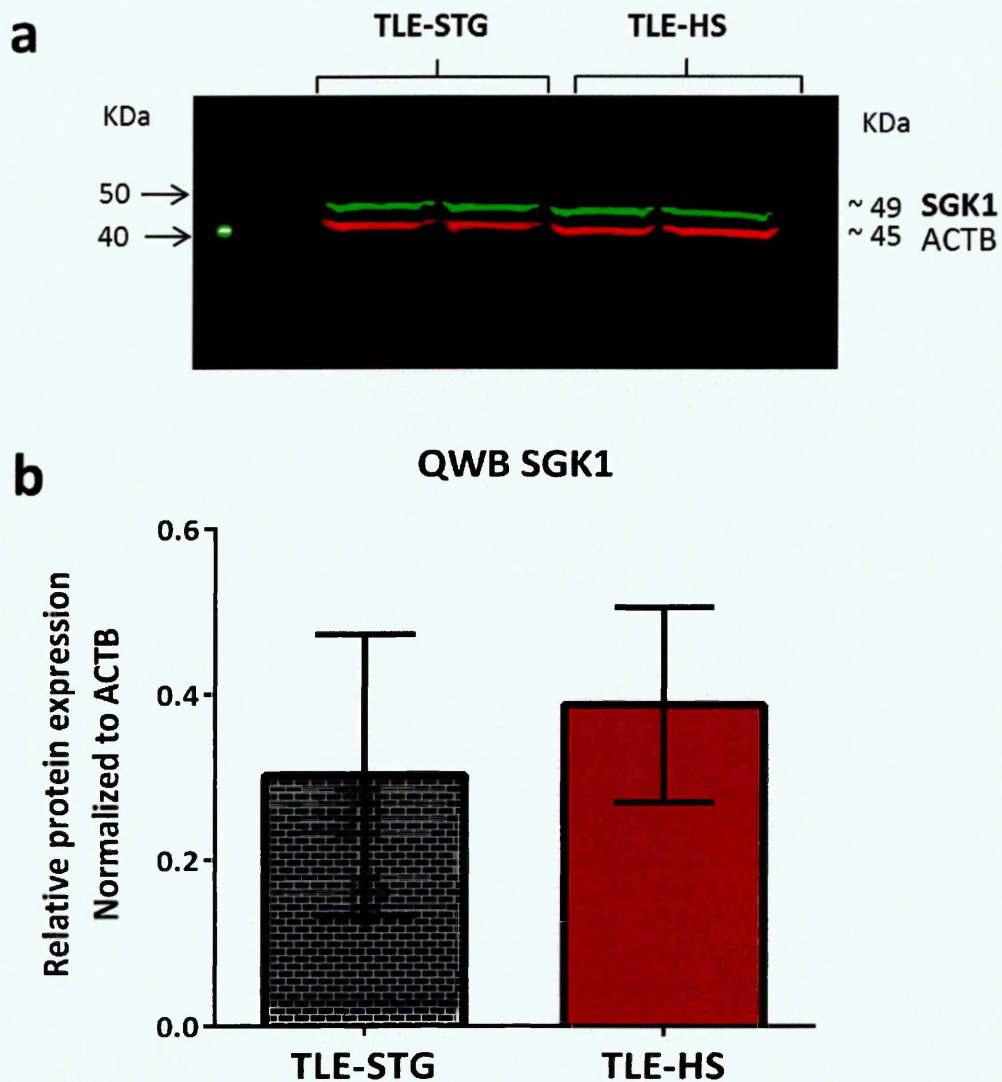
Figure 4.2 Quantitative western blotting of SGK1 in TLE-HS and TLE-STG

(a) Two-colour WBs showing expression of SGK1 and ACTB revealed by IRDye 680 and 800 secondary antibodies. (b) Quantitative expression of SGK1 relative to ACTB expression. SGK1 protein expression was higher in TLE-HS compared to TLE-STG. The quantification of the bands was done using Odyssey (1.2) and Image Studio Lite (4.0) software. Statistical analysis: Kruskal-Wallis with Conover-Inman *post hoc* analysis test was used to identify significant differences between samples (* $P < 0.05$). Number of samples: TLE-HS (n = 7) and TLE-STG (n = 4). Data presented as mean ± S.E.M.

4.3.2 Relative mRNA and protein expression of SCN4B

The SCN4B mRNA expression was investigated by qRT-PCR in TLE-HS, TLE-STG and PMC samples. The data demonstrated that, SCN4B subunit transcript was significantly up regulated in TLE-HS compared to PMC. On the other hand, SCN4B mRNA expression was significantly reduced in TLE-HS compared to TLE-STG samples as in figure 4.3.

The protein level of SCN4B in TLE-HS and TLE-STG was investigated by quantitative WB. The WB bands analysis revealed the same trend, SCN4B protein expression in TLE-HS was also significantly reduced in TLE-HS compared to TLE-STG samples as in figure 4.4. The SCN4B protein expression was mirroring the mRNA expression in TLE-HS and TLE-STG samples.

4.3.3 Relative mRNA expression of IP3R1 receptor

The IP3R1 mRNA expression was investigated by qRT-PCR in TLE-HS, TLE-STG and PMC samples. The data demonstrated that, mRNA expression of IP3R1 receptor was significantly increased in TLE-HS compared to PMC. On the other hand, IP3R1 mRNA expression was significant reduced in TLE-HS compared to TLE-STG samples as in figure 4.5.
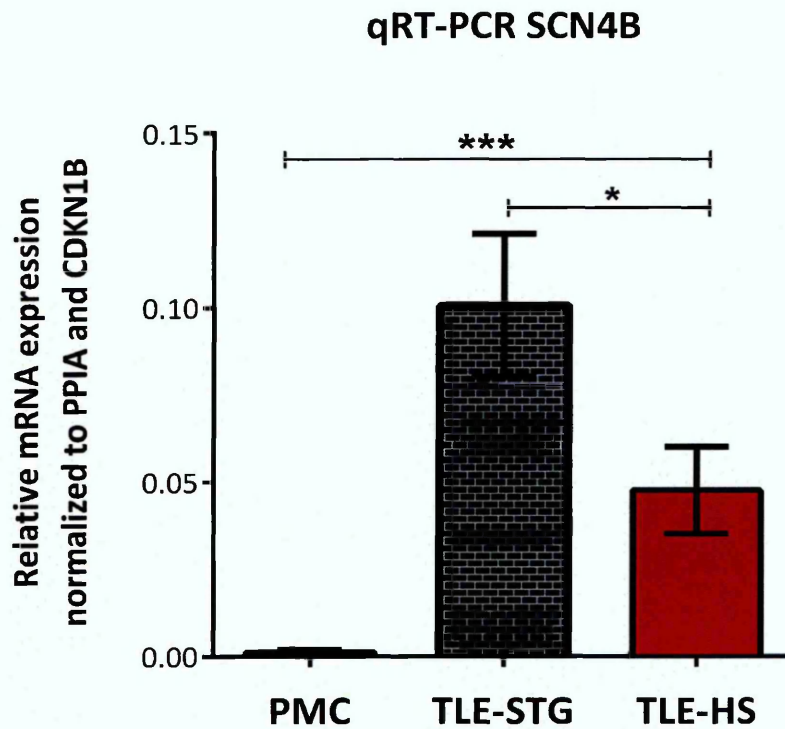
qRT-PCR SCN4B

Figure 4.3 qRT-PCR data showing the relative mRNA expression of SCN4B in TLE-HS, TLE-STG and PMC

The SCN4B mRNA level in TLE-HS was significantly up regulated compared to PMC but it was significantly down regulated compared to TLE-STG. qRT-PCR data analysis was done using $2^{-\Delta CT}$ method. Statistical analysis: Kruskal-Wallis with Conover-Inman *post hoc* analysis test was used to identify significant differences between samples (* $P <$ 0.05, ** $P <$ 0.01, *** $P <$ 0.001). Number of samples: TLE-HS (n = 10), TLE-STG (n = 5) and PMC (n = 8). Data presented as mean ± S.E.M.
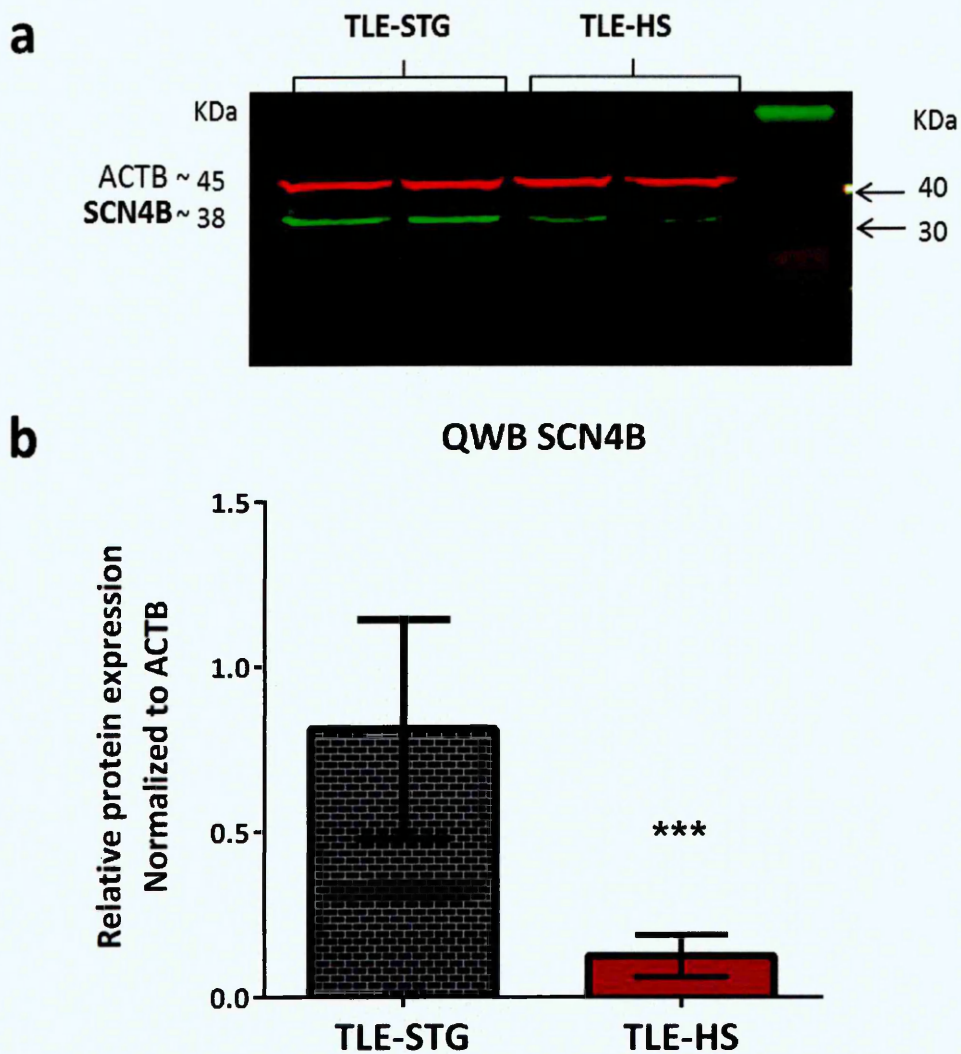
Figure 4.4 Quantitative western blotting of SCN4B in TLE-HS and TLE-STG

(a) Two-colour WBs showing expression of SCN4B and ACTB revealed by IRDye 680 and 800 secondary antibodies. **(b)** Quantitative expression of SCN4B relative to ACTB expression. The protein expression of SCN4B was significantly reduced in TLE-HS compared to TLE-STG. The quantification of the bands was done using the Odyssey (1.2) and Image Studio Lite (4.0) software. Statistical analysis: Kruskal-Wallis with Conover-Inman *post hoc* analysis test was used to identify significant differences between samples (* $P < 0.05$, ** $P < 0.01$, *** $P < 0.001$). Number of samples: TLE-HS (n = 7) and TLE-STG (n = 4). Data presented as mean ± S.E.M.
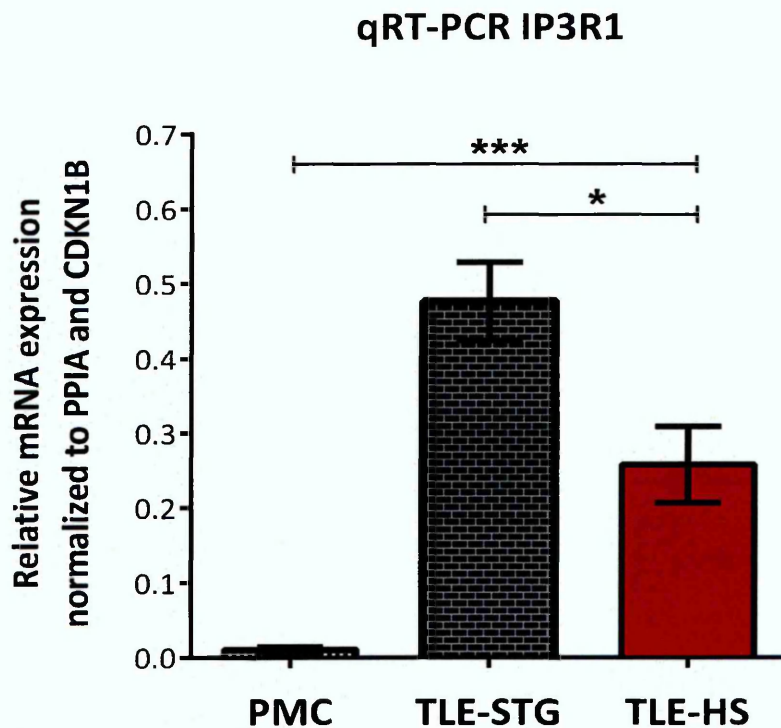
qRT-PCR IP3R1

Figure 4.5 qRT-PCR data showing the relative mRNA expression of IP3R1 in TLE-HS, TLE-STG and PMC

The IP3R1 mRNA level in TLE-HS was significantly up regulated compared to PMC but it was significantly down regulated compared to TLE-STG. qRT-PCR data analysis was done using $2^{-\Delta CT}$ method. Statistical analysis: Kruskal-Wallis with Conover-Inman *post hoc* analysis test was used to identify significant differences between samples (* $P <$ 0.05, ** $P <$ 0.01, *** $P <$ 0.001). Number of samples: TLE-HS (n = 10), TLE-STG (n = 5) and PMC (n = 8). Data presented as mean ± S.E.M.

4.3.4 Relative mRNA and protein expression of SYNPR

The synaptic vesicle SYNPR mRNA expression was investigated by qRT-PCR in TLE-HS, TLE-STG and PMC samples. The data demonstrated that, SYNPR transcript was significantly up regulated in TLE-HS compared to PMC. In contrast, SYNPR mRNA expression was significant down regulated in TLE-HS compared to TLE-STG samples as in figure 4.6.

The protein expression of SYNPR in TLE-HS and TLE-STG was investigated by quantitative WB. The densitometric analysis of WBs bands showed that SYNPR protein expression in TLE-HS was also significantly reduced in TLE-HS compared to TLE-STG samples as in figure 4.7.
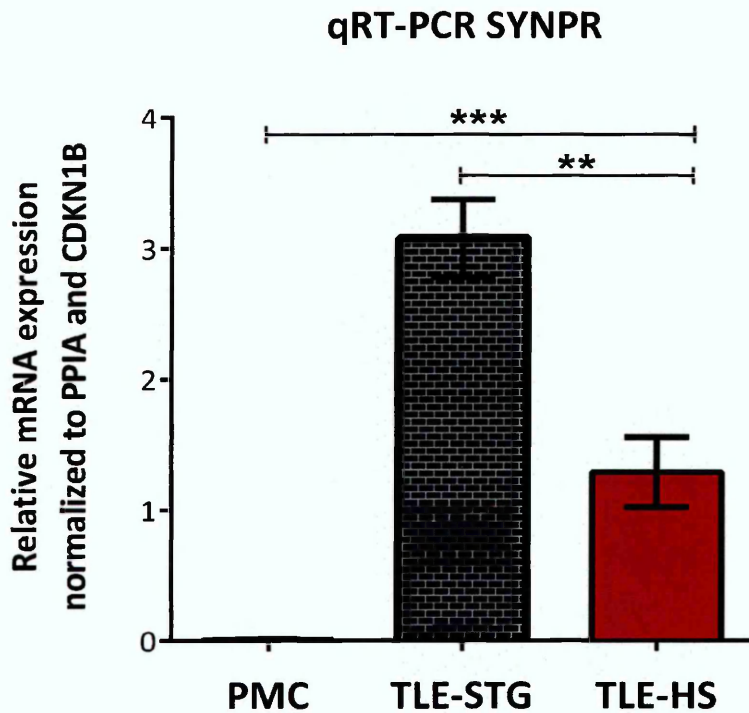
qRT-PCR SYNPR

Figure 4.6 qRT-PCR data showing the relative mRNA expression of SYNPR in TLE-HS, TLE-STG and PMC

The SYNPR mRNA level in TLE-HS was significantly up regulated compared to PMC but it was significantly down regulated compared to TLE-STG. The qRT-PCR data analysis was done using $2^{-\Delta CT}$ method. Statistical analysis: Kruskal-Wallis with Conover-Inman *post hoc* analysis test was used to identify significant differences between samples (* *P* < 0.05, ** *P* < 0.01, *** *P* < 0.001). Number of samples: TLE-HS (n = 10), TLE-STG (n = 5) and PMC (n = 8). Data presented as mean ± S.E.M.
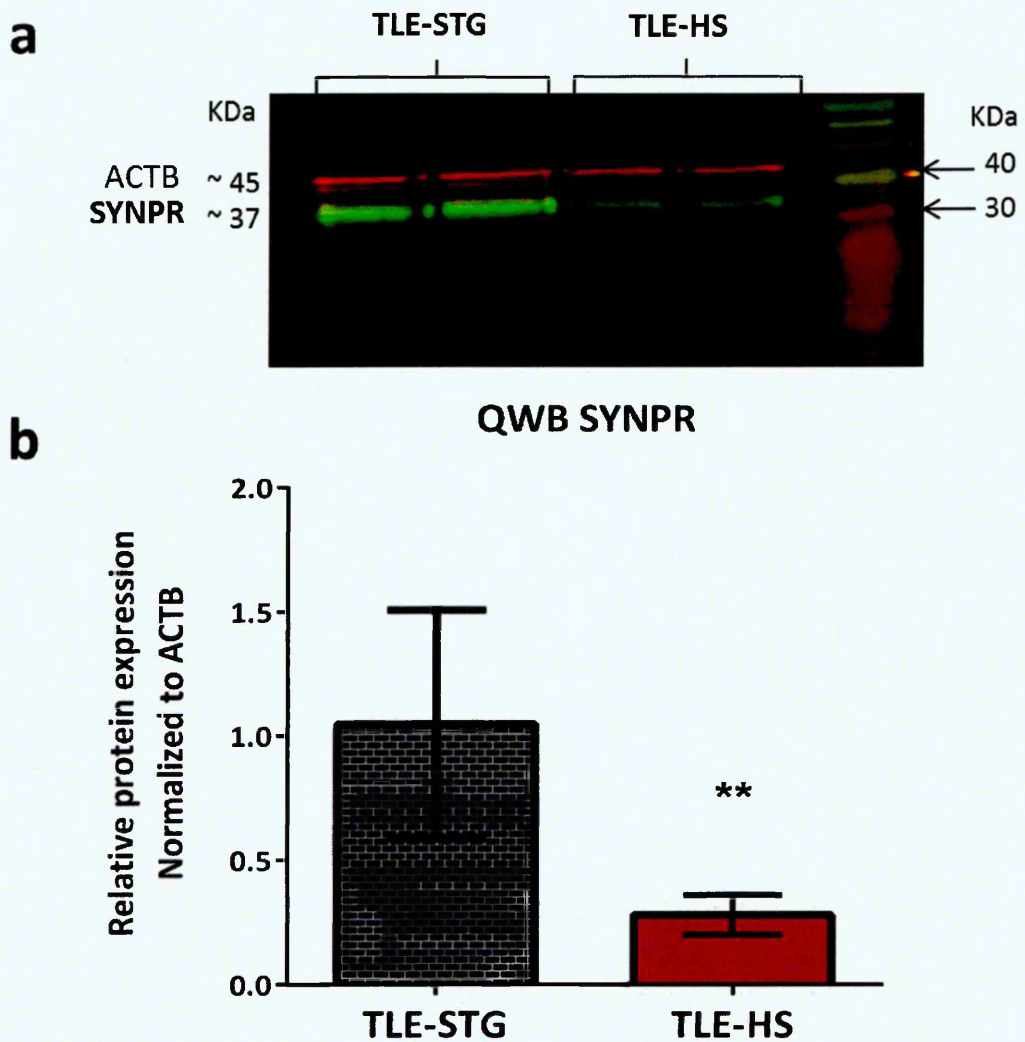
Figure 4.7 Quantitative western blotting of SYNPR in TLE-HS and TLE-STG

(a) Two-colour WBs showing expression of SYNPR and ACTB revealed by IRDye 680 and 800 secondary antibodies. (b) Quantitative expression of SYNPR relative to ACTB expression. The protein expression of SYNPR was significantly decreased in TLE-HS compared to TLE-STG. The bands quantification was done using Odyssey (1.2) and Image Studio Lite (4.0) software. Statistical analysis: Kruskal-Wallis with Conover-Inman *post hoc* analysis test was used to identify significant differences between samples (* $P < 0.05$, ** $P < 0.01$). Number of samples: TLE-HS (n = 7) and TLE-STG (n = 4). Data presented as mean ± S.E.M.

4.4 Discussion

Previous studies in animal models indicated that changes in SGK1 (Lang *et al.*, 2006; Wang *et al.*, 2010), SCN4B (Borges *et al.*, 2007; Miyazaki *et al.*, 2014), SYNPR (Singec *et al.*, 2002; Lee *et al.*, 2013) and IP3R1 (Cai *et al.*, 2004; Nicolay *et al.*, 2007) could be implicated in the pathophysiology of pharmacoresistant TLE associated with HS. The key findings of this study were: 1) the SGK1, SCN4B, SYNPR and IP3R1 mRNA levels were significantly altered in drug resistant TLE-HS hippocampi compared to TLE-STG and PMC hippocampi; 2) the quantification of SGK1, SCN4B and SYNPR protein levels were also altered in TLE-HS compared to TLE-STG samples.

4.4.1 SGK1 expression in TLE-HS

The SGK1 has a role in regulating neurone excitability; it up regulates glutamate transporters and activates VGKCs. This suggests that it could have a role in TLE (Boehmer *et al.*, 2006; Wang *et al.*, 2010). In this study we found that there was a significant up regulation of SGK1 mRNA level in the sclerotic hippocampi of refractory TLE-HS compared to both TLE-STG and PMC. This corroborates Wang *et al.*, 2010 research as they have investigated SGK1 expression in the anterior temporal neocortex tissue of drug resistant epilepsy patients. They found that SGK1 mRNA and protein were significantly up regulated compared to PMC. In the present study the SGK1 protein level was increased in TLE-HS compared to TLE-STG, though it was not significant which could be attributed to the variability and low numbers of TLE-STG samples. However, it still supports our data as SGK1 showed the same trend of increased expression in the high frequency seizure experiencing tissue.

127

In a lithium-pilocarpine rat model of epilepsy, SGK1 and EAAT3 mRNA and protein expression were investigated at different time points (6 hrs - 2 months) after the onset of *status epilepticus*. They found that SGK1 expression was significantly up regulated at all-time points after the onset of *status epilepticus*. This increase in SGK1 was also accompanied by the significant up regulation of the glutamate transporter EAAT3 suggesting the neuroprotective role of SGK1 after seizures (Wang *et al.*, 2010).

It is recognised that SGK1 expression was increased after neuronal injury and neuronal excitotoxicity (Imaizumi *et al.*, 1994; Hollister *et al.*, 1997) and it was found that seizures of *status epilepticus* induce neuronal injury in animal models (Torolira *et al.*, 2016). Therefore, SGK1 up regulation in drug resistant TLE-HS patients might play a neuroprotective role in response to recurrent seizures.

4.4.2 SCN4B expression in TLE-HS

For the first time, this study reports that SCN4B mRNA was significantly up regulated in TLE-HS compared to PMC. It also reports that both mRNA and protein expression of SCN4B subunit were significantly down regulated in the drug resistant TLE-HS compared to TLE-STG obtained from patients undergoing surgical resection. The VGSCs β subunits have multiple functions; they modulate the gating kinetics and voltage dependence of VGSCs and regulate cell adhesion, migration and neurite outgrowth. They regulate action potential firing and therefore are vital for controlling neuronal excitability (Cannon and Bean, 2010; Catterall *et al.*, 2010; Miyazaki *et al.*, 2014). The altered expression of β1, β2 and β3 subunits have been previously reported in human TLE-HS hippocampi and TLE animal models but not β4 subunit (Gastaldi *et al.*, 1998; Aronica *et al.*, 2003; van Gassen *et al.*, 2008; 2009).

The β4 subunit facilitates the action potential firing in the neurons making them more sensitive to excitatory stimuli (Amen *et al.*, 2009). Therefore, the significant up regulation of SCN4B mRNA in TLE-HS compared to PMC could explain partially the increased seizure susceptibility of the sclerotic hippocampi in TLE patients. Miyazaki *et al.* (2014) found that in response to repetitive stimulation, mice that are deficient in Scn4b showed a decrease in repetitive firing frequency of action potentials as well as a significant reduction in resurgent Na^+ currents. Whether the significant down regulation of SCN4B in TLE-HS compared to TLE-STG is a compensatory mechanism or not, it needs to be further investigated. In conclusion, the altered expression of SCN4B subunit indicates that it does seem to be involved in TLE pathophysiology.

4.4.3 IP3R1 expression in TLE-HS

In this study we found that there was a significant up regulation of calcium channel receptor IP3R1 mRNA level in the sclerotic hippocampi of refractory TLE-HS compared to PMC and IP3R1 was significantly down regulated in TLE-HS compared to TLE-STG.

The calcium signalling has been increasingly recognised in having a role in the development of epilepsy (epileptogenesis). The intracellular Ca^{2+} level affects neuronal excitability and neurotransmitter release. Therefore IP3R1 is essential in regulating intracellular Ca^{2+} homeostasis and hence neuronal excitability and neurotransmitter release (Matsumoto and Nagata, 1999; Pal *et al.*, 2001; Cai *et al.*, 2004; Steinlein, 2014).

It was found that the expression of IP3R1 in hippocampal neurons is regulated by synaptic activity (Cai *et al.*, 2004). In hippocampal neurons, IP3R1 expression was increased by the activation of NMDA receptors and VGCCs (Greaf *et al.*, 1999). On the

other hand, chronic activation of mGluRs as well as other plasma membrane receptors linked to IP3 production down regulated the IP3R1 expression in cerebellar granule cells (Cai *et al.*, 2004).

In conditions such as refractory TLE there is a chronic over activation of NMDA receptors by glutamate, and as a consequence this is accompanied by excessive influx of calcium into the neurons making them more prone to seizures. In this study, sclerotic hippocampi, which are the seizure's focus, from refractory TLE showed a significant up regulation of IP3R1 expression, compared to PMC; this could be a contributing factor to the increased neuronal excitability seen in TLE-HS. On the other hand there was a significant down regulation of IP3R1 expression in TLE-HS compared to TLE-STG, suggesting that this reduction could be a compensatory mechanism to reduce the intracellular calcium. However, in conclusion there does seem to be impairment in the intracellular Ca^{2+} homeostasis mechanism that plays a major role in imbalance between inhibitory and excitatory state in epilepsy. Therefore, further research into IP3R1 role in TLE pathophysiology may provide new drug targets for the development of AEDS.

4.4.4   SYNPR expression in TLE-HS

In this study, for the first time, the SYNPR mRNA and protein were investigated in TLE-HS and TLE-STG obtained from patients undergoing surgical resection as well as in PMC hippocampi. We found that SYNPR mRNA was significantly up regulated in TLE-HS compared to PMC. On the other hand, both mRNA and protein expression of SYNPR were significantly down regulated in the TLE-HS compared to TLE-STG.

Synaptoporin is used as a marker for mossy fibres in many studies investigating TLE pathogenesis in animal models (Wilczynski *et al.*, 2008; Volz *et al.*, 2011; Häussler *et al.*, 2015). Mossy fiber-CA3 synapses in the hippocampus are essential in preventing the seizure generation in the CA3 network. The presynaptic synaptoporin in the mossy fibre- CA3 synapses is vital for maintaining the homeostatic synaptic plasticity and reducing excitation (Lee *et al.*, 2013). In CA3 the down regulation of synaptoporin increased the recurrent CA3 excitation and thus enhances seizure susceptibility (Lawrence and McBain 2003; Queenan and Pak *et al.*, 2013). Synaptoporin was also found to be expressed in the inhibitory GABAergic nerve terminals in the different hippocampal layers (Singec *et al.*, 2002). In this study there was an increase in synaptoporin expression in TLE-HS compared to PMC, which could be an indicator of a compensatory increase in inhibitory GABAergic synapses. In contrast the down regulation of synaptoporin in TLE-HS compared to TLE-STG, seem to enhance excitation and seizure susceptibility in TLE -HS samples. Therefore, alteration in synaptoporin expression needs to be further exploited in order to provide a new insight into TLE-HS pathophysiology.

4.5 Conclusion

In epileptic brains, specifically refractory TLE hippocampus there are frequent uncontrolled seizures that are affecting neuronal activity and overwhelming many of the homeostatic mechanisms such as intracellular calcium homeostasis and homeostatic synaptic plasticity. All of the genes investigated in this study play a vital role in regulating neuronal excitability. Their expression was significantly altered in TLE-HS patients indicating the complexity of drug resistant TLE pathophysiology. Therefore a vast amount of research is still needed to unravel the epileptogenesis and pathophysiology involved in TLE-HS.

Chapter 5

Transcriptome analysis of sclerotic TLE hippocampi from refractory TLE-HS patients

5 Transcriptome analysis of sclerotic TLE hippocampi from refractory TLE-HS patients

5.1 Introduction

Transcriptome analysis is the examination of expression levels of mRNAs, transcribed in a given cell population or tissue. It is also known as expression profiling analysis because it reflects only the actively expressed genes in a tissue at a given time. This analysis often uses high-throughput techniques based on microarray technology. They provide a vital screening tool to investigate many disease pathologies (Wang *et al.*, 2009). The transcriptional profiles obtained could also provide predictive biomarkers of the disease (Trevino *et al.*, 2007).

In TLE-HS there is a need to develop new AEDs that also have anti-epileptogenic effect to stop the progression of TLE. However, TLE-HS pathophysiology remains poorly understood despite the vast amount of research done, and deciphering its pathophysiology will help in the development of new anti-epileptogenic drugs. Therefore, the transcriptome analysis is a powerful tool to investigate TLE-HS pathophysiology as it assesses the gene expression in a comprehensive and unbiased fashion.

There are a limited numbers of studies that investigated human TLE specimens by microarray analysis. Becker *et al.* (2002) found that 21 genes (from total of 588) that are involved in cell death, gliosis and neuronal plasticity were significantly altered in surgical TLE-HS samples compared to Non-HS from patients with extra-hippocampal

mass lesion. Lee *et al.* (2007) investigated gene expression in the CA1 region and found that 137 genes (from total of 14,500) were significantly altered in TLE-HS compared to Non-HS. Those genes were involved in gliosis and immune response. In another study, the transcriptome profiles of spiking and non-spiking specimens from TLE temporal cortex found that; 76 genes (from total of 14,500) were significantly altered. Those genes were involved in GABA signalling, iron metabolism and MAPK pathway (Arion *et al.*, 2006).

On the other hand; the transcriptome analysis of entorhinal cortex from TLE patients with dual pathology (HS and cortical atrophy) investigated by cDNA microarray analysis found that only 6 genes (from 2400 genes) were differentially expressed in TLE compared to autopsy controls. These genes were involved in complement cascade and synaptic transmission (Jamali *et al.*, 2006). The previous studies are limited by the use of cDNA arrays that have less target specificity and only represent a small fraction of the human transcriptome. Recently two transcriptome studies have used the new oligonucleotide microarrays that are more representative of the whole human transcriptome. The oligonucleotide microarrays also have higher target specificity that provides better discrimination of highly similar genes and splice variants (Kreil *et al.*, 2006). In the van Gassen *et al.* (2008) study, hippocampal specimens from TLE patients with and without HS and autopsy controls (n = 4 per group) were investigated. They found that most of the 618 (from 21,329) differentially expressed genes identified were implicated in innate immunity. While, Venugopal *et al.* (2012) performed microarray analysis on spiking and non-spiking hippocampal specimens from TLE

patients (n = 10 per group). They identified 413 genes that were differentially expressed; some of them were GABA-associated and astrocyte-associated genes.

The analysis approach by the previous transcriptome studies focused primarily on the list of genes that are differentially expressed in TLE compared to control, these lists of genes are relatively large and according to (Mirza *et al.*, 2011) only a small proportion of those genes are consistent across the different studies. This may be due to the small number of samples, different microarray platform used and different methods of analysis (Ahmed *et al.*, 2004). However, TLE is a multifactorial condition where many genes are simultaneously affected and contributing to TLE-HS phenotype. In order for the transcriptome analysis to have significant impact on our understanding of TLE pathophysiology, we ought to look at the biological processs and pathways that are affected rather than single genes.

5.1.1 Aims of the study

The aim of this study was to do transcriptome analysis of TLE-HS and TLE-STG from TLE patients with hippocampal sclerosis, in addition to post-mortem hippocampi samples. This was followed by transcriptome enrichment analysis of microarray data, where genes are functionally clustered based on their cellular component, molecular function, biological process and pathways they are involved in. This will give us more understanding of pathways and biological processes affected in TLE-HS pathophysiology.

5.2 Materials and methods

5.2.1 Patient clinical information

For microarray analysis, only TLE patients with hippocampal sclerosis were included and any patients with cortical dysplasia or neoplastic TLE lesion were excluded from the study. In total the number of patients used for microarray analysis study were seven TLE patients (2M + 5F) their age at surgery was 36 ± 11 years, age at onset of first non-febrile seizure 10 ± 8 years and duration of epilepsy 26 ± 15 years. Five post-mortem (2M + 3F) hippocampi from individuals with no known brain disease were used for transcriptome analysis; their age 78 ± 5 years and PMI 42 ± 12 hrs. The full clinical information for TLE-STG and TLE-HS samples investigated in this chapter is described in Appendix I.

5.2.2 Study design

The transcriptome profiling of TLE-STG (n = 7), TLE-HS (n = 7) and PMC (n = 5) samples was done by microarray analysis (MA) then it was followed by the enrichment analysis of dysregulated genes that were identified by Rank Product test. The validation of MA data was done by qRT-PCR for 11 genes in TLE-STG (n = 10), TLE-HS (n = 22) and PMC (n = 7) samples. Significant difference between the samples was identified by Kruskal-Wallis with Conover-Inman *post hoc* analysis test.

5.2.3 Microarray experiment (MA)

Briefly the total RNA was extracted by SV Total RNA Isolation System (section 2.4.1). Then cDNA samples were synthesized and labelled with Cy3 or Cy5 using the Two-colour Low Input Quick Amp Labelling Kit (Agilent Technologies, 5190-2306). Following

the labelling of TLE-HS hippocampi with Cy5 and TLE-STG samples with Cy3, equal amounts of each samples were co-hybridized onto SurePrint G3 Human Gene Expression 8x60K microarrays (Agilent Technologies, G4851A). The microarray was washed and then scanned using Agilent Technologies SureScan microarray Scanner (section 2.9).

5.2.4 MA data analysis

There are three main stages in microarray data analysis: raw data processing and normalization, identification of differentially expressed genes (DEGs) and DAVID enrichment analysis of the DEGs as shown in figure 5.1.
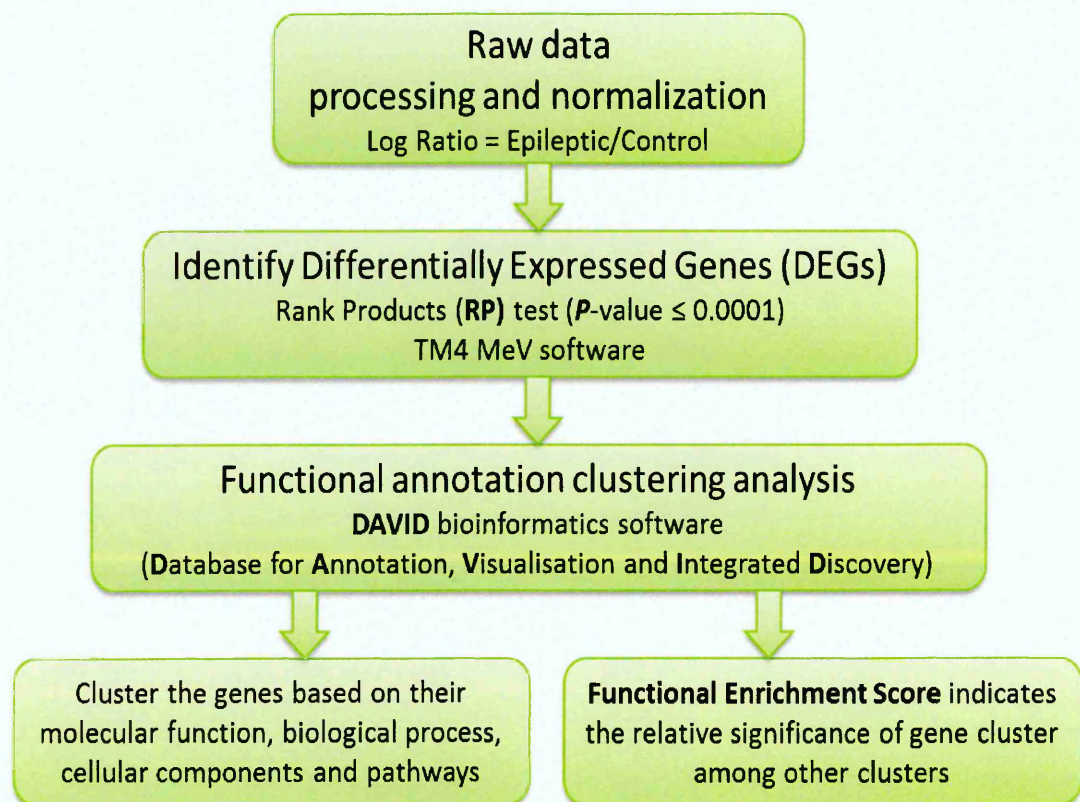
Figure 5.1 Schematic diagram presenting main steps in microarray data analysis

5.2.4.1 Raw data processing and normalization

The raw data is extracted using Agilent feature extraction software. A feature is the gene specific probe that is printed on the microarray slide. The feature's local background signal is subtracted and the dye bias between the 2 dyes is corrected by using linear and locally weighted scatter plot smoothing (LOWESS) normalization methods. The LOWESS dye normalization factor is calculated by fitting the locally weighted linear regression curve to the chosen normalization features. The processed signal is then calculated by multiplying the background-subtracted signal by the LOWESS dye normalization factor (Agilent Technologies, G4460-90052). For every probe or gene, the differential expression between 2 samples (labelled with either green or red dye) is calculated as a Log ratio as follows:

$$\text{Log ratio} = \text{Log}_{10} \text{ (red processed signal/ green processed signal)}$$

5.2.4.2 Identification of differentially expressed genes (DEGs) in TLE-HS by RP

The Rank Product (RP) method is a robust, sensitive and highly specific microarray analysis method that is powerful in identifying biologically relevant gene expression changes (Breitling et al., 2004; Koziol, 2010). Therefore in the present study, RP method is used to identify differentially expressed genes between TLE-STG, PMC and epileptic TLE-HS samples. The RP test with false discovery rate (FDR) ≤ 0.1 was done using TM4 Multi-Experiment Viewer (MeV) software, version 4.9 (Saeed et al., 2003). Only genes with FDR ≤ 0.1 and $P < 0.05$ were considered differentially expressed and were used for functional enrichment analysis.

5.2.4.3 Functional enrichment analysis of DEGs by DAVID

The functional enrichment analysis is done using the **D**atabase for **A**nnotation, **V**isualisation and **I**ntegrated **D**iscovery **(DAVID)** bioinformatics resources v6.7 (http://david.abcc.ncifcrf.gov). The DAVID database consists of an integrated biological knowledge database and analytical tools. It provides functional annotation tools for understanding the biological meaning behind a large list of genes (Huang *et al.*, 2009a; 2009b).

The functional annotation clustering analysis in DAVID, groups genes with similar annotations together into clusters and then links them to an annotation term. The term enrichment P-value represents the association of genes to an annotation term in a cluster. Then every cluster is given an enrichment score, which is a geometric mean (in $-\log_{10}$ scale) of member's P-values in that cluster. The enrichment score helps to rank the overall importance of a cluster among others. A cluster is considered of significant biological importance if the enrichment score is more than 1.3 ($P = 0.05$) (Huang *et al.*, 2009b).

In the present study, the analysis was done by following the method in Huang *et al.*, (2009b). The gene lists (Agilent probe ID list) of differentially expressed genes were uploaded into DAVID separately. They were mapped to DAVID default gene IDs and the background annotation was set to *Homo sapiens*. All submitted gene lists were analysed by the functional annotation clustering method using the annotation search categories in table 5.1. The functional classification stringency was set to medium with enrichment threshold of 0.05 (enrichment P - value).

Table 5.1 Annotation search categories used in functional enrichment analysis of DEGs

Functional categories	
COG_Ontology	Clusters of Orthologous Groups of proteins database
SP_PIR _KEYWORDS	SwissProt protein knowledgebase and Protein Information Resource combined annotations
UP_SEQ_feature	Uniprot Sequence annotations
Gene Ontology	
GOTERM_BP_FAT	Gene ontology term: Biological Processes
GOTERM_CC_FAT	Gene ontology term: Cellular Components
GOTERM_MF_FAT	Gene ontology term: Molecular Functions
Pathways	
BBID	Biological Biochemical Image Database
BIOCARTA	Biological pathways resource
KEGG_pathway	Kyoto Encyclopaedia of Genes and Genomes pathways
Protein_ Domains	
INTERPRO	Protein sequence analysis and classification resource
PIR_SUPERFAMILY	Protein Information Resource -Superfamily protein annotation
SMART	Simple Modular Architecture Research Tool

5.2.5   qRT-PCR

In brief, the total RNA extracted was reverse transcribed using SuperScript^{TM} III first strand synthesis system (section 2.4). Stable housekeeping genes were selected for the normalization of target gene expression (section 2.5.3) then followed by the qRT-PCR using TaqMan$^©$ gene expression assays (section 2.5.5). **qRT-PCR statistical analysis**: Kruskal-Wallis with Conover-Inman *post hoc* analysis test was used to identify significant differences between samples (* $P < 0.05$).

5.3   Results

5.3.1   Microarray quality control (QC)

The Agilent feature extraction software generates a detailed quality control report for every microarray analysed to evaluate its quality. In order for the microarray to be considered for further analysis it should be within the range of the 16 metrics parameters. The percentage of outlier features that are non-uniform should be less than 1%. The average of background-subtracted signal of the negative control should be -20 to 4 and its standard deviation < 15 for both channels.

In the present study all of the microarrays that were run were within the range of the above parameters as in table 5.2. This indicates good hybridization with minimum outlier probes and no non-specific binding. The reproducibility metrics of MA include calculating signal coefficient of variation (*CV*)% for replicated non-control probes and Agilent spike-in positive control (E1A) probes. The median of *CV*% for replicated probes should be 0 - 18 (both channels). This indicates a good reproducibility between replicates. The median of *CV*% of the Agilent spike-in positive control (E1A) probes should also be 0 - 18 (both channels). In our study all microarrays are within the ideal range as in table 5.3 and this indicates good and reliable reproducibility.

The Spike-in linearity is also checked by plotting the observed log ratio against the expected log ratio. The plot slope and regression coefficient (R^2) should be more than 0.85 and 0.86 respectively. In this study all the microarrays had R^2 more than 0.96 indicating high reproducibility and an excellent quality (table 5.4).

Table 5.2 Microarray quality control metrics 1

	MA	% of feature outliers in both channels	Green negative control metrics		Red negative control metrics	
			Average Signal	Std. Dev	Average Signal	Std. Dev
1	E1 C1	0.003	-2.52	1.52	-3.55	2.63
2	E2 C2	0.035	-2.67	1.46	-3.78	2.65
3	E3 C3	0.003	-2.47	1.41	-3.58	2.52
4	E4 C4	0.016	-2.51	1.44	-4.09	2.76
5	E5 C5	0.030	-3.33	1.67	-3.78	2.77
6	E6 C6	0.014	-3.36	1.58	-3.73	2.53
7	E8 C8	0.025	-3.29	1.65	-4.00	2.64
8	C3 E3	0.017	-2.82	1.58	-3.74	2.63
9	E1 PM1	0.033	-2.10	1.29	-2.29	2.30
10	E2 PM2	0.003	-2.57	1.40	-2.64	2.49
11	E3 PM3	0.008	-2.25	1.38	-2.56	2.47
12	E4 PM4	0.008	-2.48	1.50	-2.58	2.50
13	E5 PM6	0.014	-2.56	1.41	-2.51	2.36
14	E6 PM6	0.021	-2.07	1.39	-2.65	2.59
15	E8 PM3	0.027	-3.29	1.38	-2.78	2.41
16	PM1 E1	0.022	-1.76	1.25	-3.48	2.61
QC range		< 1 %	-20 to 10	< 15	-20 to 4	< 6

C: Non-spiking superior temporal gyrus TLE-STG from TLE patients. **E:** sclerotic hippocampi from TLE patients. **MA:** Microarray. **PM:** *post-mortem* hippocampi. **Signal:** background subtracted signal.

Table 5.3 Microarray quality control metrics 2

	MA	Median % CV Non-Control probe Signal		Median % CV spike-in E1A probe Signal	
		Green	Red	Green	Red
1	E1 C1	10.7	11.8	10.2	10.7
2	E2 C2	11.2	11.0	10.8	9.7
3	E3 C3	11.0	10.4	10.0	9.8
4	E4 C4	11.2	9.9	10.4	9.6
5	E5 C5	12.3	14.9	10.9	14.9
6	E6 C6	11.8	12.1	10.6	10.6
7	E8 C8	11.5	10.8	10.7	9.6
8	C3 E3	11.8	12.6	10.8	12.1
9	E1 PM1	10.6	12.9	10.0	10.6
10	E2 PM2	10.3	11.9	9.5	9.2
11	E3 PM3	11.3	13.6	9.8	11.6
12	E4 PM4	10.6	13.3	9.1	9.4
13	E5 PM6	11.4	12.5	10.1	11.0
14	E6 PM6	11.6	12.6	10.2	11.8
15	E8 PM3	11.4	14.0	11.2	12.0
16	PM1 E1	12.1	13.7	10.3	12.9
QC range		0 to 18	0 to 18	0 to 18	0 to 18

C: Non-spiking superior temporal gyrus TLE-STG from TLE patients. E: sclerotic hippocampi from TLE patients. MA: Microarray. PM: *post-mortem* hippocampi. Signal: background subtracted signal.

Table 5.4 Microarray quality control metrics 3

	MA	E1A Spike-in Observed log ratio Vs expected plot		Direction dependent noise	
		R^2	Slope	Green	Red
1	E1 C1	0.98	0.86	3	-8
2	E2 C2	0.98	0.84	3	-8
3	E3 C3	0.98	0.84	3	-8
4	E4 C4	0.99	0.85	3	-8
5	E5 C5	0.98	0.82	3	-8
6	E6 C6	0.99	0.85	3	-8
7	E8 C8	0.98	0.86	3	-8
8	C3 E3	0.98	0.85	3	-8
9	E1 PM1	0.97	0.84	3	-8
10	E2 PM2	0.98	0.84	3	-8
11	E3 PM3	0.97	0.86	3	-8
12	E4 PM4	0.98	0.86	3	-8
13	E5 PM6	0.98	0.83	3	-8
14	E6 PM6	0.98	0.84	3	-8
15	E8 PM3	0.97	0.85	3	-8
16	PM1 E1	0.98	0.86	3	-8
QC range		> 0.86	> 0.85	-15 to 15	-15 to 15

The direction dependent noise (DDN) metric is measured for every channel, to check for noise during scanning. Our microarray scanning DNN noise was within the range of a good quality array. **C:** Non-spiking superior temporal gyrus TLE-STG from TLE patients. **E:** sclerotic hippocampi from TLE patients. **MA:** Microarray. **PM:** *post-mortem* hippocampi.

5.3.2 Identification of differentially expressed genes (DEGs) in TLE-HS using RP

In comparing epileptic TLE-HS transcriptome to TLE-STG, there were 1821 genes that were significantly up regulated, while 1511 genes were significantly down regulated. In comparing TLE-HS to PMC samples, the transcriptome analysis revealed that there were; 1961 significantly up regulated genes and 2867 significantly down regulated genes as in TLE-HS tissue figure 5.2.

The comparison of TLE-HS transcriptome to both TLE-STG and PMC, showed that there were an overlapping 464 genes that are up regulated and 350 genes down regulated in TLE-HS as in figure 5.3. The functional enrichment analysis was done for those overlapping differentially expressed genes.

a   MA1: TLE-HS vs TLE-STG
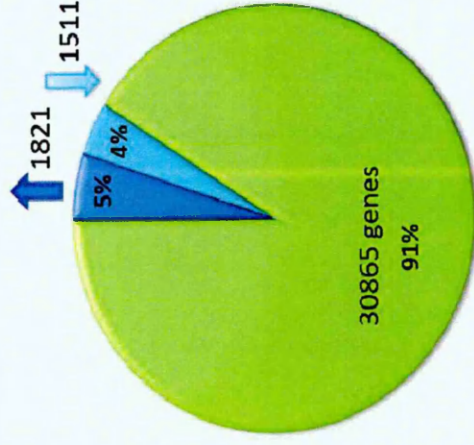
b   MA2: TLE-HS vs PMC
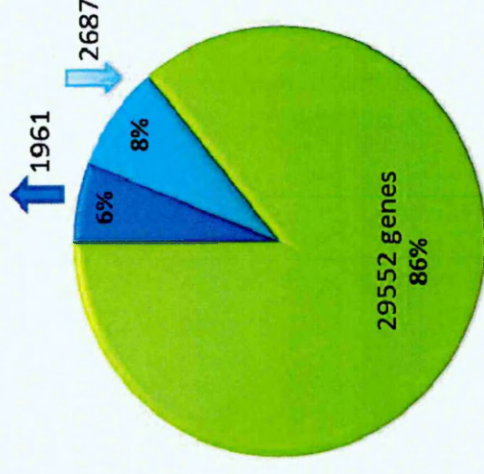
- Up regulated   ■ Down regulated   ■ non-significant

Figure 5.2 Differentially expressed genes in TLE-HS compared to TLE-STG and PMC

Differentially expressed genes in TLE-HS compared to TLE-STG and PMC. **(a) TLE-HS vs TLE-STG:** there are 1821 genes that were significantly up regulated and 1511 genes that were significantly down regulated. **(b) TLE-HS vs PMC:** there are 1961 genes that were significantly up regulated and 2687 genes that were significantly down regulated in TLE-HS. **MA statistical analysis:** rank products test was used to identify significant differences between samples ($P \leq 0.0001$). MA number of samples: TLE-HS (n = 7); TLE-STG (n = 7); PMC (n = 5). **MA:** Microarray.

147

Up-regulated genes

MA1   MA2

1357   **464**   1497

P-value < 0.0001

Down-regulated genes

MA1   MA2

1161   **350**   2337

P-value < 0.0001
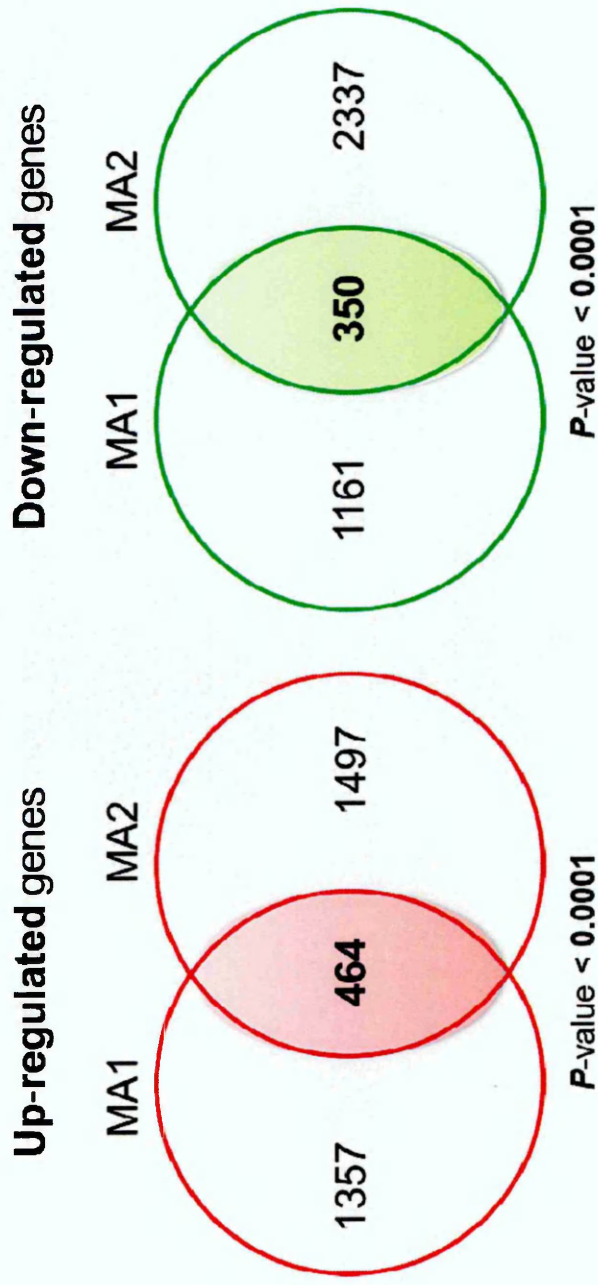
Figure 5.3 Venn diagrams showing the overlapping DEGs in TLE-HS samples compared to both TLE-STG and PMC

There were 464 genes that were significantly up regulated and 350 genes down regulated in TLE-HS. **MA**: Microarray. **MA1:** TLE-HS vs TLE-STG MA

analysis. **MA2:** TLE-HS vs PMC MA analysis.

148

5.3.3 Functional enrichment analysis of DEGs by DAVID

5.3.3.1 Functional enrichment analysis of all DEGs

The function annotation clustering analysis for both the up and down DEGs produced 34 significantly enriched clusters (enrichment score > 1.3) with the first cluster having 6.72 enrichment score.

The DEGs in clusters 1, 2 and 3 with high enrichment score 6.72, 5.96, and 5.51 respectively, were closely related to signal, glycoprotein and cytokine activity terms. They were mainly related to the extracellular region of the cellular component and were significantly associated with the biological process of inflammatory and defence response as in table 5.5. The association of individual genes to the annotation term in cluster 3 is shown in figure 5.4.

The DEGs in clusters 4, with enrichment score 3.79, were associated with biological processes such as inflammatory response, cytokine activity, cytokine-cytokine receptor interaction, chemotaxis and chemokine activity as in table 5.6. The association of genes to the annotation term in cluster 4 is shown in figure 5.5. The DEGs in clusters 5 with enrichment score 2.82; were related to neuropeptide signalling pathway and nuclear pore complex interacting proteins as in table 5.6. (See appendix IV for all 34 clusters).

Table 5.5 Functional annotation clustering of DEGs: Cluster 1-3

Annotation Cluster 1	Enrichment Score: 6.72		
Category	Term	Count	*P* Value
SP_PIR_KEYWORDS	signal	97	4.44E-09
SP_PIR_KEYWORDS	disulphide bond	90	4.90E-09
UP_SEQ_FEATURE	signal peptide	97	6.18E-09
UP_SEQ_FEATURE	disulphide bond	87	1.20E-08
UP_SEQ_FEATURE	glycosylation site: N-linked (GlcNAc...)	98	1.72E-04
SP_PIR_KEYWORDS	glycoprotein	101	1.76E-04
Annotation Cluster 2	**Enrichment Score: 5.96**		
Category	Term	Count	*P* Value
SP_PIR_KEYWORDS	signal	97	4.44E-09
UP_SEQ_FEATURE	signal peptide	97	6.18E-09
SP_PIR_KEYWORDS	Secreted	55	2.51E-06
GOTERM_CC_FAT	GO:0044421~extracellular region part	39	3.49E-06
GOTERM_CC_FAT	GO:0005576~extracellular region	64	4.44E-06
GOTERM_MF_FAT	GO:0005125~cytokine activity	15	1.02E-05
SP_PIR_KEYWORDS	cytokine	14	1.15E-05
GOTERM_CC_FAT	GO:0005615~extracellular space	30	1.67E-05
Annotation Cluster 3	**Enrichment Score: 5.51**		
Category	Term	Count	*P* Value
GOTERM_BP_FAT	GO:0006954~inflammatory response	22	8.58E-07
GOTERM_BP_FAT	GO:0006952~defense response	31	1.59E-06
GOTERM_BP_FAT	GO:0009611~response to wounding	26	2.18E-05

BP: Biological Processes. **CC:** Cellular Components. **GO:** Gene ontology. **GOTERM:** Gene ontology term. **INTERPRO:** protein sequence analysis & classification resource. **KEGG:** Kyoto Encyclopaedia of Genes and Genomes. **MF:** Molecular Functions. **PIR:** Protein Information Resource annotation. **SMART:** Simple Modular Architecture Research Tool. **SP:** SwissProt Protein Knowledgebase. **UP_SEQ_FEATURE:** Uniprot Sequence annotations.

Table 5.6 Functional annotation clustering of DEGs: Cluster 4 and 5

Annotation Cluster 4	Enrichment Score: 3.79		
Category	Term	Count	*P* Value
GOTERM_BP_FAT	GO:0007610~behavior	27	8.00E-07
GOTERM_BP_FAT	GO:0006954~inflammatory response	22	8.58E-07
SP_PIR_KEYWORDS	inflammation	7	2.79E-06
GOTERM_MF_FAT	GO:0005125~cytokine activity	15	1.02E-05
SP_PIR_KEYWORDS	cytokine	14	1.15E-05
KEGG_PATHWAY	hsa04060:Cytokine-cytokine receptor interaction	18	1.21E-05
GOTERM_CC_FAT	GO:0005615~extracellular space	30	1.67E-05
PIR_SUPERFAMILY	PIRSF500569:macrophage inflammatory protein 1, alpha/beta	4	2.97E-05
SP_PIR_KEYWORDS	inflammatory response	9	4.27E-05
SP_PIR_KEYWORDS	chemotaxis	8	1.96E-04
GOTERM_BP_FAT	GO:0006935~chemotaxis	12	2.17E-04
GOTERM_BP_FAT	GO:0042330~taxis	12	2.17E-04
INTERPRO	IPR001811:Small chemokine, interleukin-8-like	6	6.40E-04
GOTERM_BP_FAT	GO:0007626~locomotory behaviour	15	6.84E-04
INTERPRO	IPR000827:Small chemokine, C-C group, conserved site	5	7.99E-04
SMART	SM00199:SCY	6	9.42E-04
PIR_SUPERFAMILY	PIRSF001950:small inducible chemokine, C/CC types	5	9.63E-04
GOTERM_MF_FAT	GO:0008009~chemokine activity	6	0.00129
GOTERM_MF_FAT	GO:0042379~chemokine receptor binding	6	0.00172
GOTERM_BP_FAT	GO:0006928~cell motion	18	0.00828
Annotation Cluster 5	Enrichment Score: 2.82		
Category	Term	Count	*P* Value
GOTERM_BP_FAT	GO:0007218~neuropeptide signalling pathway	10	6.13E-05
INTERPRO	IPR009443:Nuclear pore complex interacting	4	9.54E-05
INTERPRO	IPR000203: GPCR proteolytic site	4	0.0269
SMART	SM00303: GPCR proteolytic site	4	0.03371

BP: Biological Processes. CC: Cellular Components. GO: Gene ontology. GOTERM: Gene ontology term. INTERPRO: protein sequence analysis & classification resource. KEGG: Kyoto Encyclopaedia of Genes and Genomes. MF: Molecular Functions. PIR: Protein Information Resource annotation. SMART: Simple Modular Architecture Research Tool. SP: SwissProt Protein Knowledgebase. UP_SEQ_FEATURE: Uniprot Sequence annotations.
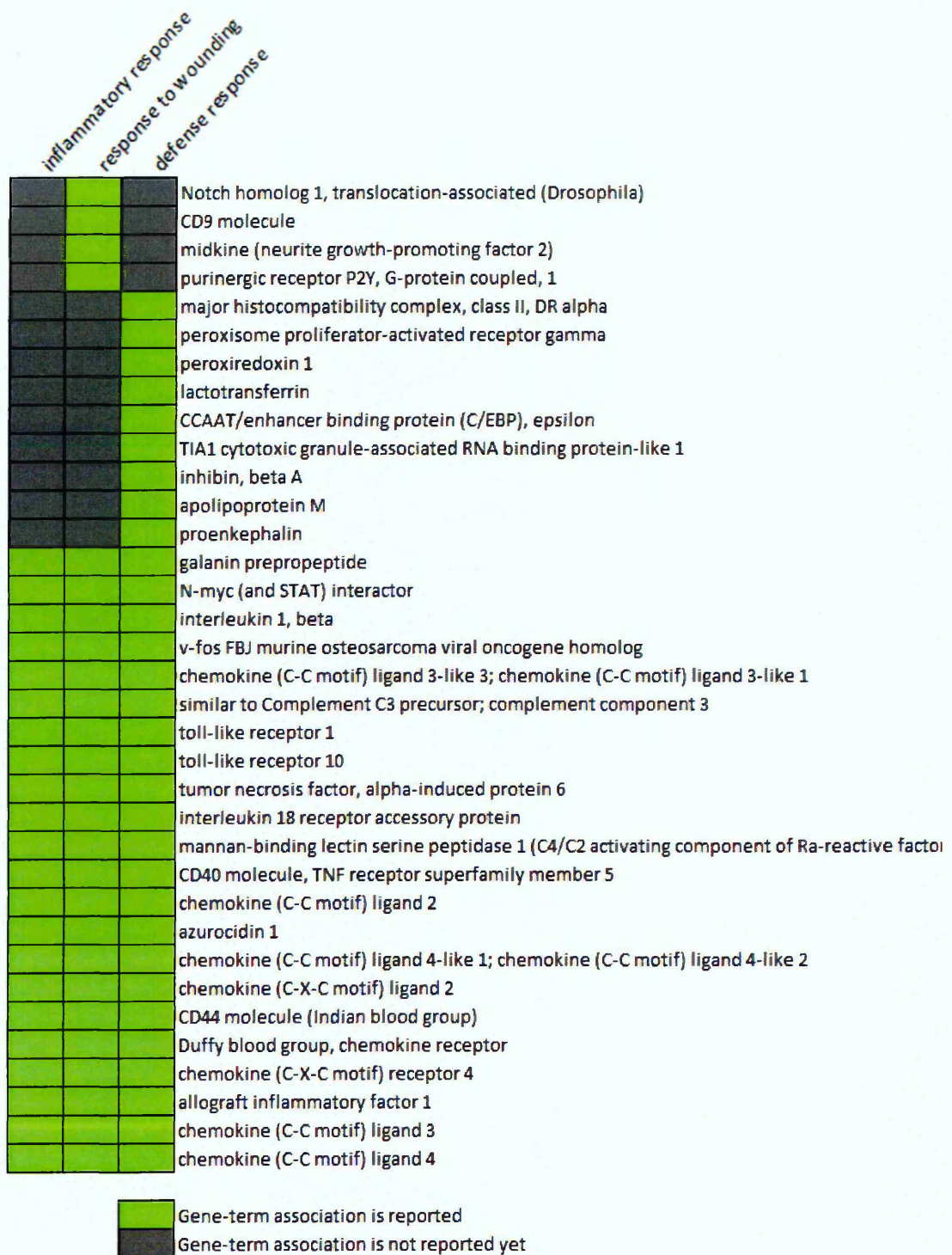
Figure 5.4 Genes in functional annotation cluster 3

Functional annotation cluster 3: the association of genes to annotation terms in the cluster with an enrichment score of 5.51.
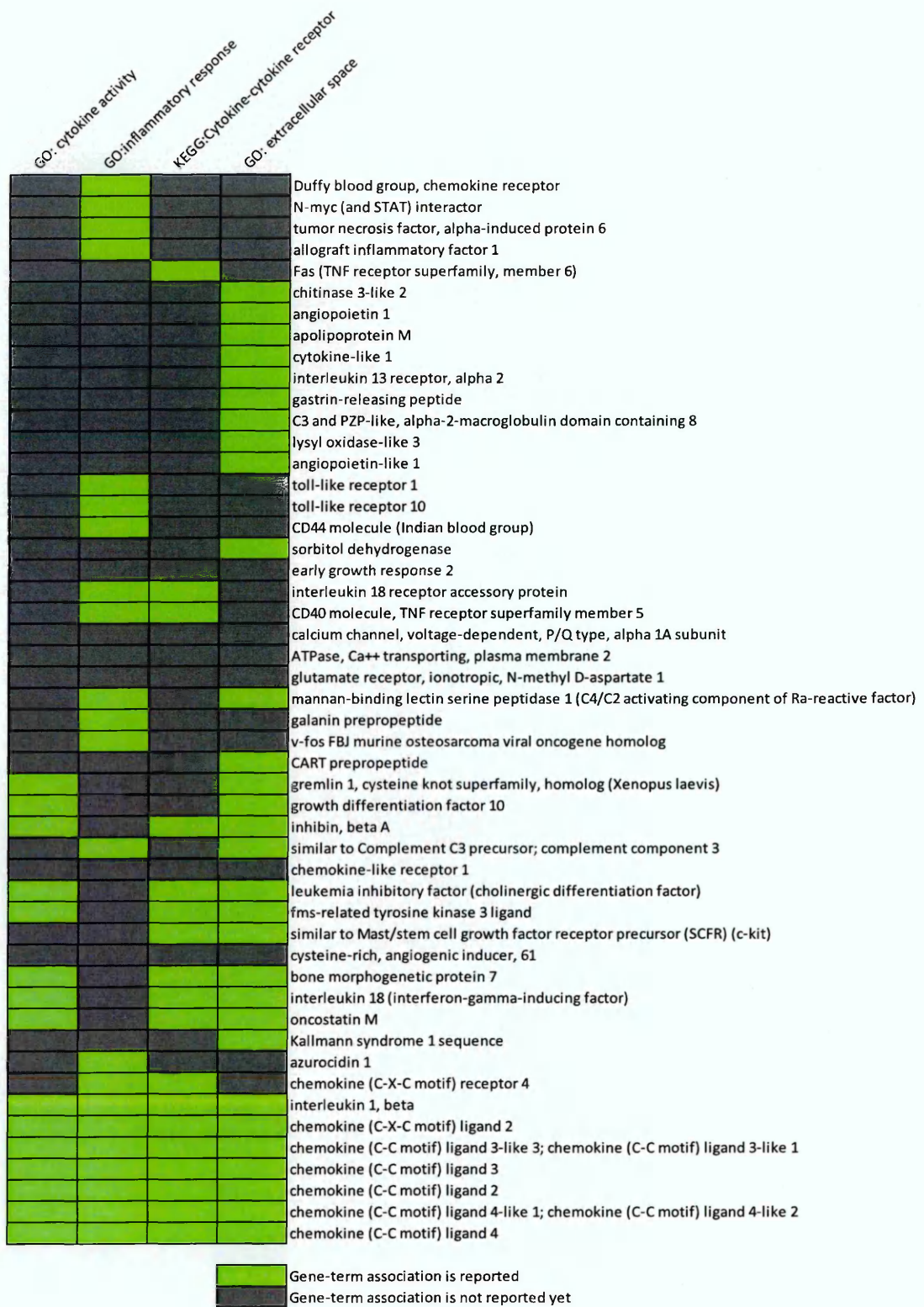
Figure 5.5 Genes in functional annotation cluster 4

Functional annotation cluster 4: the association of genes to some annotation terms in the cluster 4 with an enrichment score of 3.79.

5.3.3.2 Functional enrichment analysis of up and down regulated genes

Following the functional analysis of all DEGs, the up regulated and down regulated genes functional analysis was done separately. The functional analysis of the up regulated genes generated 21 clusters that are significantly enriched (enrichment score > 1.3). The analysis of the down regulated genes generated 6 significantly enriched clusters as in figure 5.6.
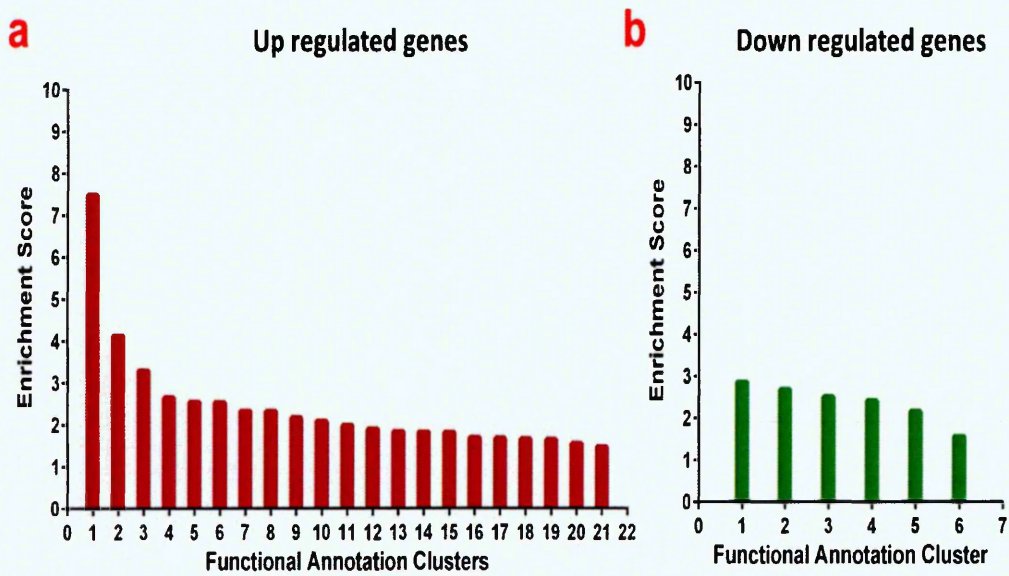
Figure 5.6 Enrichment scores of annotation clusters obtained by functional enrichment analysis

(a) Up regulated genes had 21 significantly enriched clusters with enrichment score from 7.45 to 1.46. (b) Down regulated genes only had 6 significantly enriched clusters with enrichment score from 2.85 to 1.55.

Functional annotation clusters of up regulated genes

The first cluster of up regulated genes demonstrated that 82 genes with enrichment P-value 4.2×10^{-12} were significantly associated with signalling and glycoprotein terms; their cellular component was in the extracellular space or region. The genes in the second cluster were significantly associated with biological processes of inflammatory and defence responses and chemotaxis. They were also enriched in cytokine-cytokine receptor interaction pathway in addition to molecular function such as chemokine activity and chemokine receptor binding. The genes in annotation cluster 5 were associated with neuropeptide signalling pathway as in table 5.7.

Functional annotation clusters of down regulated genes

The annotation cluster 1 of down regulated genes demonstrated that those genes were associated with calmodulin and actin binding molecular functions; their cellular component was in the actin cytoskeleton region and they were associated with biological processes of actin and actomyosin cytoskeleton organization as well as regulation of cellular component biogenesis as in table 5.8. Furthermore; the genes in annotation cluster 3 were associated with cellular components such as synapse, cell junction, dendrite, postsynaptic membrane and postsynaptic density. In addition, the down regulated genes in annotation cluster 5 were associated with biological processes such as ligand- and voltage-gated channel activity, ion transport, calcium transport and calcium signalling pathway. They were also involved in the regulation of cellular localization, synapse organization and regulation of synaptic plasticity as in table 5.8.

Table 5.7 Functional annotation clustering of up regulated genes

Annotation Cluster 1	Enrichment Score: 7.48		
Category	Term	Count	*P* Value
SP_PIR_KEYWORDS	signal	82	4.21E-12
UP_SEQ_FEATURE	signal peptide	82	5.88E-12
SP_PIR_KEYWORDS	disulphide bond	72	5.60E-10
UP_SEQ_FEATURE	disulphide bond	70	1.02E-09
SP_PIR_KEYWORDS	Secreted	50	2.25E-09
GOTERM_CC_FAT	GO:0005576~extracellular region	58	3.76E-09
GOTERM_CC_FAT	GO:0044421~extracellular region part	37	6.99E-09
GOTERM_CC_FAT	GO:0005615~extracellular space	28	2.73E-07
UP_SEQ_FEATURE	glycosylation site: N-linked (GlcNAc...)	74	1.15E-04
SP_PIR_KEYWORDS	glycoprotein	76	1.29E-04
UP_SEQ_FEATURE	topological domain:Cytoplasmic	54	0.01577
Annotation Cluster 2	Enrichment Score: 4.12		
Category	Term	Count	*P* Value
GOTERM_BP_FAT	GO:0006952~defense response	27	2.55E-07
GOTERM_BP_FAT	GO:0006954~inflammatory response	19	4.62E-07
GOTERM_BP_FAT	GO:0009611~response to wounding	23	3.13E-06
SP_PIR_KEYWORDS	inflammatory response	9	3.36E-06
GOTERM_BP_FAT	GO:0007610~behavior	21	6.08E-06
KEGG_PATHWAY	hsa04060:Cytokine-cytokine receptor interaction	16	7.48E-06
GOTERM_MF_FAT	GO:0005125~cytokine activity	13	8.07E-06
SP_PIR_KEYWORDS	inflammation	6	9.40E-06
SP_PIR_KEYWORDS	cytokine	12	1.01E-05
PIR_SUPERFAMILY	PIRSF500569:macrophage inflammatory protein 1, alpha/beta	4	1.23E-05
INTERPRO	IPR001811:Small chemokine, interleukin-8-like	6	1.31E-04
SMART	SM00199:SCY	6	1.56E-04
SP_PIR_KEYWORDS	chemotaxis	7	2.01E-04
INTERPRO	IPR000827:Small chemokine, C-C group, conserved site	5	2.17E-04
GOTERM_MF_FAT	GO:0008009~chemokine activity	6	2.97E-04
PIR_SUPERFAMILY	PIRSF001950:small inducible chemokine, C/CC types	5	3.18E-04
GOTERM_BP_FAT	GO:0042330~taxis	10	3.38E-04
GOTERM_BP_FAT	GO:0006935~chemotaxis	10	3.38E-04
GOTERM_MF_FAT	GO:0042379~chemokine receptor binding	6	4.00E-04
GOTERM_BP_FAT	GO:0006928~cell motion	16	0.00213

Table 5.7 Functional annotation clustering of up regulated genes (continued)

Annotation Cluster 3	Enrichment Score: 3.29		
Category	Term	Count	P Value
GOTERM_BP_FAT	GO:0009991~response to extracellular stimulus	14	9.74E-06
GOTERM_BP_FAT	GO:0010033~response to organic substance	25	4.39E-05
GOTERM_BP_FAT	GO:0009725~response to hormone stimulus	16	1.49E-04
GOTERM_BP_FAT	GO:0033273~response to vitamin	7	2.69E-04
GOTERM_BP_FAT	GO:0048545~response to steroid hormone stimulus	11	2.97E-04
GOTERM_BP_FAT	GO:0031667~response to nutrient levels	11	3.64E-04
GOTERM_BP_FAT	GO:0009719~response to endogenous stimulus	16	4.28E-04
GOTERM_BP_FAT	GO:0007584~response to nutrient	9	6.52E-04
GOTERM_BP_FAT	GO:0051384~response to glucocorticoid stimulus	7	6.66E-04
GOTERM_BP_FAT	GO:0031960~response to corticosteroid stimulus	7	0.00105
GOTERM_BP_FAT	GO:0043434~response to peptide hormone stimulus	9	0.00121
GOTERM_BP_FAT	GO:0043627~response to estrogen stimulus	6	0.01427
GOTERM_BP_FAT	GO:0032570~response to progesterone stimulus	3	0.02977
Annotation Cluster 4	Enrichment Score: 2.64		
Category	Term	Count	P Value
GOTERM_BP_FAT	GO:0009628~response to abiotic stimulus	15	5.11E-04
GOTERM_BP_FAT	GO:0009612~response to mechanical stimulus	6	9.60E-04
GOTERM_BP_FAT	GO:0014070~response to organic cyclic substance	7	0.00617
GOTERM_BP_FAT	GO:0042493~response to drug	9	0.00946
Annotation Cluster 5	Enrichment Score: 2.54		
Category	Term	Count	P Value
SP_PIR_KEYWORDS	cleavage on pair of basic residues	13	9.07E-05
GOTERM_BP_FAT	GO:0007218~neuropeptide signalling pathway	7	0.00167
GOTERM_MF_FAT	GO:0005179~hormone activity	6	0.01278
GOTERM_MF_FAT	GO:0005184~neuropeptide hormone activity	3	0.03487

Table 5.8 Functional annotation clustering of down regulated genes

Annotation Cluster 1	Enrichment Score: 2.85		
Category	Term	Count	*P* Value
GOTERM_MF_FAT	GO:0005516~calmodulin binding	9	4.0E-07
SP_PIR_KEYWORDS	calmodulin-binding	7	2.9E-05
SP_PIR_KEYWORDS	actin binding	5	4.5E-05
GOTERM_BP_FAT	GO:0031032~actomyosin structure organization	4	4.0E-04
GOTERM_MF_FAT	GO:0008092~cytoskeletal protein binding	10	7.7E-04
GOTERM_MF_FAT	GO:0003779~actin binding	8	1.1E-03
GOTERM_CC_FAT	GO:0015629~actin cytoskeleton	7	2.0E-03
SP_PIR_KEYWORDS	actin-binding	6	7.6E-03
GOTERM_CC_FAT	GO:0005856~cytoskeleton	14	1.6E-02
GOTERM_BP_FAT	GO:0030036~actin cytoskeleton organization	5	3.0E-02
GOTERM_BP_FAT	GO:0044087~regulation of cellular component biogenesis	4	3.7E-02
INTERPRO	IPR001715:Calponin-like actin-binding	3	4.8E-02
Annotation Cluster 2	Enrichment Score: 2.67		
Category	Term	Count	*P* Value
INTERPRO	IPR009443:Nuclear pore complex interacting	4	2.4E-06
INTERPRO	IPR001024:Lipoxygenase, LH2	3	6.3E-03
INTERPRO	IPR000203:GPS	3	1.5E-02
SMART	SM00303:GPS	3	2.2E-02
Annotation Cluster 3	Enrichment Score: 2.50		
Category	Term	Count	*P* Value
GOTERM_CC_FAT	GO:0045211~postsynaptic membrane	6	5.2E-04
GOTERM_CC_FAT	GO:0030054~cell junction	10	9.2E-04
GOTERM_CC_FAT	GO:0044456~synapse part	7	1.3E-03
SP_PIR_KEYWORDS	postsynaptic cell membrane	5	2.2E-03
SP_PIR_KEYWORDS	cell junction	8	3.6E-03
SP_PIR_KEYWORDS	synapse	6	4.1E-03
GOTERM_CC_FAT	GO:0014069~postsynaptic density	4	5.1E-03
GOTERM_CC_FAT	GO:0045202~synapse	7	7.9E-03
GOTERM_CC_FAT	GO:0030425~dendrite	5	8.5E-03
GOTERM_CC_FAT	GO:0043197~dendritic spine	3	1.5E-02
Annotation Cluster 4	Enrichment Score: 2.40		
Category	Term	Count	*P* Value
GOTERM_CC_FAT	GO:0015629~actin cytoskeleton	7	0.0020
GOTERM_CC_FAT	GO:0044449~contractile fibre part	5	0.0023

Table 5.8 Functional annotation clustering of down regulated genes (continued)

Annotation Cluster 5	Enrichment Score: 2.15		
Category	Term	Count	P Value
GOTERM_MF_FAT	GO:0005516~calmodulin binding	9	4.0E-07
GOTERM_MF_FAT	GO:0022836~gated channel activity	8	8.0E-04
GOTERM_BP_FAT	GO:0006816~calcium ion transport	6	8.3E-04
SP_PIR_KEYWORDS	ionic channel	8	1.0E-03
GOTERM_BP_FAT	GO:0044057~regulation of system process	8	1.1E-03
GOTERM_MF_FAT	GO:0046873~metal ion transmembrane transporter activity	8	1.1E-03
GOTERM_BP_FAT	GO:0006811~ion transport	12	1.8E-03
GOTERM_BP_FAT	GO:0015674~di-, tri-valent inorganic cation transport	6	2.2E-03
SP_PIR_KEYWORDS	ion transport	10	2.2E-03
GOTERM_BP_FAT	GO:0030001~metal ion transport	9	2.7E-03
GOTERM_MF_FAT	GO:0005216~ion channel activity	8	2.8E-03
GOTERM_MF_FAT	GO:0022838~substrate specific channel activity	8	3.3E-03
GOTERM_MF_FAT	GO:0015267~channel activity	8	4.0E-03
GOTERM_MF_FAT	GO:0022803~passive transmembrane transporter activity	8	4.1E-03
KEGG_PATHWAY	hsa04020:Calcium signalling pathway	5	6.2E-03
GOTERM_MF_FAT	GO:0005262~calcium channel activity	4	6.9E-03
GOTERM_BP_FAT	GO:0006812~cation transport	9	7.5E-03
GOTERM_CC_FAT	GO:0034704~calcium channel complex	3	7.8E-03
GOTERM_CC_FAT	GO:0030425~dendrite	5	8.5E-03
SP_PIR_KEYWORDS	calcium transport	4	8.6E-03
GOTERM_BP_FAT	GO:0043062~extracellular structure organization	5	1.0E-02
GOTERM_MF_FAT	GO:0005261~cation channel activity	6	1.1E-02
GOTERM_BP_FAT	GO:0022037~metencephalon development	3	1.4E-02
GOTERM_CC_FAT	GO:0034702~ion channel complex	5	1.8E-02
GOTERM_MF_FAT	GO:0022834~ligand-gated channel activity	4	2.5E-02
GOTERM_CC_FAT	GO:0034703~cation channel complex	4	2.7E-02
GOTERM_BP_FAT	GO:0050804~regulation of synaptic transmission	4	3.3E-02
GOTERM_MF_FAT	GO:0022843~voltage-gated cation channel activity	4	3.6E-02
SP_PIR_KEYWORDS	calcium channel	3	3.7E-02
SP_PIR_KEYWORDS	voltage-gated channel	4	3.8E-02
GOTERM_BP_FAT	GO:0030902~hindbrain development	3	3.9E-02

Table 5.8 Functional annotation clustering of down regulated genes (continued)

Annotation Cluster 5	Enrichment Score: 2.15		
Category	Term	Count	*P* Value
GOTERM_BP_FAT	GO:0060341~regulation of cellular localization	5	3.9E-02
GOTERM_BP_FAT	GO:0050808~synapse organization	3	4.0E-02
GOTERM_BP_FAT	GO:0051969~regulation of transmission of nerve impulse	4	4.1E-02
GOTERM_BP_FAT	GO:0050905~neuromuscular process	3	4.1E-02
GOTERM_BP_FAT	GO:0048167~regulation of synaptic plasticity	3	4.3E-02
GOTERM_BP_FAT	GO:0031644~regulation of neurological system process	4	4.5E-02
GOTERM_MF_FAT	GO:0005230~extracellular ligand-gated ion channel activity	3	4.9E-02

5.3.3.3 The KEGG pathway enrichment analysis of DEGs

The KEGG pathway enrichment analysis of up regulated genes, displayed in table 5.9, showed that the genes were most significantly associated with cytokine-cytokine receptor interaction pathway (P = 7.5 X 10^{-6}), Toll-like receptor signalling pathway (P = 4.3 X 10^{-3}) and MAPK signalling pathway (P = 2.0 X 10^{-2}). While the KEGG pathway enrichment analysis of down regulated genes showed that the genes were significantly associated with the calcium signalling pathway (P = 0.006) as displayed in table 5.10.

5.3.4 The mRNA expression of cytokines in TLE-HS

The KEGG pathway functional enrichment analysis of DEGs showed that cytokine-cytokine receptor interaction pathway (16 genes) had the highest enrichment P - value. In addition, the functional annotation analysis of up regulated genes showed that these cytokine genes were in the first and second highest clusters of functional enrichment analysis. Therefore, the mRNA expression of IL-1β, IL-18, Fas, ICAM-1, CCL2, CCL4, CXCL1, CXCL2, CXCL12, CXCR4 and CX3CR1 from MA analysis were further validated by qRT-PCR (Gene names are fully described in section 2.5, table 2.4).

Table 5.9 KEGG pathway enrichment analysis of up regulated DEGs

KEGG_PATHWAY	Count	P Value
hsa04060: Cytokine-cytokine receptor interaction	16	7.5E-06
hsa04620: Toll-like receptor signalling pathway	7	4.3E-03
hsa04640: Hematopoietic cell lineage	6	9.9E-03
hsa05330: Allograft rejection	4	1.7E-02
hsa04010: MAPK signalling pathway	10	2.0E-02
hsa05332: Graft-versus-host disease	4	2.1E-02
hsa04940: Type I diabetes mellitus	4	2.6E-02
hsa04672: Intestinal immune network for IgA production	4	3.9E-02
hsa05320: Autoimmune thyroid disease	4	4.3E-02
hsa04350: TGF-beta signalling pathway	5	4.4E-02
hsa04623: Cytosolic DNA-sensing pathway	4	5.2E-02
hsa04062: Chemokine signalling pathway	7	6.6E-02
hsa04621: NOD-like receptor signalling pathway	4	6.9E-02
hsa05310: Asthma	3	7.2E-02
hsa03320: PPAR signalling pathway	4	8.9E-02
hsa05020: Prion diseases	3	1.0E-01

Table 5.10 KEGG pathway enrichment analysis of down regulated DEGs

KEGG_PATHWAY	Count	P Value
hsa04260: Cardiac muscle contraction	4	0.00433
hsa04020: Calcium signalling pathway	5	0.00622
hsa05410: Hypertrophic cardiomyopathy (HCM)	3	0.05139
hsa05414: Dilated cardiomyopathy	3	0.05918

5.1.1.1 IL-1β, IL-18, Fas and ICAM-1 mRNA expression

The MA and qRT-PCR data demonstrated that gene expression of inflammatory cytokines IL-1β, IL-18 and Fas were significantly increased in TLE-HS compared to both PMC and TLE-STG. The intracellular adhesion molecule 1 (ICAM-1) gene expression in TLE-HS was significantly increased compared to TLE-STG. However compared to PMC, only MA data show a significant increased expression of ICAM-1 as shown in figure 5.7.

5.1.1.2 CCL2, CCL4, CXCL1 and CXCL2 mRNA expression

The gene expression of chemokines CCL2, CCL4 and CXCL2 determined by both MA and qRT-PCR, were significantly up regulated in TLE-HS compared to both PMC and TLE-STG. The MA gene expression of CXCL1 was significantly up regulated in TLE-HS compared to PMC; while the CXCL1 qRT-PCR data showed a significant up regulation in TLE-HS compared to both PMC and TLE-STG as shown in figure 5.8.

5.1.1.3 CXCL12, CXCR4 and CX3CR1 mRNA expression

The gene expression of the chemokine CXCL12 and its receptor CXCR4 determined by both MA and qRT-PCR; showed a significant up regulation in TLE-HS compared to both TLE-STG and PMC. The CX3CR1 expression in TLE-HS investigated by MA showed a slight increase in expression compared to TLE-STG and a significant increased expression compared to PMC. On the other hand, CX3CR1 expression in TLE-HS investigated by qRT-PCR revealed a significant up regulation compared to both PMC and TLE-STG as shown in figure 5.9.

163
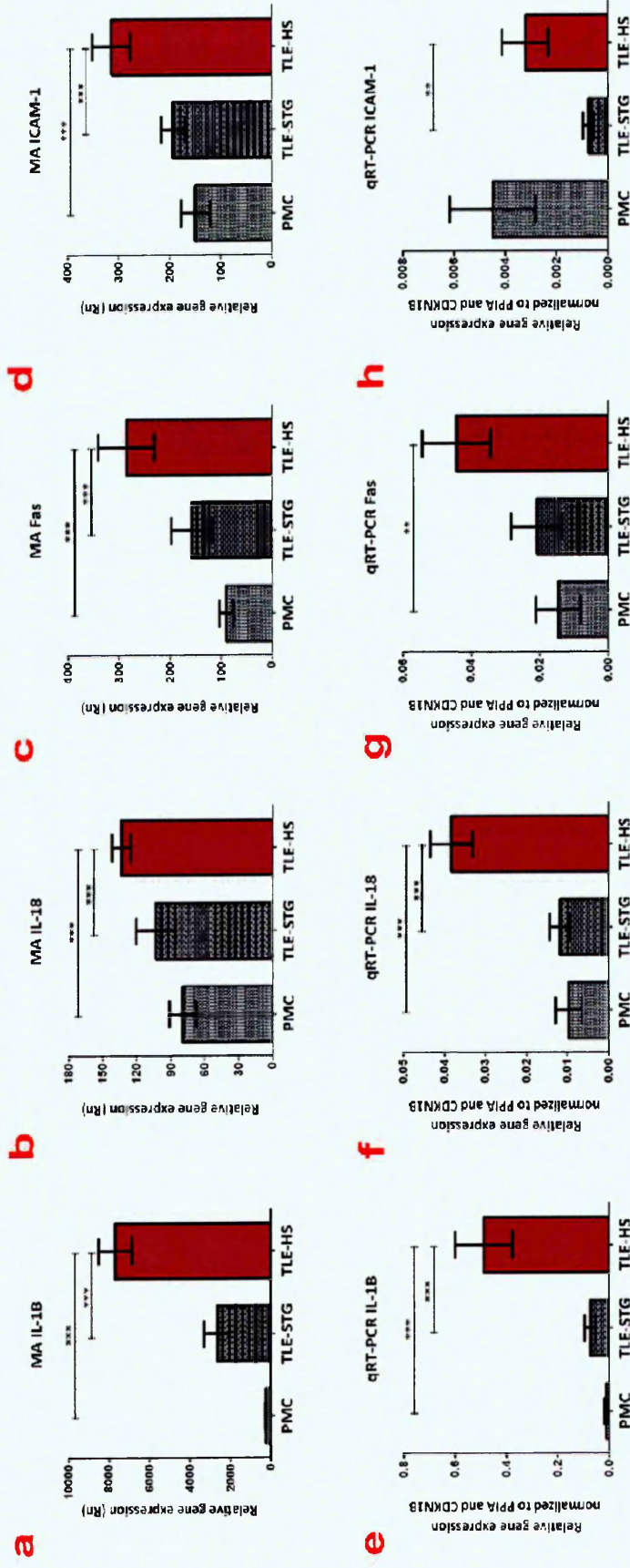
Figure 5.7 Gene expression of IL-1β, IL-18, Fas and ICAM-1 in PMC, TLE-STG and TLE-HS

IL-1β, IL-18 and Fas gene expression was increased in TLE-HS compared to PMC and TLE-STG when investigated by MA (a, b, c) and qRT-PCR (e, f, g). ICAM-1 expression was up regulated in TLE-HS compared to PMC and TLE-STG by MA (d) while qRT-PCR show that its expression was up regulated in TLE-HS only compared to TLE-STG (h). Significant differences indicated by * $P < 0.05$; ** $P < 0.01$, *** $P < 0.001$. Number of samples for **MA**: PMC (n = 5), TLE-STG (n = 7), TLE-HS (n = 7); **qRT-PCR**: PMC (n = 7) TLE-STG (n = 10); TLE-HS (n = 22). **MA**: Microarray. Data presented as mean ± S.E.M.

164
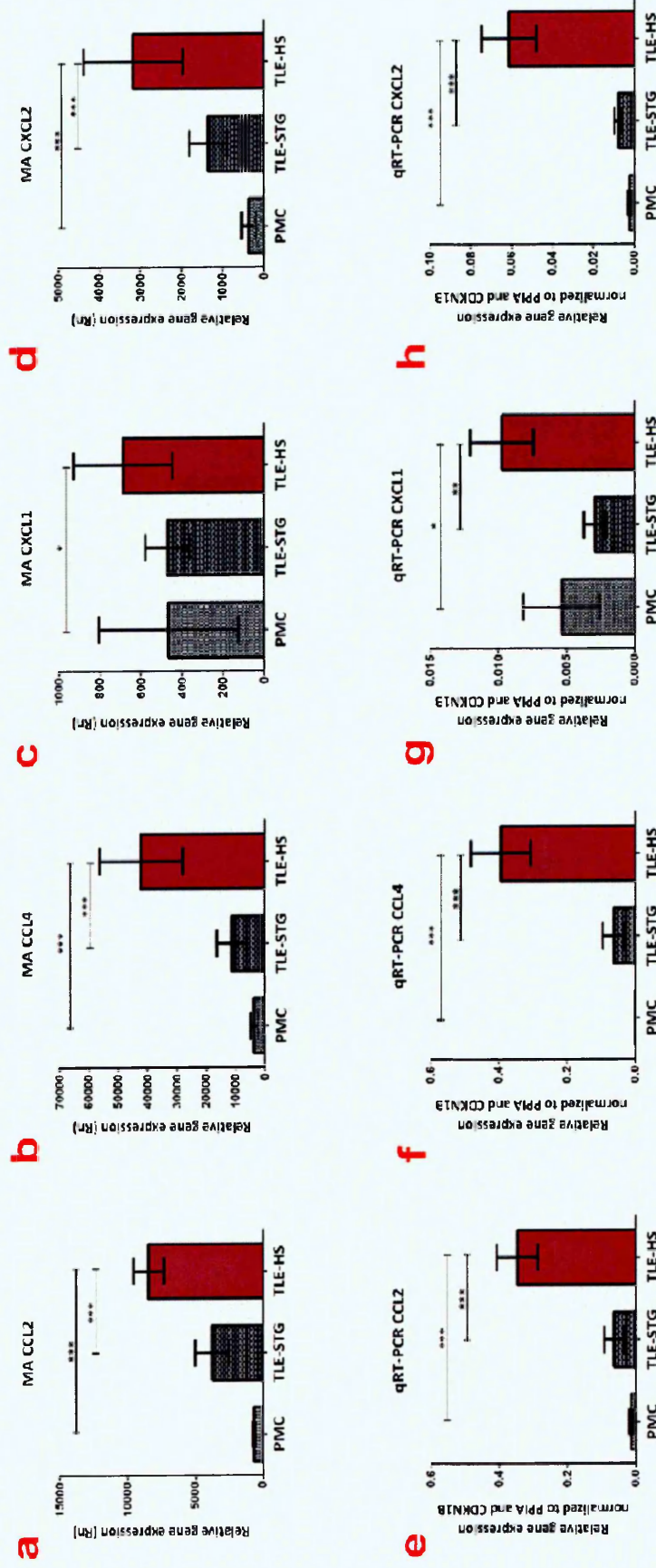
Figure 5.8 Gene expression of chemokines CCL2, CCL4, CXCL1 and CXCL2 in PMC, TLE-STG and TLE-HS

CCL2, CCL4, CXCL1 and CXCL2 gene expression was up regulated in TLE-HS compared to PMC and TLE-STG when investigated by MA (a, b, c, d) and qRT-PCR (e, f, g, h). Significant differences indicated by * $P < 0.05$; ** $P < 0.01$, *** $P < 0.001$. Number of samples for **MA**: PMC (n = 5), TLE-STG (n = 7), TLE-HS (n = 7); **qRT-PCR**: PMC (n = 7) TLE-STG (n = 10); TLE-HS (n = 22). **MA**: Microarray. Data presented as mean ± S.E.M.
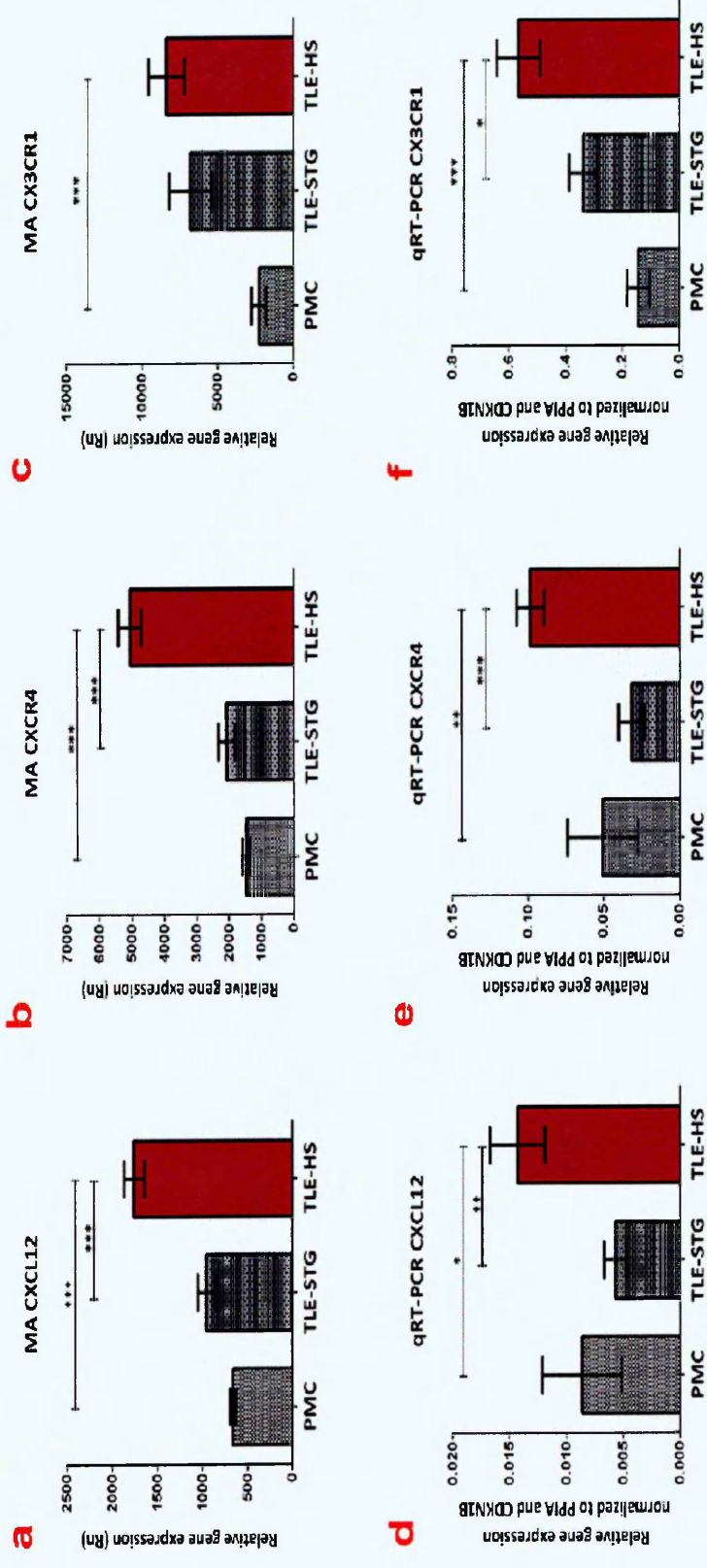
Figure 5.9 Gene expression of chemokine CXCL12 and chemokine receptors CXCR4 and CX3CR1 in PMC, TLE-STG and TLE-HS

CXCL12, CXCR4 and CX3CR1 gene expression in TLE-HS compared to PMC and TLE-STG when investigated by MA (a, b, c) and qRT-PCR (d, e, f). Significant differences indicated by * $P < 0.05$; ** $P < 0.01$, *** $P < 0.001$. Number of samples for **MA**: PMC (n = 5), TLE-STG (n = 7), TLE-HS (n = 7); **qRT-PCR**: PMC (n = 7) TLE-STG (n = 10); TLE-HS (n = 22). **MA**: Microarray. Data presented as mean ± S.E.M

5.4 Discussion

In the few microarray studies done the analysis focused on the list of genes that are differentially expressed. In addition, there was only a small proportion of genes that overlap between these studies. In physiological conditions a biological process is done by a group of genes that work together simultaneously. Hence in a pathological condition it is more rational to investigate the abnormal genes in a group-based analysis. Therefore in the present study, enrichment analysis of microarray data was performed as group-oriented analysis, rather than gene-oriented analysis. The differentially expressed genes are clustered into groups based on their cellular component, molecular function, biological processes and pathways. This will provide a better understanding of molecular functions and biological processes that are affected in the intractable TLE-HS pathology and thus providing new aspects for developing effective treatments for the pharmacoresistant TLE patients.

As a result of comparing the transcriptome profile of the epileptogenic TLE-HS tissue to TLE-STG and PMC samples, a total of 464 up regulated and 350 down regulated DEGs were identified. According to DAVID enrichment analysis of these genes, the up regulated gene clusters had higher enrichment scores than the down regulated clusters. Interestingly, the up regulated genes in TLE-HS tissue were significantly enriched in cytokine activity molecular functions and biological processes of inflammatory and defence responses. Furthermore the KEGG pathway analysis of up regulated DEGs showed that the cytokine-cytokine receptor interaction, Toll-like

receptor and MAPK signalling pathways were significantly enriched in epileptogenic TLE-HS tissue. Recent evidence suggested that these pathways have a role in the neuropathology of epilepsy (Ravizza *et al.*, 2008; Vezzani *et al.*, 2008; Maroso *et al.*, 2011; Lopes *et al.*, 2012).

The enrichment of down regulated genes in TLE-HS tissue was significantly associated with synaptic, cell junction, dendritic, postsynaptic membrane and ion transport genes; which are one of the characteristics of epileptic sclerotic hippocampi. One of the novel findings of this study; we report that $GABA_A$ receptor, epsilon subunit is down regulated in TLE-HS. However, its down regulation needs to be further validated and its role in TLE pathophysiology needs to be further explored.

5.4.1 Role of cytokines in TLE-HS

In this study, the enrichment analysis of microarray data revealed that 27 genes associated with inflammatory and defence responses were significantly up regulated in TLE-HS tissue (Table 5.7). From those 27 significantly up regulated genes, 16 were cytokines. The mRNA up regulation of inflammatory cytokines IL-1β, IL-18 and Fas as well as the intercellular adhesion molecule 1 (ICAM-1) were validated by qRT-PCR analysis.

IL-1β expression in TLE-HS

In this study there was a significant up regulation of pro-inflammatory IL-1β in epileptogenic TLE-HS tissue compared to TLE-STG and PMC, that further supports the data obtained from other studies done on TLE patients (Ravizza *et al.*, 2008; Maroso *et*

al., 2011). However, in addition to the classical role of cytokines in inflammation, cytokines also play a role in neuronal excitability. Recent evidence found that binding of IL-1β to its neuronal IL-1B receptor leads to the phosphorylation and activation of the NMDA receptor. Thus increasing the NMDA receptor induced Ca^{2+} influx into neurons, and enhancing seizure susceptibility and excitotoxicity (Viviani *et al.*, 2003; Vezzani *et al.*, 2008). Furthermore, it was reported that IL-1β and TNF-α inhibited the astrocytic glutamate uptake and thus promoting glutamate excitotoxicity in TLE-HS (Hu *et al.*, 2000). Moreover, IL-1β inhibited the $GABA_A$ receptor current in surgically resected hippocampal tissue obtained from TLE patients (Wang *et al.*, 2000; Roseti *et al.*, 2015). In many animal models of epilepsy, the administration of IL-1β receptor antagonist or caspase-1 inhibitor had an anticonvulsive effect (Maroso *et al.*, 2011). Therefore, blocking the action of IL-1β appears as a good drug target for treatment of refractory TLE-HS patients.

IL-18 expression in TLE-HS

IL-18 also known as interferon-gamma (IFN-γ) inducing factor is a potent cytokine that belongs to IL-1 family of pro-inflammatory cytokines. It has many immunological and inflammatory roles such as induction of chemokines and growth factors (Kanno *et al.*, 2004; Felderhoff-Muese *et al.*, 2005). IL-18 is expressed in the brain constitutively but its expression is increased significantly in neurons, microglia, astrocytes and endothelial cells in response to brain injury (Johnson *et al.*, 2015).

IL-18 has a key role in neuroinflammation and neurodegeneration; it induces the production of pro-inflammatory IL-1β, TNF-α and matrix metalloproteinases (MMPs) from activated microglia. It also amplifies the effect of leukocyte extravasation by inducing chemokine production from activated microglia and the up regulation of ICAM-1 on endothelial cells. In inflammatory conditions, IL-18 increases Fas-mediated neuronal apoptosis via the induction of IFN-γ secretion (Gerdes *et al.*, 2002; Felderhoff-Muese *et al.*, 2005; Johnson *et al.*, 2015). Furthermore, it was reported that IL-18 affects hippocampal synaptic transmission where it stimulated synaptic glutamate release and enhances the currents of AMPA receptors in CA1 pyramidal neurons of a mouse hippocampal slice (Kanno *et al.*, 2004).

In a rat model of SE, the expression of IL-18 was significantly up regulated in DG neurons, pyramidal cells of CA1-3, astrocytes and microglia 1-3 days following SE , while IFN-γ was only up regulated in astrocytes (Ryu *et al.*, 2010) . In addition, they found that administration of IL-18 or IFN-γ reduced the neuronal damage caused by SE. Therefore, suggesting that both IL-18 and IFN-γ may have a protective role on neurons (Ryu *et al.*, 2010). The IL-18 expression was significantly up regulated in hippocampus following SE in a rat model of sustained SE. However, IL-18 showed the highest expression in endothelial cells where there was vasculature injury. Thus, indicating that IL-18 might also play a role in angiogenesis (Johnson *et al.*, 2015). In addition, the mRNA expression of IL-18 was also up regulated in microvascular endothelial cells derived from the sclerotic hippocampus from TLE patients (Lachos *et al.*, 2011).

In the present study we report, for the first time, the up regulation of IL-18 in epileptogenic tissue from TLE-HS patients supporting the previous experimental data (Ryu *et al.*, 2010). Taking into consideration: (1) the excitatory effect of IL-18 on hippocampal synaptic transmission reported by Kanno *et al.* (2004); (2) the anticonvulsant VX-765 drug which is an inhibitor of interleukin converting enzyme (ICE)/caspase-1 that affects both IL-1β and IL-18, is showing promising results in phase II clinical trials (Walker and Sills, 2012; Vezzani, 2015). We hypothesize that this up-regulation in IL-18 is contributing to TLE-HS pathophysiology and represents a novel drug target to develop new AEDs.

Fas expression in TLE-HS

Fas (CD95) is the prototypical cell death receptor that belongs to the TNF receptor superfamily. It induces the extrinsic or receptor-mediated apoptotic pathway by binding to Fas ligand receptor and recruiting the cytoplasmic Fas-associated protein with Death Domain (FADD). FADD also has a Death Effector Domain that activates caspase 8 and 9 and starts the caspase cascade leading to apoptosis (Vermeulen *et al.*, 2005). Many experimental animal models and human studies of TLE-HS reported neuronal loss connected to apoptosis in TLE tissue (Bengzon *et al.*, 2002; Pitkanen and Sutula, 2002; Henshall, and Simon, 2005: Xu *et al.*, 2007). In a rat model of TLE, there was an increase in Fas expression indicating Fas-mediated apoptosis in TLE (Tan *et al.*, 2002). Furthermore, there was also overexpression of Fas in sclerotic hippocampi obtained from drug resistant TLE patients (Xu *et al.*, 2007).

In addition to the role of Fas in apoptosis, accumulating evidence supports Fas pro-inflammatory role (Choi *et al.*, 2001; 2003; Chorpade *et al.*, 2003; Park *et al.*, 2003). It was found that Fas can initiate an inflammatory response by the inducing the release of pro-inflammatory cytokines such as TNF-α from monocytes and macrophages (Park *et al.*, 2003). It was also reported that Fas increased the expression of ICAM-1 in human astroglioma cells (Choi *et al.*, 2003). In addition, it was found that IL-1β induces the astrocytic expression of Fas (Chorpade *et al.*, 2003). In the present study, there was a significant increase in Fas expression in TLE-HS further corroborating the Fas-mediated apoptosis demonstrated by previous studies. However, the Fas up regulation could also be implicated in the inflammatory aspect of TLE-HS pathophysiology.

ICAM-1 expression in TLE-HS

Cell adhesion molecules such as ICAM-1 play a major role in inflammation as they are responsible for T-cells activation and leukocyte recruitment to sites of inflammation (Ren *et al.*, 2010). The pro-inflammatory cytokines Fas, IL-1β and TNF-α significantly enhance the expression of ICAM-1 (Kuppner *et al.*, 1990). As mentioned earlier IL-18 also increased the expression of ICAM-1 on endothelial cells (Gerdes *et al.*, 2002). Interestingly it was found that increased expression of ICAM-1 causes an enhanced translation of IL-1β mRNA (Allan *et al.*, 2005).

In the hippocampi of experimental models of TLE, there was an up regulation of ICAM-1 expression on the endothelial cells that was followed by the infiltration of leukocytes (Akiyama *et al.*, 1994; Zattoni *et al.*, 2011). It was also reported that there was an up

regulation of ICAM-1 expression in the endothelial cells in sclerotic hippocampi (n = 4) from TLE patients (Nakahara *et al.*, 2010). This supports our finding of significant increase in ICAM-1 mRNA level in TLE-HS. Regarding the T-lymphocyte infiltration in sclerotic hippocampi from TLE-HS, there were more cytotoxic T-cells (CD8+) than Th-cells (CD4+) suggesting that it might be contributing to the neurodegeneration in TLE-HS (Nakahara *et al.*, 2010). Therefore, we suggest that ICAM-1 overexpression plays a vital role in triggering and aggravating leukocyte infiltration and thus further contributes to TLE-HS neuropathology.

5.4.2   Role of chemokines in TLE-HS

In the present study, the enrichment analysis of microarray data revealed that 27 significantly up regulated genes in TLE-HS tissue were associated with inflammatory and defence responses (Table 5.7). From those, 16 cytokine genes including 6 chemokines were significantly altered. The transcript up regulation of inflammatory chemokines CCL2, CCL4, CXCL1, CXCL2, CXCL12, as well as chemokine receptors CXCR4 and CX3CR were validated by qRT-PCR analysis. Chemokines are a class of cytokines. They are small secreted proteins that play an important role in inflammation. One of their main functions is leukocyte chemoattraction but they are also involved in angiogenesis, proliferation and apoptosis. The primary sources of chemokines following CNS injury are microglia and astrocytes (Mantovani *et al.*, 2006). Recent evidence highlighted the role of pro-inflammatory chemokines such as CCL2, CCL3 and CCL4 in TLE neuropathology (Van Gassen *et al.*, 2008; Kan *et al.*, 2012; Arisi *et al.*, 2015).

CCL2 and CCL4 expression in TLE-HS

In animal models of TLE, there was a significant up regulation of CCL2, CCL3 and CCL4 chemokines in the hippocampus during the acute and early phases of SE indicating their role in early stages of epileptogenesis (Gorter *et al.*, 2006; Arisi *et al.*, 2015). A study of sclerotic hippocampus from drug resistant TLE patients also showed high expression levels of CCL3 and CCL4 that are consistent with our results and further implicate their role in chronic stages of epileptogenesis. CCL2, CCL3 and CCL4 affect endothelial cells and increase the permeability of the BBB, thus facilitating the infiltration of leukocytes into the brain. Once within the brain they activate microglia and astrocytes, which participate in cytokine-mediated neuroinflammation (Stamatovic *et al*, 2005; Louboutin *et al.*, 2011). In addition, it was found that CCL2 and CCL4 are involved in neuronal damage and excitotoxicity following SE (Kalehua *et al.*, 2004; Sheehan *et al.*, 2007; Louboutin *et al.*, 2011). Therefore, their up regulation is a contributing factor to the TLE-HS pathology.

CXCL1 and CXCL2 expression in TLE-HS

The inflammatory chemokines CXCL1 and CXCL2 hippocampal expression were found to be up regulated following SE in animal models (Kalehua *et al.*, 2004; Kim *et al.*, 2010; Johnson *et al.*, 2011). The secretion of CXCL1 and CXCL2 by microglia, astrocytes, neurons and endothelial cells is essential for leukocyte recruitment and neutrophil infiltration during neuroinflammation (Wu *et al.*, 2015). The neutrophil infiltration further amplifies the inflammatory response by releasing proteolytic enzymes and inducing pro-inflammatory cytokines production (Kim *et al.*, 2010). In addition, *in vitro*

174

and *in vivo* studies found that high levels of CXCL2 induced hippocampal neuronal damage via apoptotic pathways (Kalehua *et al*., 2004). Therefore, the significant up regulation of CXCL1 and 2 in the epileptogenic tissue from TLE-HS patients seem to be implicated in its neuropathology. Thus, blocking their receptor CXCR2 might have a beneficial effect in ameliorating neuroinflammation in TLE-HS.

CXCL12 and CXCR4 expression in TLE-HS

In TLE animal models, the homeostatic chemokine CXCL12 was up regulated in the hippocampus in response to KA-induced seizures (Hartmen *et al*., 2010; Song *et al*., 2016). In adults, CXCL12 plays a role in neuroinflammation by leukocytes chemoattraction and infiltration (Guyon, 2014). In addition, CXCL12 and its receptor CXCR4 play a vital role in hippocampal neurogenesis. CXCL12 regulates the migration, differentiation and functional integration of newly formed neurons into the existing neuronal networks (Marquez-Curtis *et al*., 2013). In drug refractory TLE-HS, there is an abnormal hippocampal neurogenesis that seem to contribute to TLE-HS neuropathology. In a TLE animal model, the administration of CXCR4 antagonist (AMD3100) showed anticonvulsant activity where it suppressed long-term seizure activity and altered neurogenesis (Song *et al*., 2016). In the present study there was a significant up regulation of CXCL12 and CXCR4 in sclerotic hippocampus from TLE patients further supporting its role in TLE-HS pathophysiology. However, further studies are still needed to confirm the beneficial role of CXCR4 antagonists in TLE patients.

CX3CR1 expression in TLE-HS

The inflammatory chemokine receptor CX3CR1 is expressed primarily on microglia and it regulates microglia activation and phagocytic activity (Ali *et al.*, 2015). In animal models, microglia activation preceded SE-induced neuronal death and it was found that microglia activation plays an important factor in TLE epileptogenesis (Kang *et al.*, 2006; Abiega *et al.*, 2016).

The CX3CR1 ligand, CX3CL1, expression was significantly increased in neurons and astrocytes in the hippocampus following SE in animal models (Yeo *et al.*, 2011). It was also up regulated in tissue obtained from drug resistant TLE patients (Xu *et al.*, 2012). In addition, it was found that CX3CL1 reduced GABA currents in neurons obtained from TLE-HS patients and the increased expression of CX3CR1 further affected the GABA inhibitory current (Roseti *et al.*, 2013).

The expression of CX3CR1 was investigated in rat hippocampus following SE and its expression was found to be up regulated following seizures (Yeo *et al.*, 2011; Ali *et al.*, 2015). The high expression of CX3CR1 was associated with SE-induced neuronal death and blocking CX3CR1 led to a reduction in SE-induced neuronal damage (Yeo *et al.*, 2011). In the present study, there was a significant up regulation of CX3CR1 in the epileptogenic TLE-HS tissue from drug resistant TLE patients. This further supports the pathological role of CX3CR1 up regulation in TLE-HS as it contributes to elevated microglia activation and GABAergic activity reduction. Therefore, CX3CR1 might be a potential new drug target for TLE-HS.

5.5 Conclusion

The enrichment analysis of TLE-HS transcriptome provided an overview of molecular functions and biological processes that are affected and possibly contributing to TLE-HS. The up regulated cytokine and chemokine genes in cluster 1 and 2 (Table 5.7), which had the highest enrichment scores associating them to TLE-HS pathology. In the present study, we had further corroborated the pathological role of some thoroughly investigated cytokines such as IL-1β and Fas in TLE epilepsy. In addition, the expression of some cytokines and their receptors such as IL-18, CXCL1, CXCL2, CXCL12, CXCR4 and CX3CR1 are reported for the first time in human TLE-HS tissue, implicating them in TLE-HS pathophysiology. However, further research to investigate the spatial and temporal pattern of these cytokines and chemokines during TLE will help in developing new AEDs for refractory TLE-HS.

Chapter 6

Expression of Aquaporins in sclerotic hippocampi from refractory

TLE-HS patients

6 Expression of AQPs in sclerotic hippocampi from refractory TLE-HS patients

6.1 Introduction

The excitability of the hippocampus was found to be affected by alteration in water movement and osmotic changes. It was reported that hypo-osmolality promoted epileptiform activity in hippocampal brain slices and induced seizures (Andrew, 1990). Imaging studies in TLE-HS patients did demonstrate that there is water accumulation in the sclerotic hippocampi, compared to non-sclerotic ones. Magnetic resonance imaging (MRI) of the TLE-HS shows an increase in T2 and T2-weighted signal indicating higher free water content in sclerotic hippocampi tissue (Bronen *et al.*, 1991; Dawe *et al.*, 2014). In addition, diffusion-weighted imaging also demonstrated higher diffusion coefficient in TLE-HS hippocampi. This supports the T2 MRI findings as the diffusion coefficient is a measure of water movement within tissues determined by MRI (Hugg *et al.*, 1999; Heuser *et al.*, 2010). Therefore the roles of aquaporins were investigated in TLE-HS as they are important regulators of transcellular water flow in the brain.

6.1.1 Aquaporins (AQPs)

AQPs are a family of small membrane transporter proteins. They form channels by assembling into stable tetramers in the membrane (Nielsen *et al.*, 1993; Tait *et al.*, 2008). AQPs mainly regulate the bidirectional water movement across cell membranes in response to osmotic gradients. In humans there are 13 AQPs that are initially divided into 2 subfamilies: orthodox aquaporins and the aquaglyceroporins. The orthodox

179

aquaporins such as AQP1, AQP4, AQP5 and AQP8 selectively transport water. The aquaglyceroporins such as AQP3, AQP7 and AQP9 transport glycerol, urea and other small solutes, in addition to water (Amiry-Moghaddam and Ottersen, 2003; Tait *et al.*, 2008; Papadopoulos and Verkmen, 2013; Day *et al.*, 2014). Recently a third subfamily of AQPs called superaquaporins, such as AQP11 and AQP12, was identified and thought to play a role in intracellular water transport (Gorelick *et al.*, 2006; Ishibashi *et al.*, 2014).

6.1.2 AQP expression in the brain

The AQPs that are expressed in rodent brain are AQP1, AQP3, AQP4, AQP5, AQP8 and AQP9 (Badaut *et al.*, 2014). In human brain, **AQP4** is the most abundant aquaporin and it is widely expressed in all brain structures in contact with the cerebral vascular compartment. In the human hippocampus, AQP4 is found in CA1 and DG areas. It is highly expressed in the astrocyte end-feet that ensheath the glutamatergic synapses. However, it shows the highest expression at the astrocyte perivascular end-feet processes, which is known as AQP4 polarized expression (Eid *et al.*, 2005; Lee *et al.*, 2004).

AQP1 is expressed in the epithelial cells of the choroid plexus. In physiological conditions AQP1 is not expressed in cerebrovascular endothelium, AQP1 expression is induced only in pathological situations where there is a disruption in BBB (Papadopoulos and Verkmen, 2013; Badaut *et al.*, 2014). **AQP9** is weakly expressed in the brain; it has been reported in some neurons and astrocytes (Papadopoulos and Verkmen, 2013). In the rodent hippocampus, AQP9 is expressed in the astrocyte cell

bodies and processes but it is not polarized (Badaut and Regli, 2004; Yang *et al.*, 2011). It is also found in some catecholaminergic neurons (Badaut *et al.*, 2014). In rat hippocampus, **AQP3**, **AQP5** and **AQP8** are expressed in the DG area. They were found in both astrocytes and neurons as their expression was co-localized with GFAP and NeuN positive cells in the DG (Yang *et al.*, 2009). **AQP11** is an intracellular AQP expressed on the ER membrane (Morishita *et al.*, 2005). In rat brain, AQP11 is expressed in the cerebral cortex neurons and in CA1 and CA2 hippocampal neurons (Gorelick *et al.*, 2006).

6.1.3 AQPs in TLE

It is well-known that water and ion homeostasis are important factors that modulate seizure susceptibility (Andrew, 1990; Schwartzkroin *et al.*, 1998; Lee *et al.*, 2012). The role of AQP1, -4 and -9 in TLE pathophysiology has been studied as they are key players in maintaining water homeostasis in the brain (Lee *et al.*, 2004; Eid *et al.*, 2005; Bebek *et al.*, 2013). Alterations in AQP expression were observed in epileptic animal models as AQP1, AQP4 and AQP9 were investigated in chronic pilocarpine -induced SE rat model (Kim *et al.*, 2009). AQP4 expression was also investigated in a kainic acid-induced SE mouse model (Lee *et al.*, 2012).

In human TLE-HS specimens, alterations of AQP1 and AQP4 expression were observed in a few studies (Lee *et al.*, 2004; Eid *et al.*, 2005; Bebek *et al.*, 2013). The expression of AQP1 and AQP4 were studied in sclerotic hippocampi obtained from TLE patients and was compared to non-sclerotic hippocampi obtained from mass associated- and paradoxical TLE patients (Lee *et al.*, 2004). AQP1 transcript was slightly increased and

181

AQP4 expression was significantly up regulated in TLE-HS specimens compared to Non-HS (Lee *et al.*, 2004). The overall AQP4 protein expression was also significantly up regulated in TLE-HS compared to Non-HS; however, there was also a mislocalization of AQP4 expression and a significant loss in perivascular expression in TLE-HS (Eid *et al.*, 2005). The loss of perivascular AQP4 causes a perturbed flux of water through astrocytes which is accompanied with an impaired extracellular K^+ homeostasis. This altered K^+ homeostasis leads to prolonged and aggravated epileptic seizures (Eid *et al.*, 2005). The gene expression of AQP1 and AQP4 investigated in TLE-HS, showed no significant alterations in their expression when compared with autopsy hippocampi as a control (Bebek *et al.*, 2013).

6.1.4   Aims of the study

The expression of AQP1 and AQP4 has been investigated in human TLE-HS specimens and were found to be involved in pathology of TLE-HS. Nevertheless, little is known about the expression of other AQPs such as AQP3, AQP5 AQP8, AQP9 and AQP11. Thus, the aim of this study was to investigate the expression of AQP3, AQP5 AQP8, AQP9 and AQP11 in human TLE-HS hippocampi to see if they play a role in the pathophysiology of TLE-HS.

6.2   Materials and methods

6.2.1   Patient clinical information

Clinical information for TLE-STG and TLE-HS samples investigated in this chapter is described in Appendix I.

6.2.2 Study design

The mRNA level of AQP1, AQP3, AQP4, AQP5 AQP8, AQP9 and AQP11 as well as NeuN and GFAP were investigated by microarray analysis (n = 7) and qRT-PCR in TLE-STG (n = 5) and TLE-HS (n = 10) samples.

6.2.3 Methods

Microarray analysis (MA): Briefly the total RNA was extracted by SV Total RNA Isolation System (section 2.3.1). Then cDNA samples were synthesized and labelled with Cy3 or Cy5 using the Two-colour Low Input Quick Amp Labeling Kit (Agilent Technologies, 5190-2306). Following the labelling of TLE-HS hippocampi with Cy5 and TLE-STG samples with Cy3, equal amounts of the two samples were co-hybridized onto SurePrint G3 Human Gene Expression 8x60K Microarrays (Agilent Technologies, G4851A). The microarray array was washed and then scanned on Agilent Technologies SureScan Microarray Scanner (section 2.9). Raw data was extracted using Agilent feature extraction software and analysis was done on Multi-experiment Viewer (MeV) software (section 5.2.4). **MA statistical analysis**: rank products test was used to identify significant differences between samples (*** $P < 0.0001$).

qRT-PCR: In brief, the total RNA extracted was reverse transcribed using SuperScript[TM] III first strand synthesis system (section 2.4). Stable housekeeping genes were selected for the normalization of target gene expression (section 2.5.3) then followed by the qRT-PCR using TaqMan[©] gene expression assays (section 2.5.5). **qRT-PCR statistical analysis**: Kruskal-Wallis with Conover-Inman *post hoc* analysis test was used to identify significant differences between samples (* $P < 0.05$).

183

6.3 Results

6.3.1 NeuN and GFAP mRNA expression

The neuronal marker, NeuN mRNA expression obtained from microarray analysis showed a significant decrease in TLE-HS tissue compared to TLE-STG. The NeuN mRNA expression determined by qRT-PCR analysis also showed the same trend of a reduced expression in TLE-HS tissue though it was not significant as in figure 6.1.

The mRNA expression of GFAP, which is an astrocyte marker determined by microarray analysis and qRT-PCR showed a significant up regulation in TLE-HS samples compared to TLE-STG as in figure 6.1. The expression level of NeuN and GFAP does confirm the hallmarks of TLE-HS which are neuronal loss and gliosis.
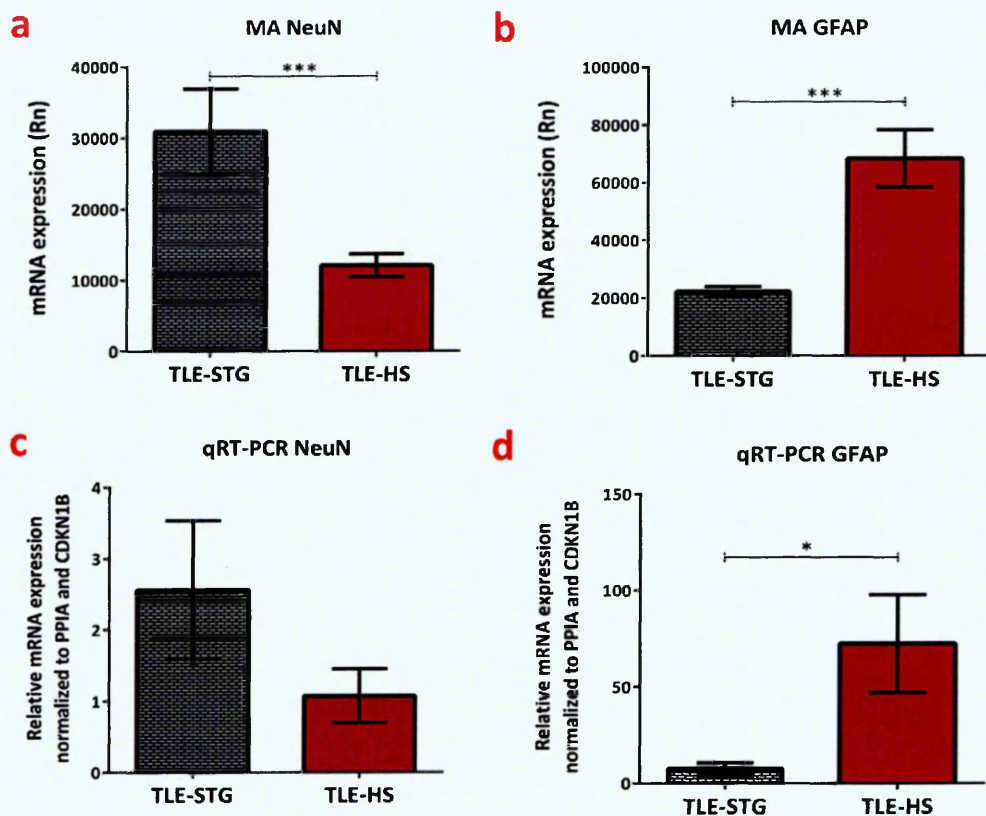
Figure 6.1 NeuN and GFAP mRNA expression in TLE-HS and TLE-STG

The neuronal marker, NeuN, mRNA level investigated by MA (a) and qRT-PCR (c) showed a reduced expression in TLE-HS. The astrocyte marker, GFAP, mRNA level investigated by MA (b) and qRT-PCR (d) showed a significant higher expression in TLE-HS. **MA statistical analysis**: rank products test was used to identify significant differences between samples (*** $P < 0.0001$). MA number of samples: TLE-STG (n = 7); TLE-HS (n = 7). **qRT-PCR statistical analysis**: Kruskal-Wallis with Conover-Inman *post hoc* analysis test was used to identify significant differences between samples (* $P < 0.05$); qRT-PCR number of samples: TLE-STG (n = 5); TLE-HS (n = 10). All data presented as mean ± S.E.M. **MA**: Microarray analysis; **Rn**: Normalized fluorescence intensity.

185

6.3.2 The AQP abundance in TLE-STG samples

The transcript expression of AQPs was investigated in the non-spiking TLE-STG samples by both MA and qRT-PCR. The data demonstrate that AQP4 was the most abundant aquaporin, showing highest expression, and then there was AQP5 and AQP11 that were moderately expressed. Followed by AQP1, AQP3, AQP8 and AQP9 that were less abundant and showing lowest expression compared to AQP4 as shown in figure 6.2.

6.3.3 AQP1 and AQP4 mRNA expression in TLE-HS

The microarray analysis revealed that AQP1 and AQP4 expression was significantly up regulated in TLE-HS samples. The qRT-PCR data showed an increase in AQP1 and AQP4 expression; even though it was not significant but it was still the same trend as MA data as shown in figure 6.3.

6.3.4 AQP3 and AQP5 mRNA expression in TLE-HS

The data obtained from MA and qRT-PCR demonstrated that there was an increase in AQP3 transcript level in TLE-HS compared to TLE-STG. In contrast, AQP5 transcript level revealed a reduced expression in TLE-HS compared to TLE-STG as shown in figure 6.4.
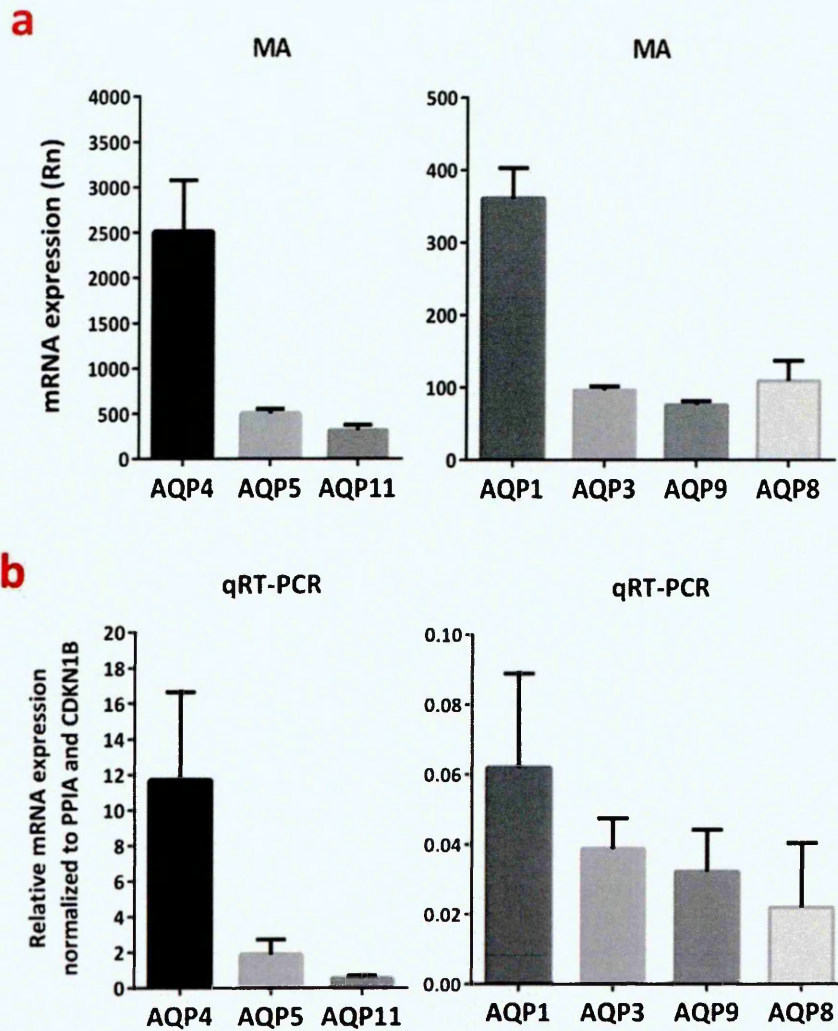
Figure 6.2 mRNA expression of AQPs in TLE-STG

AQPs expression in TLE-STG investigated by (a) MA and (b) qRT-PCR showed that AQP4 has highest expression, AQP5 and AQP11 showed moderate expression and AQP1, AQP3, AQP8 and AQP9 showed the lowest expression in the TLE-STG specimens. Number of TLE-STG samples: MA (n = 5); qRT-PCR (n = 7). All data presented as mean ± S.E.M. **MA**: Microarray analysis; **Rn**: Normalized fluorescence intensity.
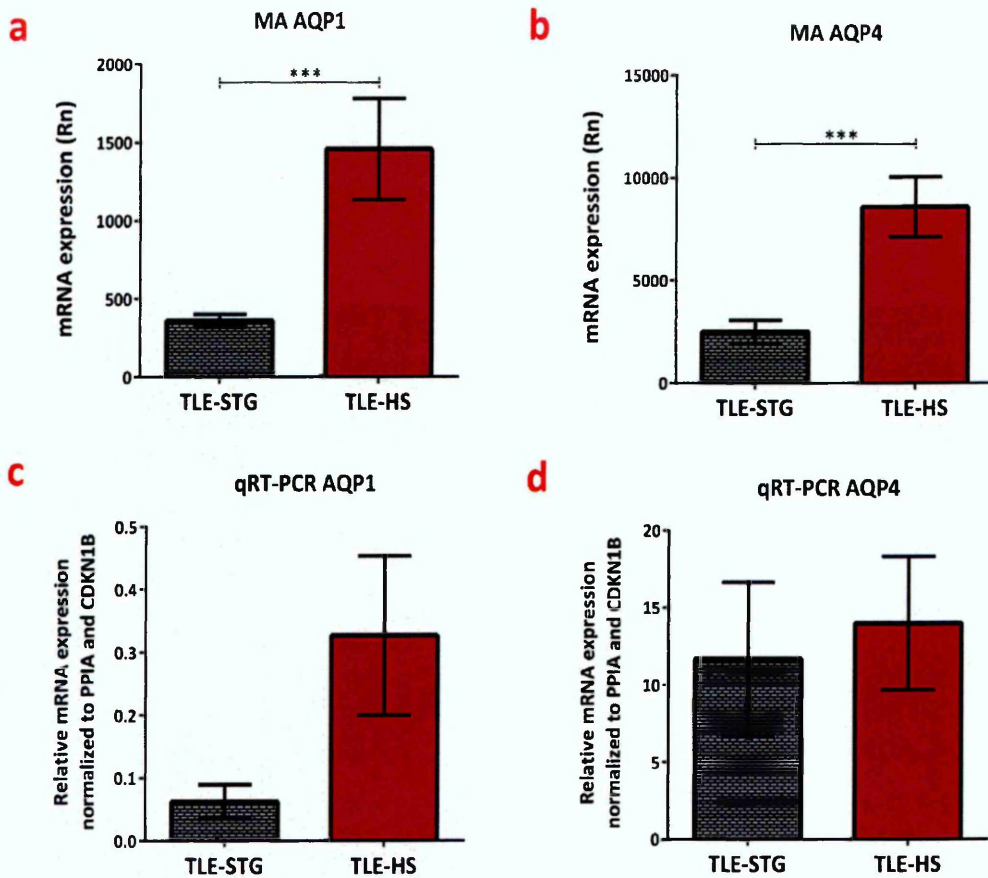
Figure 6.3 AQP1 and AQP4 mRNA expression in TLE-HS and TLE-STG

MA data showed that mRNA levels of AQP1 (a) and AQP4 (b) were significantly up regulated in TLE-HS. qRT-PCR data also showed that both AQP1 (c) and AQP4 (d) expression was higher in TLE-HS compared to TLE-STG but it was not significant. **MA statistical analysis**: rank products test was used to identify significant differences between samples (*** $P < 0.0001$). **MA** number of samples: TLE-STG (n = 7); TLE-HS (n = 7). **qRT-PCR statistical analysis**: Kruskal-Wallis with Conover-Inman *post hoc* analysis test was used to identify significant differences between samples (* $P < 0.05$). **qRT-PCR** number of samples: TLE-STG (n = 5); TLE-HS (n = 10). All data presented as mean ± S.E.M. **MA**: Microarray analysis; **Rn**: Normalized fluorescence fluorescence intensity.
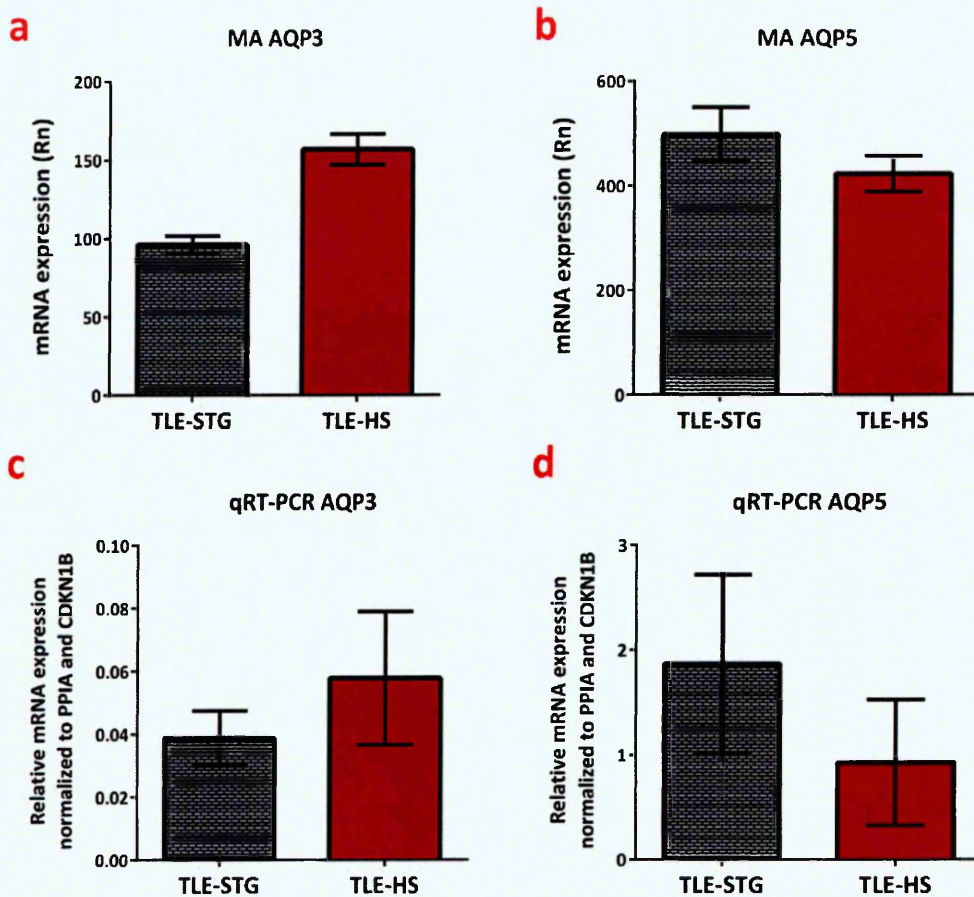
Figure 6.4 AQP3 and AQP5 mRNA expression in TLE-HS and TLE-STG

AQP3 mRNA level explored by MA (a) and qRT-PCR (c), showed an increased expression in TLE-HS. While AQP5 mRNA level investigated by MA (b) and qRT-PCR (d), showed a reduced expression in TLE-HS compared with TLE-STG. **MA statistical analysis**: rank products test was used to identify significant differences between samples. MA number of samples: TLE-STG (n = 7), TLE-HS (n = 7). **qRT-PCR statistical analysis**: Kruskal-Wallis with Conover-Inman *post hoc* analysis test was used to identify significant differences between samples. No significant differences were detected. qRT-PCR number of samples: TLE-STG (n = 5); TLE-HS (n = 10). All data presented as mean ± S.E.M. **MA**: Microarray analysis; **Rn**: Normalized fluorescence intensity.

6.3.5   AQP8 and AQP9 mRNA expression in TLE-HS

The mRNA expression data obtained from MA and qRT-PCR demonstrate that there was a slight reduction in AQP8 transcript level in TLE-HS samples. In TLE-STG samples, there was more variability seen in AQP8 expression compared to TLE-HS. The data also showed a reduced level of AQP9 mRNA expression in TLE-HS compared with TLE-STG as shown in figure 6.5.

6.3.6   AQP11 mRNA expression in TLE-HS

The MA data revealed a modest reduction in AQP11 mRNA expression in TLE-HS compared to TLE-STG. Nevertheless, the qRT-PCR data showed a significant down regulation in TLE-HS compared to TLE-STG as shown in figure 6.6.
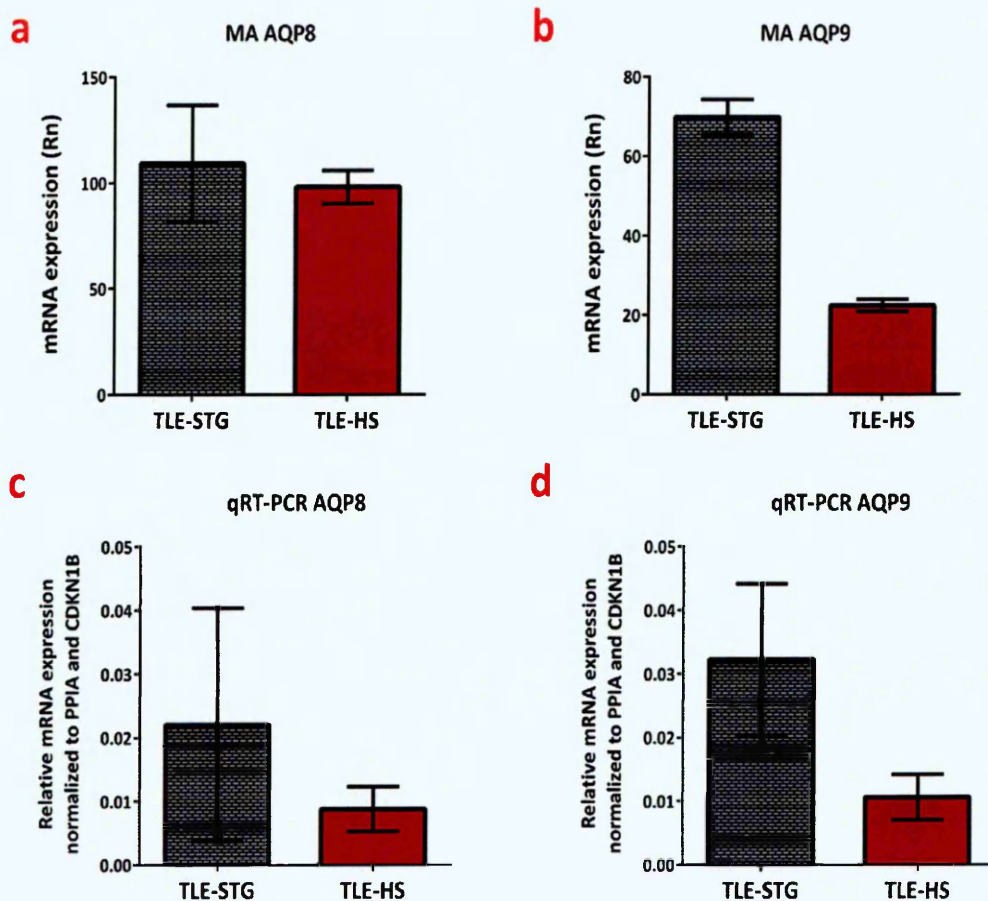
Figure 6.5 AQP8 and AQP9 mRNA expression in TLE-HS and TLE-STG

AQP8 mRNA level data obtained from MA (a) and qRT-PCR (c), showed a slight decreased expression in TLE-HS. AQP9 mRNA level investigated by MA (b) and qRT-PCR (d) also showed a reduced expression in TLE-HS compared with TLE-STG. **MA statistical analysis**: rank products test was used to identify significant differences between samples. MA number of samples: TLE-STG (n = 7), TLE-HS (n = 7). **qRT-PCR statistical analysis**: Kruskal-Wallis with Conover-Inman *post hoc* analysis test was used to identify significant differences between samples. No significant differences were detected. qRT-PCR number of samples: TLE-STG (n = 5); TLE-HS (n = 10). All data presented as Mean ± S.E.M. **MA**: Microarray analysis; **Rn**: Normalized fluorescence intensity.
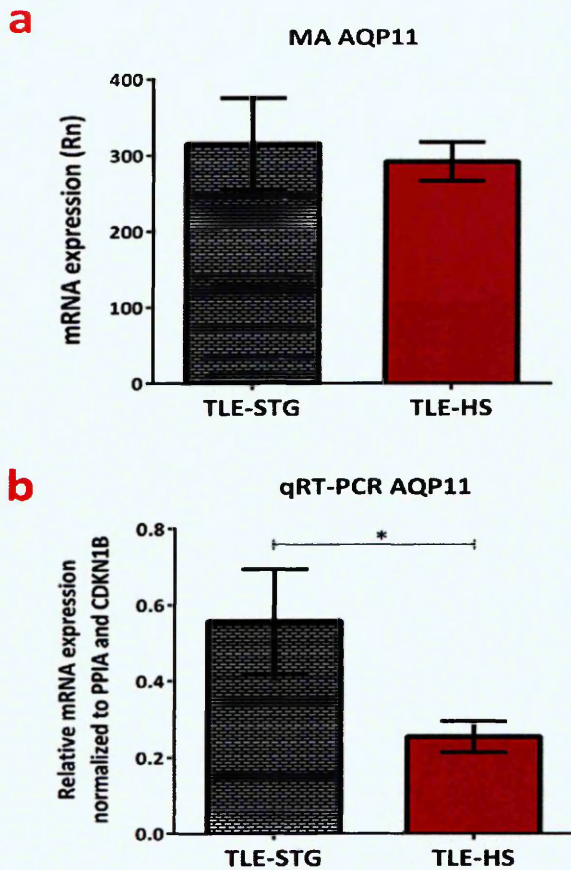
Figure 6.6 AQP11 mRNA expression in TLE-HS and TLE-STG

AQP11 mRNA level obtained from MA (a) showed a slight decreased expression in TLE-HS. While expression data obtained from qRT-PCR (b) showed a significant reduction of AQP11 in TLE-HS compared to TLE-STG. **MA statistical analysis**: rank products test was used to identify significant differences between samples. MA number of samples: TLE-STG (n = 7), TLE-HS (n = 7). **qRT-PCR statistical analysis**: Kruskal-Wallis with Conover-Inman *post hoc* analysis test was used to identify significant differences between samples (* $P < 0.05$). qRT-PCR number of samples: TLE-STG (n = 5); TLE-HS (n = 10). All data presented as mean ± S.E.M. **MA**: Microarray analysis; **Rn**: Normalized fluorescence intensity.

6.4 Discussion

As pointed out in the introduction, there is evidence of impaired water homeostasis in sclerotic hippocampi resected from TLE patients (Bronen *et al.*, 1991; Lee *et al.*, 2004; Heuser *et al.*, 2010; Dawe *et al.*, 2014). Previous studies in human TLE-HS specimens indicated that changes in AQP4 expression (Lee *et al.*, 2004; Eid *et al.*, 2005) is implicated in the pathophysiology of pharmacoresistant TLE associated with HS. In summary the novel findings of this study were: 1) Reporting the transcript expression of AQP3, AQP5 AQP8, AQP9 and AQP11 in human hippocampus; 2) the expression of AQ1 is significantly increased in TLE-HS hippocampi; 3) the expression of AQP11 is significantly reduced in TLE-HS; 4) there was a slight increase in AQP3 expression and a small decreases in AQP5, AQP8 and AQP9 expression in TLE-HS compared to TLE-STG.

6.4.1   AQP transcript abundance in TLE-HS

AQP3, AQP5 AQP8, AQP9 and AQP11 were previously reported to be expressed in rodent hippocampus (Badaut and Regli, 2004; Gorelick *et al.*, 2006; Yang *et al.*, 2009). However, for the first time the presence of AQP3, AQP5 AQP8, AQP9 and AQP11 transcripts are described in human hippocampi. This indicates that these AQPs also play a physiological role in maintaining water and ion homeostasis in the hippocampus, in addition to AQP1 and 4 that are widely studied.

6.4.2   AQP4 expression in TLE-HS

AQP4 is widely expressed in astrocytes and it was one of the first AQPs studied in human TLE hippocampi by Lee *et al.*, (2004). In the present study AQP4 was used as a positive control, its total mRNA expression was increased in TLE-HS compared to TLE-STG supporting the findings of Lee *et al.*, (2004) and Eid *et al.*, (2005).

6.4.3   AQP1 expression in TLE-HS

In the present study, AQP1 mRNA is significantly up regulated in TLE-HS compared to TLE-STG. Normally in the hippocampus, the water transporting AQP1 is not observed in astrocytes or cerebrovascular endothelial cells. However, in a chronic model of SE, AQP1 expression was observed in astrocytes at 4 weeks after SE and became significantly up regulated at 6 weeks compared to control that was followed by a sustained up regulation of AQP1 in epileptic hippocampi (Kim *et a*l., 2009). This is supporting our data and indicates that AQP1 astrocyte expression is increased as the number of uncontrolled seizures increases, which could be a compensatory mechanism to overcome the loss in perivascular AQP4 expression.

In addition, AQP1 expression in cerebrovascular endothelial cells is only seen in conditions where the BBB is disrupted such as malignant brain tumours (Papadopoulos and Verkmen, 2013). In chronic seizures there is transient opening of BBB during seizures in the epileptogenic foci that plays a role in the epileptogenic process (Kovacs *et al.*, 2012; Gorter *et al.*, 2015). Therefore in drug resistant TLE hippocampi, the AQP1 expression could be induced in endothelial cells to facilitate water movement across BBB. In summary the up regulation of AQP1 seen in TLE-HS tissue seems to be the

result of AQP1 induced expression in astrocytes and endothelial cells, in response to the uncontrolled seizures. Therefore, this data suggests that AQP1 does have a role in water homeostasis in the drug resistant sclerotic hippocampi from TLE patients.

6.4.4   AQP3 and AQP9 expression in TLE-HS

Seizures represent a massive metabolic burden to neurons and glia as the restoration of the ion gradients requires energy and an enhanced oxygen and glucose consumption (Kovacs *et al.*, 2012; Ullah *et al.*, 2015). It was found that during epileptic activity there is a reduction in the level of glucose and ATP in the tissue as well as an increase in the level of lactate (Kovacs *et al.*, 2012). In order for the neurons to meet this enormous metabolic demand they use glycerol and lactate as a source of energy (Magistretti *et al.*, 1999; Badaut and Regli, 2004). The aquaglyceroporins, AQP3 and AQP9, are expressed in both astrocytes and neurons in the brain. They act as a metabolite channel that transports glycerol and other solutes such as lactate to astrocytes and neurons. Therefore they play a vital role in astrocyte and neuronal energy metabolism (Amiry-Moghaddam and Ottersen, 2003, Badaut *et al.*, 2004).

In the present study, the total AQP9 transcript level is reduced in TLE-HS compared to TLE-STG. In chronic epileptic rats, the metabolic disturbance was manifested by accumulation of CO_2 and lactic acid in the extracellular space that lead to extracellular lactic acidosis in CA1 (Kim *et al.*, 2009). There was also an up regulation of AQP9 expression in CA1 area in the chronic epilepsy rats after 6 weeks from SE. This increased AQP9 expression in the astrocytes enabled the uptake of excess lactate, due to AQP9 permeability to lactate. Therefore suggesting that AQP9 up regulation is very

important in inhibiting the extracellular lactic acidosis induced by repeated spontaneous seizures (Ribeiro *et al.*, 2006; Kim *et al.*, 2009). Therefore, the reduced AQP9 level seen in this study indicates that AQP9 might be one of the many contributing factors to the pathophysiology of TLE-HS.

In the present study, AQP3 expression was not significantly up regulated in TLE-HS tissue compared to TLE-STG. AQP3 expression investigated in rat hippocampus showed that AQP3 mRNA and protein are expressed in CA1, CA2 and CA3 hippocampal subregions. AQP3 is expressed in both astrocytes and neurons (Yang *et al.*, 2009; 2011). So far there are no studies that investigate the role of AQP3 in epilepsy. However in ischemia, similarly to seizure, there is massive metabolic burden on neurons as they need energy to restore the ion gradient across the cell membrane (Kim *et al.*, 2009; Ullah *et al.*, 2015). In a rat model of focal ischemia, AQP3 expression was significantly increased in the hippocampus following ischemia to cope with the increased energy demand (Yang *et al.*, 2011). Therefore, the non-significant up regulation of AQP3 seen in this study in the TLE-HS tissue, which is the site of repeated spontaneous seizures, indicates an impaired neuronal energy metabolism in TLE-HS that might be contributing to its pathophysiology.

6.4.5 AQP5 and AQP8 expression in TLE-HS

In rat hippocampus AQP5 and AQP8 are expressed in neurons and astrocytes. They both have very similar distribution in CA1, CA2 and CA3 areas suggesting that they may co-operate with each other to regulate water homeostasis in neurons and astrocytes (Yang *et al.*, 2011). To date, there are no studies that investigate the role of AQP5 and

AQP8 in the epileptogenic process. In the present study, there is a slight non-significant reduction in the expression of AQP5 and AQP8 in the TLE-HS samples. This finding suggests that AQP5 and AQP8 do seem to have a role in neuronal water homeostasis. However, whether they have a role in TLE pathophysiology needs to be investigated by further research.

6.4.6   AQP11 expression in TLE-HS

AQP11 is one of the recently described superaquaporin that have a relatively low homology with the other AQPs (Gorelick *et al.*, 2006; Yakata *et al.*, 2011). It has low but constant water permeability (Yakata *et al.*, 2011). In the kidneys, AQP11 has an intracellular localization as it was expressed on the endoplasmic reticulum membrane (Morishita *et al.*, 2005). It has an important role in ER function as the kidney cells from AQP11 knockout mice show an up regulation of both apoptosis and ER stress genes (Ishibashi *et al.*, 2014).

It is proposed that AQP11 has a distinct role in CNS function. In rat brain AQP11 has a unique intracellular expression in Purkinje cell dendrites, while having a membrane expression in the neurons of the cerebral cortex and hippocampal CA1 and CA2 neurons (Gorelick *et al.*, 2006). AQP11 is also expressed in cerebral endothelial cells, suggesting it might have a protective role in brain oedema (Ishibashi *et al.*, 2014). However, the exact biological function of AQP11 in the brain still needs to be elucidated and so far, the role of AQP11 in TLE-HS have not been investigated.

In the present study, there was a significant reduction in AQP11 expression in the epileptogenic foci of TLE-HS compared to TLE-STG. This indicates that AQP11 down regulation might also be linked to the neuroinflammation in seizure foci. A recent study revealed that AQP11 is expressed in retina glial cells. It also found that, in a chronic inflammatory retinal disease, the down regulation of AQP11 was linked to neuroinflammation in the retina (Deeg *et al.*, 2016). In pharmacoresistant epilepsies such as TLE-HS, many clinical and experimental studies demonstrate that there is neuroinflammation in the epileptogenic foci contributing to its pathophysiology (Walker and Sills, 2012; Vezzani *et al.*, 2013; 2015). Therefore, the novel and vital role of AQP11 in TLE-HS pathophysiology needs to be further explored.

6.5 Conclusion

In the sclerotic epileptic hippocampus all AQPs investigated showed an altered expression compared to TLE-STG. The different AQPs have distinct roles involving neuronal excitability, neuronal and astrocytic ion and water homeostasis, neuronal and astrocytic energy metabolism and neuroinflammation. Therefore, the selective regulation of the different AQPs may provide new therapeutic approaches to TLE-HS epilepsy treatment.

Chapter 7

General discussion and conclusions

7 General discussion and conclusions

7.1 General discussion

Temporal lobe epilepsy is a common type of adult epilepsy. The AEDs available modulate and control seizures in 70% of TLE patients. However, there is a need to develop new AEDs as 30% of TLE patients do not respond to the available AEDs. Those patients experience recurrent uncontrolled seizures that cause a decline in their cognitive functions and affect their quality of life (Pitkänen and Sutula, 2002; Blümcke et al., 2012). In addition, TLE-HS surgical treatment, by the resection of the epileptic focus, causes memory impairments and psychopathological disturbances. Furthermore, surgical resection is only effective in controlling seizures in 60% of refractory TLE patients (Blümcke et al., 2012; Cleary et al., 2012; Coras and Blümcke, 2015). Therefore it is a necessity to further understand TLE-HS pathophysiology so new AEDs could be developed for treatment of refractory TLE-HS patients.

In the present study the expression of many genes were investigated in TLE-HS, TLE-STG and PMC specimens, in order to further understand TLE-HS pathophysiology and identify potential drug targets. The use of the surgically resected non-sclerotic, non-spiking TLE-STG samples from TLE patients (Lee et al., 2006; Ravizza et al., 2008; Teichgräber et al., 2009; Bartolomei et al., 2010; Rocha et al., 2015) has many advantages. The samples do not have the *post-mortem* confounding factors such as *post-mortem* interval time and method of collection (Preece and Carins, 2003; Tomita et al., 2004). They have less inter-individual variation as samples are from the same

TLE patient so they are age matched and have the same AED history. However, the epileptogenicity of non-spiking TLE-STG could not be excluded. Even though the TLE-STG sample is a non-spiking tissue, and we cannot exclude that it might be epileptogenic, it is still less epileptogenic compared to chronic epileptogenic TLE-HS tissue which is the seizure focus.

7.1.1 Dysregulation of GABA$_B$ receptor in TLE-HS

In the present study, we found that there was a dysregulation in GABA$_B$ receptor subunits B1 and B2 expression that seem to be contributing to the impaired GABAergic inhibition in TLE-HS patients (Figure 3.10 and 3.13). The total GABA$_{B1}$ and GABA$_{B2}$ subunits expression in TLE-HS showed an apparent elevation compared to PMC. On the other hand, comparing epileptogenic TLE-HS to TLE-STG, we found a significant down regulation of GABA$_{B2}$ subunit. This affects the formation of a functional heterodimeric GABA$_B$ receptor and contributes to the slow GABAergic inhibition impairment in epileptogenic TLE-HS. Therefore, drugs that target and increase GABA$_{B2}$ subunit expression could promote and prolong the late inhibitory postsynaptic potential in the seizure foci tissue and counteracts the excitatory hyperactivity in TLE-HS.

7.1.2 Dysregulation of SGK1 and SCN4B in TLE-HS

In the present study, we found that there was an up regulation of SGK1 in the epileptogenic TLE-HS tissue compared to non-spiking TLE-STG and PMC samples (Figure 4.1 and 4.2). SGK1 is a potent regulator of neuronal excitability (Lang *et al.*, 2006; 2010) and its increased expression may have a protective role in TLE as it induces

prolonged IPSP by the activation and up regulation of VGKCs. It also plays a role in the neuronal and glial re-uptake of glutamate by the up regulation of sodium-dependent glutamate transporters (Lang *et al.*, 2006; Boehmer *et al.*, 2006). Therefore, the activation of SGK1 might be a potential drug target for controlling excessive neuronal excitability.

In addition, this study reports for the first time the expression of SCN4B subunit in TLE. There was a significant up regulation of SCN4B mRNA level in the drug resistant TLE-HS compared to PMC (Figure 4.3 and 4.4). This elevated expression of SCN4B seems to contribute to the increased seizure susceptibility of the sclerotic hippocampi in TLE patients, as β4 subunit favours the Na^+ channel activation and facilitates the action potential firing in neurons. The up regulation of SCN4B may also be contributing to the drug resistance in TLE-HS patients; hence they were resistant to sodium channels blockers such as phenytoin and lamotrigine that stabilize the inactive form of VGSCs. On the other hand, SCN4B subunit was significantly down regulated in the epileptogenic TLE-HS compared to TLE-STG obtained from drug resistant TLE patients. However, whether this down regulation of SCN4B is a compensatory mechanism in response to increased number of seizures, still needs to be further investigated. Nevertheless, modulating VGSCs via targeting SCN4B subunit seem to be a potential drug target for TLE-HS treatment.

7.1.3 Dysregulation of IP3R1 and SYNPR in TLE-HS

In this study we found that there was a significant up regulation of intracellular calcium channel receptor IP3R1 transcript in the sclerotic hippocampi of refractory TLE-HS

202

compared to PMC (Figure 4.5). The up regulation of IP3R1 increases the intracellular Ca^{2+} concentration, neuronal excitability and neurotransmitter release (Cai *et al.*, 2004; Steinlein, 2014). Therefore, IP3R1 up regulation seems to be an additional contributing factor to the increased neuronal excitability seen in TLE-HS as there is already excessive influx of calcium into the neurons caused by excessive glutamate release and chronic NMDA receptor activation. On the other hand, IP3R1 was significantly down regulated in high seizure-frequency TLE-HS tissue compared to TLE-STG indicating an alteration in intracellular Ca^{2+} homeostasis. In conclusion, impairment in Ca^{2+} homeostasis seems to play a role in TLE-HS pathophysiology and IP3R1 may be a potential drug targets for the development of new AEDs.

This study also found that presynaptic SYNPR that is involved in calcium dependent neurotransmitter release was significantly up regulated in TLE-HS compared to PMC (Figure 4.6 and 4.7). SYNPR is found in the inhibitory GABAergic nerve terminals in the hippocampus (Singec *et al.*, 2002). Therefore, SYNPR up regulation in TLE-HS compared to PMC may be an indicator of a compensatory increase in inhibitory GABAergic synapses. On the other hand, both mRNA and protein expression of SYNPR were significantly down regulated in the TLE-HS compared to TLE-STG. This SYNPR down regulation seem to be contributing to the enhanced seizure susceptibility of TLE -HS samples. Nevertheless, role of synaptoporin dysregulation in TLE-HS pathophysiology needs to be further exploited as it might represent a good drug target for TLE-HS patients.

7.1.4 Up regulation of cytokines and chemokines in TLE-HS

The enrichment analysis of TLE-HS transcriptome done in this study presented an overview of molecular functions and biological processes that are affected and possibly contributing to TLE-HS pathophysiology. The clusters of up regulated genes had higher enrichment analysis than the down regulated clusters (Figure 5.6). The up regulated cytokine and chemokine genes were in both the first and second clusters (Table 5.7) and they had the highest enrichment analysis scores associating them to TLE-HS pathophysiology. In addition to the thoroughly investigated cytokines such as IL-1β, and Fas, this study reports for the first time the up regulation of some cytokines and their receptors such as IL-18, CXCL1, CXCL2, CXCL12, CXCR4 and CX3CR1 in TLE-HS, implicating them in TLE pathophysiology (Figure 5.7 - 5.9). The up regulated cytokines are mediating and aggravating neuroinflammation in the epileptogenic TLE-HS tissue. Furthermore, the up regulation of cytokines IL-1β and IL-18 enhances neuronal excitability either via activation of NMDA, AMPA receptors or reduction in inhibitory $GABA_A$ currents (Kanno *et al.*, 2004; Vezzani *et al.*, 2008; Roseti *et al.*, 2015). Therefore, inhibiting the cytokines' effect by means of receptor antagonists or drugs that inhibit their activation provides a worthy therapeutic approach for treatment of refractory TLE-HS.

The up regulation of chemokines CCL2, CCL4, CXCL1, CXCL2 and CXCL12 and the up regulation of chemokine receptors CXCR4 and CX3CR1 (Figure 5.8 and 5.9) are also contributing to the neuroinflammation in the epileptogenic TLE-HS tissue. As they increase the BBB permeability and thus facilitate the infiltration of leukocytes into the

brain. The infiltrated leukocytes further amplify the inflammatory response by releasing proteolytic enzymes and inducing pro-inflammatory cytokines production (Kim *et al.*, 2010; Wu *et al.*, 2015). In addition, the high expression of CCL2, CCL4, CXCL2 and CX3CR1 is probably contributing to the neuronal loss in TLE-HS hence their up regulation was associated with neuronal death in SE animal models (Kalehua *et al.*, 2004; Yeo *et al.*, 2011). Furthermore, high expression of CX3CR1 contributes to increased neuronal hyperactivity via the reduction in inhibitory $GABA_A$ currents (Roseti *et al.*, 2013). Therefore, inhibiting the chemokine effect by means of antagonists for CCR2, CCR5, CXCR2, CXCR4, CX3CR1 receptors or RNA interference therapy might provide a new viable therapeutic approach for treatment of refractory TLE-HS.

It is also important to point out that, activated microglia are the main source of many inflammatory cytokines that are up regulated in TLE-HS such as IL-1β, IL-18, CCL2, CCL4, CXCL1, CXCL2, CXCL12 and CX3CL1. Therefore, drugs that target microglial activation would halt the cycle of recurrent cytokine secretion and microglial autoactivation that causes neuronal damage. Thus they would represent a novel approach for treatment of refractory TLE-HS.

7.1.5   Up regulation of ICAM-1 in TLE-HS

In the present study there was an up regulation of ICAM-1 expression in the epileptogenic TLE-HS tissue (Figure 5.7). This increase in ICAM-1 expression in TLE-HS causes leukocyte recruitment and T-lymphocyte infiltration that contributes to the neurodegeneration and neuroinflammation in TLE-HS. Therefore, targeting ICAM-1 would help in reducing neuroinflammatory response in TLE-HS.

7.1.6   Dysregulation of AQPs in TLE-HS

The present study demonstrates an altered expression of AQP1, AQP3, AQP4, AQP5 AQP8, AQP9 and AQP11 in TLE-HS compared to TLE-STG. There was an up regulation of AQP1 and AQP4 in the seizure foci tissue (TLE-HS) that seems to play a role in astrocyte and epithelial cell water homeostasis (Figure 6.3). There was also an elevation in AQP3 expression in TLE-HS tissue that is experiencing high frequency seizures (Figure 6.4). AQP3 is vital for astrocyte and neuronal energy metabolism and its increased expression in TLE-HS samples might be a way of coping with the massive metabolic burden caused by seizures. On the other hand, there was a down regulation in neuronal AQPs such as AQP5, AQP8, AQP9 and AQP11 in the TLE-HS tissue (Figure 6.4 - 6.6). This indicates that there is impairment in the neuronal ion and water homeostasis, thus making the neurons more vulnerable to water changes in the TLE-HS tissues. Therefore, the selective targeting of the different AQPs may provide new therapeutic approaches to TLE-HS epilepsy treatment.

7.2 Conclusion and future directions

In this thesis, there was an alteration in expression of many genes in the epileptogenic TLE-HS specimens compared to TLE-STG and PMC as shown in the summary table 7.1. The genes investigated were involved in different biological processes; some were involved in neuronal excitability, neuroinflammation, neuronal and astrocytic energy metabolism. Other genes were involved in neurogenesis, apoptosis, intracellular calcium and water homeostasis. Furthermore the investigated genes and the associated proteins produced that were dysregulated in TLE-HS, were expressed or released by neurons, astrocytes, activated microglia and BBB endothelial cells. This highlights that TLE-HS pathophysiology is a complex condition that is caused by combination of astrocytic, microglial and endothelial cells dysfunction, in addition to the neuronal dysfunction. Therefore, developing drugs that address the dysfunction of all cells involved in TLE-HS pathophysiology gives hope for anti-epileptogenic drugs rather than just anti-seizure drugs. In conclusion, many of dysregulated genes identified by this study gave us more insight in TLE-HS pathophysiology and they represent potential drug targets for TLE-HS treatment. However, further research is needed to understand the temporal and spatial changes of those genes and their proteins in TLE-HS.

Table 7.1 Summary of thesis key findings on gene and protein expression in TLE-HS

Target	TLE-HS mRNA expression		TLE-HS protein expression	
	vs TLE-STG	vs PMC	vs TLE-STG	vs PMC
GABA$_{B1}$	↓	No change	↓	↑ *
GABA$_{B2}$	↓ *	↑	↓ *	↑ *
SGK1	↑ *	↑ *	↑	—
SCN4B	↓ *	↑ *	↓ *	—
IP3R1	↓ *	↑ *	—	—
SYNPR	↓ *	↑ *	↓ *	—

Target	TLE-HS mRNA expression (MA)		TLE-HS mRNA expression (qRT-PCR)	
	vs TLE-STG	vs PMC	vs TLE-STG	vs PMC
IL-1β	↑ *	↑ *	↑ *	↑ *
IL-18	↑ *	↑ *	↑ *	↑ *
Fas	↑ *	↑ *	↑	↑ *
ICAM-1	↑ *	↑ *	↑ *	↑
CCL2	↑ *	↑ *	↑ *	↑ *
CCL4	↑ *	↑ *	↑ *	↑ *
CXCL1	↑	↑ *	↑ *	↑ *
CXCL2	↑ *	↑ *	↑ *	↑ *
CXCL12	↑ *	↑ *	↑ *	↑ *
CXCR4	↑ *	↑ *	↑ *	↑ *
CX3CR1	↑	↑ *	↑ *	↑ *
AQP1	↑ *	—	↑	—
AQP3	↑	—	↑	—
AQP4	↑ *	—	↑	—
AQP5	↓	—	↓	—
AQP8	↓	—	↓	—
AQP9	↓	—	↓	—
AQP11	↓	—	↓ *	—

↓ Down regulated   ↑ Up regulated   — Not available

* Significant $P < 0.05$

References

References

ABIEGA, O., BECCARI, S., DIAZ-APARICIO, I., NADJAR, A., LAYÉ, S., LEYROLLE, Q., GÓMEZ-NICOLA, D., DOMERCQ, M., PÉREZ-SAMARTÍN, A. and SÁNCHEZ-ZAFRA, V., 2016. Neuronal Hyperactivity Disturbs ATP Microgradients, Impairs Microglial Motility, and Reduces Phagocytic Receptor Expression Triggering Apoptosis/Microglial Phagocytosis Uncoupling. *PLoS Biol,* **14**(5), pp. e1002466.

AHMED, A.A., VIAS, M., IYER, N.G., CALDAS, C. and BRENTON, J.D., 2004. Microarray segmentation methods significantly influence data precision. *Nucleic Acids Research,* **32**(5), pp. e50.

AKIYAMA, H., TOOYAMA, I., KONDO, H., IKEDA, K., KIMURA, H., MCGEER, E.G. and MCGEER, P.L., 1994. Early response of brain resident microglia to kainic acid-induced hippocampal lesions. *Brain Research,* **635**(1-2), pp. 257-268.

ALI, I., CHUGH, D. and EKDAHL, C.T., 2015. Role of fractalkine–CX3CR1 pathway in seizure-induced microglial activation, neurodegeneration, and neuroblast production in the adult rat brain. *Neurobiology of Disease,* **74**, pp. 194-203.

ALLAN, S.M., TYRRELL, P.J. and ROTHWELL, N.J., 2005. Interleukin-1 and neuronal injury. *Nature Reviews Immunology,* **5**(8), pp. 629-640.

ALONSO-NANCLARES, L. and DEFELIPE, J., 2014. Alterations of the microvascular network in the sclerotic hippocampus of patients with temporal lobe epilepsy. *Epilepsy & Behavior,* **38**, pp. 48-52.

AMAN, T.K., GRIECO-CALUB, T.M., CHEN, C., RUSCONI, R., SLAT, E.A., ISOM, L.L. and RAMAN, I.M., 2009. Regulation of persistent Na current by interactions between beta subunits of voltage-gated Na channels. *The Journal of Neuroscience: the official journal of the Society for Neuroscience,* **29**(7), pp. 2027-2042.

AMBROZ, K., 2006. Improving quantification accuracy for western blots. *PDF).Image Analysis,* **33**. pp. 33-35.

AMIRY-MOGHADDAM, M. and OTTERSEN, O.P., 2003. The molecular basis of water transport in the brain. *Nature Reviews Neuroscience,* **4**(12), pp. 991-1001.

ANDREW, R.D., 1991. Seizure and acute osmotic change: clinical and neurophysiological aspects. *Journal of the Neurological Sciences,* **101**(1), pp. 7-18.

ARION, D., SABATINI, M., UNGER, T., PASTOR, J., ALONSO-NANCLARES, L., BALLESTEROS-YÁNEZ, I., SOLA, R.G., MUNOZ, A., MIRNICS, K. and DEFELIPE, J., 2006. Correlation of transcriptome profile with electrical activity in temporal lobe epilepsy. *Neurobiology of Disease,* **22**(2), pp. 374-387.

ARISI, G.M., FORESTI, M.L., KATKI, K. and SHAPIRO, L.A., 2015. Increased CCL2, CCL3, CCL5, and IL-1β cytokine concentration in piriform cortex, hippocampus, and neocortex after pilocarpine-induced seizures. *Journal of Neuroinflammation,* **12**(1), pp. 1-7.

ARONICA, E., TROOST, D., ROZEMULLER, A.J., YANKAYA, B., JANSEN, G.H., ISOM, L.L. and GORTER, J.A., 2003. Expression and regulation of voltage-gated sodium channel 1 subunit protein in human gliosis-associated pathologies. *Acta Neuropathologica,* **5**(105), pp. 515-523.

BADAUT, J. and REGLI, L., 2004. Distribution and possible roles of aquaporin 9 in the brain. *Neuroscience,* **129**(4), pp. 969-979.

BADAUT, J., FUKUDA, A.M., JULLIENNE, A. and PETRY, K.G., 2014. Aquaporin and brain diseases. *Biochimica et Biophysica Acta (BBA)-General Subjects,* **1840**(5), pp. 1554-1565.

BARTOLOMEI, F., COSANDIER-RIMELE, D., MCGONIGAL, A., AUBERT, S., RÉGIS, J., GAVARET, M., WENDLING, F. and CHAUVEL, P., 2010. From mesial temporal lobe to temporoperisylvian seizures: a quantified study of temporal lobe seizure networks. *Epilepsia,* **51**(10), pp. 2147-2158.

BAULAC, M. and LEPPIK, I.E., 2007. Efficacy and safety of adjunctive zonisamide therapy for refractory partial seizures. *Epilepsy Research,* **75**(2), pp. 75-83.

BEBEK, N., ÖZDEMIR, Ö., SAYITOGLU, M., HATIRNAZ, Ö., BAYKAN, B., GÜRSES, C., SENCER, A., KARASU, A., TÜZÜN, E. and ÜZÜN, I., 2013. Expression analysis and clinical correlation of aquaporin 1 and 4 genes in human hippocampal sclerosis. *Journal of Clinical Neuroscience,* **20**(11), pp. 1564-1570.

BECKER, A.J., CHEN, J., PAUS, S., NORMANN, S., BECK, H., ELGER, C.E., WIESTLER, O.D. and BLÜMCKE, I., 2002. Transcriptional profiling in human epilepsy: expression array and single cell real-time qRT-PCR analysis reveal distinct cellular gene regulation. *Neuroreport,* **13**(10), pp. 1327-1333.

BEN-ARI, Y. and DUDEK, F.E., 2010. Primary and secondary mechanisms of epileptogenesis in the temporal lobe: there is a before and an after. *Epilepsy Currents,* **10**(5), pp. 118-125.

BENARROCH, E.E., 2012. GABA_B receptors: structure, functions, and clinical implications. *Neurology, 78*(8), pp. 578-584.

BENGZON, J., MOHAPEL, P., EKDAHL, C.T. and LINDVALL, O., 2002. Neuronal apoptosis after brief and prolonged seizures. *Progress in Brain Research, 135*, pp. 111-119.

BENKE, D., HONER, M., MICHEL, C., BETTLER, B. and MOHLER, H., 1999. gamma-aminobutyric acid type B receptor splice variant proteins GBR1a and GBR1b are both associated with GBR2 in situ and display differential regional and subcellular distribution. *The Journal of Biological Chemistry, 274*(38), pp. 27323-27330.

BENKE, D., ZEMOURA, K. and MAIER, P.J., 2012. Modulation of cell surface GABA(B) receptors by desensitization, trafficking and regulated degradation. *World Journal of Biological Chemistry, 3*(4), pp. 61-72.

BERG, A.T. and SCHEFFER, I.E., 2011. New concepts in classification of the epilepsies: entering the 21st century. *Epilepsia, 52*(6), pp. 1058-1062.

BESAG, F. and PATSALOS, P.N., 2012. New developments in the treatment of partial-onset epilepsy. *Neuropsychiatric Disease and Treatment, 8*, pp. 455-464.

BETTLER, B., KAUPMANN, K., MOSBACHER, J. and GASSMANN, M., 2004. Molecular structure and physiological functions of GABA(B) receptors. *Physiological Reviews, 84*(3), pp. 835-867.

BIALER, M. and WHITE, H.S., 2010. Key factors in the discovery and development of new antiepileptic drugs. *Nature Reviews Drug Discovery, 9*(1), pp. 68-82.

BILLINTON, A., BAIRD, V.H., THOM, M., DUNCAN, J.S., UPTON, N. and BOWERY, N.G., 2001. GABA B (1) mRNA expression in hippocampal sclerosis associated with human temporal lobe epilepsy. *Molecular Brain Research, 86*(1), pp. 84-89.

BILLINTON, A., BAIRD, V.H., THOM, M., DUNCAN, J.S., UPTON, N. and BOWERY, N.G., 2001. GABA_B receptor autoradiography in hippocampal sclerosis associated with human temporal lobe epilepsy. *British Journal of Pharmacology, 132*(2), pp. 475-480.

BILLINTON, A., IGE, A.O., WISE, A., WHITE, J.H., DISNEY, G.H., MARSHALL, F.H., WALDVOGEL, H.J., FAULL, R.L. and EMSON, P.C., 2000. GABA B receptor heterodimer-component localisation in human brain. *Molecular Brain Research, 77*(1), pp. 111-124.

BINDER, D.K., NAGELHUS, E.A. and OTTERSEN, O.P., 2012. Aquaporin-4 and epilepsy. *Glia, 60*(8), pp. 1203-1214.

BLÜMCKE, I., CORAS, R., MIYATA, H. and ÖZKARA, C., 2012. Defining Clinico-Neuropathological Subtypes of Mesial Temporal Lobe Epilepsy with Hippocampal Sclerosis. *Brain Pathology,* **22**(3), pp. 402-411.

BOEHMER, C., PALMADA, M., RAJAMANICKAM, J., SCHNIEPP, R., AMARA, S. and LANG, F., 2006. Post-translational regulation of EAAT2 function by co-expressed ubiquitin ligase Nedd4-2 is impacted by SGK kinases. *Journal of Neurochemistry,* **97**(4), pp. 911-921.

BORGES, K., SHAW, R. and DINGLEDINE, R., 2007. Gene expression changes after seizure preconditioning in the three major hippocampal cell layers. *Neurobiology of Disease,* **26**(1), pp. 66-77.

BRAGIN, A., WILSON, C. and ENGEL, J., 2000. Chronic epileptogenesis requires development of a network of pathologically interconnected neuron clusters: a hypothesis. *Epilepsia,* **41**(s6), pp. S144-S152.

BREITLING, R., ARMENGAUD, P., AMTMANN, A. and HERZYK, P., 2004. Rank products: a simple, yet powerful, new method to detect differentially regulated genes in replicated microarray experiments. *FEBS Letters,* **573**(1), pp. 83-92.

BRODIE, M.J., COVANIS, A., GIL-NAGEL, A., LERCHE, H., PERUCCA, E., SILLS, G.J. and WHITE, H.S., 2011. Antiepileptic drug therapy: does mechanism of action matter? *Epilepsy & Behavior,* **21**(4), pp. 331-341.

BRONEN, R.A., CHEUNG, G., CHARLES, J.T., KIM, J.H., SPENCER, D.D., SPENCER, S.S., SZE, G. and MCCARTHY, G., 1991. Imaging findings in hippocampal sclerosis: correlation with pathology. *American Journal of Neuroradiology,* **12**(5), pp. 933-940.

BROWN, R.E., JARVIS, K.L. and HYLAND, K.J., 1989. Protein measurement using bicinchoninic acid: elimination of interfering substances. *Analytical Biochemistry,* **180**(1), pp. 136-139.

CAI, W., HISATSUNE, C., NAKAMURA, K., NAKAMURA, T., INOUE, T. and MIKOSHIBA, K., 2004. Activity-dependent expression of inositol 1,4,5-trisphosphate receptor type 1 in hippocampal neurons. *The Journal of Biological Chemistry,* **279**(22), pp. 23691-23698.

CANNON, S.C. and BEAN, B.P., 2010. Sodium channels gone wild: resurgent current from neuronal and muscle channelopathies. *The Journal of Clinical Investigation,* **120**(1), pp. 80-83.

CASILLAS-ESPINOSA, P.M., POWELL, K.L. and O'BRIEN, T.J., 2012. Regulators of synaptic transmission: roles in the pathogenesis and treatment of epilepsy. *Epilepsia,* **53**(s9), pp. 41-58.

CASTELLI, L., NIGRO, M.J. and MAGISTRETTI, J., 2007. Analysis of resurgent sodium-current expression in rat parahippocampal cortices and hippocampal formation. *Brain Research,* **1163**, pp. 44-55.

CATTERALL, W.A., KALUME, F. and OAKLEY, J.C., 2010. NaV1. 1 channels and epilepsy. *The Journal of Physiology,* **588**(11), pp. 1849-1859.

CAVAZOS, J. and SUTULA, T., 1990. Progressive neuronal loss induced by kindling: a possible mechanism for mossy fiber synaptic reorganization and hippocampal sclerosis. *Brain Research,* **527**(1), pp. 1-6.

CAVAZOS, J.E., DAS, I. and SUTULA, T.P., 1994. Neuronal loss induced in limbic pathways by kindling: evidence for induction of hippocampal sclerosis by repeated brief seizures. *The Journal of Neuroscience: the official journal of the Society for Neuroscience,* **14**(5 Pt 2), pp. 3106-3121.

CAVUS, I., KASOFF, W.S., CASSADAY, M.P., JACOB, R., GUEORGUIEVA, R., SHERWIN, R.S., KRYSTAL, J.H., SPENCER, D.D. and ABI-SAAB, W.M., 2005. Extracellular metabolites in the cortex and hippocampus of epileptic patients. *Annals of Neurology,* **57**(2), pp. 226-235.

CHARLES, K., DEUCHARS, J., DAVIES, C. and PANGALOS, M., 2003. GABA B receptor subunit expression in glia. *Molecular and Cellular Neuroscience,* **24**(1), pp. 214-223.

CHEN, L.S., WONG, J.G., BANERJEE, P.K. and SNEAD III, O.C., 1996. Kainic acid-induced focal cortical seizure is associated with an increase of synaptophysin immunoreactivity in the cortex. *Experimental Neurology,* **141**(1), pp. 25-31.

CHOI, C., XU, X., OH, J.W., LEE, S.J., GILLESPIE, G.Y., PARK, H., JO, H. and BENVENISTE, E.N., 2001. Fas-induced expression of chemokines in human glioma cells: involvement of extracellular signal-regulated kinase 1/2 and p38 mitogen-activated protein kinase. *Cancer Research,* **61**(7), pp. 3084-3091.

CHOI, J., NORDLI, D.R., ALDEN, T.D., DIPATRI, A., LAUX, L., KELLEY, K., ROSENOW, J., SCHUELE, S.U., RAJARAM, V. and KOH, S., 2009. Cellular injury and neuroinflammation in children with chronic intractable epilepsy. *Journal of Neuroinflammation,* **6**(1), pp. 1-14.

CLEARY, R.A., THOMPSON, P.J., FOX, Z. and FOONG, J., 2012. Predictors of psychiatric and seizure outcome following temporal lobe epilepsy surgery. *Epilepsia,* **53**(10), pp. 1705-1712.

CORAS, R. and BLÜMCKE, I., 2015. Clinico-pathological subtypes of hippocampal sclerosis in temporal lobe epilepsy and their differential impact on memory impairment. *Neuroscience,* **309**, pp. 153-161.

COWAN, D., LINIAL, M. and SCHELLER, R.H., 1990. Torpedo synaptophysin: evolution of a synaptic vesicle protein. *Brain Research,* **509**(1), pp. 1-7.

DAI, J., JI, C., GU, S., WU, Q., WANG, L., XU, J., ZENG, L., YE, X., YIN, G. and XIE, Y., 2003. Cloning and sequence analysis of the human cDNA encoding the synaptoporin (Δ), a highly conservative synaptic vesicle protein. *Molecular Biology Reports,* **30**(3), pp. 185-191.

DAVIES, K.G., SCHWEITZER, J.B., LOONEY, M.R., BUSH, A.J., DOHAN, F.C. and HERMANN, B.P., 1998. Synaptophysin immunohistochemistry densitometry measurement in resected human hippocampus: implication for the etiology of hippocampal sclerosis. *Epilepsy Research,* **32**(3), pp. 335-344.

DAWE, R.J., BENNETT, D.A., SCHNEIDER, J.A., LEURGANS, S.E., KOTROTSOU, A., BOYLE, P.A. and ARFANAKIS, K., 2014. Ex vivo T 2 relaxation: associations with age-related neuropathology and cognition. *Neurobiology of Aging,* **35**(7), pp. 1549-1561.

DAY, R.E., KITCHEN, P., OWEN, D.S., BLAND, C., MARSHALL, L., CONNER, A.C., BILL, R.M. and CONNER, M.T., 2014. Human aquaporins: regulators of transcellular water flow. *Biochimica et Biophysica Acta (BBA)-General Subjects,* **1840**(5), pp. 1492-1506.

DE CASTRO RIBEIRO, M., HIRT, L., BOGOUSSLAVSKY, J., REGLI, L. and BADAUT, J., 2006. Time course of aquaporin expression after transient focal cerebral ischemia in mice. *Journal of Neuroscience Research,* **83**(7), pp. 1231-1240.

DEEG, C.A., AMANN, B., LUTZ, K., HIRMER, S., LUTTERBERG, K., KREMMER, E. and HAUCK, S.M., 2016. Aquaporin 11, a regulator of water efflux at retinal Müller glial cell surface decreases concomitant with immune-mediated gliosis. *Journal of Neuroinflammation,* **13**(1), pp. 1.

EID, T., LEE, T.S., THOMAS, M.J., AMIRY-MOGHADDAM, M., BJORNSEN, L.P., SPENCER, D.D., AGRE, P., OTTERSEN, O.P. and DE LANEROLLE, N.C., 2005. Loss of perivascular aquaporin 4 may underlie deficient water and K+ homeostasis in the human epileptogenic hippocampus. *Proceedings of the National Academy of Sciences of the United States of America,* **102**(4), pp. 1193-1198.

215

ENGEL, T. and HENSHALL, D.C., 2009. Apoptosis, Bcl-2 family proteins and caspases: the ABCs of seizure-damage and epileptogenesis. *International Journal of Physiology, Pathophysiology and Pharmacology,* **1**(2), pp. 97-115.

ENGEL, T., SCHINDLER, C.K., SANZ-RODRIGUEZ, A., CONROY, R.M., MELLER, R., SIMON, R.P. and HENSHALL, D.C., 2011. Expression of neurogenesis genes in human temporal lobe epilepsy with hippocampal sclerosis. *International Journal of Physiology, Pathophysiology and Pharmacology,* **3**(1), pp. 38-47.

ERRANTE, L.D., WILLIAMSON, A., SPENCER, D.D. and PETROFF, O.A., 2002. Gabapentin and vigabatrin increase GABA in the human neocortical slice. *Epilepsy Research,* **49**(3), pp. 203-210.

FELDERHOFF-MUESER, U., SCHMIDT, O.I., OBERHOLZER, A., BÜHRER, C. and STAHEL, P.F., 2005. IL-18: a key player in neuroinflammation and neurodegeneration? *Trends in Neurosciences,* **28**(9), pp. 487-493.

FELDERHOFF-MUESER, U., SCHMIDT, O.I., OBERHOLZER, A., BÜHRER, C. and STAHEL, P.F., 2005. IL-18: a key player in neuroinflammation and neurodegeneration? *Trends in Neurosciences,* **28**(9), pp. 487-493.

FISHER, R.S., ACEVEDO, C., ARZIMANOGLOU, A., BOGACZ, A., CROSS, J.H., ELGER, C.E., ENGEL, J., FORSGREN, L., FRENCH, J.A. and GLYNN, M., 2014. ILAE official report: a practical clinical definition of epilepsy. *Epilepsia,* **55**(4), pp. 475-482.

FROTSCHER, M., JONAS, P. and SLOVITER, R.S., 2006. Synapses formed by normal and abnormal hippocampal mossy fibers. *Cell and Tissue Research,* **326**(2), pp. 361-367.

GAMPER, N., FILLON, S., FENG, Y., FRIEDRICH, B., LANG, P., HENKE, G., HUBER, S., KOBAYASHI, T., COHEN, P. and LANG, F., 2002a. K channel activation by all three isoforms of serum-and glucocorticoid-dependent protein kinase SGK. *Pflügers Archiv,* **445**(1), pp. 60-66.

GAMPER, N., FILLON, S., HUBER, S., FENG, Y., KOBAYASHI, T., COHEN, P. and LANG, F., 2002b. IGF-1 up-regulates K channels via PI3-kinase, PDK1 and SGK1. *Pflügers Archiv,* **443**(4), pp. 625-634.

GASSMANN, M. and BETTLER, B., 2012. Regulation of neuronal GABAB receptor functions by subunit composition. *Nature Reviews Neuroscience,* **13**(6), pp. 380-394.

GASTALDI, M., ROBAGLIA-SCHLUPP, A., MASSACRIER, A., PLANELLS, R. and CAU, P., 1998. mRNA coding for voltage-gated sodium channel β2 subunit in rat central nervous system: cellular distribution and changes following kainate-induced seizures. *Neuroscience Letters,* **249**(1), pp. 53-56.

GERDES, N., SUKHOVA, G.K., LIBBY, P., REYNOLDS, R.S., YOUNG, J.L. and SCHONBECK, U., 2002. Expression of interleukin (IL)-18 and functional IL-18 receptor on human vascular endothelial cells, smooth muscle cells, and macrophages: implications for atherogenesis. *The Journal of Experimental Medicine,* **195**(2), pp. 245-257.

GHORPADE, A., HOLTER, S., BORGMANN, K., PERSIDSKY, R. and WU, L., 2003. HIV-1 and IL-1β regulate Fas ligand expression in human astrocytes through the NF-κB pathway. *Journal of Neuroimmunology,* **141**(1), pp. 141-149.

GOLDIN, A.L., 2003. Mechanisms of sodium channel inactivation. *Current Opinion in Neurobiology,* **13**(3), pp. 284-290.

GORELICK, D.A., PRAETORIUS, J., TSUNENARI, T., NIELSEN, S. and AGRE, P., 2006. Aquaporin-11: a channel protein lacking apparent transport function expressed in brain. *BMC Biochemistry,* **7**(14), pp. 1-14.

GORTER, J.A., VAN VLIET, E.A. and ARONICA, E., 2015. Status epilepticus, blood–brain barrier disruption, inflammation, and epileptogenesis. *Epilepsy & Behavior,* **49**, pp. 13-16.

GORTER, J.A., VAN VLIET, E.A., ARONICA, E., BREIT, T., RAUWERDA, H., LOPES DA SILVA, F.H. and WADMAN, W.J., 2006. Potential new antiepileptogenic targets indicated by microarray analysis in a rat model for temporal lobe epilepsy. *The Journal of Neuroscience: the official journal of the Society for Neuroscience,* **26**(43), pp. 11083-11110.

GRABS, D., BERGMANN, M., SCHUSTER, T., FOX, P., BRICH, M. and GRATZL, M., 1994. Differential Expression of Synaptophysin and Synaptoporin During Pre-and Postnatal Development of the Rat Hippocampal Network. *European Journal of Neuroscience,* **6**(11), pp. 1765-1771.

GRAEF, I.A., MERMELSTEIN, P.G., STANKUNAS, K., NEILSON, J.R., DEISSEROTH, K., TSIEN, R.W. and CRABTREE, G.R., 1999. L-type calcium channels and GSK-3 regulate the activity of NF-ATc4 in hippocampal neurons. *Nature,* **401**(6754), pp. 703-708.

GRIECO, T.M., MALHOTRA, J.D., CHEN, C., ISOM, L.L. and RAMAN, I.M., 2005. Open-channel block by the cytoplasmic tail of sodium channel β4 as a mechanism for resurgent sodium current. *Neuron,* **45**(2), pp. 233-244.

GRYDER, D.S. and ROGAWSKI, M.A., 2003. Selective antagonism of GluR5 kainate-receptor-mediated synaptic currents by topiramate in rat basolateral amygdala neurons. *The Journal of Neuroscience : the official journal of the Society for Neuroscience,* **23**(18), pp. 7069-7074.

GUYON, A., 2015. CXCL12 chemokine and GABA neurotransmitter systems crosstalk and their putative roles. *Frontiers in Cellular Neuroscience.,* **5**(115), pp.1-7.

HARTMAN, N.W., CARPENTINO, J.E., LAMONICA, K., MOR, D.E., NAEGELE, J.R. and GRABEL, L., 2010. CXCL12-mediated guidance of migrating embryonic stem cell-derived neural progenitors transplanted into the hippocampus. *PLoS One,* **5**(12), pp. e15856.

HÄUSSLER, U., RINAS, K., KILIAS, A., EGERT, U. and HAAS, C.A., 2015. Mossy fiber sprouting and pyramidal cell dispersion in the hippocampal CA2 region in a mouse model of temporal lobe epilepsy. *Hippocampus,* **26**(5), pp. 577-588.

HELMSTAEDTER, C., LOER, B., WOHLFAHRT, R., HAMMEN, A., SAAR, J., STEINHOFF, B.J., QUISKE, A. and SCHULZE-BONHAGE, A., 2008. The effects of cognitive rehabilitation on memory outcome after temporal lobe epilepsy surgery. *Epilepsy & Behavior,* **12**(3), pp. 402-409.

HENSHALL, D.C. and SIMON, R.P., 2005. Epilepsy and apoptosis pathways. *Journal of Cerebral Blood Flow & Metabolism,* **25**(12), pp. 1557-1572.

HENSHALL, D.C., CLARK, R.S., ADELSON, P.D., CHEN, M., WATKINS, S.C. and SIMON, R.P., 2000. Alterations in bcl-2 and caspase gene family protein expression in human temporal lobe epilepsy. *Neurology,* **55**(2), pp. 250-257.

HESDORFFER, D.C., LOGROSCINO, G., BENN, E.K., KATRI, N., CASCINO, G. and HAUSER, W.A., 2011. Estimating risk for developing epilepsy: a population-based study in Rochester, Minnesota. *Neurology,* **76**(1), pp. 23-27.

HEUSER, K., EID, T., LAURITZEN, F., THOREN, A.E., VINDEDAL, G.F., TAUBOLL, E., GJERSTAD, L., SPENCER, D.D., OTTERSEN, O.P., NAGELHUS, E.A. and DE LANEROLLE, N.C., 2012. Loss of perivascular Kir4.1 potassium channels in the sclerotic hippocampus of patients with mesial temporal lobe epilepsy. *Journal of Neuropathology and Experimental Neurology,* **71**(9), pp. 814-825.

HEUSER, K., NAGELHUS, E.A., TAUBØLL, E., INDAHL, U., BERG, P.R., LIEN, S., NAKKEN, S., GJERSTAD, L. and OTTERSEN, O.P., 2010. Variants of the genes encoding AQP4 and Kir4. 1 are associated with subgroups of patients with temporal lobe epilepsy. *Epilepsy Research,* **88**(1), pp. 55-64.

HOLLISTER, R., PAGE, K. and HYMAN, B., 1997. Distribution of the messenger RNA for the extracellularly regulated kinases 1, 2 and 3 in rat brain: effects of excitotoxic hippocampal lesions. *Neuroscience,* **79**(4), pp. 1111-1119.

HU, S., SHENG, W.S., EHRLICH, L.C., PETERSON, P.K. and CHAO, C.C., 2000. Cytokine effects on glutamate uptake by human astrocytes. *Neuroimmunomodulation,* **7**(3), pp. 153-159.

HUANG DA, W., SHERMAN, B.T. and LEMPICKI, R.A., 2009. Bioinformatics enrichment tools: paths toward the comprehensive functional analysis of large gene lists. *Nucleic Acids Research,* **37**(1), pp. 1-13.

HUANG, D.W., SHERMAN, B.T. and LEMPICKI, R.A., 2009. Systematic and integrative analysis of large gene lists using DAVID bioinformatics resources. *Nature Protocols,* **4**(1), pp. 44-57.

HUGG, J.W., BUTTERWORTH, E.J. and KUZNIECKY, R.I., 1999. Diffusion mapping applied to mesial temporal lobe epilepsy: preliminary observations. *Neurology,* **53**(1), pp. 173-176.

HUYGHE, D., NAKAMURA, Y., TERUNUMA, M., FAIDEAU, M., HAYDON, P., PANGALOS, M.N. and MOSS, S.J., 2014. Glutamine synthetase stability and subcellular distribution in astrocytes are regulated by gamma-aminobutyric type B receptors. *The Journal of Biological Chemistry,* **289**(42), pp. 28808-28815.

IMAIZUMI, K., TSUDA, M., WANAKA, A., TOHYAMA, M. and TAKAGI, T., 1994. Differential expression of sgk mRNA, a member of the Ser/Thr protein kinase gene family, in rat brain after CNS injury. *Molecular Brain Research,* **26**(1-2), pp. 189-196.

ISHIBASHI, K., TANAKA, Y. and MORISHITA, Y., 2014. The role of mammalian superaquaporins inside the cell. *Biochimica et Biophysica Acta (BBA)-General Subjects,* **1840**(5), pp. 1507-1512.

JACOB, T.C., MOSS, S.J. and JURD, R., 2008. GABAA receptor trafficking and its role in the dynamic modulation of neuronal inhibition. *Nature Reviews Neuroscience,* **9**(5), pp. 331-343.

JAMALI, S., BARTOLOMEI, F., ROBAGLIA-SCHLUPP, A., MASSACRIER, A., PERAGUT, J.C., REGIS, J., DUFOUR, H., RAVID, R., ROLL, P., PEREIRA, S., ROYER, B., ROECKEL-TREVISIOL, N., FONTAINE, M., GUYE, M., BOUCRAUT, J., CHAUVEL, P., CAU, P. and SZEPETOWSKI, P., 2006. Large-scale expression study of human mesial temporal lobe epilepsy: evidence for dysregulation of the neurotransmission and complement systems in the entorhinal cortex. *Brain: A Journal of Neurology,* **129**(Pt 3), pp. 625-641.

JENSEN, E.C., 2012. The basics of western blotting. *The Anatomical Record,* **295**(3), pp. 369-371.

JOHNSON, E.A., DAO, T.L., GUIGNET, M.A., GEDDES, C.E., KOEMETER-COX, A.I. and KAN, R.K., 2011. Increased expression of the chemokines CXCL1 and MIP-1a by resident brain cells precedes neutrophil infiltration in the brain following prolonged somaninduced *status epilepticus* in rats. *J Neuroinflammation,* **8** (41), pp.1-10.

JOHNSON, E.A., GUIGNET, M.A., DAO, T.L., HAMILTON, T.A. and KAN, R.K., 2015. Interleukin-18 expression increases in response to neurovascular damage following soman-induced *status epilepticus* in rats. *Journal of Inflammation,* **12**(48), pp. 1-11.

JOHNSON, M.R., BEHMOARAS, J., BOTTOLO, L., KRISHNAN, M.L., PERNHORST, K., SANTOSCOY, P.L.M., ROSSETTI, T., SPEED, D., SRIVASTAVA, P.K. and CHADEAU-HYAM, M., 2015. Systems genetics identifies Sestrin 3 as a regulator of a proconvulsant gene network in human epileptic hippocampus. *Nature Communications,* **6**(23).pp. 1-11.

JOHNSTON, G.A., 2005. GABA$_A$ receptor channel pharmacology. *Current Pharmaceutical Design,* **11**(15), pp. 1867-1885.

KALEHUA, A., NAGEL, J., WHELCHEL, L., GIDES, J., PYLE, R., SMITH, R., KUSIAK, J. and TAUB, D., 2004. Monocyte chemoattractant protein-1 and macrophage inflammatory protein-2 are involved in both excitotoxin-induced neurodegeneration and regeneration. *Experimental Cell Research,* **297**(1), pp. 197-211.

KAN, A.A., DE JAGER, W., DE WIT, M., HEIJNEN, C., VAN ZUIDEN, M., FERRIER, C., VAN RIJEN, P., GOSSELAAR, P., HESSEL, E. and VAN NIEUWENHUIZEN, O., 2012. Protein expression profiling of inflammatory mediators in human temporal lobe epilepsy reveals co-activation of multiple chemokines and cytokines. *J Neuroinflammation,* **9**, pp. 207.

KANG, T., KIM, D., KWAK, S., KIM, J., WON, M.H., KIM, D., CHOI, S. and KWON, O., 2006. Epileptogenic roles of astroglial death and regeneration in the dentate gyrus of experimental temporal lobe epilepsy. *Glia,* **54**(4), pp. 258-271.

KANNO, T., NAGATA, T., YAMAMOTO, S., OKAMURA, H. and NISHIZAKI, T., 2004. Interleukin-18 stimulates synaptically released glutamate and enhances postsynaptic AMPA receptor responses in the CA1 region of mouse hippocampal slices. *Brain Research,* **1012**(1), pp. 190-193.

KAUPMANN, K., MALITSCHEK, B., SCHULER, V., HEID, J., FROESTL, W., BECK, P., MOSBACHER, J., BISCHOFF, S., KULIK, A. and SHIGEMOTO, R., 1998. GABAB-receptor subtypes assemble into functional heteromeric complexes. *Nature,* **396**(6712), pp. 683-687.

KIM, J., RYU, H., YEO, S., SEO, C., LEE, B., CHOI, I., KIM, D. and KANG, T., 2009. Differential expressions of aquaporin subtypes in astroglia in the hippocampus of chronic epileptic rats. *Neuroscience,* **163**(3), pp. 781-789.

KIM, J., RYU, H.J., YEO, S. and KANG, T., 2010. P2X7 receptor regulates leukocyte infiltrations in rat frontoparietal cortex following status epilepticus. *J Neuroinflammation,* **7**(6), pp. 65-70.

KINGSBURY, A.E., BRAY, E.L. and FOSTER, O.J., 1996. A simplified and rapid procedure for in situ hybridization on human, flash-frozen, post-mortem brain and its combination with immunohistochemistry. *Journal of Neuroscience Methods,* **69**(2), pp. 213-227.

KLITGAARD, H., MATAGNE, A., NICOLAS, J., GILLARD, M., LAMBERTY, Y., DE RYCK, M., KAMINSKI, R.M., LECLERCQ, K., NIESPODZIANY, I. and WOLFF, C., 2016. Brivaracetam: Rationale for discovery and preclinical profile of a selective SV2A ligand for epilepsy treatment. *Epilepsia,* **57**(4), pp. 538–548.

KOVÁCS, R., HEINEMANN, U. and STEINHÄUSER, C., 2012. Mechanisms underlying blood–brain barrier dysfunction in brain pathology and epileptogenesis: role of astroglia. *Epilepsia,* **53**(s6), pp. 53-59.

KOYAMA, R. and IKEGAYA, Y., 2004. Mossy fiber sprouting as a potential therapeutic target for epilepsy. *Current Neurovascular Research,* **1**(1), pp. 3-10.

KOZIOL, J.A., 2010. The rank product method with two samples. *FEBS Letters,* **584**(21), pp. 4481-4484.

KREIL, D.P., RUSSELL, R.R. and RUSSELL, S., 2006. [4] Microarray Oligonucleotide Probes. *Methods in Enzymology,* **410**, pp. 73-98.

KUCZEWSKI, N., FUCHS, C., FERRAND, N., JOVANOVIC, J.N., GAIARSA, J. and PORCHER, C., 2011. Mechanism of GABAB receptor-induced BDNF secretion and promotion of GABAA receptor membrane expression. *Journal of Neurochemistry,* **118**(4), pp. 533-545.

KUO, C. and BEAN, B.P., 1994. Na channels must deactivate to recover from inactivation. *Neuron,* **12**(4), pp. 819-829.

KUO, C.C., LIN, B.J., CHANG, H.R. and HSIEH, C.P., 2004. Use-dependent inhibition of the N-methyl-D-aspartate currents by felbamate: a gating modifier with selective binding to the desensitized channels. *Molecular Pharmacology,* **65**(2), pp. 370-380.

KUPPNER, M., MEIR, E., HAMOU, M. and TRIBOLET, N.D., 1990. Cytokine regulation of intercellular adhesion molecule-1 (ICAM-1) expression on human glioblastoma cells. *Clinical & Experimental Immunology,* **81**(1), pp. 142-148.

KURIEN, B.T. and SCOFIELD, R.H., 2006. Western blotting. *Methods,* **38**(4), pp. 283-293.

KURUBA, R., HATTIANGADY, B. and SHETTY, A.K., 2009. Hippocampal neurogenesis and neural stem cells in temporal lobe epilepsy. *Epilepsy & Behavior,* **14**(1), pp. 65-73.

KWAN, P., ARZIMANOGLOU, A., BERG, A.T., BRODIE, M.J., ALLEN HAUSER, W., MATHERN, G., MOSHÉ, S.L., PERUCCA, E., WIEBE, S. and FRENCH, J., 2010. Definition of drug resistant epilepsy: consensus proposal by the ad hoc Task Force of the ILAE Commission on Therapeutic Strategies. *Epilepsia,* **51**(6), pp. 1069-1077.

LACHOS, J., ZATTONI, M., WIESER, H.G., FRITSCHY, J.M., LANGMANN, T., SCHMITZ, G., ERREDE, M., VIRGINTINO, D., YONEKAWA, Y. and FREI, K., 2011. Characterization of the gene expression profile of human hippocampus in mesial temporal lobe epilepsy with hippocampal sclerosis. *Epilepsy Research and Treatment,* **2011**, pp. 758407.

LAI, H.C. and JAN, L.Y., 2006. The distribution and targeting of neuronal voltage-gated ion channels. *Nature Reviews Neuroscience,* **7**(7), pp. 548-562.

LANG, F., BOHMER, C., PALMADA, M., SEEBOHM, G., STRUTZ-SEEBOHM, N. and VALLON, V., 2006. (Patho)physiological significance of the serum- and glucocorticoid-inducible kinase isoforms. *Physiological Reviews,* **86**(4), pp. 1151-1178.

LANG, F., STRUTZ-SEEBOHM, N., SEEBOHM, G. and LANG, U.E., 2010. Significance of SGK1 in the regulation of neuronal function. *The Journal of Physiology,* **588**(18), pp. 3349-3354.

LAWRENCE, J.J. and MCBAIN, C.J., 2003. Interneuron diversity series: containing the detonation—feedforward inhibition in the CA3 hippocampus. *Trends in Neurosciences,* **26**(11), pp. 631-640.

LEE, D.J., HSU, M.S., SELDIN, M.M., ARELLANO, J.L. and BINDER, D.K., 2012. Decreased expression of the glial water channel aquaporin-4 in the intrahippocampal kainic acid model of epileptogenesis. *Experimental Neurology,* **235**(1), pp. 246-255.

LEE, K.J., QUEENAN, B.N., ROZEBOOM, A.M., BELLMORE, R., LIM, S.T., VICINI, S. and PAK, D.T., 2013. Mossy fiber-CA3 synapses mediate homeostatic plasticity in mature hippocampal neurons. *Neuron,* **77**(1), pp. 99-114.

LEE, T., BJØRNSEN, L.P., PAZ, C., KIM, J.H., SPENCER, S.S., SPENCER, D.D., EID, T. and DE LANEROLLE, N.C., 2006. GAT1 and GAT3 expression are differently localized in the human epileptogenic hippocampus. *Acta Neuropathologica,* **111**(4), pp. 351-363.

LEE, T.S., EID, T., MANE, S., KIM, J.H., SPENCER, D.D., OTTERSEN, O.P. and DE LANEROLLE, N.C., 2004. Aquaporin-4 is increased in the sclerotic hippocampus in human temporal lobe epilepsy. *Acta Neuropathologica,* **108**(6), pp. 493-502.

LEE, T.S., MANE, S., EID, T., ZHAO, H., LIN, A., GUAN, Z., KIM, J.H., SCHWEITZER, J., KING-STEVENS, D., WEBER, P., SPENCER, S.S., SPENCER, D.D. and DE LANEROLLE, N.C., 2007. Gene expression in temporal lobe epilepsy is consistent with increased release of glutamate by astrocytes. *Molecular Medicine (Cambridge, Mass.),* **13**(1-2), pp. 1-13.

LEMUTH, K. and RUPP, S., 2015. Microarrays as Research Tools and Diagnostic Devices. *RNA and DNA Diagnostics.* Springer, pp. 259-280.

LINVAK, K. and SCHMITTGEN, T., 2001. Analysis of relative gene expression data using real-time quantitative PCR and $2^{-\Delta\Delta CT}$. *Methods,* **25**(4), pp. 402-408.

LIU, Q., JIN, Y., WANG, K., MENG, X., YANG, Y., YANG, Z., ZHAO, Y., ZHAO, M. and ZHANG, J., 2014. Study of the residues involved in the binding of β1 to β3 subunits in the sodium channel. *Comptes Rendus Biologies,* **337**(2), pp. 73-77.

LOPES, M.W., SOARES, F.M.S., DE MELLO, N., NUNES, J.C., DE CORDOVA, F.M., WALZ, R. and LEAL, R.B., 2012. Time-dependent modulation of mitogen activated protein kinases and AKT in rat hippocampus and cortex in the pilocarpine model of epilepsy. *Neurochemical Research,* **37**(9), pp. 1868-1878.

LOUBOUTIN, J.P., CHEKMASOVA, A., MARUSICH, E., AGRAWAL, L. and STRAYER, D.S., 2011. Role of CCR5 and its ligands in the control of vascular inflammation and leukocyte recruitment required for acute excitotoxic seizure induction and neural damage. *FASEB Journal: official publication of the Federation of American Societies for Experimental Biology,* **25**(2), pp. 737-753.

MAGISTRETTI, P.J., PELLERIN, L., ROTHMAN, D.L. and SHULMAN, R.G., 1999. Energy on demand. *Science,* **283**(5401), pp. 496.

MANGAN, P.S. and LOTHMAN, E.W., 1996. Profound disturbances of pre- and postsynaptic GABAB-receptor-mediated processes in region CA1 in a chronic model of temporal lobe epilepsy. *Journal of Neurophysiology,* **76**(2), pp. 1282-1296.

MANTOVANI, A., BONECCHI, R. and LOCATI, M., 2006. Tuning inflammation and immunity by chemokine sequestration: decoys and more. *Nature Reviews Immunology,* **6**(12), pp. 907-918.

MAROSO, M., BALOSSO, S., RAVIZZA, T., LIU, J., BIANCHI, M. and VEZZANI, A., 2011. Interleukin-1 type 1 receptor/Toll-like receptor signalling in epilepsy: the importance of IL-1beta and high-mobility group box 1. *Journal of Internal Medicine,* **270**(4), pp. 319-326.

MARQUEZ-CURTIS, L.A. and JANOWSKA-WIECZOREK, A., 2013. Enhancing the migration ability of mesenchymal stromal cells by targeting the SDF-1/CXCR4 axis. *BioMed Research International,* **2013**, pp. 561098.

MATHERN, G.W., BABB, T.L., VICKREY, B.G., MELENDEZ, M. and PRETORIUS, J.K., 1995. The clinical-pathogenic mechanisms of hippocampal neuron loss and surgical outcomes in temporal lobe epilepsy. *Brain : a Journal of Neurology,* **118** (1), pp. 105-118.

MATSUMOTO, M. and NAGATA, E., 1999. Type 1 inositol 1, 4, 5-trisphosphate receptor knock-out mice: their phenotypes and their meaning in neuroscience and clinical practice. *Journal of Molecular Medicine,* **77**(5), pp. 406-411.

MIRZA, N., VASIEVA, O., MARSON, A.G. and PIRMOHAMED, M., 2011. Exploring the genomic basis of pharmacoresistance in epilepsy: an integrative analysis of large-scale gene expression profiling studies on brain tissue from epilepsy surgery. *Human Molecular Genetics,* **20**(22), pp. 4381-4394.

MIYAZAKI, H., OYAMA, F., INOUE, R., AOSAKI, T., ABE, T., KIYONARI, H., KINO, Y., KUROSAWA, M., SHIMIZU, J. and OGIWARA, I., 2014. Singular localization of sodium channel β4 subunit in unmyelinated fibres and its role in the striatum. *Nature Communications,* **5**(5525),pp. 1-15.

MORISHITA, Y., MATSUZAKI, T., HARA-CHIKUMA, M., ANDOO, A., SHIMONO, M., MATSUKI, A., KOBAYASHI, K., IKEDA, M., YAMAMOTO, T., VERKMAN, A., KUSANO, E., OOKAWARA, S., TAKATA, K., SASAKI, S. and ISHIBASHI, K., 2005. Disruption of aquaporin-11 produces polycystic kidneys following vacuolization of the proximal tubule. *Molecular and Cellular Biology,* **25**(17), pp. 7770-7779.

MUÑOZ, A., ARELLANO, J.I. and DEFELIPE, J., 2002. GABABR1 receptor protein expression in human mesial temporal cortex: changes in temporal lobe epilepsy. *Journal of Comparative Neurology,* **449**(2), pp. 166-179.

NAKAHARA, H., KONISHI, Y., G. BEACH, T., YAMADA, N., MAKINO, S. and TOOYAMA, I., 2010. Infiltration of T lymphocytes and expression of icam-1 in the hippocampus of patients with hippocampal sclerosis. *Acta Histochemica et Cytochemica,* **43**(6), pp. 157-162.

NAMADURAI, S., YEREDDI, N.R., CUSDIN, F.S., HUANG, C.L., CHIRGADZE, D.Y. and JACKSON, A.P., 2015. A new look at sodium channel beta subunits. *Open Biology,* **5**(1), pp. 140192.

NICOLAY, N.H., HERTLE, D., BOEHMERLE, W., HEIDRICH, F.M., YECKEL, M. and EHRLICH, B.E., 2007. Inositol 1, 4, 5 trisphosphate receptor and chromogranin B are concentrated in different regions of the hippocampus. *Journal of Neuroscience Research,* **85**(9), pp. 2026-2036.

NIELSEN, S., SMITH, B.L., CHRISTENSEN, E.I., KNEPPER, M.A. and AGRE, P., 1993. CHIP28 water channels are localized in constitutively water-permeable segments of the nephron. *The Journal of Cell Biology,* **120**(2), pp. 371-383.

OKA, M., WADA, M., WU, Q., YAMAMOTO, A. and FUJITA, T., 2006. Functional expression of metabotropic GABA B receptors in primary cultures of astrocytes from rat cerebral cortex. *Biochemical and Biophysical Research Communications,* **341**(3), pp. 874-881.

PAL, S., SUN, D., LIMBRICK, D., RAFIQ, A. and DELORENZO, R., 2001. Epileptogenesis induces long-term alterations in intracellular calcium release and sequestration mechanisms in the hippocampal neuronal culture model of epilepsy. *Cell Calcium,* **30**(4), pp. 285-296.

PAPADOPOULOS, M.C. and VERKMAN, A.S., 2013. Aquaporin water channels in the nervous system. *Nature Reviews Neuroscience,* **14**(4), pp. 265-277.

PARK, D.R., THOMSEN, A.R., FREVERT, C.W., PHAM, U., SKERRETT, S.J., KIENER, P.A. and LILES, W.C., 2003. Fas (CD95) induces proinflammatory cytokine responses by human monocytes and monocyte-derived macrophages. *Journal of Immunology (Baltimore, Md.: 1950),* **170**(12), pp. 6209-6216.

PARK, K.D., YANG, X., LEE, H., DUSTRUDE, E.T., WANG, Y., KHANNA, R. and KOHN, H., 2013. Discovery of lacosamide affinity bait agents that exhibit potent voltage-gated sodium channel blocking properties. *ACS Chemical Neuroscience,* **4**(3), pp. 463-474.

PERUCCA, E., YASOTHAN, U., CLINCKE, G. and KIRKPATRICK, P., 2008. Lacosamide. *Nature Reviews Drug Discovery,* **7**(12), pp. 973-974.

PICARIELLO, L., SALA, S.C., MARTINETI, V., GOZZINI, A., ARAGONA, P., TOGNARINI, I., PAGLIERANI, M., NESI, G., BRANDI, M. and TONELLI, F., 2006. A comparison of methods for the analysis of low abundance proteins in desmoid tumor cells. *Analytical Biochemistry,* **354**(2), pp. 205-212.

PITKÄNEN, A. and SUTULA, T.P., 2002. Is epilepsy a progressive disorder? Prospects for new therapeutic approaches in temporal-lobe epilepsy. *The Lancet Neurology,* **1**(3), pp. 173-181.

PREECE, P. and CAIRNS, N.J., 2003. Quantifying mRNA in postmortem human brain: influence of gender, age at death, postmortem interval, brain pH, agonal state and inter-lobe mRNA variance. *Molecular Brain Research,* **118**(1), pp. 60-71.

PRINCIVALLE, A., DUNCAN, J., THOM, M. and BOWERY, N., 2002. Studies of $GABA_B$ receptors labelled with $[^3H]$-CGP62349 in hippocampus resected from patients with temporal lobe epilepsy. *British Journal of Pharmacology,* **136**(8), pp. 1099-1106.

PRINCIVALLE, A., DUNCAN, J., THOM, M. and BOWERY, N., 2003. $GABA_{B1a}$, $GABA_{B1b}$ and $GABA_{B2}$ mRNA variants expression in hippocampus resected from patients with temporal lobe epilepsy. *Neuroscience,* **122**(4), pp. 975-984.

PROPER, E.A., HOOGLAND, G., KAPPEN, S.M., JANSEN, G.H., RENSEN, M.G., SCHRAMA, L.H., VAN VEELEN, C.W., VAN RIJEN, P.C., VAN NIEUWENHUIZEN, O., GISPEN, W.H. and DE GRAAN, P.N., 2002. Distribution of glutamate transporters in the hippocampus of patients with pharmaco-resistant temporal lobe epilepsy. *Brain : a Journal of Neurology,* **125**(1), pp. 32-43.

QUEENAN, B.N. and PAK, D.T., 2013. Homeostatic synaptic plasticity in the hippocampus: therapeutic prospects for seizure control? *Future Neurology,* **8**(4), pp. 361-363.

RADONIĆ, A., THULKE, S., MACKAY, I.M., LANDT, O., SIEGERT, W. and NITSCHE, A., 2004. Guideline to reference gene selection for quantitative real-time PCR. *Biochemical and Biophysical Research Communications,* **313**(4), pp. 856-862.

RAJALU, M., FRITZIUS, T., ADELFINGER, L., JACQUIER, V., BESSEYRIAS, V., GASSMANN, M. and BETTLER, B., 2015. Pharmacological characterization of GABA B receptor subtypes assembled with auxiliary KCTD subunits. *Neuropharmacology,* **88**, pp. 145-154.

RANG, H.P., RITTER, J.M., FLOWER, R.J. and HENDERSON, G., 2014. *Rang & Dale's Pharmacology: With student consult online access.* Elsevier Health Sciences.

RAVIZZA, T. and VEZZANI, A., 2006. *Status epilepticus* induces time-dependent neuronal and astrocytic expression of interleukin-1 receptor type I in the rat limbic system. *Neuroscience,* **137**(1), pp. 301-308.

RAVIZZA, T., GAGLIARDI, B., NOÉ, F., BOER, K., ARONICA, E. and VEZZANI, A., 2008. Innate and adaptive immunity during epileptogenesis and spontaneous seizures: evidence from experimental models and human temporal lobe epilepsy. *Neurobiology of Disease,* **29**(1), pp. 142-160.

REN, G., ZHAO, X., ZHANG, L., ZHANG, J., L'HUILLIER, A., LING, W., ROBERTS, A.I., LE, A.D., SHI, S., SHAO, C. and SHI, Y., 2010. Inflammatory cytokine-induced intercellular adhesion molecule-1 and vascular cell adhesion molecule-1 in mesenchymal stem cells are critical for immunosuppression. *Journal of Immunology (Baltimore, Md.: 1950),* **184**(5), pp. 2321-2328.

ROCHA, L., ALONSO-VANEGAS, M., MARTINEZ-JUAREZ, I.E., OROZCO-SUAREZ, S., ESCALANTE-SANTIAGO, D., FERIA-ROMERO, I.A., ZAVALA-TECUAPETLA, C., CISNEROS-FRANCO, J.M., BUENTELLO-GARCIA, R.M. and CIENFUEGOS, J., 2015. GABAergic alterations in neocortex of patients with pharmacoresistant temporal lobe epilepsy can explain the comorbidity of anxiety and depression: the potential impact of clinical factors. *Frontiers in Cellular Neuroscience,* **8**, pp. 442.

ROGAWSKI, M.A. and LÖSCHER, W., 2004. The neurobiology of antiepileptic drugs. *Nature Reviews Neuroscience,* **5**(7), pp. 553-564.

ROSETI, C., FUCILE, S., LAURO, C., MARTINELLO, K., BERTOLLINI, C., ESPOSITO, V., MASCIA, A., CATALANO, M., ARONICA, E. and LIMATOLA, C., 2013. Fractalkine/CX3CL1 modulates GABAA currents in human temporal lobe epilepsy. *Epilepsia,* **54**(10), pp. 1834-1844.

ROSETI, C., VAN VLIET, E.A., CIFELLI, P., RUFFOLO, G., BAAYEN, J.C., DI CASTRO, M.A., BERTOLLINI, C., LIMATOLA, C., ARONICA, E. and VEZZANI, A., 2015. GABA A currents are decreased by IL-1β in epileptogenic tissue of patients with temporal lobe epilepsy: implications for ictogenesis. *Neurobiology of Disease,* **82**, pp. 311-320.

ROTHSTEIN, J.D., VAN KAMMEN, M., LEVEY, A.I., MARTIN, L.J. and KUNCL, R.W., 1995. Selective loss of glial glutamate transporter GLT-1 in amyotrophic lateral sclerosis. *Annals of Neurology,* **38**(1), pp. 73-84.

RYU, H., KIM, J., KIM, M., KWON, H., SUH, S., SONG, H. and KANG, T., 2010. The protective effects of interleukin-18 and interferon-γ on neuronal damages in the rat hippocampus following status epilepticus. *Neuroscience,* **170**(3), pp. 711-721.

SAEED, A.I., SHAROV, V., WHITE, J., LI, J., LIANG, W., BHAGABATI, N., BRAISTED, J., KLAPA, M., CURRIER, T., THIAGARAJAN, M., STURN, A., SNUFFIN, M., REZANTSEV, A., POPOV, D., RYLTSOV, A., KOSTUKOVICH, E., BORISOVSKY, I., LIU, Z., VINSAVICH, A., TRUSH, V. and QUACKENBUSH, J., 2003. TM4: a free, open-source system for microarray data management and analysis. *BioTechniques,* **34**(2), pp. 374-378.

SARAC, S., AFZAL, S., BROHOLM, H., MADSEN, F.F., PLOUG, T. and LAURSEN, H., 2009. Excitatory amino acid transporters EAAT-1 and EAAT-2 in temporal lobe and hippocampus in intractable temporal lobe epilepsy. *Apmis,* **117**(4), pp. 291-301.

SCHARFMAN, H.E., SOLLAS, A.L., BERGER, R.E. and GOODMAN, J.H., 2003. Electrophysiological evidence of monosynaptic excitatory transmission between granule cells after seizure-induced mossy fiber sprouting. *Journal of Neurophysiology,* **90**(4), pp. 2536-2547.

SCHULER, V., LÜSCHER, C., BLANCHET, C., KLIX, N., SANSIG, G., KLEBS, K., SCHMUTZ, M., HEID, J., GENTRY, C. and URBAN, L., 2001. Epilepsy, hyperalgesia, impaired memory, and loss of pre-and postsynaptic GABA B responses in mice lacking GABA B (1). *Neuron,* **31**(1), pp. 47-58.

SCHUTZ-GESCHWENDER, A., ZHANG, Y., HOLT, T., MCDERMITT, D. and OLIVE, D.M., 2004. Quantitative, two-color western blot detection with infrared fluorescence. *LI-COR Biosciences,* pp. 1-7.

SCHWARTZKROIN, P.A., BARABAN, S.C. and HOCHMAN, D.W., 1998. Osmolarity, ionic flux, and changes in brain excitability. *Epilepsy Research,* **32**(1), pp. 275-285.

SHAPIRO, L.A., WANG, L. and RIBAK, C.E., 2008. Rapid astrocyte and microglial activation following pilocarpine-induced seizures in rats. *Epilepsia,* **49**(s2), pp. 33-41.

SHEEHAN, J.J., ZHOU, C., GRAVANIS, I., ROGOVE, A.D., WU, Y.P., BOGENHAGEN, D.F. and TSIRKA, S.E., 2007. Proteolytic activation of monocyte chemoattractant protein-1 by plasmin underlies excitotoxic neurodegeneration in mice. *The Journal of Neuroscience : the Official Journal of the Society for Neuroscience,* **27**(7), pp. 1738-1745.

SILLS, G.J., 2006. The mechanisms of action of gabapentin and pregabalin. *Current Opinion in Pharmacology,* **6**(1), pp. 108-113.

SILLS, G.J., 2010. SV2A in epilepsy: the plot thickens. *Epilepsy Currents,* **10**(2), pp. 47-49.

SILLS, G.J., BUTLER, E., THOMPSON, G.G. and BRODIE, M.J., 1999. Vigabatrin and tiagabine are pharmacologically different drugs. A pre-clinical study. *Seizure,* **8**(7), pp. 404-411.

SINGEC, I., KNOTH, R., DITTER, M., HAGEMEYER, C.E., ROSENBROCK, H., FROTSCHER, M. and VOLK, B., 2002. Synaptic vesicle protein synaptoporin is differently expressed by subpopulations of mouse hippocampal neurons. *Journal of Comparative Neurology,* **452**(2), pp. 139-153.

SKEBERDIS, V.A., CHEVALEYRE, V., LAU, C.G., GOLDBERG, J.H., PETTIT, D.L., SUADICANI, S.O., LIN, Y., BENNETT, M.V., YUSTE, R. and CASTILLO, P.E., 2006. Protein kinase A regulates calcium permeability of NMDA receptors. *Nature Neuroscience,* **9**(4), pp. 501-510.

SLOVITER, R.S., 2005. The neurobiology of temporal lobe epilepsy: too much information, not enough knowledge. *Comptes Rendus Biologies,* **328**(2), pp. 143-153.

SMITHSON, W.H. and WALKER, M.C., 2012. *ABC of Epilepsy.* John Wiley & Sons.

SONG, C., XU, W., ZHANG, X., WANG, S., ZHU, G., XIAO, T., ZHAO, M. and ZHAO, C., 2015. CXCR4 Antagonist AMD3100 Suppresses the Long-Term Abnormal Structural Changes of Newborn Neurons in the Intraventricular Kainic Acid Model of Epilepsy. *Molecular Neurobiology,* **53**, pp. 1518–1532.

STAMATOVIC, S.M., SHAKUI, P., KEEP, R.F., MOORE, B.B., KUNKEL, S.L., VAN ROOIJEN, N. and ANDJELKOVIC, A.V., 2005. Monocyte chemoattractant protein-1 regulation of blood–brain barrier permeability. *Journal of Cerebral Blood Flow & Metabolism,* **25**(5), pp. 593-606.

STEINHÄUSER, C., GRUNNET, M. and CARMIGNOTO, G., 2016. Crucial role of astrocytes in temporal lobe epilepsy. *Neuroscience,* **323**, pp. 157-169.

STEINLEIN, O.K., 2014. Calcium signaling and epilepsy. *Cell and Tissue Research,* **357**(2), pp. 385-393.

STEKEL, D., 2003. *Microarray Bioinformatics.* Cambridge University Press.

STRAESSLE, A., LOUP, F., ARABADZISZ, D., OHNING, G.V. and FRITSCHY, J., 2003. Rapid and long-term alterations of hippocampal GABAB receptors in a mouse model of temporal lobe epilepsy. *European Journal of Neuroscience,* **18**(8), pp. 2213-2226.

STRUTZ-SEEBOHM, N., SEEBOHM, G., SHUMILINA, E., MACK, A.F., WAGNER, H., LAMPERT, A., GRAHAMMER, F., HENKE, G., JUST, L. and SKUTELLA, T., 2005. Glucocorticoid adrenal steroids and glucocorticoid-inducible kinase isoforms in the regulation of GluR6 expression. *The Journal of Physiology,* **565**(2), pp. 391-401.

SUN, T., XIAO, H., ZHOU, P., LU, Y., BAO, L. and ZHANG, X., 2006. Differential expression of synaptoporin and synaptophysin in primary sensory neurons and up-regulation of synaptoporin after peripheral nerve injury. *Neuroscience,* **141**(3), pp. 1233-1245.

TAIT, M.J., SAADOUN, S., BELL, B.A. and PAPADOPOULOS, M.C., 2008. Water movements in the brain: role of aquaporins. *Trends in Neurosciences,* **31**(1), pp. 37-43.

TAN, Z., SANKAR, R., TU, W., SHIN, D., LIU, H., WASTERLAIN, C.G. and SCHREIBER, S.S., 2002. Immunohistochemical study of p53-associated proteins in rat brain following lithium–pilocarpine status epilepticus. *Brain Research,* **929**(1), pp. 129-138.

TATULIAN, L., DELMAS, P., ABOGADIE, F.C. and BROWN, D.A., 2001. Activation of expressed KCNQ potassium currents and native neuronal M-type potassium currents by the anti-convulsant drug retigabine. *The Journal of Neuroscience : the Official Journal of the Society for Neuroscience,* **21**(15), pp. 5535-5545.

TAYLOR, C.W. and TOVEY, S.C., 2010. IP(3) receptors: toward understanding their activation. *Cold Spring Harbor Perspectives in Biology,* **2**(12), pp. a004010.

TEICHGRÄBER, L.A., LEHMANN, T., MEENCKE, H., WEISS, T., NITSCH, R. and DEISZ, R.A., 2009. Impaired function of GABAB receptors in tissues from pharmacoresistant epilepsy patients. *Epilepsia,* **50**(7), pp. 1697-1716.

TELEZHKIN, V., BROWN, D.A. and GIBB, A.J., 2012. Distinct subunit contributions to the activation of M-type potassium channels by PI(4,5)P2. *The Journal of General Physiology,* **140**(1), pp. 41-53.

TELLEZ-ZENTENO, J.F. and HERNANDEZ-RONQUILLO, L., 2012. A review of the epidemiology of temporal lobe epilepsy. *Epilepsy Research and Treatment,* **2012**, pp. 630853.

THOMPSON, S.J., ASHLEY, M.D., STOHR, S., SCHINDLER, C., LI, M., MCCARTHY-CULPEPPER, K.A., PEARSON, A.N., XIONG, Z.G., SIMON, R.P., HENSHALL, D.C. and MELLER, R., 2011. Suppression of TNF receptor-1 signaling in an in vitro model of epileptic tolerance. *International Journal of Physiology, Pathophysiology and Pharmacology,* **3**(2), pp. 120-132.

TOMITA, H., VAWTER, M.P., WALSH, D.M., EVANS, S.J., CHOUDARY, P.V., LI, J., OVERMAN, K.M., ATZ, M.E., MYERS, R.M. and JONES, E.G., 2004. Effect of agonal and postmortem factors on gene expression profile: quality control in microarray analyses of postmortem human brain. *Biological Psychiatry,* **55**(4), pp. 346-352.

TOROLIRA, D., SUCHOMELOVA, L., WASTERLAIN, C.G. and NIQUET, J., 2016. Widespread neuronal injury in a model of cholinergic *status epilepticus* in postnatal day 7 rat pups. *Epilepsy Research,* **120**, pp. 47-54.

TREVINO, V. and FALCIANI, F., 2006. GALGO: an R package for multivariate variable selection using genetic algorithms. *Bioinformatics (Oxford, England),* **22**(9), pp. 1154-1156.

TREVINO, V., FALCIANI, F. and BARRERA-SALDAÑA, H.A., 2007. DNA microarrays: a powerful genomic tool for biomedical and clinical research. *Molecular Medicine-Cambridge Ma Then New York-,* **13**(9/10), pp. 527.

TRINKA, E., STEINHOFF, B., NIKANOROVA, M. and BRODIE, M., 2016. Perampanel for focal epilepsy: insights from early clinical experience. *Acta Neurologica Scandinavica,* **133**(3), pp. 160-172.

TURECEK, R., SCHWENK, J., FRITZIUS, T., IVANKOVA, K., ZOLLES, G., ADELFINGER, L., JACQUIER, V., BESSEYRIAS, V., GASSMANN, M. and SCHULTE, U., 2014. Auxiliary GABA B receptor subunits uncouple G protein βγ subunits from effector channels to induce desensitization. *Neuron,* **82**(5), pp. 1032-1044.

ULLAH, G., WEI, Y., DAHLEM, M.A., WECHSELBERGER, M. and SCHIFF, S.J., 2015. The Role of Cell Volume in the Dynamics of Seizure, Spreading Depression, and Anoxic Depolarization. *PLoS Comput Biol,* **11**(8), pp. e1004414.

VALENZUELA, J.I., JAUREGUIBERRY-BRAVO, M., SALAS, D.A., RAMIREZ, O.A., CORNEJO, V.H., LU, H.E., BLANPIED, T.A. and COUVE, A., 2014. Transport along the dendritic endoplasmic reticulum mediates the trafficking of GABAB receptors. *Journal of Cell Science,* **127**(Pt 15), pp. 3382-3395.

VAN DER HEL, W.S., NOTENBOOM, R.G., BOS, I.W., VAN RIJEN, P.C., VAN VEELEN, C.W. and DE GRAAN, P.N., 2005. Reduced glutamine synthetase in hippocampal areas with neuron loss in temporal lobe epilepsy. *Neurology,* **64**(2), pp. 326-333.

VAN DER VELDEN, V., HOCHHAUS, A., CAZZANIGA, G., SZCZEPANSKI, T., GABERT, J. and VAN DONGEN, J., 2003. Detection of minimal residual disease in hematologic malignancies by real-time quantitative PCR: principles, approaches, and laboratory aspects. *Leukemia,* **17**(6), pp. 1013-1034.

VAN GASSEN, K. L., DE WIT, M., KOERKAMP, M.J., RENSEN, M.G., VAN RIJEN, P.C., HOLSTEGE, F.C., LINDHOUT, D. and DE GRAAN, P.N., 2008. Possible role of the innate immunity in temporal lobe epilepsy. *Epilepsia,* **49**(6), pp. 1055-1065.

VAN GASSEN, K. L., DE WIT, M., VAN KEMPEN, M., SASKIA VAN DER HEL, W, VAN RIJEN, P.C., JACKSON, A.P., LINDHOUT, D. and DE GRAAN, P.N., 2009. Hippocampal Navβ3 expression in patients with temporal lobe epilepsy. *Epilepsia,* **50**(4), pp. 957-962.

VANDESOMPELE, J., DE PRETER, K., PATTYN, F., POPPE, B., VAN ROY, N., DE PAEPE, A. and SPELEMAN, F., 2002. Accurate normalization of real-time quantitative RT-PCR data by geometric averaging of multiple internal control genes. *Genome Biology,* **3**(7), pp. 1-12.

VENUGOPAL, A.K., SAMEER KUMAR, G.S., MAHADEVAN, A., SELVAN, L.D., MARIMUTHU, A., DIKSHIT, J.B., TATA, P., RAMACHANDRA, Y., CHAERKADY, R., SINHA, S., CHANDRAMOULI, B., ARIVAZHAGAN, A., SATISHCHANDRA, P., SHANKAR, S. and PANDEY, A., 2012. Transcriptomic Profiling of Medial Temporal Lobe Epilepsy. *Journal of Proteomics & Bioinformatics,* **5**(2), pp. 1000210.

VERKHRATSKY, A., RODRÍGUEZ, J.J. and PARPURA, V., 2013. Astroglia in neurological diseases. *Future Neurology,* **8**(2), pp. 149-158.

VERMEULEN, K., VAN BOCKSTAELE, D.R. and BERNEMAN, Z.N., 2005. Apoptosis: mechanisms and relevance in cancer. *Annals of Hematology,* **84**(10), pp. 627-639.

VEZZANI, A., 2015. Anti-inflammatory drugs in epilepsy: does it impact epileptogenesis? *Expert Opinion on Drug Safety,* **14**(4), pp. 583-592.

VEZZANI, A., BALOSSO, S. and RAVIZZA, T., 2008. The role of cytokines in the pathophysiology of epilepsy. *Brain, Behavior, and Immunity,* **22**(6), pp. 797-803.

VEZZANI, A., FRIEDMAN, A. and DINGLEDINE, R.J., 2013. The role of inflammation in epileptogenesis. *Neuropharmacology,* **69**, pp. 16-24.

VIVIANI, B., BARTESAGHI, S., GARDONI, F., VEZZANI, A., BEHRENS, M.M., BARTFAI, T., BINAGLIA, M., CORSINI, E., DI LUCA, M., GALLI, C.L. and MARINOVICH, M., 2003. Interleukin-1beta enhances NMDA receptor-mediated intracellular calcium increase through activation of the Src family of kinases. *The Journal of Neuroscience : the Official Journal of the Society for Neuroscience,* **23**(25), pp. 8692-8700.

VOLZ, F., BOCK, H.H., GIERTHMUEHLEN, M., ZENTNER, J., HAAS, C.A. and FREIMAN, T.M., 2011. Stereologic estimation of hippocampal GluR2/3-and calretinin-immunoreactive hilar neurons (presumptive mossy cells) in two mouse models of temporal lobe epilepsy. *Epilepsia,* **52**(9), pp. 1579-1589.

WALKER, J.M., 2009. The bicinchoninic acid (BCA) assay for protein quantitation. *The Protein Protocols Handbook,* pp. 11-15.

WALKER, L. and SILLS, G.J., 2012. Inflammation and epilepsy: the foundations for a new therapeutic approach in epilepsy? *Epilepsy Currents,* **12**(1), pp. 8-12.

WANG, Z., GERSTEIN, M. and SNYDER, M., 2009. RNA-Seq: a revolutionary tool for transcriptomics. *Nature Reviews Genetics,* **10**(1), pp. 57-63.

WEBSTER, M.K., GOYA, L., GE, Y., MAIYAR, A.C. and FIRESTONE, G.L., 1993. Characterization of sgk, a novel member of the serine/threonine protein kinase gene family which is transcriptionally induced by glucocorticoids and serum. *Molecular and Cellular Biology,* **13**(4), pp. 2031-2040.

WHITWORTH, T.L. and QUICK, M.W., 2001. Upregulation of gamma-aminobutyric acid transporter expression: role of alkylated gamma-aminobutyric acid derivatives. *Biochemical Society Transactions,* **29**(Pt 6), pp. 736-741.

WICKENDEN, A.D., YU, W., ZOU, A., JEGLA, T. and WAGONER, P.K., 2000. Retigabine, a novel anti-convulsant, enhances activation of KCNQ2/Q3 potassium channels. *Molecular Pharmacology,* **58**(3), pp. 591-600.

WIERSCHKE, S., GIGOUT, S., HORN, P., LEHMANN, T., DEHNICKE, C., BRÄUER, A.U. and DEISZ, R.A., 2010. Evaluating reference genes to normalize gene expression in human epileptogenic brain tissues. *Biochemical and Biophysical Research Communications,* **403**(3), pp. 385-390.

WILCZYNSKI, G.M., KONOPACKI, F.A., WILCZEK, E., LASIECKA, Z., GORLEWICZ, A., MICHALUK, P., WAWRZYNIAK, M., MALINOWSKA, M., OKULSKI, P., KOLODZIEJ, L.R., KONOPKA, W., DUNIEC, K., MIODUSZEWSKA, B., NIKOLAEV, E., WALCZAK, A., OWCZAREK, D., GORECKI, D.C., ZUSCHRATTER, W., OTTERSEN, O.P. and KACZMAREK, L., 2008. Important role of matrix metalloproteinase 9 in epileptogenesis. *The Journal of Cell Biology,* **180**(5), pp. 1021-1035.

WONG, M.L. and MEDRANO, J.F., 2005. Real-time PCR for mRNA quantitation. *BioTechniques,* **39**(1), pp. 75.

WORLD MEDICAL ASSOCIATION., 2001. World Medical Association Declaration of Helsinki. Ethical principles for medical research involving human subjects. *Bulletin of the World Health Organization,* **79**(4), pp. 373-374.

233

WU, F., ZHAO, Y., JIAO, T., SHI, D., ZHU, X., ZHANG, M., SHI, M. and ZHOU, H., 2015. CXCR2 is essential for cerebral endothelial activation and leukocyte recruitment during neuroinflammation. *Journal of Neuroinflammation,* **12**, pp. 98.

XU, C., ZHANG, W., RONDARD, P., PIN, J.P. and LIU, J., 2014. Complex GABAB receptor complexes: how to generate multiple functionally distinct units from a single receptor. *Frontiers in Pharmacology,* **5**, pp. 12.

XU, L., HE, D. and BAI, Y., 2015. Microglia-mediated inflammation and neurodegenerative disease. *Molecular Neurobiology,* **53**, pp. 1-7.

XU, S., PANG, Q., LIU, Y., SHANG, W., ZHAI, G. and GE, M., 2007. Neuronal apoptosis in the resected sclerotic hippocampus in patients with mesial temporal lobe epilepsy. *Journal of Clinical Neuroscience,* **14**(9), pp. 835-840.

XU, Y., ZENG, K., HAN, Y., WANG, L., CHEN, D., XI, Z., WANG, H., WANG, X. and CHEN, G., 2012. Altered expression of CX3CL1 in patients with epilepsy and in a rat model. *The American Journal of Pathology,* **180**(5), pp. 1950-1962.

YAKATA, K., TANI, K. and FUJIYOSHI, Y., 2011. Water permeability and characterization of aquaporin-11. *Journal of Structural Biology,* **174**(2), pp. 315-320.

YANG, M., GAO, F., LIU, H., YU, W., HE, G., ZHUO, F., QIU, G. and SUN, S., 2011. Immunolocalization of aquaporins in rat brain. *Anatomia, Histologia, Embryologia,* **40**(4), pp. 299-306.

YANG, M., GAO, F., LIU, H., YU, W.H. and SUN, S.Q., 2009. Temporal changes in expression of aquaporin3,-4,-5 and-8 in rat brains after permanent focal cerebral ischemia. *Brain Research,* **1290**, pp. 121-132.

YAROV-YAROVOY, V., BROWN, J., SHARP, E.M., CLARE, J.J., SCHEUER, T. and CATTERALL, W.A., 2001. Molecular determinants of voltage-dependent gating and binding of pore-blocking drugs in transmembrane segment IIIS6 of the Na(+) channel alpha subunit. *The Journal of Biological Chemistry,* **276**(1), pp. 20-27.

YEO, S., KIM, J., RYU, H., SEO, C., LEE, B., CHOI, I., KIM, D. and KANG, T., 2011. The roles of fractalkine/CX3CR1 system in neuronal death following pilocarpine-induced status epilepticus. *Journal of Neuroimmunology,* **234**(1), pp. 93-102.

YILMAZER-HANKE, D.M., WOLF, H.K., SCHRAMM, J., ELGER, C.E., WIESTLER, O.D. and BLUMCKE, I., 2000. Subregional pathology of the amygdala complex and entorhinal region in surgical specimens from patients with pharmacoresistant temporal lobe epilepsy. *Journal of Neuropathology and Experimental Neurology,* **59**(10), pp. 907-920.

YOON, E.J., GERACHSHENKO, T., SPIEGELBERG, B.D., ALFORD, S. and HAMM, H.E., 2007. Gbetagamma interferes with Ca2+-dependent binding of synaptotagmin to the soluble N-ethylmaleimide-sensitive factor attachment protein receptor (SNARE) complex. *Molecular Pharmacology, 72*(5), pp. 1210-1219.

YU, F.H., WESTENBROEK, R.E., SILOS-SANTIAGO, I., MCCORMICK, K.A., LAWSON, D., GE, P., FERRIERA, H., LILLY, J., DISTEFANO, P.S., CATTERALL, W.A., SCHEUER, T. and CURTIS, R., 2003. Sodium channel beta4, a new disulfide-linked auxiliary subunit with similarity to beta2. *The Journal of Neuroscience : the Official Journal of the Society for Neuroscience, 23*(20), pp. 7577-7585.

ZACCARA, G., 2016. Brivaracetam: new compound approved for the treatment of epilepsy. *Drugs of Today (Barcelona, Spain : 1998), 52*(4), pp. 219-227.

ZATTONI, M., MURA, M.L., DEPREZ, F., SCHWENDENER, R.A., ENGELHARDT, B., FREI, K. and FRITSCHY, J.M., 2011. Brain infiltration of leukocytes contributes to the pathophysiology of temporal lobe epilepsy. *The Journal of Neuroscience : the Official Journal of the Society for Neuroscience, 31*(11), pp. 4037-4050.

ZHANG, F., SUN, Q., ZHENG, X., LIN, Y., SHANG, W., WANG, A., DUAN, R. and CHI, Z., 2014. Abnormal expression of synaptophysin, SNAP-25, and synaptotagmin 1 in the hippocampus of kainic acid-exposed rats with behavioral deficits. *Cellular and Molecular Neurobiology, 34*(6), pp. 813-824.

ZHOU, T., ZHANG, Z., LIU, J., ZHANG, J. and JIAO, B., 2012. Glycosylation of the sodium channel β4 subunit is developmentally regulated and involves in neuritic degeneration. *International Journal of Biological Sciences, 8*(5), pp. 630-639.

Appendix

Appendix I: The clinical data of patients used in each chapter of the thesis and analytical technique applied

Pt. No	sex	Family history	age at surgery (yrs)	TLE duration (yrs)	sample	Current AED	previous AEDs	Chapter 3		Chapter 4		Chapter 5		Chapter 6
								PCR	WB	PCR	WB	MA	PCR	PCR
Pt. 01	M	No	59	15	TLE-HS TLE-STG	PGB	LMT, LEV,CBZ			X				
Pt. 02	M	No	40	32	TLE-HS TLE-STG	PHT	PHT, LEV,CBZ			X				
Pt. 03	M	No	37	12	TLE-HS TLE-STG	CBZ, LEV	PVA			X				
Pt. 04	M	No	50	48.5	TLE-HS TLE-STG	LEV, ZNS, PGB	CBZ, TPM, PB, VPA,GBP,PHT			X				
Pt. 05	F	NA	34	NA	TLE-HS	NA	NA			X				
Pt. 06	F	NA	44	28	TLE-HS TLE-STG	TPM	LMT,CBZ,LEV CLB	X					X	
Pt. 07	F	No	39	26	TLE-HS TLE-STG	None	CBZ, PHT, LEV LMT			X				
Pt. 08	F	No	26	18	TLE-HS	LEV, PHT, CLB	CBZ,LMT	X	X	X				
Pt. 09	F	No	34	33.5	TLE-HS TLE-STG	LMT,LEV	PB, PHT, CBZ, VPA	X		X		X	X	
Pt. 10	F	No	36	32	TLE-HS	PHT,VPA	PGB, LEV,LM CBZ,TPM,ZNS	X		X			X	

Hippocampal sclerotic specimens (**TLE-HS**) and superior temporal gyrus specimens (**TLE-STG**) obtained from temporal lobe epilepsy patients. Antiepileptic drugs (**AEDs**): **CBZ**, Carbamazepine; **CLB**, Clobazam; **CNP**, Clonazepam; **GBP**, Gabapentin; **LCS**, Lacosamide; **LEV**, Levetiracetam; **LMT**, Lamotrigine; **OXC**, Oxcabazepine; **PB**, Phenobarbital; **PER**, Perampanel; **PGB**, Pregabalin; **PHT**, Phenytoin; **TPM**, Topiramate; **TGB**, Tiagabine; **VPA**, Valproate; **VGB**, Vigabatrin; **ZNS**, Zonisamide. **NA**: not available.

Pt. No	sex	Family history	age at surgery (yrs)	TLE duration (yrs)	sample	Current AED	previous AEDs	Chapter 3		Chapter 4		Chapter 5		Chapter 6
								PCR	WB	PCR	WB	MA	PCR	PCR
Pt. 11	M	No	42	40	TLE-HS	CBZ, ZNS, PHT	PB,VPA,GBP, LEV	X		X			X	
Pt. 12	M	NA	54	NA	TLE-HS	CBZ, ZNS	PB, PHT, PGB, CNP,LEV	X		X			X	
Pt. 13	F	No	24	23	TLE-HS	LCS, LEV	CBZ, LMT	X					X	
Pt. 14	M	NA	42	NA	TLE-HS TLE-STG	CBZ,CNP, ZNS	NA	X					X	
Pt. 15	F	Yes	32	13	TLE-HS TLE-STG	LMT, CBZ, GBP	LEV	X				X	X	
Pt. 16	M	No	25	23	TLE-HS	ZNS, TPM	CBZ,VPA,GBP	X	X				X	
Pt. 17	M	NA	61	NA	TLE-HS TLE-STG	NA	NA	X	X					
Pt. 18	M	Yes	48	47	TLE-HS TLE-STG	PER, CBZ	PHT, LEV,LMT, GBP,TPM,PGB, ZNS	X	X			X	X	X
Pt. 19	F	No	51	40	TLE-HS TLE-STG	LCS, LEV	CBZ, LMT, VPA	X	X			X	X	X
Pt. 20	M	No	30	2	TLE-HS	LEV, TPM, LCS	LMT	X	X					
Pt. 21	M	Yes	32	3	TLE-HS TLE-STG	LMT, OXC	CBZ, LEV	X	X		X		X	

Hippocampal sclerotic specimens (**TLE-HS**) and superior temporal gyrus specimens (**TLE-STG**) obtained from temporal lobe epilepsy patients. Antiepileptic drugs (**AEDs**): **CBZ**, Carbamazepine; **CLB**, Clobazam; **CNP**, Clonazepam; **GBP**, Gabapentin; **LCS**, Lacosamide; **LEV**, Levetiracetam; **LMT**, Lamotrigine; **OXC**, Oxcabazepine; **PB**, Phenobarbital; **PER**, Perampanel; **PGB**, Pregabalin, **PHT**, Phenytoin; **TGB**, Tiagabine; **TPM**, Topiramate; **VGB**, Vigabatrin; **VPA**, Valproate; **ZNS**, Zonisamide.

Pt. No	sex	Family history	age at surgery (yrs)	TLE duration (yrs)	sample	Current AED	previous AEDs	Chapter 3		Chapter 4		Chapter 5		Chapter 6
								PCR	WB	PCR	WB	MA	PCR	PCR
Pt. 22	M	No	51	6	TLE-HS / TLE-STG	NA	NA	X					X	
Pt. 23	M	No	35	18	TLE-HS / TLE-STG	CBZ, LEV	TPM, LMT, VPA	X	X					
Pt. 24	F	No	54	53	TLE-HS / TLE-STG	LMT, PGB	GBP, VPA, PHT, CBZ, PB, LEV, CNP, LCS	X					X	X
Pt. 25	M	No	41	29	TLE-HS / TLE-STG	CBZ, LMT	LEV, ZNS, PGB	X				X	X	X
Pt. 26	F	No	22	13	TLE-HS / TLE-STG	LCS, LMT, TPM, PB	VPA	X				X	X	
Pt. 27	F	No	25	6	TLE-HS / TLE-STG	NA	NA	X	X		X	X	X	X
Pt. 28	F	No	44	22	TLE-HS / TLE-STG	LMT, VPA, PHT	CBZ, LEV, TPM	X					X	
Pt. 29	F	No	24	20	TLE-HS / TLE-STG	LMT	VPA, TPM, CBZ			X	X		X	
Pt. 30	M	NA	35	NA	TLE-HS / TLE-STG	NA	NA				X		X	
Pt. 31	F	NA	44	10	TLE-HS	LCS, LEV, PHT	OXC, LMT				X		X	

Hippocampal sclerotic specimens (**TLE-HS**) and superior temporal gyrus specimens (**TLE-STG**) obtained from temporal lobe epilepsy patients. Antiepileptic drugs (**AEDs**): **CBZ**, Carbamazepine; **CLB**, Clobazam; **CNP**, Clonazepam; **GBP**, Gabapentin; **LCS**, Lacosamide; **LEV**, Levetiracetam; **LMT**, Lamotrigine; **OXC**, Oxcabazepine; **PB**, Phenobarbital; **PER**, Perampanel; **PGB**, Pregabalin; **PHT**, Phenytoin; **TGB**, Tiagabine; **TPM**, Topiramate; **VGB**, Vigabatrin; **VPA**, Valproate; **ZNS**, Zonisamide.

Pt. No	sex	Family history	age at surgery (yrs)	TLE duration (yrs)	sample	Current AED	previous AEDs	Chapter 3		Chapter 4		Chapter 5		Chapter 6
								PCR	WB	PCR	WB	MA	PCR	PCR
Pt. 32	M	NA	32	NA	TLE-HS	NA	NA				X		X	
Pt. 33	M	NA	35	14	TLE-HS	LMT, CLB	VPA, ZNS, CBZ				X		X	
Pt. 34	F	NA	31	NA	TLE-HS TLE-STG	NA	NA							X
Pt. 35	M	NA		NA	TLE-HS TLE-STG	NA	NA							X
Pt. 36	M	NA	42	NA	TLE-HS TLE-STG	NA	NA							X
Pt. 37	F	No	45	16	TLE-HS	None	CBZ,LEV,PGB, CLB	X						X
Pt. 38	M	NA	33	24	TLE-HS	None	CBZ,VPA, LEV	X						X
Pt. 39	M	No	33	31	TLE-HS	LEV, LMT	CBZ,VPA, CLB	X						
Pt. 40	F	NA	22	NA	TLE-HS	CBZ,LMT	CNP,LEV,ZNS	X						
Pt. 41	F	No	39	37	TLE-HS	None	GBP,LEV, LMT	X						
Pt. 42	F	No	29	28	TLE-HS	CBZ,LMT	CLB, LCS, LEV PGB,VPA, ZNS	X						
Pt. 43	M	No	23	16	TLE-HS	LMT	CLB,LEV, TPM	X						
Pt. 44	F	No	27	9	TLE-HS	CBZ, LEV	CLB,LMT, TPM	X						

Hippocampal sclerotic specimens (**TLE-HS**) and superior temporal gyrus specimens (**TLE-STG**) obtained from temporal lobe epilepsy patients. Antiepileptic drugs (**AEDs**): **CBZ**, Carbamazepine; **CLB**, Clobazam; **CNP**, Clonazepam; **GBP**, Gabapentin; **LCS**, Lacosamide; **LEV**, Levetiracetam; **LMT**, Lamotrigine; **OXC**, Oxcabazepine; **PB**, Phenobarbital; **PER**, Perampanel; **PGB**, Pregabalin; **PHT**, Phenytoin; **TGB**, Tiagabine; **TPM**, Topiramate; **VGB**, Vigabatrin; **VPA**, Valproate; **ZNS**, Zonisamide.

Pt. No	sex	Family history	age at surgery (yrs)	TLE duration (yrs)	sample	Current AED	previous AEDs	Chapter 3		Chapter 4		Chapter 5		Chapter 6
								PCR	WB	PCR	WB	MA	PCR	PCR
Pt. 45	M	No	31	20	TLE-HS	CBZ,LEV, LCS	PGB, VGB	X						
Pt. 46	M	No	48	41	TLE-HS	None	CBZ,LMT, VPA, PHT,VGB, CLB, TPM,TGB	X						
Pt. 47	M	NA	48	NA	TLE-HS	LEV, VPA	OXC	X						
Pt. 48	F	NA	44	NA	TLE-HS	PGB,VPA	LEV, LMT	X						
Pt. 49	M	No	63	46	TLE-HS	LEV,CLB	VPA,VGB, PB,ZNS	X						

Hippocampal sclerotic specimens (**TLE-HS**) and superior temporal gyrus specimens (**TLE-STG**) obtained from temporal lobe epilepsy patients. Antiepileptic drugs (**AEDs**): **CBZ**, Carbamazepine; **CLB**, Clobazam; **CNP**, Clonazepam; **GBP**, Gabapentin; **LCS**, Lacosamide; **LEV**, Levetiracetam; **LMT**, Lamotrigine; **OXC**, Oxcabazepine; **PB**, Phenobarbital; **PER**, Perampanel; **PGB**, Pregabalin, **PHT**, Phenytoin; **TGB**, Tiagabine; **TPM**, Topiramate; **VGB**, Vigabatrin; **VPA**, Valproate; **ZNS**, Zonisamide.

Appendix II: Regression analysis between the age at death, post-mortem interval and GABA$_B$ subunits expression:
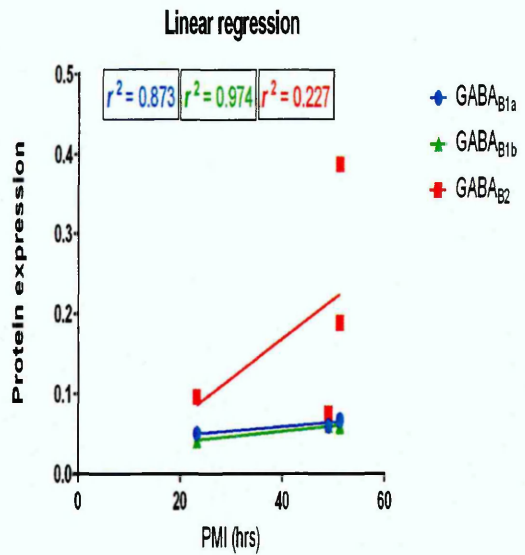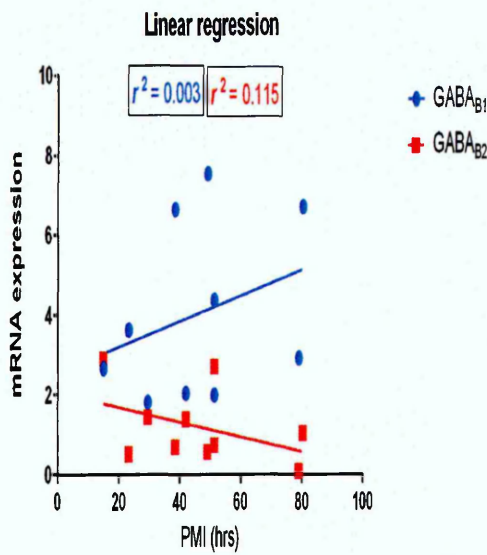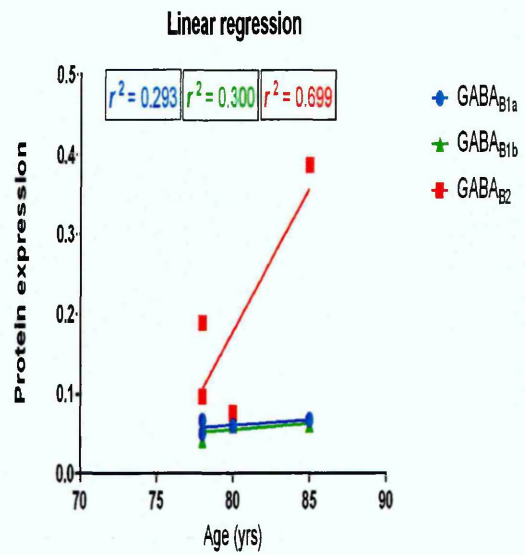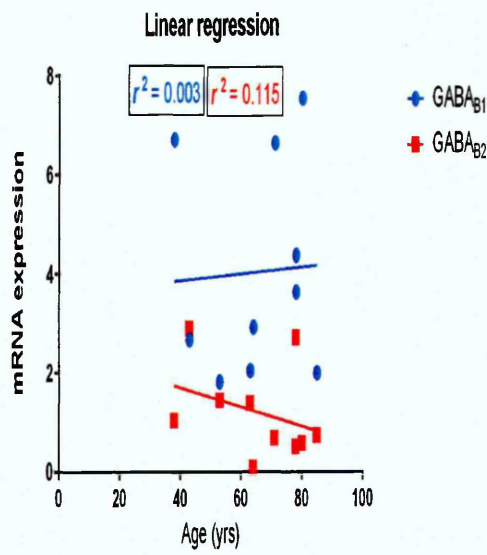
Appendix III: Suppliers:

Abcam, 330 Cambridge Science Park, Cambridge, CB4 0FL, UK; **Agilent Technologies**, 610 Wharfedale Road, IQ Winnersh, Wokingham, Berkshire, RG41 5TP, UK; **Applied Biosystems,** Lingley House, 120 Birchwood Boulevard, Warrington, WA3 7QH, UK; **Cell Signaling Technology, Inc**. 3 Trask Lane, Danvers, MA, 01923, USA; **Fisher Scientific Inc,** Bishop Meadow Rd., Loughborough, Leicestershire, LE11 5RG, UK; **Invitrogen,** 3 Fountain Drive, Inchinnan Business Park, Paisley, PA4 9RF, UK; **LI-COR Biotechnology (UK) Ltd**, St. John's Innovation Centre, Cowley Road, Cambridge, CB4 0WS, UK; **Life Technologies Ltd.**, (Invitrogen, Arcturus) 3 Fountain Drive, Inchinnan Business Park, Paisley, PA4 9RF, UK; **Merck Millipore® (UK) Limited**, Suite 21, Building 6, Croxley Green Business Park, Watford, Hertfordshire, WD18 8YH, UK; **New England BioLab ,** 75-77 Knowl Piece, Wilbury Way, Hitchin, Herts, SG4 0TY, UK; **Promega UK Ltd,** Delta House, Southampton Science Park, Southampton, Hampshire, SO16 7NS, UK; **QIAGEN Ltd**, Skelton House, Lloyd Street North, Manchester, M15 6SH, UK; **Santa Cruz Biotechnology, Inc.,** Bergheimer Str. 89-2, 69115, Heidelberg, Germany; **Sigma-Aldrich**, The Old Brickyard, New Road, Gillingham, Dorset, SP8 4XT, UK; **STARLAB (UK), Ltd,** 5 Tanners Drive, Blakelands, Milton Keynes, MK14 5BU, UK.

Appendix IV: Functional Annotation Clustering analysis of both up and down differentially regulated genes:

Annotation Cluster 1	Enrichment Score: 6.718867155915662		
Category	Term	Count	P-Value
SP_PIR_KEYWORDS	signal	97	4.44E-09
SP_PIR_KEYWORDS	disulfide bond	90	4.90E-09
UP_SEQ_FEATURE	signal peptide	97	6.18E-09
UP_SEQ_FEATURE	disulfide bond	87	1.20E-08
UP_SEQ_FEATURE	glycosylation site:N-linked (GlcNAc...)	98	1.72E-04
SP_PIR_KEYWORDS	glycoprotein	101	1.76E-04
Annotation Cluster 2	Enrichment Score: 5.9600103646605636		
Category	Term	Count	P-Value
SP_PIR_KEYWORDS	signal	97	4.44E-09
UP_SEQ_FEATURE	signal peptide	97	6.18E-09
SP_PIR_KEYWORDS	Secreted	55	2.51E-06
GOTERM_CC_FAT	GO:0044421~extracellular region part	39	3.49E-06
GOTERM_CC_FAT	GO:0005576~extracellular region	64	4.44E-06
GOTERM_MF_FAT	GO:0005125~cytokine activity	15	1.02E-05
SP_PIR_KEYWORDS	cytokine	14	1.15E-05
GOTERM_CC_FAT	GO:0005615~extracellular space	30	1.67E-05
Annotation Cluster 3	Enrichment Score: 5.509099942728049		
Category	Term	Count	P-Value
GOTERM_BP_FAT	GO:0006954~inflammatory response	22	8.58E-07
GOTERM_BP_FAT	GO:0006952~defense response	31	1.59E-06
GOTERM_BP_FAT	GO:0009611~response to wounding	26	2.18E-05
Annotation Cluster 4	Enrichment Score: 3.785753187273131		
Category	Term	Count	P-Value
GOTERM_BP_FAT	GO:0007610~behaviour	27	8.00E-07
GOTERM_BP_FAT	GO:0006954~inflammatory response	22	8.58E-07
SP_PIR_KEYWORDS	inflammation	7	2.79E-06
GOTERM_MF_FAT	GO:0005125~cytokine activity	15	1.02E-05
SP_PIR_KEYWORDS	cytokine	14	1.15E-05
KEGG_PATHWAY	hsa04060:Cytokine-cytokine receptor interaction	18	1.21E-05
GOTERM_CC_FAT	GO:0005615~extracellular space	30	1.67E-05
PIR_SUPERFAMILY	PIRSF500569:macrophage inflammatory protein 1, alpha/beta types	4	2.97E-05
SP_PIR_KEYWORDS	inflammatory response	9	4.27E-05
SP_PIR_KEYWORDS	chemotaxis	8	1.96E-04
GOTERM_BP_FAT	GO:0006935~chemotaxis	12	2.17E-04

Category	Term	Count	P-Value
GOTERM_BP_FAT	GO:0042330~taxis	12	2.17E-04
INTERPRO	IPR001811:Small chemokine, interleukin-8-like	6	6.40E-04
GOTERM_BP_FAT	GO:0007626~locomotory behaviour	15	6.84E-04
INTERPRO	IPR000827:Small chemokine, C-C group, conserved site	5	7.99E-04
SMART	SM00199:SCY	6	9.42E-04
PIR_SUPERFAMILY	PIRSF001950:small inducible chemokine, C/CC types	5	9.63E-04
GOTERM_MF_FAT	GO:0008009~chemokine activity	6	0.001292
GOTERM_MF_FAT	GO:0042379~chemokine receptor binding	6	0.001721
GOTERM_BP_FAT	GO:0006928~cell motion	18	0.008276
GOTERM_BP_FAT	GO:0019079~viral genome replication	3	0.035438
GOTERM_BP_FAT	GO:0019058~viral infectious cycle	4	0.046561
Annotation Cluster 5	**Enrichment Score: 2.8189143497033533**		
Category	Term	Count	P-Value
GOTERM_BP_FAT	GO:0007218~neuropeptide signalling pathway	10	6.13E-05
INTERPRO	IPR009443:Nuclear pore complex interacting	4	9.54E-05
INTERPRO	IPR000203:GPS	4	0.0269
SMART	SM00303:GPS	4	0.033711
Annotation Cluster 6	**Enrichment Score: 2.7386591027193132**		
Category	Term	Count	P-Value
GOTERM_BP_FAT	GO:0009991~response to extracellular stimulus	16	1.77E-05
GOTERM_BP_FAT	GO:0010033~response to organic substance	28	4.89E-04
GOTERM_BP_FAT	GO:0031667~response to nutrient levels	12	0.001253
GOTERM_BP_FAT	GO:0007584~response to nutrient	10	0.001302
GOTERM_BP_FAT	GO:0033273~response to vitamin	7	0.001463
GOTERM_BP_FAT	GO:0009725~response to hormone stimulus	17	0.001567
GOTERM_BP_FAT	GO:0009719~response to endogenous stimulus	18	0.001678
GOTERM_BP_FAT	GO:0048545~response to steroid hormone stimulus	11	0.003416
GOTERM_BP_FAT	GO:0051384~response to glucocorticoid stimulus	7	0.003433
GOTERM_BP_FAT	GO:0031960~response to corticosteroid stimulus	7	0.005246

Category	Term	Count	P-Value
GOTERM_BP_FAT	GO:0043434~response to peptide hormone stimulus	9	0.008606
GOTERM_BP_FAT	GO:0043627~response to estrogen stimulus	6	0.047747
Annotation Cluster 7	**Enrichment Score: 2.653103007394828**		
Category	Term	Count	P-Value
GOTERM_BP_FAT	GO:0045944~positive regulation of transcription from RNA polymerase II promoter	20	7.48E-05
GOTERM_BP_FAT	GO:0045893~positive regulation of transcription, DNA-dependent	21	6.86E-04
GOTERM_BP_FAT	GO:0051254~positive regulation of RNA metabolic process	21	7.68E-04
GOTERM_BP_FAT	GO:0010557~positive regulation of macromolecule biosynthetic process	25	0.001337
GOTERM_BP_FAT	GO:0010628~positive regulation of gene expression	23	0.001422
GOTERM_BP_FAT	GO:0045941~positive regulation of transcription	22	0.002233
GOTERM_BP_FAT	GO:0051173~positive regulation of nitrogen compound metabolic process	24	0.0024
GOTERM_BP_FAT	GO:0031328~positive regulation of cellular biosynthetic process	25	0.002479
GOTERM_BP_FAT	GO:0009891~positive regulation of biosynthetic process	25	0.002967
GOTERM_BP_FAT	GO:0010604~positive regulation of macromolecule metabolic process	29	0.002998
GOTERM_BP_FAT	GO:0045935~positive regulation of nucleobase, nucleoside, nucleotide and nucleic acid metabolic process	23	0.003427
GOTERM_BP_FAT	GO:0051094~positive regulation of developmental process	13	0.006331
GOTERM_BP_FAT	GO:0045597~positive regulation of cell differentiation	11	0.0114
GOTERM_BP_FAT	GO:0006357~regulation of transcription from RNA polymerase II promoter	22	0.032847
Annotation Cluster 8	**Enrichment Score: 2.3801544678193176**		
Category	Term	Count	P-Value
GOTERM_MF_FAT	GO:0008092~cytoskeletal protein binding	20	0.001675
GOTERM_MF_FAT	GO:0003779~actin binding	15	0.002121
GOTERM_CC_FAT	GO:0015629~actin cytoskeleton	13	0.00362

SP_PIR_KEYWORDS	actin-binding	10	0.023435
	Enrichment Score: 2.243004058494122		
Category	Term	Count	P-Value
GOTERM_BP_FAT	GO:0031032~actomyosin structure organization	6	1.55E-04
GOTERM_BP_FAT	GO:0010927~cellular component assembly involved in morphogenesis	5	0.004459
GOTERM_BP_FAT	GO:0030239~myofibril assembly	4	0.006774
GOTERM_BP_FAT	GO:0055002~striated muscle cell development	5	0.016242
GOTERM_BP_FAT	GO:0055001~muscle cell development	5	0.020798
GOTERM_BP_FAT	GO:0048738~cardiac muscle tissue development	5	0.022048
Annotation Cluster 10	**Enrichment Score: 2.22151090895036**		
Category	Term	Count	P-Value
GOTERM_BP_FAT	GO:0007178~transmembrane receptor protein serine/threonine kinase signalling pathway	8	0.00325
GOTERM_BP_FAT	GO:0007179~transforming growth factor beta receptor signalling pathway	6	0.005287
GOTERM_BP_FAT	GO:0007167~enzyme linked receptor protein signalling pathway	14	0.012601
Annotation Cluster 11	**Enrichment Score: 2.204384901915561**		
Category	Term	Count	P-Value
GOTERM_BP_FAT	GO:0044057~regulation of system process	16	7.51E-04
GOTERM_BP_FAT	GO:0048168~regulation of neuronal synaptic plasticity	5	0.004459
GOTERM_BP_FAT	GO:0007611~learning or memory	8	0.004912
GOTERM_BP_FAT	GO:0051969~regulation of transmission of nerve impulse	9	0.006569
GOTERM_BP_FAT	GO:0048167~regulation of synaptic plasticity	6	0.006948
GOTERM_BP_FAT	GO:0031644~regulation of neurological system process	9	0.008289
GOTERM_BP_FAT	GO:0050804~regulation of synaptic transmission	8	0.014272
GOTERM_BP_FAT	GO:0030902~hindbrain development	5	0.026068
Annotation Cluster 12	**Enrichment Score: 2.2042064385802975**		
Category	Term	Count	P-Value
GOTERM_CC_FAT	GO:0031982~vesicle	24	0.00236
GOTERM_CC_FAT	GO:0031410~cytoplasmic vesicle	23	0.00297

Category	Term	Count	P-Value
GOTERM_CC_FAT	GO:0031988~membrane-bounded vesicle	20	0.00729
GOTERM_CC_FAT	GO:0016023~cytoplasmic membrane-bounded vesicle	19	0.01115
GOTERM_CC_FAT	GO:0030141~secretory granule	9	0.01668
Annotation Cluster 13	Enrichment Score: 2.1989123311431285		
Category	Term	Count	P-Value
GOTERM_MF_FAT	GO:0030246~carbohydrate binding	16	0.00179
GOTERM_MF_FAT	GO:0005539~glycosaminoglycan binding	9	0.00355
GOTERM_MF_FAT	GO:0030247~polysaccharide binding	9	0.00622
GOTERM_MF_FAT	GO:0001871~pattern binding	9	0.00622
GOTERM_MF_FAT	GO:0008201~heparin binding	7	0.01012
GOTERM_BP_FAT	GO:0045785~positive regulation of cell adhesion	5	0.02608
Annotation Cluster 14	Enrichment Score: 2.1739754579500272		
Category	Term	Count	P-Value
GOTERM_BP_FAT	GO:0003012~muscle system process	13	7.85E-05
GOTERM_BP_FAT	GO:0006936~muscle contraction	12	1.47E-04
GOTERM_CC_FAT	GO:0015629~actin cytoskeleton	13	0.00362
GOTERM_CC_FAT	GO:0044449~contractile fibre part	8	0.00433
GOTERM_CC_FAT	GO:0043292~contractile fibre	8	0.00636
GOTERM_BP_FAT	GO:0006941~striated muscle contraction	5	0.01069
SP_PIR_KEYWORDS	muscle protein	5	0.01785
GOTERM_BP_FAT	GO:0048738~cardiac muscle tissue development	5	0.02208
GOTERM_CC_FAT	GO:0005865~striated muscle thin filament	3	0.02929
GOTERM_CC_FAT	GO:0030017~sarcomere	6	0.03235
GOTERM_MF_FAT	GO:0008307~structural constituent of muscle	4	0.03837
SP_PIR_KEYWORDS	Cardiomyopathy	4	0.04588
Annotation Cluster 15	Enrichment Score: 2.0121134142077866		
Category	Term	Count	P-Value
GOTERM_BP_FAT	GO:0051591~response to cAMP	6	0.00102
INTERPRO	IPR004827:Basic-leucine zipper (bZIP) transcription factor	5	0.01276
SMART	SM00338:BRLZ	5	0.01708
UP_SEQ_FEATURE	domain:Leucine-zipper	6	0.03806
Annotation Cluster 16	Enrichment Score: 2.0057516111940923		
Category	Term	Count	P-Value

Category	Term	Count	P-Value
GOTERM_BP_FAT	GO:0046888~negative regulation of hormone secretion	5	0.00131
GOTERM_BP_FAT	GO:0060341~regulation of cellular localization	12	0.00727
GOTERM_BP_FAT	GO:0051046~regulation of secretion	10	0.01417
GOTERM_BP_FAT	GO:0051048~negative regulation of secretion	5	0.01953
GOTERM_BP_FAT	GO:0046883~regulation of hormone secretion	5	0.03535
Annotation Cluster 17	**Enrichment Score: 1.948891880528446**		
Category	Term	Count	P-Value
GOTERM_BP_FAT	GO:0007626~locomotory behaviour	15	6.84E-04
GOTERM_BP_FAT	GO:0019725~cellular homeostasis	20	0.00127
GOTERM_BP_FAT	GO:0055082~cellular chemical homeostasis	16	0.00557
GOTERM_BP_FAT	GO:0030003~cellular cation homeostasis	12	0.00868
GOTERM_BP_FAT	GO:0030005~cellular di-, tri-valent inorganic cation homeostasis	11	0.01075
GOTERM_BP_FAT	GO:0006873~cellular ion homeostasis	15	0.01124
GOTERM_BP_FAT	GO:0042592~homeostatic process	24	0.01445
GOTERM_BP_FAT	GO:0055066~di-, tri-valent inorganic cation homeostasis	11	0.01499
GOTERM_BP_FAT	GO:0048878~chemical homeostasis	18	0.01665
GOTERM_BP_FAT	GO:0055080~cation homeostasis	12	0.01947
GOTERM_BP_FAT	GO:0006874~cellular calcium ion homeostasis	9	0.02236
GOTERM_BP_FAT	GO:0050801~ion homeostasis	15	0.02263
GOTERM_BP_FAT	GO:0055074~calcium ion homeostasis	9	0.02579
GOTERM_BP_FAT	GO:0006875~cellular metal ion homeostasis	9	0.03167
GOTERM_BP_FAT	GO:0055065~metal ion homeostasis	9	0.03981
Annotation Cluster 18	**Enrichment Score: 1.9260615339996585**		
Category	Term	Count	P-Value
GOTERM_BP_FAT	GO:0032101~regulation of response to external stimulus	9	0.01037
GOTERM_BP_FAT	GO:0048585~negative regulation of response to stimulus	7	0.01137
GOTERM_BP_FAT	GO:0032102~negative regulation of response to external stimulus	5	0.01422
Annotation Cluster 19	**Enrichment Score: 1.9099746554025676**		
Category	Term	Count	P-Value
GOTERM_CC_FAT	GO:0031226~intrinsic to plasma membrane	37	0.00206

Category	Term	Count	P-Value
GOTERM_CC_FAT	GO:0044459~plasma membrane part	58	0.00249
GOTERM_CC_FAT	GO:0005887~integral to plasma membrane	35	0.00473
SP_PIR_KEYWORDS	transmembrane protein	20	0.01176
SP_PIR_KEYWORDS	receptor	39	0.01459
UP_SEQ_FEATURE	topological domain:Extracellular	60	0.021956
GOTERM_CC_FAT	GO:0005886~plasma membrane	82	0.03896
UP_SEQ_FEATURE	topological domain:Cytoplasmic	70	0.042817
SP_PIR_KEYWORDS	cell membrane	48	0.04356
Annotation Cluster 20	**Enrichment Score: 1.8740906263654176**		
Category	Term	Count	P-Value
GOTERM_CC_FAT	GO:0000267~cell fraction	33	0.003835
GOTERM_CC_FAT	GO:0005624~membrane fraction	24	0.020742
GOTERM_CC_FAT	GO:0005626~insoluble fraction	24	0.030003
Annotation Cluster 21	**Enrichment Score: 1.8540373271456263**		
Category	Term	Count	P-Value
GOTERM_MF_FAT	GO:0022838~substrate specific channel activity	16	0.005108
GOTERM_MF_FAT	GO:0015267~channel activity	16	0.006951
GOTERM_MF_FAT	GO:0022803~passive transmembrane transporter activity	16	0.007114
GOTERM_MF_FAT	GO:0005216~ion channel activity	14	0.020878
SP_PIR_KEYWORDS	ion transport	17	0.034047
SP_PIR_KEYWORDS	ionic channel	11	0.041838
Annotation Cluster 22	**Enrichment Score: 1.8385165551147895**		
Category	Term	Count	P-Value
GOTERM_BP_FAT	GO:0048754~branching morphogenesis of a tube	6	0.007415
GOTERM_BP_FAT	GO:0001763~morphogenesis of a branching structure	6	0.012631
GOTERM_BP_FAT	GO:0035239~tube morphogenesis	7	0.032577
Annotation Cluster 23	**Enrichment Score: 1.8029687642885472**		
Category	Term	Count	P-Value
GOTERM_BP_FAT	GO:0010035~response to inorganic substance	11	0.005412
GOTERM_BP_FAT	GO:0000302~response to reactive oxygen species	6	0.013332
GOTERM_BP_FAT	GO:0034614~cellular response to reactive oxygen species	4	0.018276
GOTERM_BP_FAT	GO:0034599~cellular response to oxidative stress	4	0.046561
Annotation Cluster 24	**Enrichment Score: 1.7646634444180525**		
Category	Term	Count	P-Value

INTERPRO	IPR013151:Immunoglobulin	10	0.008101
INTERPRO	IPR003598:Immunoglobulin subtype 2	10	0.008883
INTERPRO	IPR003599:Immunoglobulin subtype	13	0.011646
SP_PIR_KEYWORDS	Immunoglobulin domain	16	0.012886
INTERPRO	IPR013783:Immunoglobulin-like fold	18	0.014611
SMART	SM00408:IGc2	10	0.014824
SMART	SM00409:IG	13	0.021059
INTERPRO	IPR007110:Immunoglobulin-like	16	0.025599
UP_SEQ_FEATURE	domain:Ig-like C2-type 1	8	0.041802
UP_SEQ_FEATURE	domain:Ig-like C2-type 2	8	0.042801
Annotation Cluster 25	**Enrichment Score: 1.746953414787051**		
Category	Term	Count	P-Value
SP_PIR_KEYWORDS	postsynaptic cell membrane	7	0.010372
GOTERM_CC_FAT	GO:0045211~postsynaptic membrane	8	0.011308
GOTERM_CC_FAT	GO:0030054~cell junction	16	0.048969
Annotation Cluster 26	**Enrichment Score: 1.6895442129153926**		
Category	Term	Count	P-Value
GOTERM_CC_FAT	GO:0000323~lytic vacuole	10	0.014577
GOTERM_CC_FAT	GO:0005764~lysosome	10	0.014577
GOTERM_CC_FAT	GO:0005773~vacuole	10	0.040181
Annotation Cluster 27	**Enrichment Score: 1.6785307237329645**		
Category	Term	Count	P-Value
GOTERM_BP_FAT	GO:0051726~regulation of cell cycle	15	0.004006
GOTERM_BP_FAT	GO:0042325~regulation of phosphorylation	17	0.014868
GOTERM_BP_FAT	GO:0019220~regulation of phosphate metabolic process	17	0.020987
GOTERM_BP_FAT	GO:0051174~regulation of phosphorus metabolic process	17	0.020987
GOTERM_BP_FAT	GO:0007243~protein kinase cascade	14	0.022755
GOTERM_BP_FAT	GO:0045860~positive regulation of protein kinase activity	10	0.025141
GOTERM_BP_FAT	GO:0033674~positive regulation of kinase activity	10	0.030589
GOTERM_BP_FAT	GO:0051347~positive regulation of transferase activity	10	0.037925
GOTERM_BP_FAT	GO:0001932~regulation of protein amino acid phosphorylation	8	0.044919
Annotation Cluster 28	**Enrichment Score: 1.5955104866674612**		
Category	Term	Count	P-Value
GOTERM_BP_FAT	GO:0001568~blood vessel development	11	0.017467
GOTERM_BP_FAT	GO:0001944~vasculature	11	0.020372

Category	Term	Count	P-Value
	development		
GOTERM_BP_FAT	GO:0048514~blood vessel morphogenesis	9	0.045942

Annotation Cluster 29	Enrichment Score: 1.5808777697129992		
Category	Term	Count	P-Value
BIOCARTA	h_bbcellPathway: Bystander B Cell Activation	3	0.015545
KEGG_PATHWAY	hsa05330:Allograft rejection	4	0.033818
BIOCARTA	h_asbcellPathway: Antigen Dependent B Cell Activation	3	0.034406
Annotation Cluster 30	Enrichment Score: 1.560897193242292		
Category	Term	Count	P-Value
GOTERM_BP_FAT	GO:0002521~leukocyte differentiation	8	0.011799
GOTERM_BP_FAT	GO:0045321~leukocyte activation	10	0.039338
GOTERM_BP_FAT	GO:0001775~cell activation	11	0.044736
Annotation Cluster 31	Enrichment Score: 1.5248021584253257		
Category	Term	Count	P-Value
GOTERM_BP_FAT	GO:0019319~hexose biosynthetic process	4	0.019959
GOTERM_BP_FAT	GO:0006006~glucose metabolic process	8	0.025436
GOTERM_BP_FAT	GO:0046364~monosaccharide biosynthetic process	4	0.031795
GOTERM_BP_FAT	GO:0046165~alcohol biosynthetic process	4	0.049299
Annotation Cluster 32	Enrichment Score: 1.4727030120557136		
Category	Term	Count	P-Value
GOTERM_BP_FAT	GO:0051249~regulation of lymphocyte activation	8	0.02168
GOTERM_BP_FAT	GO:0002694~regulation of leukocyte activation	8	0.037228
GOTERM_BP_FAT	GO:0050865~regulation of cell activation	8	0.047311
Annotation Cluster 33	Enrichment Score: 1.466199596760949		
Category	Term	Count	P-Value
GOTERM_BP_FAT	GO:0043065~positive regulation of apoptosis	15	0.03288
GOTERM_BP_FAT	GO:0043068~positive regulation of programmed cell death	15	0.034281
GOTERM_BP_FAT	GO:0010942~positive regulation of cell death	15	0.035433

Annotation Cluster 34	Enrichment Score: 1.3847563772782288		
Category	Term	Count	P-Value
KEGG_PATHWAY	hsa05330:Allograft rejection	4	0.033818
KEGG_PATHWAY	hsa05332:Graft-versus-host disease	4	0.04149
KEGG_PATHWAY	hsa04940:Type I diabetes mellitus	4	0.049962

Appendix V: Functional Annotation Clustering analysis of up regulated genes:

Annotation Cluster 1	Enrichment Score: 7.48		
Category	Term	Count	P Value
SP_PIR_KEYWORDS	signal	82	4.21E-12
UP_SEQ_FEATURE	signal peptide	82	5.88E-12
SP_PIR_KEYWORDS	disulfide bond	72	5.60E-10
UP_SEQ_FEATURE	disulfide bond	70	1.02E-09
SP_PIR_KEYWORDS	Secreted	50	2.25E-09
GOTERM_CC_FAT	GO:0005576~extracellular region	58	3.76E-09
GOTERM_CC_FAT	GO:0044421~extracellular region part	37	6.99E-09
GOTERM_CC_FAT	GO:0005615~extracellular space	28	2.73E-07
UP_SEQ_FEATURE	glycosylation site:N-linked (GlcNAc...)	74	1.15E-04
SP_PIR_KEYWORDS	glycoprotein	76	1.29E-04
UP_SEQ_FEATURE	topological domain:Cytoplasmic	54	0.01577
Annotation Cluster 2	Enrichment Score: 4.12		
Category	Term	Count	P Value
GOTERM_BP_FAT	GO:0006952~defense response	27	2.55E-07
GOTERM_BP_FAT	GO:0006954~inflammatory response	19	4.62E-07
GOTERM_BP_FAT	GO:0009611~response to wounding	23	3.13E-06
SP_PIR_KEYWORDS	inflammatory response	9	3.36E-06
GOTERM_BP_FAT	GO:0007610~behaviour	21	6.08E-06
KEGG_PATHWAY	hsa04060:Cytokine-cytokine receptor interaction	16	7.48E-06
GOTERM_MF_FAT	GO:0005125~cytokine activity	13	8.07E-06
SP_PIR_KEYWORDS	inflammation	6	9.40E-06
SP_PIR_KEYWORDS	cytokine	12	1.01E-05
PIR_SUPERFAMILY	PIRSF500569:macrophage inflammatory protein 1, alpha/beta types	4	1.23E-05
INTERPRO	IPR001811:Small chemokine, interleukin-8-like	6	1.31E-04
SMART	SM00199:SCY	6	1.56E-04
SP_PIR_KEYWORDS	chemotaxis	7	2.01E-04

Category	Term	Count	P Value
INTERPRO	IPR000827:Small chemokine, C-C group, conserved site	5	2.17E-04
GOTERM_MF_FAT	GO:0008009~chemokine activity	6	2.97E-04
PIR_SUPERFAMILY	PIRSF001950:small inducible chemokine, C/CC types	5	3.18E-04
GOTERM_BP_FAT	GO:0042330~taxis	10	3.38E-04
GOTERM_BP_FAT	GO:0006935~chemotaxis	10	3.38E-04
GOTERM_MF_FAT	GO:0042379~chemokine receptor binding	6	4.00E-04
GOTERM_BP_FAT	GO:0006928~cell motion	16	0.00213
GOTERM_BP_FAT	GO:0007626~locomotory behaviour	10	0.01274
GOTERM_BP_FAT	GO:0019079~viral genome replication	3	0.01948
GOTERM_BP_FAT	GO:0019058~viral infectious cycle	4	0.02051
Annotation Cluster 3	**Enrichment Score: 3.29**		
Category	Term	Count	*P* Value
GOTERM_BP_FAT	GO:0009991~response to extracellular stimulus	14	9.74E-06
GOTERM_BP_FAT	GO:0010033~response to organic substance	25	4.39E-05
GOTERM_BP_FAT	GO:0009725~response to hormone stimulus	16	1.49E-04
GOTERM_BP_FAT	GO:0033273~response to vitamin	7	2.69E-04
GOTERM_BP_FAT	GO:0048545~response to steroid hormone stimulus	11	2.97E-04
GOTERM_BP_FAT	GO:0031667~response to nutrient levels	11	3.64E-04
GOTERM_BP_FAT	GO:0009719~response to endogenous stimulus	16	4.28E-04
GOTERM_BP_FAT	GO:0007584~response to nutrient	9	6.52E-04
GOTERM_BP_FAT	GO:0051384~response to glucocorticoid stimulus	7	6.66E-04
GOTERM_BP_FAT	GO:0031960~response to corticosteroid stimulus	7	0.00105
GOTERM_BP_FAT	GO:0043434~response to peptide hormone stimulus	9	0.00121
GOTERM_BP_FAT	GO:0043627~response to stimulus	6	0.01427
GOTERM_BP_FAT	GO:0032570~response to progesterone stimulus	3	0.02977
Annotation Cluster 4	**Enrichment Score: 2.64**		
Category	Term	Count	*P* Value
GOTERM_BP_FAT	GO:0009628~response to abiotic stimulus	15	5.11E-04

GOTERM_BP_FAT	GO:0009612~response to mechanical stimulus	6	9.60E-04
GOTERM_BP_FAT	GO:0014070~response to organic cyclic substance	7	0.00617
GOTERM_BP_FAT	GO:0042493~response to drug	9	0.00946
Annotation Cluster 5	**Enrichment Score: 2.54**		
Category	Term	Count	*P* Value
SP_PIR_KEYWORDS	cleavage on pair of basic residues	13	9.07E-05
GOTERM_BP_FAT	GO:0007218~neuropeptide signalling pathway	7	0.00167
GOTERM_MF_FAT	GO:0005179~hormone activity	6	0.01278
GOTERM_MF_FAT	GO:0005184~neuropeptide hormone activity	3	0.03487
Annotation Cluster 6	**Enrichment Score: 2.53**		
Category	Term	Count	*P* Value
GOTERM_MF_FAT	GO:0030246~carbohydrate binding	14	6.59E-04
GOTERM_MF_FAT	GO:0005539~glycosaminoglycan binding	8	0.00221
GOTERM_MF_FAT	GO:0030247~polysaccharide binding	8	0.00376
GOTERM_MF_FAT	GO:0001871~pattern binding	8	0.00376
GOTERM_MF_FAT	GO:0008201~heparin binding	6	0.01056
Annotation Cluster 7	**Enrichment Score: 2.32**		
Category	Term	Count	*P* Value
BIOCARTA	h_Ccr5Pathway:Pertussis toxin-insensitive CCR5 Signalling in Macrophage	5	1.01E-04
GOTERM_BP_FAT	GO:0007179~transforming growth factor beta receptor signalling pathway	5	0.00893
GOTERM_BP_FAT	GO:0007178~transmembrane receptor protein serine/threonine kinase signalling pathway	6	0.01322
GOTERM_BP_FAT	GO:0007167~enzyme linked receptor protein signalling pathway	10	0.04433
Annotation Cluster 8	**Enrichment Score: 2.32**		
Category	Term	Count	*P* Value
GOTERM_CC_FAT	GO:0031982~vesicle	20	0.00128
GOTERM_CC_FAT	GO:0031410~cytoplasmic vesicle	19	0.00196
GOTERM_CC_FAT	GO:0031988~membrane-bounded vesicle	16	0.00791
GOTERM_CC_FAT	GO:0030141~secretory granule	8	0.0097
GOTERM_CC_FAT	GO:0016023~cytoplasmic membrane-bounded vesicle	15	0.0137

Annotation Cluster 9	Enrichment Score: 2.16		
Category	Term	Count	*P* Value
GOTERM_BP_FAT	GO:0045944~positive regulation of transcription from RNA polymerase II promoter	15	5.54E-04
GOTERM_BP_FAT	GO:0045597~positive regulation of cell differentiation	10	0.00413
GOTERM_BP_FAT	GO:0051094~positive regulation of developmental process	11	0.00476
GOTERM_BP_FAT	GO:0045893~positive regulation of transcription, DNA-dependent	15	0.00566
GOTERM_BP_FAT	GO:0010628~positive regulation of gene expression	17	0.00582
GOTERM_BP_FAT	GO:0051254~positive regulation of RNA metabolic process	15	0.00608
GOTERM_BP_FAT	GO:0010604~positive regulation of macromolecule metabolic process	22	0.00635
GOTERM_BP_FAT	GO:0051173~positive regulation of nitrogen compound metabolic process	18	0.00683
GOTERM_BP_FAT	GO:0010557~positive regulation of macromolecule biosynthetic process	18	0.00791
GOTERM_BP_FAT	GO:0045941~positive regulation of transcription	16	0.01015
GOTERM_BP_FAT	GO:0045935~positive regulation of nucleobase, nucleoside, nucleotide and nucleic acid metabolic process	17	0.01115
GOTERM_BP_FAT	GO:0031328~positive regulation of cellular biosynthetic process	18	0.01217
GOTERM_BP_FAT	GO:0009891~positive regulation of biosynthetic process	18	0.01387
GOTERM_MF_FAT	GO:0043566~structure-specific DNA binding	6	0.0393
Annotation Cluster 10	Enrichment Score: 2.08		
Category	Term	Count	*P* Value
GOTERM_BP_FAT	GO:0009612~response to mechanical stimulus	6	9.60E-04
INTERPRO	IPR004827:Basic-leucine zipper (bZIP) transcription factor	5	0.00386
SMART	SM00338:BRLZ	5	0.00444
UP_SEQ_FEATURE	domain:Leucine-zipper	6	0.00993
UP_SEQ_FEATURE	DNA-binding region:Basic motif	7	0.01238
GOTERM_MF_FAT	GO:0043566~structure-specific DNA binding	6	0.0393

Annotation Cluster 11	Enrichment Score: 1.98		
Category	Term	Count	*P* Value
GOTERM_BP_FAT	GO:0019725~cellular homeostasis	16	0.00177
GOTERM_BP_FAT	GO:0042592~homeostatic process	20	0.00673
GOTERM_BP_FAT	GO:0055082~cellular chemical homeostasis	12	0.01492
GOTERM_BP_FAT	GO:0048878~chemical homeostasis	14	0.02279
GOTERM_BP_FAT	GO:0006873~cellular ion homeostasis	11	0.03198
Annotation Cluster 12	Enrichment Score: 1.89		
Category	Term	Count	*P* Value
GOTERM_BP_FAT	GO:0002673~regulation of acute inflammatory response	4	0.00275
GOTERM_BP_FAT	GO:0050727~regulation of inflammatory response	5	0.01989
GOTERM_BP_FAT	GO:0045087~innate immune response	6	0.04024
Annotation Cluster 13	Enrichment Score: 1.83		
Category	Term	Count	*P* Value
GOTERM_BP_FAT	GO:0002521~leukocyte differentiation	8	0.00208
GOTERM_BP_FAT	GO:0030097~hemopoiesis	9	0.0155
GOTERM_BP_FAT	GO:0001775~cell activation	10	0.01672
GOTERM_BP_FAT	GO:0045321~leukocyte activation	9	0.01776
GOTERM_BP_FAT	GO:0046649~lymphocyte activation	8	0.01905
GOTERM_BP_FAT	GO:0048534~hemopoietic or lymphoid organ development	9	0.02591
GOTERM_BP_FAT	GO:0002520~immune system development	9	0.03513
Annotation Cluster 14	Enrichment Score: 1.82		
Category	Term	Count	*P* Value
GOTERM_CC_FAT	GO:0031226~intrinsic to plasma membrane	27	0.00873
GOTERM_CC_FAT	GO:0005887~integral to plasma membrane	26	0.01233
UP_SEQ_FEATURE	topological domain:Cytoplasmic	54	0.01577
UP_SEQ_FEATURE	topological domain:Extracellular	45	0.01772
SP_PIR_KEYWORDS	receptor	29	0.01934
SP_PIR_KEYWORDS	transmembrane protein	15	0.01988
Annotation Cluster 15	Enrichment Score: 1.80		
Category	Term	Count	P Value
GOTERM_BP_FAT	GO:0001568~blood vessel development	10	0.00636

GOTERM_BP_FAT	GO:0001944~vasculature development	10	0.00743
GOTERM_BP_FAT	GO:0048754~branching morphogenesis of a tube	5	0.01177
GOTERM_BP_FAT	GO:0001525~angiogenesis	7	0.01571
GOTERM_BP_FAT	GO:0001763~morphogenesis of a branching structure	5	0.01822
GOTERM_BP_FAT	GO:0048514~blood vessel morphogenesis	8	0.0254
GOTERM_BP_FAT	GO:0035239~tube morphogenesis	6	0.02967
GOTERM_BP_FAT	GO:0007389~pattern specification process	9	0.02971
Annotation Cluster 16	Enrichment Score: 1.68		
Category	Term	Count	*P* Value
INTERPRO	IPR013151:Immunoglobulin	8	0.01173
INTERPRO	IPR003598:Immunoglobulin subtype 2	8	0.01264
SMART	SM00408:IGc2	8	0.0152
INTERPRO	IPR013783:Immunoglobulin-like fold	14	0.01755
SP_PIR_KEYWORDS	Immunoglobulin domain	12	0.02352
INTERPRO	IPR007110:Immunoglobulin-like	12	0.04158
INTERPRO	IPR003599:Immunoglobulin subtype	9	0.04844
Annotation Cluster 17	Enrichment Score: 1.67		
Category	Term	Count	*P* Value
GOTERM_BP_FAT	GO:0019319~hexose biosynthetic process	4	0.00841
GOTERM_BP_FAT	GO:0046364~monosaccharide biosynthetic process	4	0.0137
GOTERM_BP_FAT	GO:0006006~glucose metabolic process	7	0.01811
GOTERM_BP_FAT	GO:0046165~alcohol biosynthetic process	4	0.0218
GOTERM_BP_FAT	GO:0006094~gluconeogenesis	3	0.04498
GOTERM_BP_FAT	GO:0019318~hexose metabolic process	7	0.0475
Annotation Cluster 18	Enrichment Score: 1.65		
Category	Term	Count	*P* Value
GOTERM_BP_FAT	GO:0051249~regulation of lymphocyte activation	8	0.00411
GOTERM_BP_FAT	GO:0002694~regulation of leukocyte activation	8	0.00758
GOTERM_BP_FAT	GO:0050865~regulation of cell activation	8	0.00997
GOTERM_BP_FAT	GO:0050670~regulation of lymphocyte proliferation	5	0.0265

GOTERM_BP_FAT	GO:0070663~regulation of leukocyte proliferation	5	0.02754
GOTERM_BP_FAT	GO:0032944~regulation of mononuclear cell proliferation	5	0.02754
GOTERM_BP_FAT	GO:0050671~positive regulation of lymphocyte proliferation	4	0.03878
GOTERM_BP_FAT	GO:0032946~positive regulation of mononuclear cell proliferation	4	0.04057
GOTERM_BP_FAT	GO:0070665~positive regulation of leukocyte proliferation	4	0.04057
GOTERM_BP_FAT	GO:0051251~positive regulation of lymphocyte activation	5	0.04326
GOTERM_BP_FAT	GO:0002684~positive regulation of immune system process	8	0.04424
Annotation Cluster 19	**Enrichment Score: 1.64**		
Category	Term	Count	P Value
BIOCARTA	h_bbcell Pathway:Bystander B Cell Activation	3	0.00954
KEGG_PATHWAY	hsa05330:Allograft rejection	4	0.01724
KEGG_PATHWAY	hsa05332:Graft-versus-host disease	4	0.02136
BIOCARTA	h_asbcell Pathway:Antigen Dependent B Cell Activation	3	0.02143
GOTERM_CC_FAT	GO:0009897~external side of plasma membrane	7	0.02473
KEGG_PATHWAY	hsa04940:Type I diabetes mellitus	4	0.02597
KEGG_PATHWAY	hsa04672:Intestinal immune network for IgA production	4	0.03863
KEGG_PATHWAY	hsa05320:Autoimmune thyroid disease	4	0.04273
Annotation Cluster 20	**Enrichment Score: 1.55**		
Category	Term	Count	P Value
GOTERM_CC_FAT	GO:0005764~lysosome	8	0.02148
GOTERM_CC_FAT	GO:0000323~lytic vacuole	8	0.02148
GOTERM_CC_FAT	GO:0005773~vacuole	8	0.04882
Annotation Cluster 21	**Enrichment Score: 1.46**		
Category	Term	Count	P Value
GOTERM_BP_FAT	GO:0043065~positive regulation of apoptosis	12	0.0332
GOTERM_BP_FAT	GO:0043068~positive regulation of programmed cell death	12	0.03465
GOTERM_BP_FAT	GO:0010942~positive regulation of cell death	12	0.03565

Appendix VI: Functional Annotation Clustering analysis of down regulated genes:

Annotation Cluster 1	Enrichment Score: 2.85		
Category	Term	Count	*P* Value
GOTERM_MF_FAT	GO:0005516~calmodulin binding	9	4.0E-07
SP_PIR_KEYWORDS	calmodulin-binding	7	2.9E-05
SP_PIR_KEYWORDS	actin binding	5	4.5E-05
GOTERM_BP_FAT	GO:0031032~actomyosin structure organization	4	4.0E-04
GOTERM_MF_FAT	GO:0008092~cytoskeletal protein binding	10	7.7E-04
GOTERM_MF_FAT	GO:0003779~actin binding	8	1.1E-03
GOTERM_CC_FAT	GO:0015629~actin cytoskeleton	7	2.0E-03
SP_PIR_KEYWORDS	actin-binding	6	7.6E-03
GOTERM_CC_FAT	GO:0005856~cytoskeleton	14	1.6E-02
GOTERM_BP_FAT	GO:0030036~actin cytoskeleton organization	5	3.0E-02
GOTERM_BP_FAT	GO:0030029~actin filament-based process	5	3.6E-02
GOTERM_BP_FAT	GO:0044087~regulation of cellular component biogenesis	4	3.7E-02
INTERPRO	IPR001715:Calponin-like actin-binding	3	4.8E-02
Annotation Cluster 2	Enrichment Score: 2.67		
Category	Term	Count	*P* Value
INTERPRO	IPR009443:Nuclear pore complex interacting	4	2.4E-06
INTERPRO	IPR001024:Lipoxygenase, LH2	3	6.3E-03
SMART	SM00308:LH2	3	9.1E-03
INTERPRO	IPR000203:GPS	3	1.5E-02
SMART	SM00303:GPS	3	2.2E-02
Annotation Cluster 3	Enrichment Score: 2.50		
Category	Term	Count	*P* Value
GOTERM_CC_FAT	GO:0045211~postsynaptic membrane	6	5.2E-04
GOTERM_CC_FAT	GO:0030054~cell junction	10	9.2E-04
GOTERM_CC_FAT	GO:0044456~synapse part	7	1.3E-03
SP_PIR_KEYWORDS	postsynaptic cell membrane	5	2.2E-03
SP_PIR_KEYWORDS	cell junction	8	3.6E-03
SP_PIR_KEYWORDS	synapse	6	4.1E-03
GOTERM_CC_FAT	GO:0014069~postsynaptic density	4	5.1E-03
GOTERM_CC_FAT	GO:0045202~synapse	7	7.9E-03
GOTERM_CC_FAT	GO:0030425~dendrite	5	8.5E-03
GOTERM_CC_FAT	GO:0043197~dendritic spine	3	1.5E-02

Annotation Cluster 4	Enrichment Score: 2.40		
Category	Term	Count	*P* Value
GOTERM_CC_FAT	GO:0015629~actin cytoskeleton	7	0.0020
GOTERM_CC_FAT	GO:0044449~contractile fibre part	5	0.0023
GOTERM_CC_FAT	GO:0043292~contractile fibre	5	0.0030
SP_PIR_KEYWORDS	muscle protein	4	0.0033
GOTERM_BP_FAT	GO:0006936~muscle contraction	5	0.0081
GOTERM_BP_FAT	GO:0003012~muscle system process	5	0.0111
Annotation Cluster 5	Enrichment Score: 2.15		
Category	Term	Count	P Value
GOTERM_MF_FAT	GO:0005516~calmodulin binding	9	4.0E-07
GOTERM_MF_FAT	GO:0022836~gated channel activity	8	8.0E-04
GOTERM_BP_FAT	GO:0006816~calcium ion transport	6	8.3E-04
SP_PIR_KEYWORDS	ionic channel	8	1.0E-03
GOTERM_BP_FAT	GO:0044057~regulation of system process	8	1.1E-03
GOTERM_MF_FAT	GO:0046873~metal ion transmembrane transporter activity	8	1.1E-03
GOTERM_BP_FAT	GO:0006811~ion transport	12	1.8E-03
GOTERM_BP_FAT	GO:0015674~di-, tri-valent inorganic cation transport	6	2.2E-03
SP_PIR_KEYWORDS	ion transport	10	2.2E-03
GOTERM_BP_FAT	GO:0030001~metal ion transport	9	2.7E-03
GOTERM_MF_FAT	GO:0005216~ion channel activity	8	2.8E-03
GOTERM_MF_FAT	GO:0022838~substrate specific channel activity	8	3.3E-03
GOTERM_MF_FAT	GO:0015267~channel activity	8	4.0E-03
GOTERM_MF_FAT	GO:0022803~passive transmembrane transporter activity	8	4.1E-03
KEGG_PATHWAY	hsa04020:Calcium signaling pathway	5	6.2E-03
GOTERM_MF_FAT	GO:0005262~calcium channel activity	4	6.9E-03
GOTERM_BP_FAT	GO:0006812~cation transport	9	7.5E-03
GOTERM_CC_FAT	GO:0034704~calcium channel complex	3	7.8E-03
GOTERM_CC_FAT	GO:0030425~dendrite	5	8.5E-03
SP_PIR_KEYWORDS	calcium transport	4	8.6E-03
GOTERM_BP_FAT	GO:0043062~extracellular structure organization	5	1.0E-02
GOTERM_MF_FAT	GO:0005261~cation channel activity	6	1.1E-02
GOTERM_BP_FAT	GO:0022037~metencephalon development	3	1.4E-02
GOTERM_CC_FAT	GO:0034702~ion channel complex	5	1.8E-02
GOTERM_MF_FAT	GO:0022834~ligand-gated channel activity	4	2.5E-02

Category	Term	Count	P Value
GOTERM_MF_FAT	GO:0015276~ligand-gated ion channel activity	4	2.5E-02
GOTERM_CC_FAT	GO:0034703~cation channel complex	4	2.7E-02
GOTERM_BP_FAT	GO:0050804~regulation of synaptic transmission	4	3.3E-02
GOTERM_MF_FAT	GO:0022843~voltage-gated cation channel activity	4	3.6E-02
SP_PIR_KEYWORDS	calcium channel	3	3.7E-02
SP_PIR_KEYWORDS	voltage-gated channel	4	3.8E-02
GOTERM_BP_FAT	GO:0030902~hindbrain development	3	3.9E-02
GOTERM_BP_FAT	GO:0060341~regulation of cellular localization	5	3.9E-02
GOTERM_BP_FAT	GO:0050808~synapse organization	3	4.0E-02
GOTERM_BP_FAT	GO:0051969~regulation of transmission of nerve impulse	4	4.1E-02
GOTERM_BP_FAT	GO:0050905~neuromuscular process	3	4.1E-02
GOTERM_BP_FAT	GO:0048167~regulation of synaptic plasticity	3	4.3E-02
GOTERM_BP_FAT	GO:0031644~regulation of neurological system process	4	4.5E-02
GOTERM_MF_FAT	GO:0005230~extracellular ligand-gated ion channel activity	3	4.9E-02
Annotation Cluster 6	Enrichment Score: 1.55		
Category	Term	Count	P Value
GOTERM_BP_FAT	GO:0007517~muscle organ development	5	0.0237
GOTERM_BP_FAT	GO:0014706~striated muscle tissue development	4	0.0237
GOTERM_BP_FAT	GO:0042692~muscle cell differentiation	4	0.0248
GOTERM_BP_FAT	GO:0060537~muscle tissue development	4	0.0269
GOTERM_BP_FAT	GO:0055002~striated muscle cell development	3	0.0296
GOTERM_BP_FAT	GO:0055001~muscle cell development	3	0.0340